Online ISSN: 1920-3853

Vol. 8, No. 3, October 2014

Print ISSN : 1715-9997

Canadian Journal of pure & applied sciences

an International Journal

SENRA
Academic Publishers
British Columbia

The Canadian Journal of Pure and Applied Sciences (CJPAS-ISSN 1715-9997) is a peer reviewed multi-disciplinary specialist journal aimed at promoting research worldwide in Agricultural Sciences, Biological Sciences, Chemical Sciences, Computer and Mathematical Sciences, Engineering, Environmental Sciences, Medicine and Physics (all subjects).

Every effort is made by the editors, board of editorial advisors and publishers to see that no inaccurate or misleading data, opinions, or statements appear in this journal, they wish to make clear that data and opinions appearing in the articles are the sole responsibility of the contributor concerned. The CJPAS accept no responsibility for the misleading data, opinion or statements.

CJPAS is Abstracted/Indexed in:
Thomson Reuters, EBSCO, Ulrich's Periodicals Directory, Scirus, CiteSeerX, Index Copernicus, Directory of Open Access Journals, Google Scholar, CABI, Chemical Abstracts, Zoological Records, Global Impact Factor Australia, J-Gate, HINARI, WorldCat, British Library, European Library, Biblioteca Central, The Intute Consortium, Genamics JournalSeek, bibliotek.dk, OAJSE, Zurich Open Repository and Archive Journal Database.

Global Impact Factor for 2012 = 2.657

Frequency:
3 times a year (Feb, June and Oct.)

Editorial Office
E-mail: editor@cjpas.ca
: editor@cjpas.net

SENRA Academic Publishers
5919 129 B Street Surrey
British Columbia V3X 0C5 Canada
www.cjpas.net
E-mail: senra@cjpas.ca

Print ISSN 1715-9997
Online ISSN 1920-3853

Volume 8, Number 3
October 2014

CANADIAN JOURNAL OF PURE AND APPLIED SCIENCES

Board of Editorial Advisors

Member
CANADIAN ASSOCIATION OF LEARNED JOURNALS

Canadian Journal of pure & applied sciences

Volume 8, Number 3
October 2014

CONTENTS

LIFE SCIENCES

Joga Singh, Sudhir Sharma, Paramdeep Singh, Gurjeet Singh, Ravinder Dang and Neena Bedi
Pharmacokinetic and Pharmacological Evaluation of Dov 21947 and Venlafaxine by Oral and Intranasal Administration in Mice 2985

S Stephen, AE Pillay, T Shah and E Siores
Heavy Metal Isotopic Fractionation Effects Linked to Acid Leaching of Doped Polymeric Matrix: A Study by Hyphenated Mass Spectrometry 2993

Fatma Hashem, Hemaia Motawea, Manal Shabana, Mai Khalil and Taha Al-Alfy
Ehretia wallichiana Hook. F. and Thomson Ex Gamble Reduces the Risk of Breast Cancer 2999

Issam Kobrsi
Synthesis and Characterization of Bis(5-Diisopropylamino-1,2,3,4-Tetrazolato)-Tris(Dimethylamido) Digallium: The First Example of a Gallium Tetrazolate Complex 3005

Raheela Sharmeen, M Zaheer Khan, Ghazala Yasmeen and Syed Ali Ghalib
Levels of Heavy Metals (Cadmium, Chromium, Copper and Lead) on Water and Selected Tissues of *Oreochromis mossambicus* from Different Locations of Malir River, Karachi 3011

Azza H Mohamed, Sherin K Sheir, Gamalat Y Osman and Hoda H Abd-El Azeem
Toxic Effects of Heavy Metals Pollution on Biochemical Activities of the Adult Brine Shrimp, *Artemia Salina* 3019

Mohammed I Hamzah, Mohammed AM Al-Bayati and Faisal Gh. Al-Rubaye
Serum Sialic Acid (Total Sialic Acid and Lipid Associated Sialic Acid), B-Carotene and Super Oxide Dismutase (Sod) Levels in Iraqi Patients with Knee Osteoarthritis 3029

Karim Gabol, M Zaheer Khan, M Umair A Khan, Peer Khan, Farina Fatima, Saima Siddiqui, Tanveer Jabeen, Nadeem Baig, M Asif Iqbal, M Usman A Hashmi and Muhammad Tabish
Induced Effects of Lead, Chromium and Cadmium on *Gallus domesticus* 3035

Sherimon PC, Vinu PV, Reshmy Krishnan and Youssef Saad
Ontology Driven Analysis and Prediction of Patient Risk in Diabetes 3043

Said A Damhoureyeh and Syed Ali Ghalib
An Overview of the Status and Distribution of the Mangrove Forests and their Wildlife in Sindh 3051

Short Communication

Fatin F Alkazaz, Sura A Abdulsattar, Farred MA Farred and Shahad J Mahmood
Risk Factor of Metabolism Alteration in Burn Patients 3057

PHYSICAL SCIENCES

Pakorn Leesutthipornchai, Chalermpol Charnsripinyo and Naruemon Wattanapongsakorn
Multi-Objective Evolutionary Computation Heuristic for Traffic Grooming in WDM Optical Networks 3061

Al Mutairi Alya O and Heng Chin Low
Saddlepoint Approximation to Cumulative Distribution Functions for some Difficult and Unknown Linear Combinations of Random Variables.....3081

Roland Tolulope Loto, Cleophas Akintoye Loto and Patricia Abimbola Popoola
Corrosion Inhibition of 2-Amino-5 Ethyl-1, 3, 4-Thiadiazole on Mild Steel in Hydrochloric Acid 3091

OR Adegboye, KM Odunfa and OS Ohunakin
Re-Activation of a Small Hydropower (SHP) Plant: Oyan Shp Station, Nigeria 3105

Om Parkash and Priyanka Kakkar
New Information Theoretic Models, their Detailed Properties and New Inequalities.....3115

Muhammad Asif Khan
Effectiveness of Detective and Preventative Information Security Controls in Information Systems Organizations.....3125

Ashwani K Thukral
Logarithms of Imaginary Numbers in Rectangular Form: A New Technique.....3131

A A Zakharenko
An Examination of Zero-Order Modes of Plate Pem-Sh Dispersive Acoustic Waves: Magnetically Open and Electrically Closed Plate Sides 3139

Omar Selt and Rachid Zitouni
A Comparative Study of Heuristic and Metaheuristic for three Identical Parallel Machines.....3147

SB Akpila and IW Omunguye
Soil Modulus and Undrained Cohesion of Clayey Soils from Stress-Strain Models.....3155

Short Communication

Pishtiwan O. Sabir
On Fuzzy Complex Derivatives II.....3163

SENRA Academic Publishers, British Columbia
Vol. 8, No. 3, pp. 2985-2992, October 2014
Online ISSN: 1920-3853; Print ISSN: 1715-9997

Canadian Journal of pure&applied sciences

PHARMACOKINETIC AND PHARMACOLOGICAL EVALUATION OF DOV 21947 AND VENLAFAXINE BY ORAL AND INTRANASAL ADMINISTRATION IN MICE

Joga Singh[1], Sudhir Sharma[2], Paramdeep Singh[2], Gurjeet Singh[2], Ravinder Dang[3] and *Neena Bedi[1]
[1]Department of Pharmaceutical Sciences, Guru Nanak Dev University, Amritsar-143005
[2]Department of Discovery Biology, Drug Discovery Research, Panacea Biotec Ltd., SAS Nagar (Mohali)-160055
[3]Department of Pharmacy, GGN Khalsa College, Civil Lines, Ludhiana-141001, India

ABSTRACT

Intranasal administration is a non-invasive method of drug delivery which may bypass the BBB to allow therapeutic substances direct access to the central nervous system. Recently direct delivery of drugs from nasal cavity to the CNS via the olfactory pathway is attracting increasing attention in order target the drugs directly to the CNS for the treatment of diseases like Schizophrenia, Meningitis, Parkinson's disease, Alzheimer's disease as well as depression also. This alternative approach can also lead to reduction in systemic side effects. The study investigated the plasma pharmacokinetics and brain uptake of DOV 21947 (Triple Reuptake Inhibitor) and venlafaxine a serotonin-norepinephrine reuptake inhibitor in Swiss albino mice after oral and intranasal administration. Enhanced pharmacological effect was observed which was evaluated by means of forced swimming test, suggesting that intranasal administration of drug produced higher direct delivery to CNS as well as to systemic circulation. Thus, offering a promising route of administration and an alternative to per-oral administration.

Keywords: Intranasal, per-oral, antidepressant, forced swim test, venlafaxine.

INTRODUCTION

A syndrome that reflects a sad and/or irritable mood exceeding normal sadness or grief is known as depression. According to the DSM-IV (Diagnostic and Statistical Manual of Mental Disorders) 'depression' and 'depressed mood' is a clinical syndrome, or cluster of symptoms, covering changes in effect, cognition and behaviour, and which meet the diagnostic criteria for a Major Depressive Disorder (Aaron *et al*., 2004; APA, 1996). Treatment of central nervous system (CNS) diseases is very difficult due to the blood–brain barrier's (BBB) ability to severely restrict entry of almost all the drugs except small, non-polar compounds (Berardi *et al*., 2002). Intranasal administration is a non-invasive method of drug delivery which may bypass the BBB to allow direct access of therapeutic substances to the CNS (Mumford *et al*., 1997; Charlton *et al*., 2007). The nasal route could provide an attractive needle-free alternative for currently injectable drugs which may improve patient compliance and allow extended use of self-medication for many chronic diseases/ acute conditions (Scranton *et al*., 2011; Frey *et al*., 1997).

In the present study, the possibility of using an intranasal delivery system for antidepressant drug therapy by evaluating the transport to the systemic circulation and brain and the pharmacological effect after intranasal (*i.n.*) administration were investigated. Two drugs namely venlafaxine (a serotonin-norepinephrine reuptake inhibitor i.e. SNRI) and DOV 21947 (a triple re-uptake inhibitor i.e. TUI or SNDRI) were selected. Chemically, venlafaxine is (R/S)-1-[2-(dimethylamino)-1-(4-methoxyphenyl) ethyl] cyclohexanol hydrochloride. It is used primarily for the treatment of depression, general anxiety disorder, social phobia, panic disorder and vasomotor symptoms whereas DOV 21947 is [(1R, 5S) -1-(3, 4-dichlorophenyl)-3-azabicyclo [3.1.0] hexane hydrochloride]. DOV 21,947 or EB-1010, also known as Amitifadine, is an antidepressant drug being developed by Euthymics Bioscience Inc., which is currently in clinical trials. Based upon preclinical studies, this triple reuptake inhibitor has the potential utility in treating a wide variety of central nervous system disorders including depression and obesity (Skolnick *et al*., 2003; Tizzano *et al*., 2008). Intranasal administration of antidepressant drugs (DOV 21947 and venlafaxine) was found to produce a higher direct delivery to the CNS as well as to the systemic circulation.

MATERIALS AND METHODS

Materials

Quality grade anti-depressant drug: venlafaxine hydrochloride and DOV 21947 were obtained from Panacea Biotec Ltd, Mohali (Punjab, India). Polyethylene glycol (PEG 400) and Propylene glycol (PG) were procured from Spectrochem Private Ltd, Mumbai, India.

*Corresponding author email: neenagndu@yahoo.com

Carboxy methyl cellulose sodium and sodium chloride GR were purchased from Loba Chemie Private Ltd, Mumbai and Merck Specialities Private Ltd, Mumbai, respectively. Other chemicals like Ethylene diamine tetraacetic acid (EDTA) tri potassium salt dehydrate and Tween® 80 were purchased from Sigma Life Science (Sigma-Aldrich Co.), USA and Halothane from Raman and Weil Private Ltd, Mumbai, India. All the chemicals acquired were of high quality and of analytical grade.

Animals

Animals used in this study were post weaned (4-weeks old) either sex SAM provided by Small Animal Facility for Experimentation and Breeding (SAFEB), Drug Discovery Research, Panacea Biotec Ltd, Mohali (Punjab, India) and maintained as per the guidance laid by Committee for the Purpose of Control and Supervision of Experiments on Animals (CPCSEA). Controlled conditions in animal house were light (12 hr duration light: dark), temperature and relative humidity at 21±2°C and 50-55%, respectively.

Formulation Development

To study the effect of different vehicles, drug was either solubilised in (1) R.O.Water (2) 10% PEG + 50% PG + 40% R.O.Water (3) 20% PEG + 50% PG + 30% R.O.Water. Weighed quantity of drug was taken in mortar. Two to three drops of Tween 80 (as a surfactant) was added and slowly triturated to form a homogenous paste. Drug was solubilised in the calculated amount of vehicle, added in small volumes with continuous trituration. Solution was mixed thoroughly by using vortex mixer (IKA® Werke) for about one minute so that drug gets evenly dispersed in the vehicle. Drug solutions were sonicated (Elmasonic) for two to three minutes to dissolve any remaining drug particle.

Peroral Administration of Drugs in Test Animals

Drug suspended in suitable vehicles was administered via a feeding cannula attached to a syringe at 10 mg/kg or 30 mg/kg dosage.The drug was administered to eight batches (eight time points) of group of four either sex Swiss albino mice housed in a ventilated room at ambient temperature and were fed with standard pellet diet and water *ad libitum*. The mice were fasted overnight before dosing. The animals used were between weight ranges of 25g-30g. DOV 21947 was prepared as a suspension and administrated orally at a dose of 30 mg/kg and 10 mg/kg in case of intranasal administration. The formulations were prepared on the day of dose administration and were administered within 15 minutes of preparation by oral gavage in different vehicles and proportions as indicated in table 1.

Blood samples (100 µl) were drawn by capillary bleeding from retro-orbital plexus and brain samples were also extracted. Samples were collected at pre-dose (0 h), and then 0.25, 0.5, 1, 2, 4, 8 and 24 hours after administration. Animals were sacrificed by cervical dislocation. The protocol was approved by the Institutional Animal Ethics Committee (IAEC).

Intranasal Administration of Drugs in Test Animals

Drug was administered in drop wise manner on the nostril of animal using a 50µl Hamilton syringe. Prior to administration, animals were anesthetized using an inhalational anaesthetic (Halothane) in the desiccators (Schaefer *et al*., 2002; Guerrero *et al*., 2011).

Swiss albino mice (25 to 30g) were anesthetized with halothane. Throughout the entire experiment, all mice were kept in supine position so that drug solutions can contact a larger area of nasal olfactory mucosa compared to the prone position. DOV 21947 nasal drops were administered at a dose of 10 mg/kg to each mouse. A volume of drug solution (10 µl per 30g of body weight) was administered into both nostrils carefully using a Hamilton syringe.

Before (0 minute) and after drug administration at 15, 30, 60, 120, 240, 480 and 1440 minutes, blood samples of 100 µl were withdrawn from retro-orbital plexus and then centrifuged for 6 minutes at 6000 rpm to obtain plasma. After the blood sampling, the mouse was sacrificed by cervical dislocation and brain was excised carefully. Brain sampling was completed within 5 minutes following the blood sampling. All plasma and brain samples were stored at -20 and -80°C, respectively, until analysis.

Collection of Plasma

Blood was collected by inserting the capillary into the retro-orbital sinus in labelled microfuge tubes containing EDTA at predetermined times after administration and plasma samples were obtained by centrifugation (Eppendorf Research).

Table 1.Various formulations used in the study along their composition

Formulation Code		Composition
Venlafaxine	DOV 21947	
Formulation V_1	Formulation D_1	R.O. Water + DRUG
Formulation V_2	Formulation D_2	10% PEG + 50% PG + 40% Water + DRUG
Formulation V_3	Formulation D_3	20% PEG + 50% PG + 30% Water + DRUG
Formulation V_4	Formulation D_4	30% PEG + 50% PG + 20% Water + DRUG

Extraction of Brain Samples

Animals were sacrificed by cervical dislocation. Bone cutter was used to make circumferential incision from behind the eye sockets (avoiding injury to the brain tissue) from extending to the opening for the ears in the skull to all round the cranium. Brain samples were placed in 15 ml tube having adequate amount of 0.85% NaCl and kept in ice until it was further processed.

Homogenisation of Brain Samples

Extracted brain samples were weighed individually to make 10% *w/v* brain homogenate in 0.85% NaCl solution and homogenized. Homogenizer probe was washed thoroughly first with R.O water and then with absolute ethanol in between the two samples. Finally, 1 ml from each tube was transferred to fresh, properly labelled, clean and dry micro centrifuge tubes and kept at -80°C until analysis.

Drug Quantification

The concentration of drug was determined by an appropriate HPLC method. A Symmetry C_{18} column (250 mm×4.6 mm, 5 µm, cartridge) was used for chromatographic separation. The injection volume and run time was 20 µl and 15 minutes, respectively.

A LC-MS analysis was performed using a Discovery 5µm column (5x4mm). Plasma and brain drug samples were analyzed using the above technique. Detection was performed using a 4000 Q Trap instrument. The spectrophotometer was used in MS/MS mode with MRM of fragmentation reactions selected for each drug.

Assessment of anti-depressant like activity of DOV 21947 by the most frequently used behavioural model, Forced Swim Test:

Swiss albino mice (22–28g) from the Small Animal Facility for Experimentation and Breeding (SAFEB), Drug Discovery Research, Panacea Biotec Ltd., Mohali, were used. Fifteen mice were housed per cage. The cages were placed in the experimental room 48 hour before the test for acclimatization. The animals were fed a standard laboratory diet and water *ad libitum* under standard environmental conditions (Woode *et al*., 2010; Porsolt *et al*., 1997).

Clear plastic cylinders (diameter 12 cm, height 25 cm) were filled to a depth of 10 cm with water (25ºC). Briefly, mice were dropped individually into glass cylinders and left there for 6 minutes. Behaviour was recorded on video. The duration of immobility was recorded during the last 4 minutes of the 6-minutes test using Forced swim scan™ 2.0 software by Clever Sys, Inc. The test was performed 15 minutes after administration of drug.

Animals were randomized based on body weight. At time T_{-30}, vehicle to control group, standard compounds (suitable dose mg/kg) in vehicle to standard group, test compounds (suitable dose mg/kg) in vehicle to test group were administered. Animals were individually forced to swim inside a glass jar containing 10 cm of water maintained at 23-25°C. After the initial 1-2 minute of vigorous activity the animals showed periods of immobility by floating with minimum movements. The immobility time is the time spent by the mouse floating in the water without struggling and making only those movements necessary to keep their heads above the water. Animal is considered to be immobile whenever it remained floating passively in the water in a slightly hunched but upright position, its nose above the water surface. The total immobility time for the period of 6 minutes was recorded.

RESULTS AND DISCUSSION

(A_1) Transfer of DOV 21947 to the Brain and Systemic Circulation after *p.o.* Administration

Plasma profile

The maximum plasma concentration of DOV 21947 was observed after oral administration of Formulation D_4 followed by D_3. The AUC values were calculated by trapezoidal rule. Data suggested (Plasma $t_{1/2}$ values) that in spite of low peak plasma concentration, formulation D_2 was cleared slowly from plasma (Fig. 1). For all formulations administered, highest and lowest values of tmax were observed in Formulation D_4 and Formulation D_2, respectively.

Brain profile

The drug release pattern of DOV 21947 in Formulation D_3 showed better results in brain profiling but time required to achieve the maximum concentration was minimum with Formulation D_2 out of all the tested formulations.

After analysis it was decided that formulation D_2 can be further carried for intranasal administration in mice. Comparison was done with Formulation D_1.

(A_2) Transfer of DOV 21947 to the Brain and Systemic Circulation after *i.n.* Administration

Plasma Profile

At several time points, significant differences were observed between the DOV 21947 levels in plasma and brain tissue of the intranasal and oral routes. Following oral administration, DOV 21947 in Formulation D_1 attained a peak concentration at 15 minutes, and then followed by an exponential decline with the passage of time (Fig. 2). Nasally administered DOV 21947 in Formulation D_1 displayed slightly increased levels. Comparatively, nasally administered DOV in Formulation D_3 displayed a slow and poor absorption of active drug across the nasal mucosa into the systemic circulation. The AUC and half life values of concentration time curves in

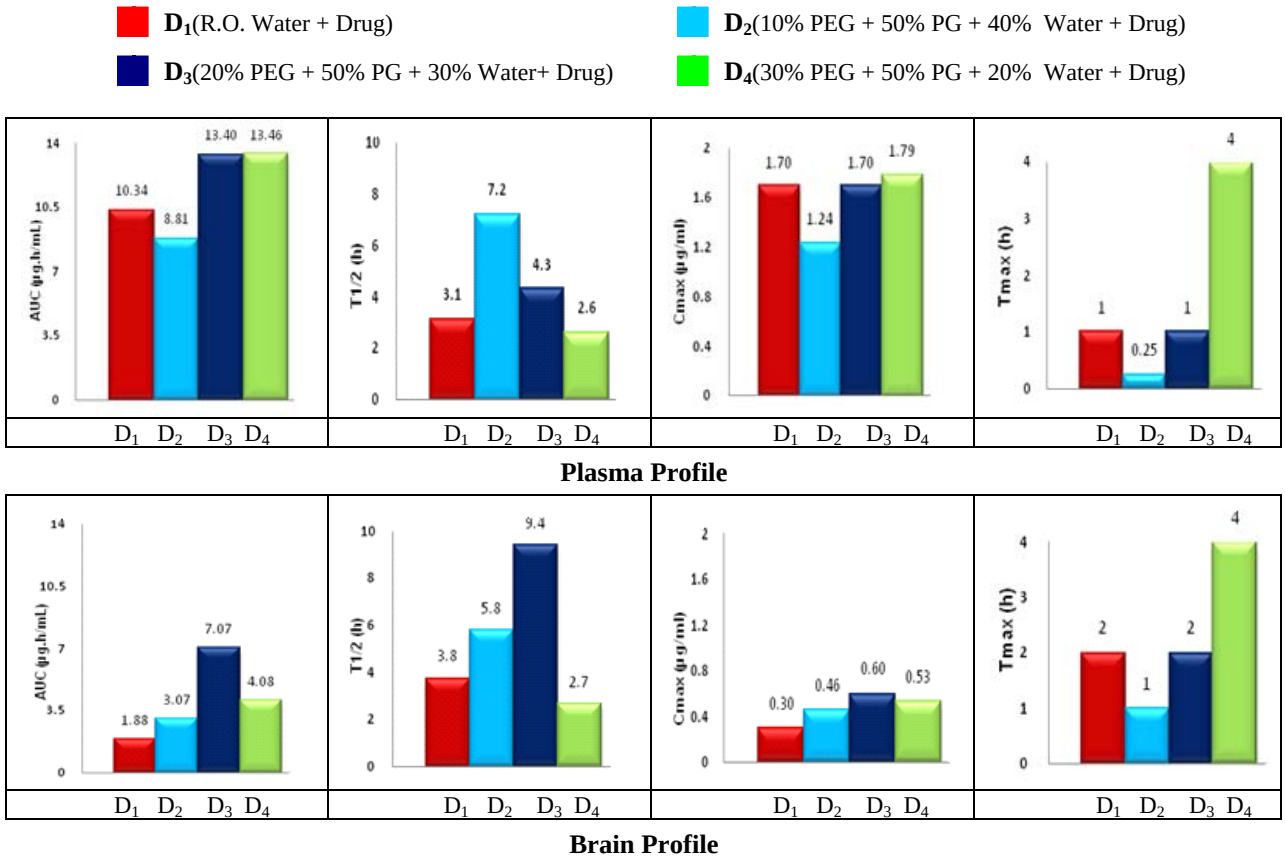

Fig. 1. Pharmocokinetic parameters of DOV 21947 in different vehicles administered orally.

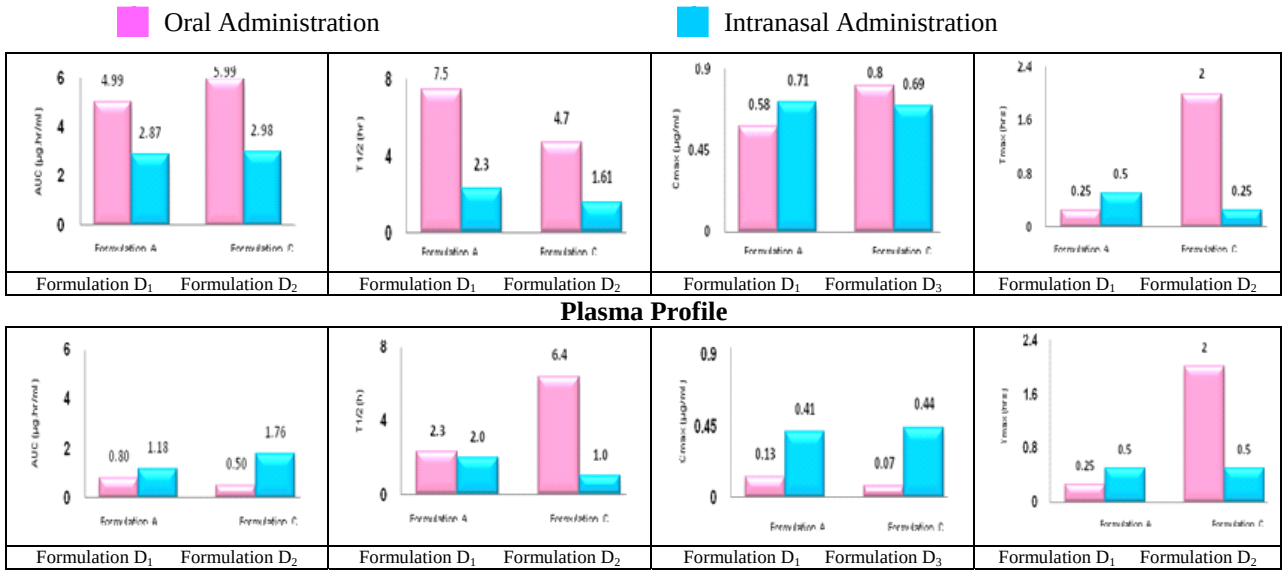

Fig. 2. Comparative pharmocokinetic parameters of DOV 21947 administered by oral and intranasal administration.

plasma after nasal administration were significantly lower than those in post oral administration in Formulations D_1 and D_3.

Brain Profile

Following DOV 21947 (in either formulation) intranasal administration, the drug levels in brain samples were all significantly higher than those in post oral administration brain samples. At 30 minutes post-nasal dose, DOV 21947 concentrations in brain reached peak values of 0.41 µg/g and 0.44 µg/g from Formulation D_1 and Formulation D_3, respectively.

(A_3) Pharmacological Effect 15 min after *i.n.* Administration of DOV 21947

Figure 3 shows the effects of treatment with DOV 21947 on the immobility time in the forced swimming test in mice. In the case of *p.o.* and *i.n.* administration of DOV 21947, the immobility time of mice was reduced significantly compared with controls, in both the formulations. Moreover, the pharmacological effect after *i.n.* administration was higher than that after *p.o.* administration and significant differences were observed for both the routes between the immobility times.

The possible CNS antidepressant effect of DOV 21947 after oral and intranasal administration was studied by the forced swim test. In this test, animals treated with both the DOV 21947 formulations (i.e. D_1 & D_2) showed decrease in their immobility times, which was significant (77.8 ± 23.1 and 139.6 ± 28.6, respectively after oral administration and 27.2 ± 7.7 and 6.3 ± 3.1, respectively after Intranasal administration) when compared with the control group (191.7 ± 10.9) (Fig. 3). Similarly, animals treated with the drug (DOV 21947 in water 32 mg/kg, oral), as expected showed a significant decrease in their immobility time (2.2 ± 0.9). $E.D_{50}$ (dose responsible for 50% of linear regression equation on percent decrease in immobility time data for both the delivery routes (oral route 15.52 and intranas maximal effect) for DOV 21947 was determined by applying al route 10.21) and significant difference was observed as depicted in figure 4.

(B_1) Transfer of Venlafaxine to the Brain and Systemic Circulation after *p.o.* Administration.

Venlafaxine was prepared as a suspension (in different vehicles and proportions as given in Table 1) and administrated orally at a dose of 30 mg/kg.

Plasma profile

Due to high solubility of drug in water, it showed better results in Formulation V_1. Out of peglated formulations, Formulation V_2 showed maximum plasma concentration as evident from figure 5.

Brain profile

In brain profiling, Formulation V_2 achieved maximum concentration and also remained there for significant duration of time.

As is relevant from the data, Formulation V_2 outshined other formulations so it was taken further for pharmacological investigations.

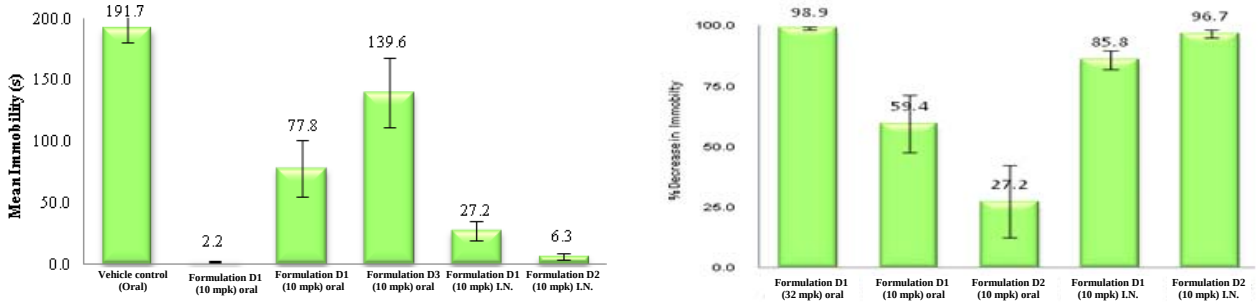

Fig. 3. Effects of DOV 21947 on the duration of immobility in the forced swim test.

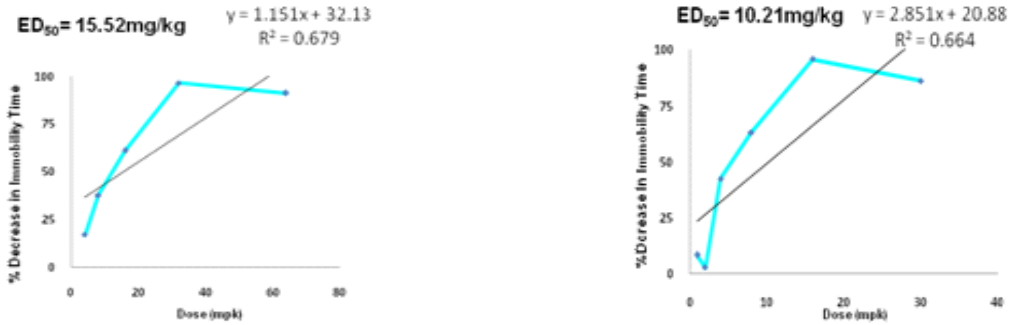

Fig. 4. ED_{50} values of DOV 21947 in the forced swim test after Oral administration (left) and after Nasal administration (right).

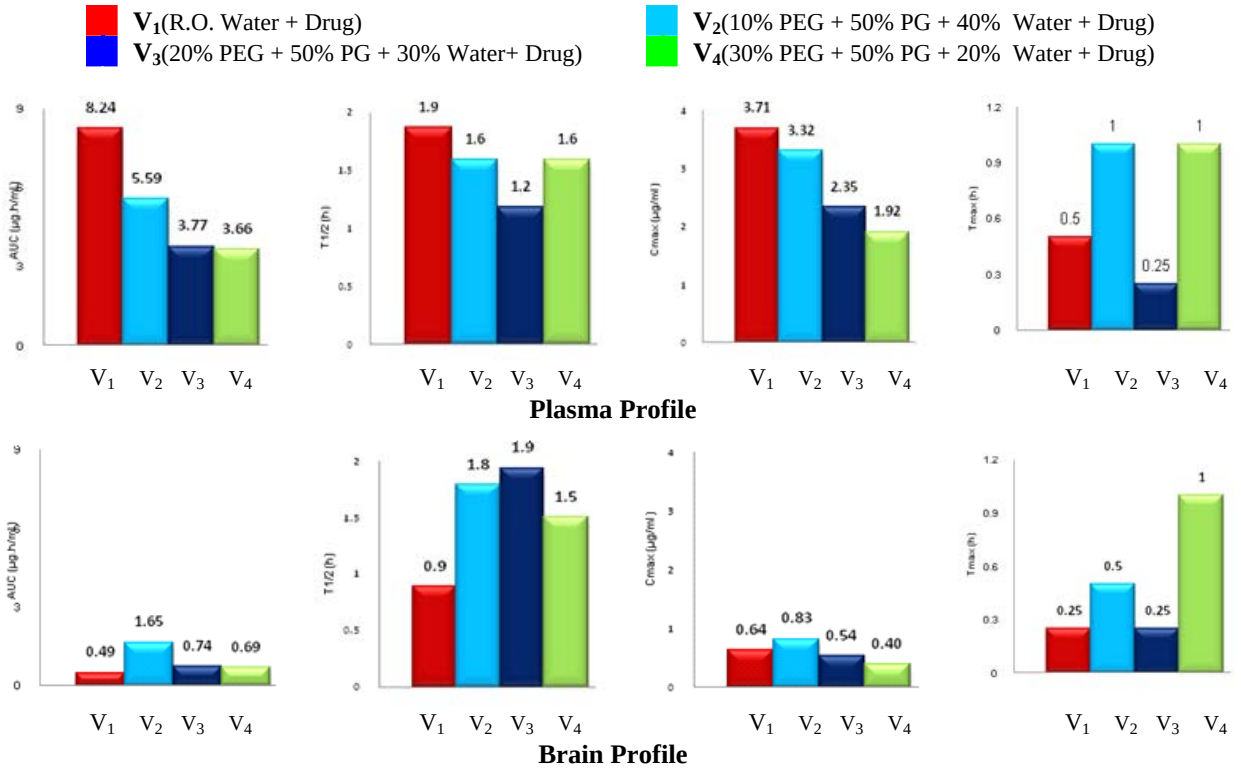

Fig. 5. Pharmocokinetic parameters of Venlafaxine in different vehicles administered orally.

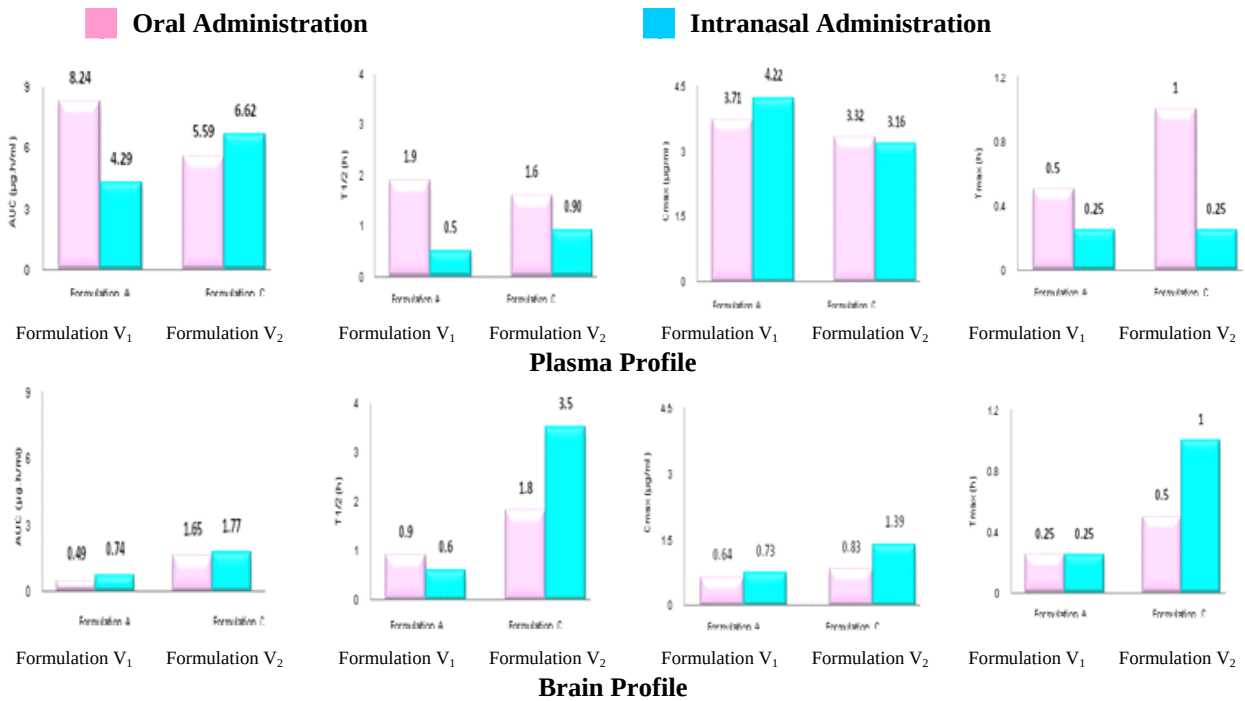

Fig. 6. Comparative pharmocokinetic parameters of Venlafaxine administered by oral and intranasal administration.

(B_2) Transfer of Venlafaxine to the Brain and Systemic Circulation after *i.n.* Administration.

Procedure and methodology was same while administering venlafaxine via intranasal route as

described in previous drug administration i.e. DOV21947. Venlafaxine nasal drops were administered at a dose of 30 mg/kg to each mouse.

Plasma Profile

At several time points, significant differences could be observed between the venlafaxine levels in plasma and brain tissue of the intranasal and oral routes. Comparatively, nasally administered venlafaxine in Formulation V_1 displayed slightly increased levels (Fig. 6) while oral administration of venlafaxine in Formulation V_2 attained a peak plasma concentration of 3.32µg/ml at 1 hour. Nasally administered venlafaxine in Formulation V_2 displayed no significant difference in peak concentration but faster absorption across the nasal mucosa into the systemic circulation as compared to orally administered venlafaxine. The half life values of concentration time curves in plasma after nasal administration were all significantly lower than those in post oral administration in both Formulation V_1 andV_2.

Brain Profile

Following venlafaxine (in formulation V_2) intranasal administration, the drug levels in brain samples were all significantly higher than those in post oral administration brain samples. At 1 hour post-nasal dose, venlafaxine concentrations in brain reached peak values of 1.39µg/g while for venlafaxine (Formulation V_1) intranasal administration, the peak drug levels in brain were of no significant difference.

(B_3) Pharmacological Effect 15 min after *i.n.* Administration of Venlafaxine

The possible CNS antidepressant effect of venlafaxine after oral and intranasal administration was studied by the forced swimming test. In this test, animals treated with both the venlafaxine formulations (i.e. V_1&V_2) showed decrease in their immobility times, which was significant (83.5 ± 29.4 and 108.3 ± 17.2, respectively after oral administration and 25.7 ± 12.6 and 27.6 ± 11.54, respectively after Intranasal administration) when

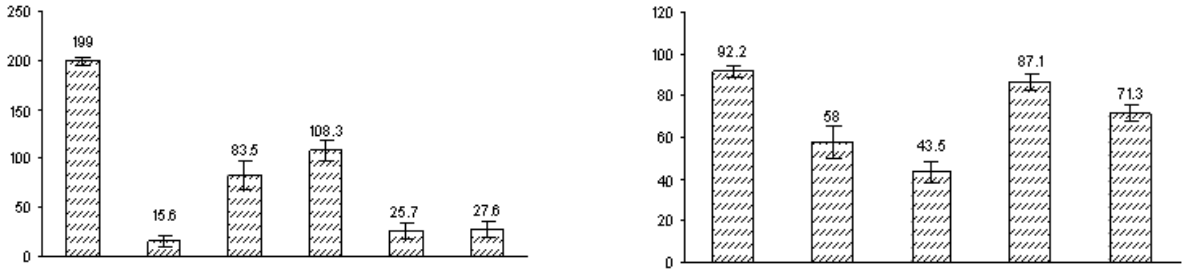

Fig. 7. Effects of Venlafaxine on the duration of immobility in the forced swim test.

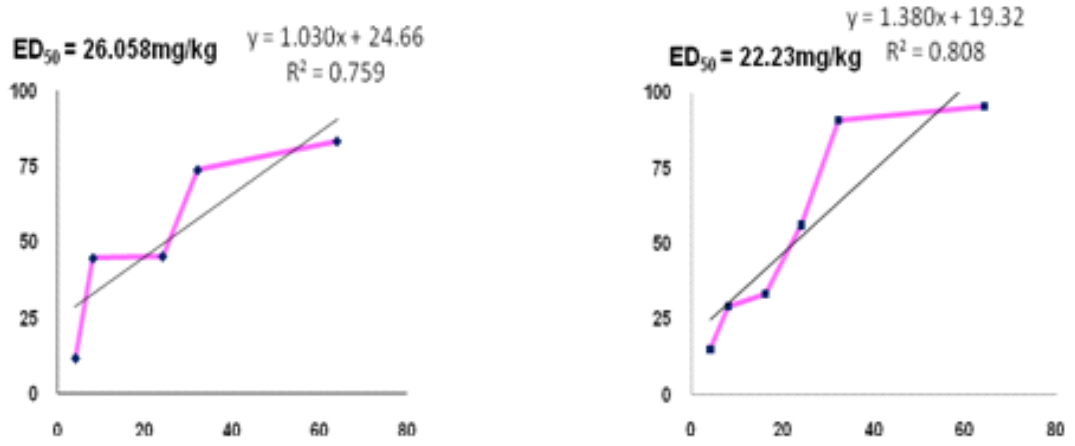

Fig 8. ED_{50} values of Venlafaxine in the forced swim test after Oral administration (left) and after Nasal Administration (right).

compared with the control group (199.0 ± 4.9). Similarly, animals treated with the drug (DOV 21947 in water 32 mg/kg, oral), as expected showed a significant decrease in their immobility time (15.6±6.5) (Fig. 7). $E.D_{50}$ (dose responsible for 50% of maximal effect) for venlafaxine was determined by applying linear regression equation onpercentage decrease in immobility time data for both the delivery routes and slight difference was observed (Fig. 8).

CONCLUSION

The present study evaluated an alternative route for direct delivery to brain of antidepressant drugs. The intra nasal administration of antidepressant drugs produces a higher direct delivery to brain suggesting that it is a promising route of administration and an alternative to per oral administration. The direct transport to brain, results in higher antidepressant effect compared to that with per oral administration. Our overall data suggest that the nasal route could be exploited to increase the availability of antidepressants inside the brain.

ACKNOWLEDGEMENT

The authors are thankful to Dr. Sanjay Trehan, President, Panacea Biotec Ltd. for granting permission and providing all facilities to conduct my project work in this prestigious institute and also express sincere gratitude to project coordinator Dr. Ajay Singh, Sr. Scientist, Biological Research Department, Panacea Biotec Ltd. for his kind and encouraging attitudes.

REFERENCES

Aaron, R., Joseph, A., Abraham, S., Muliyil, J., George, K. and Prasad, J. 2004. Suicides in young people in rural southern India. Lancet. 363:1117-1118.

American Psychiatric Association. (APA). 1996. American psychiatric association practice guidelines. Washington, DC, USA. Available Source <http://dev.summacare.com/Libraries/Documents/Depression_Guidelines.sflb.ashx>.

Berardi, D., Leggieri, G., Ceroni, GB., Rucci, P. and Pezzoli, A. 2002. Depression in primary care-a nationwide epidemiological survey. Journal of Family Practice. 19:397-400.

Charlton, S., Jones, NS., Davis, SS. and Illum, L. 2007. Distribution and clearance of bioadhesive formulations from the olfactory region in man: Effect of polymer type and nasal delivery device. European Journal of Pharmaceutical Sciences. 30:295-302.

Frey, WH. II, Liu, J., Chan, X., Thorne, RG., Fawcett, JR., Ala, TA. and Rahman, YE. 1997. Delivery of 125I-NGF to the brain via the olfactory route. Drug Delivery. 4:87-92.

Guerrero-Cazares, H., Gonzalez-Perez, O., Soriano-Navarro, M., Zamora-Berridi, G., Garcia-Verdugo, JM. and Quinones-Hinojosa, A. 2011. Cytoarchitecture of the lateral ganglionic eminence and rostral extension of the lateral ventricle in the human fetal brain. Journal of Comparative Neurology. 519:1165-1180.

Mumford, DB., Saeed, K., Ahmad, I., Latif, S. and Mubbashar, MH. 1997. Stress and psychiatric disorder in rural Punjab: a community survey. British Journal of Psychiatry. 170:473-478.

Porsolt, RD., Le-Pichon, M. and Jalfre, M. 1977. Depression: A new animal model-sensitive antidepressant treatments. Nature. 266:730-732.

Schaefer, ML., Bottger, B., Silver, WL. and Finger, TE. 2002. Trigeminalcollaterals in the nasal epithelium and olfactorybulb: a potentialroute for directmodulation of olfactory information by trigeminal stimuli. Journal of Comparative Neurology. 444(3):221-226.

Scranton, RA., Fletcher, L., Sprague, S., Jimenez, DF. and Digicaylioglu, M. 2011. The rostralmigratory stream plays a keyrole in intranasal delivery of drugs into the CNS. University of Texas Health Science Centre San Antonio, USA, America PLoS One. 6(4):e18711.

Skolnick, P., Popik, P., Janowsky, A., Beer, B. and Lippa, AS. 2003. Antidepressant like actions of DOV 21947: a "triple" reuptake inhibitor. European Journal of Pharmacology. 461:99-104.

Tizzano, JP., Stribling, DS., Pereztilve, D., Strack, A., Frassetto, A., Chen, RZ., Fong, TM., Shearman, L., Krieter, PA., Tschöp, MH., Skolnick, P. and Basile, AS. 2008. The triple uptake inhibitor (1R,5S)-(+)-1-(3,4-dichlorophenyl)-3-azabicyclo [3.1.0]hexanehydrochloride (DOV 21947) reduces body weight and plasma triglycerides in rodent models of diet-induced obesity. Journal of Pharmacology and Experimental Therapeutics. 324(3):1111-1126.

Woode, E., Boakye-Gyasi, E., Amidu, N., Ansah, C. and Duwiejua, M. 2010. Anxiolytic and Antidepressant Effects of a Leaf Extract of *Palisota hirsuta* K. Schum. (Commelinaceae) in Mice. International Journal of Pharmacology. 6(1):1-17.

Received: Feb 6, 2014; Accepted June 26, 2014

SENRA Academic Publishers, British Columbia
Vol. 8, No. 3, pp. 2993-2998, October 2014
Online ISSN: 1920-3853; Print ISSN: 1715-9997

Canadian Journal of pure&applied sciences

HEAVY METAL ISOTOPIC FRACTIONATION EFFECTS LINKED TO ACID LEACHING OF DOPED POLYMERIC MATRIX: A STUDY BY HYPHENATED MASS SPECTROMETRY

*S Stephen[1], AE Pillay[1], T Shah[2] and E Siores[2,3]
[1]Department of Chemistry, The Petroleum Institute, Abu Dhabi, UAE
[2]Institute of Material Science and Innovation, Bolton University, UK
[3]TEI – Athens, Greece

ABSTRACT

Fractionation effects associated with heavy metal isotopes leached from a doped polypropylene matrix was studied. The matrix itself was doped with oxides of Mg, Ti and Zn at levels of 3% and 10%. Acid leaching was investigated at pH3 and pH10. The leachates were analyzed by high performance ICP-MS and the results showed that normal natural abundances were recorded for Mg and Zn. However, depletion of Ti-48 and enrichment of Ti-46 were observed at statistically significant levels. At pH3, Ti-46 and Ti-48 displayed cycles of decay and growth with leaching over time for both the 3% and 10% doped polymeric materials. Such growth and decay were less pronounced for pH10, but the existence of enriched and depleted levels persisted. These data are interpreted in terms of the extraordinary crystal structure of TiO_2, and mechanisms relating to the crystal lattice arrangement of TiO_2. The mechanistic aspects were corroborated by TEM imaging. The fundamental application of our work lies in the discovery of a facile process for preparation of enriched Ti-46 solutions and depleted Ti-46 polymers.

Keywords: ICP-MS, isotopic fractionation, Ti-46/Ti48, polypropylene.

INTRODUCTION

The significance of an investigation of this nature is twofold: (i) to delineate the behavior of polymeric materials under conditions of chemical stress; and (ii) to discover new processes of enriching/depleting metal isotopes (Niederer *et al.*, 1980; Kung. 1989; Victor and Cox, 1996; Williams *et al.*, 2003; Häusser *et al.*, 1970) in polymers. The present study focused on subjecting metal-doped polymeric matrices (Pillay *et al.*, 2010) to acid leaching and observing the levels of isotopic fractionation in the leachates. There were sporadic attempts to study fractionation of metal isotopes using techniques other than ICP-MS (Jouvin *et al.*, 2012; Fujiia *et al.*, 2011; Williams *et al.*, 2014). However, research of this caliber has not been previously accomplished where fractionation effects were monitored using high-performance Inductively Coupled Plasma Mass Spectrometry (ICP-MS). ICP-MS is a notable mass-analytical technique for measurement of ultra-low levels of metal isotopes. The technique is highly sensitive, quick and accurate. Polymeric material (polypropylene) used in this study was specially doped with major concentrations of Mg, Ti and Zn at levels of 3% and 10%. These particular doping levels were selected for clear observation of fractionation processes; and to study the effects of leaching on the stability of the polymeric material. Polymer stability can be adversely affected by unabated leaching; this is of high significance in conducting polymers used in applications such as fuel cells (Mondal *et al.*, 2011).

Heavy-metal isotopic leaching studies of polymeric material are relatively unexplored because these effects are usually not appreciable and can only be detected by highly sensitive instruments. Regular mass spectrometry could be employed for such studies, but hyphenated mass spectrometry (ICP-MS) is a more powerful tool because of successful elimination of matrix effects. Clearly, one novel aspect of this research is the observation of these fractionation effects, especially in titanium isotopes; and proposal of a mechanism associated with such heavy-metal fractionation. TiO_2 is particularly prone to such effects because it can exist in various metastable phases such as β metastable Ti (Chang *et al.*, 2014) (unlike Mg and Zn) (Kung, 1989; Victor and Cox, 1996; Häusser *et al.*, 1970). Therefore, a second novel area of this study uncovers the facile capability to deplete polymeric material and concurrently enrich solutions with Ti-46. For the treatment of cancer by radioactivity (Ragde *et al.*, 2000; Maria *et al.*, 2008) titanium capsules are used but Ti-46 tends to create a problem because of the formation of unwanted radioactive Sc-46. Practical depletion techniques for Ti-46 are therefore, useful. In addition, enriched solutions (Stephen *et al.*, 2014) of Ti-46 can be used to abstract the isotope in question and convert it to Sc-46, which can be used as a tracer in oil refineries (Schweitzer, 1991). This work, therefore, has high potential for application in the oil and gas sector. Our

*Corresponding author email: sstephen@pi.ac.ae

technique at varying pHs could possibly be applied to deplete the Ti-46 in such applications.

MATERIALS AND METHODS

Sample preparation/ leaching study/ICP-MS

The sample preparation and instrumental technique associated with this work have been reported previously (Stephen *et al.*, 2014). The homopolymer HE445FB was used as base material to prepare the compounded materials, which were doped with 3% and 10% $Mg(OH)_2$, TiO_2 and ZnO (as reported earlier Stephen *et al.*, 2014). Each sample (1cm x 1cm) was kept individually in the leaching solvent of pH3 and pH10 for 24 weeks. Isotopic measurements of the leachates were undertaken at specific intervals with a Perkin Elmer SCIEX DRC-e ICP-MS. The analytical capability of the instrument was satisfactory producing relative standard deviations (RSD) <5% for repeated measurements on a certified standard (Stephen *et al.*, 2014).

Slicing polymers for TEM imaging

Thin slivers were "carved" from polymer plaques using an Ultra microtome facility (Power Tome PC, RMC Products, Boeckeler, model CRX). The microtome was equipped with a glass knife for coarse chopping and shaping prior to the final slicing. The final slices of 100 nm thickness and 4x4 mm sections were produced by employing a diamond knife. The cutting chamber was maintained at the appropriate temperature by circulating liquid nitrogen through it. The resultant thin slice of the sample was attached to a stainless steel loop dipped in 2 M sucrose solution. Sucrose solution helped to uncurl the sliver and to attach it to the steel loop. Once the slice was attached to the loop, sucrose was rinsed off using deionized water. The sliced sample was then carefully transferred to a tiny copper mesh 3.06 mm in diameter for imaging.

TEM and imaging

The grid along with the polymer slice was inserted into the electron beam path, which was guided down the vertical tubing by an accelerating voltage of 200 kV. An FEI Tecnai (model G2 20S-Twin EDAX) electron microscope was used for this study. The entire TEM was supported on a pneumatic suspension to minimize vibrations.

RESULTS AND DISCUSSION

TEM Study/Mechanism

The TEM study revealed that acid degradation of the TiO_2 bulk crystal structure leads to production of "smaller particles" suggesting that the ordered structure is broken down along planes into diminished entities. There is evidence (Kung, 1989; Victor and Cox, 1996; Häusser *et al.*, 1970) in the documented literature to indicate that when the crystal is cleaved along a plane, the new surface will be reconstructed, involving atomic rearrangement, to produce a thermodynamically stable surface (Niederer *et al.*, 1980; Kung, 1989; Victor and Cox, 1996). Evidence of atomic rearrangement cannot be deduced from the images but can be inferred from the ICP-MS data below. Crystal stability and rearrangement suggests lighter Ti-46 atoms on the surface with the heavier Ti-48 atoms supporting the interior bulk of the crystal (Kung, 1989; Victor and Cox, 1996; Häusser *et al.*, 1970). The TEM images in figures 1-4 tend to support the theory (Niederer *et al.*, 1980; Kung, 1989; Victor and Cox, 1996; Häusser *et al.*, 1970) that constant crystal cleavage and rearrangement takes place breaking down the bulk structure into minute components. Figures 1 and 2 represent the unleached and leached images of 3% dopant. A comparison of figures 1 and 2 shows the intact bulk structure at the 3% dopant level degrading into myriad constituents at pH3. It is clear from the unleached image (Fig. 1) that the bulk composite ultimately erodes to a more "grainy" conglomerate structure (Fig. 2) with time. The graininess is attributed to the cycle of cleavages followed by atomic rearrangement and formation of new peripheral boundaries (Kung, 1989; Victor and Cox, 1996; Häusser *et al.*, 1970). Figures 3 and 4 represent the unleached and leached images of 10% dopant. The depth of colour in figure 3 reflects the higher dopant concentration. Here again, we observe from these images that acid degradation leads to more grainy formations, corroborating the premise that under acid attack the crystal structure is subjected to cycles of cleavages and re-formation of stable surfaces with atomic rearrangement (Niederer *et al.*, 1980; Kung, 1989; Victor and Cox, 1996; Häusser *et al.*, 1970).

Isotopic fractionation

TiO_2 has an anomalous crystal structure (Kung, 1989; Victor and Cox, 1996), resulting in extraordinary phases and metastable phases during chemical and physical stress (Niederer *et al.*, 1980). Thus its crystal structure is prone to effects unseen in other crystal structures – such as those of Mg and Zn. Figure 5a-d represents isotopic abundances of the metals of interest under leaching conditions of pH3 and pH10. Clearly, from the plots in figure 5, significant levels of enriched/depleted Ti-46/Ti-48 were observed. It is equally clear that these plots depict cycles of growth and decay. For pH3 and dopant levels of 3% and 10% (Figs. 5a,c) Ti-46 decays sharply with corresponding growth of Ti-48. This suggests that the crystal surface is optimized (maximized) with Ti-46 at lattice points, which is gradually degraded by acid attack showing a decline of Ti-46 levels. As the acid penetrates the bulk, the Ti-48 grows. After 12 weeks the data suggest "disintegration" of the bulk crystal structure (throughout the sample, from persistent attack) into grainy formations – as supported by the TEM images – leading to atomic rearrangement and

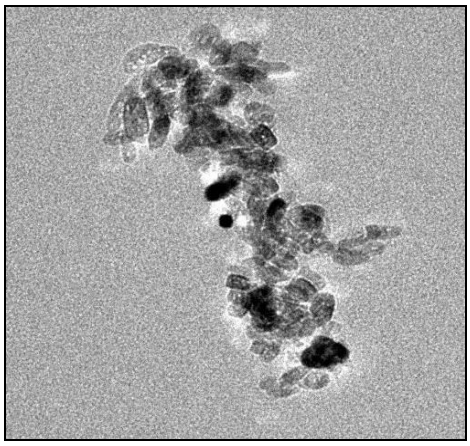

Fig. 1. Unleached 3%.

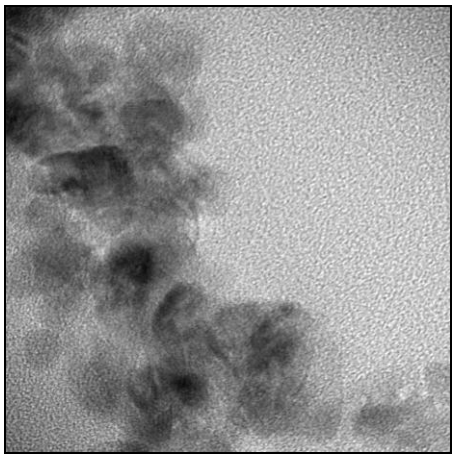

Fig. 2. Leached, 3%, pH3, 12 weeks.

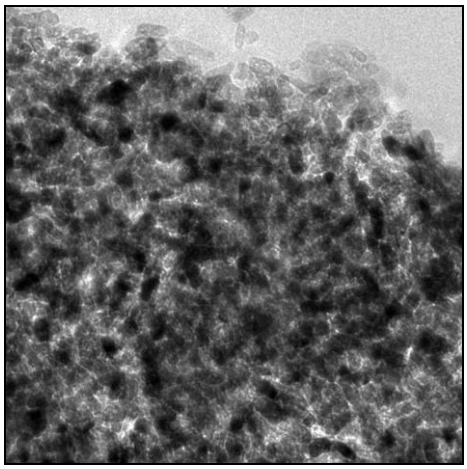

Fig. 3. Unleached 10%.

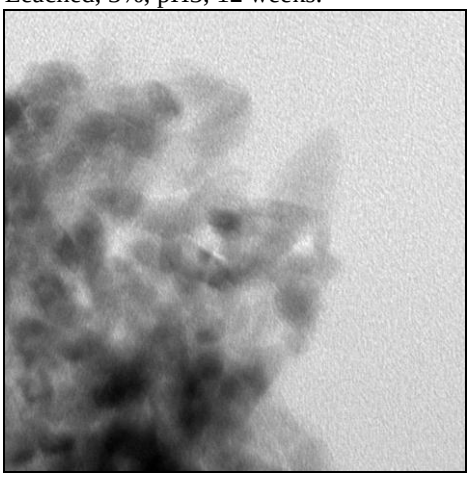

Fig. 4. Leached, 10%, pH3,12 weeks.

resulting in new cycles of growth and decay (Niederer *et al.*, 1980; Kung, 1989; Victor and Cox, 1996).

With pH10 (Figs. 5b,d) the cycles of decay and growth are reversed and less pronounced. However, the existence of maxima and minima are apparent with use of higher pH. The data suggest that at pH10 the dual combination of negatively charged hydroxide ion (OH-) and H+ (at lower concentrations) has the double capability of attacking the crystal surface and the interior bulk structure, more effectively, with minima not as deep as in the case of pH3. Inroads of OH- into the heart of the crystal releases Ti-46 from within and without – hence the plots in figures 5b,d show an initial increase in Ti-46 followed by a decline. The Ti-48, on the other hand shows a decline as these isotopes are abstracted from within the crystal structure, and their corresponding levels decrease. It is interesting to observe that in figure 5d (3% dopant) due to the diminished concentration of TiO_2 the effect is not as pronounced as that shown in figure 5b, but continued cycles of cleavage and reconstruction are still present.

From the mechanistic perspective, the ICP-MS data tend to support the hypothesis proposed by other authors that degradation of the TiO_2 structure is followed by cleavage along the planes of the crystal and atomic rearrangement (Niederer *et al.*, 1980; Kung, 1989; Victor and Cox, 1996; Häusser *et al.*, 1970). The data also support the theory that spatial arrangement of lighter Ti-46 isotopes is more probable as these are maximized on the periphery than in the interior of the bulk structure. This is logical as the heavier isotopes are needed within the crystal to provide support. If instead the interior were composed of mainly Ti-46 the crystal structure would collapse.

Kinetics/Impact of this study

The kinetics of this study is represented in figures 6 a-d and follows the same first-order format described in our previous paper (Stephen *et al.*, 2014). Inspection of figure 6 reveals that at the higher dopant level the rate of Ti-48 leaching increases with pH3 than with pH10. This suggests that at higher dopant levels the cycles of crystal cleavage and atomic re-arrangement are accelerated with higher H^+ concentration (and infiltration into the crystal bulk) leading to a steeper slope (Fig. 6a). The plot for Ti-

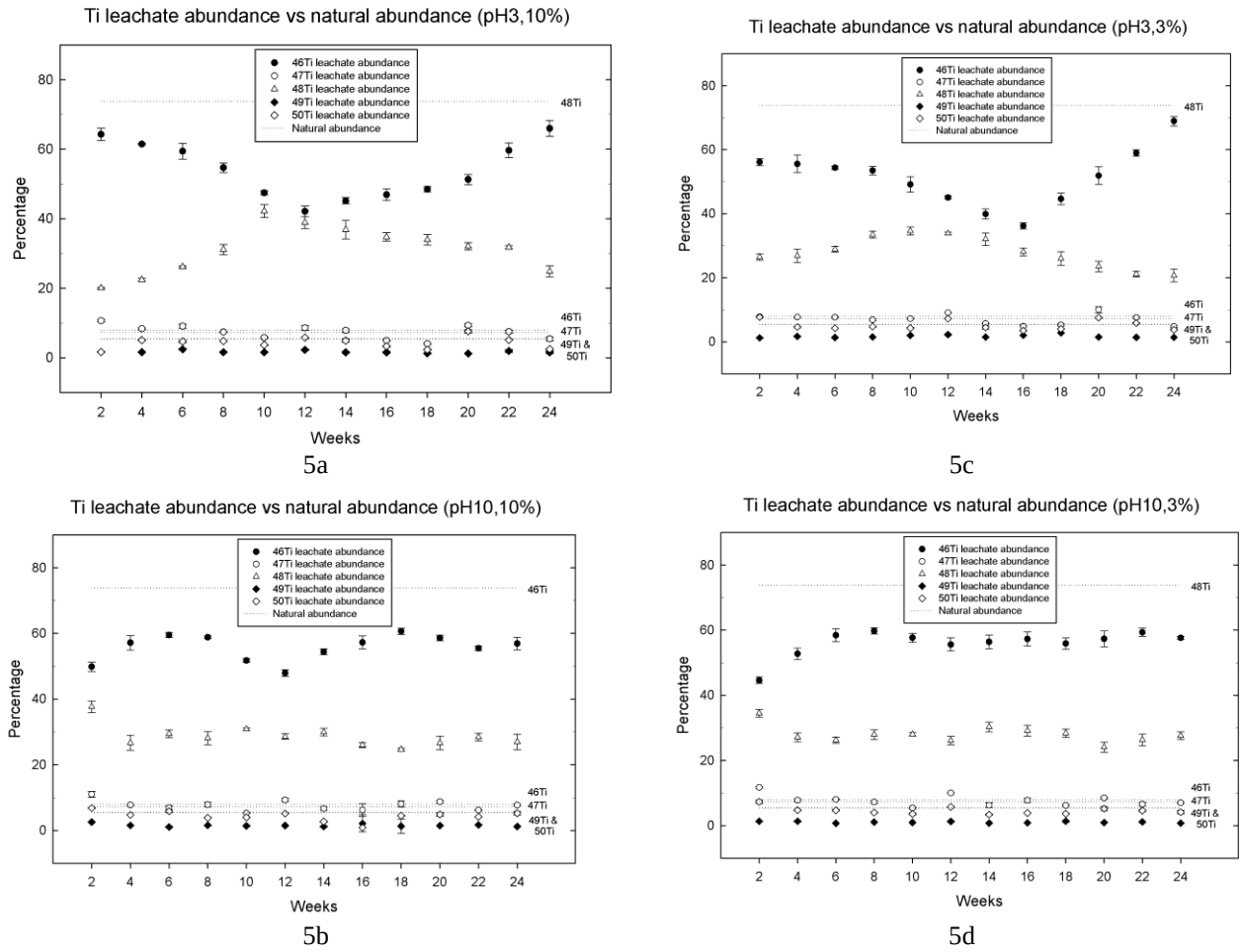

Fig. 5. a-d: Data showing cycles of growth and decay of Ti-46/ Ti-48 at pH3 and pH10.

46 is similar but less pronounced, as expected, due to lower natural abundance of this isotope. However, an interesting observation is that the levels of Ti-48 are consistently lower than those of Ti-46 supporting the theory that leaching of Ti-46 is more pronounced (but virtually constant) with constant re-arrangement of lattice structures composed predominantly of peripheral Ti-46 on the exterior of the bulk structure (Niederer *et al.*, 1980; Kung, 1989; Victor and Cox, 1996). A comparison of pH3 and pH10 (at 10%), figures 6a and 6c, reflects higher levels of Ti-48 at pH10 corroborating the view that combined OH- and H+ attack occurs as the bulk structure is infiltrated. It is important to underscore that according to the experimental data, leaching occurs with both H+ and OH-. However, the rate of leaching could be affected by interfering chemical reactions such as possible formation of titanium complexes from undesirable impurities (Stephen *et al.*, 2014). The impact of the study lies in the development of a novel facile method for production of significant enrichment of Ti-46 in solution. As suggested earlier, this enriched Ti-46 can be converted to radioactive Sc-46 for use as tracers in oil refineries (Schweitzer, 1991). Another practical application of the technique is discovery of depletion of Ti-46 in polymeric materials. This can be extended to other materials, including biomaterials, which could be used for brachytherapy treatment of prostate cancer (Ragde *et al.*, 2000).

CONCLUSION

Our study established that TiO_2 is prone to metal isotopic fractionation effects caused by acid percolation of polymeric material. We found the process to be highly pH dependent, and led to enriched Ti-46 solutions. At higher pHs the results suggested combined OH- and H+ attack of the crystal structure. Lower pHs tend to induce accelerated rates of percolation, attributed to accelerated atomic re-arrangements of the crystal structure. Cycles of growth and decay of Ti-46/Ti-48 were observed, and attributed to constant cleavage and lattice re-formation with persistent acid attack. These cycles were found to be less pronounced at higher pH due to possible chemical ramifications with dual OH- and H+ infiltration. The practical application of our study is facile production of

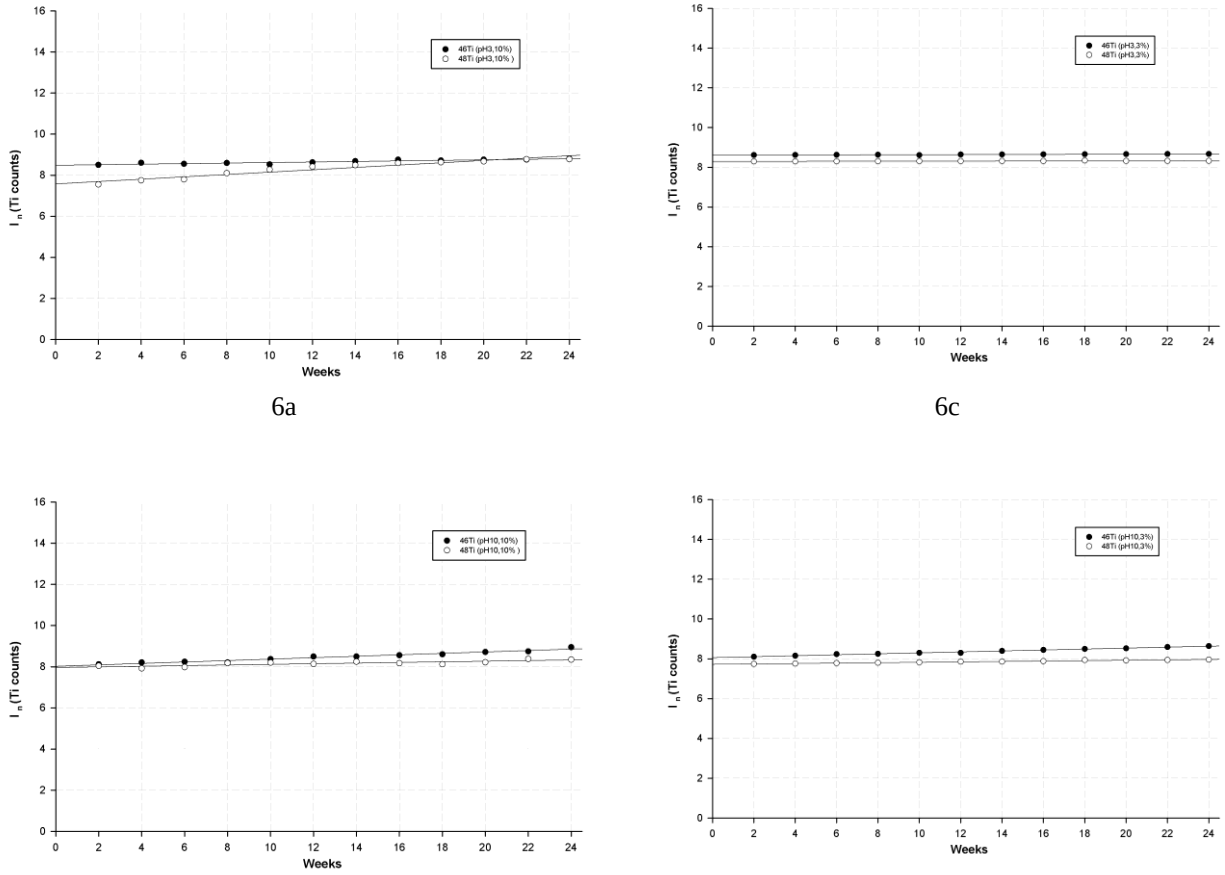

Fig. 6. a-d: Kinetic study of doped polymeric materials at pH3 and pH10.

enriched Ti-46 solutions for conversion into Sc-46 tracers for use in oil refineries (Schweitzer, 1991).

REFERENCES

Chang, H., Gautier, EA. and Zhou, L. 2014. Phase Transformation Kinetics in Metastable Titanium Alloys. Chin. Sci. Bull. 59:1773-1777.

Fujiia, T., Moynierb, F., Dauphasc, N. and Abed, M. 2011. Theoretical and experimental investigation of nickel isotopic fractionation in species relevant to modern and ancient oceans. Geochimica et Cosmochimica Acta. 75:469-482.

Häusser, O., Pelte, D., Alexander, TK. and Evans, HC. 1970. Reorientation measurements in even titanium isotopes. Nuclear Physics A. 150:417-438.

Jouvin, D., Weiss, DJ., Mason, TF., Bravin, MN., Louvat, P., Zhao, F., Ferec, F., Hinsinger, P. and Benedetti, MF. 2012. Stable Isotopes of Cu and Zn in Higher Plants: Evidence for Cu Reduction at the Root Surface and Two Conceptual Models for Isotopic Fractionation Processes. Environ. Sci. Technol. 46:2652-2266.

Kung, HH. 1989. Transition Metal Oxides: Surface Chemistry and Catalysis. (1st edi.). Elsevier, Amsterdam. 6-26.

Maria, ECMR., Paulo, RR., Carlos, AZ., Anselmo, F., José, EM., João, AM., Eduardo, SM. and Constância, PGS. 2008. Development and production of radioactive sources used for cancer treatment in Brazil NUKLEONIKA. 53:99-103.

Mondal, AN., Tripathi, BP. and Shahi, VK. 2011. Highly stable aprotic ionic-liquid doped anhydrous proton-conducting polymer electrolyte membrane for high-temperature applications. J. Mater. Chem. 21:4117-4124.

Niederer, FR., Papanastassiou, DA. and Wasserburg, GJ. 1980. Endemic Isotopic Anomalies in Titanium. The Astrophysical Journal. 240:73-77.

Pillay, AE., Vukusic, S., Stephen, S. and Abd-Elhameed, A. 2010. Rapid Ablative Laser Technique (ICP-MS) for

Monitoring Material Homogeneity in Polypropylene. Chemical Sciences Journal. 2010:1-9.

Ragde, H., Grado, GL., Nadir, B. and Abdel-Aziz, E. 2000. Modern prostate brachytherapy. A Cancer Journal for Clinicians. 50:380-393

Schweitzer, JS. 1991. Nuclear techniques in the oil industry. Nuclear Geophysics. 22.

Stephen, S., Shah, T., Pillay, AE. and Siores, E. 2014. A Study of Kinetics of Metal Leaching from Polypropylene Matrix using a Hyphenated Mass Spectrometric Technique. Candian Journal of Pure and Applied Sciences. 8(2):2925-2931.

Victor, EH. and Cox, PA. 1996. The Surface Science of Metal Oxides. Cambridge University Press, New York, USA. 14-61.

Williams, CD., Mendybaev, RA., Ushikubo, T., Bullock, ES., Janney, PE., Kita, NT., Richter, FM., MacPherson, GJ. and Wadhwa, M. 2014. 45th Lunar and Planetary Science Conference. The Woodlands, Texas, USA. p. 2146.

Williams, CK., Breyfogle, LE., Choi, SK., Nam, W., Young Jr, VG., Hillmyer, MA. and Tolman, WB. 2003. A Highly Active Zinc Catalyst for the Controlled Polymerization of Lactide. J. Am. Chem. Soc. 125:11350-11359.

Received: July 16, 2014; Accepted: Aug 19, 2014

SENRA Academic Publishers, British Columbia
Vol. 8, No. 3, pp. 2999-3003, October 2014
Online ISSN: 1920-3853; Print ISSN: 1715-9997

Canadian Journal of pure&applied sciences

EHRETIA WALLICHIANA HOOK.F. AND THOMSON EX GAMBLE REDUCES THE RISK OF BREAST CANCER

*Fatma Hashem[1], Hemaia Motawea[1], Manal Shabana[2], Mai Khalil[1] and Taha Al-Alfy[3]
[1]Department of Pharmacognosy, National Research Centre
[2]Department of Phytochemistry and Plant Systematic, National Research Centre
[3]Department of Pharmacognosy, Faculty of Pharmacy, Cairo University, Egypt

ABSTRACT

Globally researchers are agreed that diet is the single greatest contributor to human cancer, and maybe associated with 35-70% of the incidence of the disease. Although various carcinogens are present in foods, their effects are minor compared with dietary components that inhibit the cancer process. The crude extract (80% ethanol extract) of leaves of *Ehretia wallichiana* Hook. f. & Thomson ex Gamble family Borginaceae was examined for their cytotoxic activity against different cell lines. It showed higher activity against breast cancer (IC50=10 µg/mL). Petroleum ether, chloroform and ethyl acetate extracts (successive to each other), showed high activity against breast cell line. Four phenolic compounds were isolated from *Ehretia wallichiana*. Two of them are flavonoids: quercetin 3-*O*-*β*-(6"-galloyl glucopyranoside) and quercetin-3-*O*-*β*-glucopyranoside. The third is a precursor of coumarin 5-hydroxy-6-methoxybenzofuran-3-carbaldehyde and the fourth is *p*- methoxybenzoic acid (*p*-anisic acid). They were identified by their spectroscopic data.

Keywords. *Ehretia wallichiana*, phenolics, anticancer activity.

INTRODUCTION

The plants of the genus *Ehretia* Linn. is composed of about 50 species. They are mainly distributed in tropical Asia and Africa. *Ehretia* Linn. species are used in traditional Chinese herbal medicines as ethno pharmaceuticals. For example, in folklore it is used for the treatment of various ailments such as inflammation, cough, itches, swellings, pain, diarrhea, dysentery, fever, cachexia and syphilis (Iqbal *et al*., 2005).

The compounds identified in the genus mainly belong to the classes of phenolic acids, flavonoids, benzoquinones, cyanoglucosides and fatty acids. The chemical constituents of some species of *Ehretia* have been reported to be long chain aliphatic unsaturated acids (Kleiman *et al.,* 1964), baurenol (Anjaneyulu *et al.*, 1965) and allantoin (Koyama*,* 1953; Agarwal *et al*., 1980). Species of the genus *Ehretia* were reported to contain pyrrolizidine alkaloids (Suri *et al*., 1980), nitrile glucosides and rosmarinic acid with histamine-inhibitory activity (Simpol *et al*., 1994). Also, dimeric prenylbenzoquinones with antiallergic activity (Yamamura *et al*., 1995) and quinonoid xanthene with antisnake venom activity (Selvanayagam *et al*., 1996).

MATERIALS AND METHODS

Plant materials

Fresh non flowering aerial parts of *Ehretia wallichiana* Hook.f. & Thomson ex Gamble, family Boraginaceae, was collected from Giza Zoo in May 2009, Cairo, Egypt. Voucher specimen of the plant was identified by plant taxonomist Dr. M. El-Gibaly and Mrs. Trease Labib.

Total ethanol extract

Crude extract was prepared by percolating 100g dry powder of the plant with 80% ethanol until exhaustion. The filtered percolate was concentrated under reduced pressure at 40°C. It yielded a result of 22.5% w/w of solvent free extract.

Preparation of successive extracts

One kg of the air-dried powdered non flowering aerial parts of the plant was successively extracted with solvents of increasing polarities. Which were: petroleum ether, chloroform, ethyl acetate and 95% ethanol in a Soxhlet apparatus. After a complete extraction, these extracts were evaporated to dryness reduced pressure at 40°C yielding 4.48, 4.35, 1.14 and 4.85% w/w of solvent free extracts.

Isolation of flavonoids I and II

The ethanol successive extract was subjected to PC examination for the detection of flavonoids using Whatmann No. 1 sheets for developing with the two solvent systems (a) *n*-butanol - acetic acid - water (4:1: 5 v/v organic upper layer) and (b) acetic acid - water (15:85 v/v). The chromatograms were examined under UV light before and after exposure to ammonia vapour and sprayed with $AlCl_3$ solution. Spots were detected in each extract, as their R_f values in systems (a) & (b) and colors were

*Corresponding author email: fateema0@yahoo.com

being recorded. These compounds were isolated by preparative paper chromatography (PPC) on Whatmann 3MM, using solvent system (a), then purified by repeated PPC using solvent system (b). Final purification was performed on Sephadex LH-20 column and elution with methanol.

Isolation of compounds III and IV

The powdered air-dried non flowering aerial part of *Ehretia wallichiana* Hook.f. & Thomson ex Gamble (500g) was extracted with 80% ethanol in a Soxhlet apparatus. The extract was concentrated and treated with an equal volume of 10% KOH solution at room temperature for one hour to liberate potassium salt of coumarin. The alkaline alcoholic extract was diluted with water and extracted with ether. The aqueous layer was acidified with dilute HCl, refluxed for 1.5 hours, cooled and extracted with ether, whereby the ethereal extract was evaporated to dryness. The ether extract fraction was dissolved in ethanol and subjected to TLC using silica gel G60, F_{254} precoated plates, developed with benzene: ethyl acetate (8:2) and sprayed with I_2/KI reagent. Two compounds showed blue color under UV, one of which was intensified by spraying with I_2/KI reagent. Both were purified by PLC using the same solvent system and recovered from silica gel by chloroform, evaporated under reduced pressure at 40°C and then subjected to spectral analysis (MS, UV, ^{1}HNMR).

Apparatus

1- UV-Visible Spectrophotometer: UV–VIS double beam Jasco v-630.
2- Mass spectrometer: Thermo Scientific, ISQ Single Quadrupole Mass Spectrometer, an electron ionization system with ionization energy of 70eV.
3- NMR Spectrometers: Nuclear Magnetic Resonance spectrometers JEOL 500 MHz (for determination of ^{1}HNMR).

Characterization of compounds

Compound **I:** R_f values (PC): 0.52 (a), 0.32 (b). It appears as a dark spot under UV which turned yellow upon exposure to NH_3 and $AlCl_3$, on complete acid hydrolysis (2 N HCL, at 100°C for 5 hours) gave D-glucose (CoPC) in the aqueous phase, while gallic acid and quercetin were detected in the organic phase (CoPC, UV, and ^{1}HNMR spectral data).

UV:λ_{max} (MeOH): 257, 268 (sh), 356; NaOMe: 273, 325 sh, 410; $AlCl_3$: 272, 300 (sh), 413; $AlCl_3$/ HCl: 268, 295 sh, 385, 398; NaOAc: 266, 402 NaOAc/ H_3BO_3: 265, 402.

^{1}HNMR in $(CD_3)_2CO$ δ ppm 7.80 (d, *J*= 2 Hz, H-2') 7.50 (dd, *J*= 8 , 2 Hz, H- 6') 7.25 (d, *J*= 2 Hz, H-2 "and 6" of galloyl moiety) 6.90 (d, *J*= 8 Hz, H- 5'), 6.45 (d, *J*=2 Hz, H-8) 6.21 (d, *J*=2 Hz, H-6) 5.50 (d, *J*=7 Hz, H-1'"glucosyl) 5.27 (dd, *J*= 12.5 and 4.8 Hz, H- 6'"$_a$) 5.20 (dd *J*= 12.5 and 2.5 Hz, H-6'"$_b$) while glucosyl protons from 3.46- 3.60 ppm.

Compound **II:** R_f values (PC): 0.59 in (a), 0.36 in (b). It appears as a dark spot under UV, turned yellow orange upon exposure to NH_3 vapours and yellow upon exposure to $AlCl_3$. On complete acid hydrolysis it gave glucose (CoPC) and quercetin (CoPC, UV and ^{1}HNMR spectral data).

UV: λ_{max} (MeOH): 258, 270 sh, 300 sh, 360; NaOMe: 272, 328, 406; $AlCl_3$: 275, 300 sh, 330 sh, 430; $AlCl_3$/ HCl: 270, 299 sh, 365, 400; NaOAc: 269, 405; NaOAc/H_3BO_3: 263, 380.

^{1}HNMR (DMSO,d_6): δ ppm 7.53 (m, H- 2' and H- 6'), 6.80 (d, *J*= 8 Hz, H- 5'), 6.29 (d, *J*= 2 Hz, H- 8), 6.1 (d, *J*= 2 Hz, H- 6), 5.42 (d, *J*=7 Hz, H- 1'' glucosyl) while glucosyl protons (3.46- 3.80 ppm were hidden by OH groups).

Compound **III**: It was isolated as white powder at R_f0.6 in benzene: ethyl acetate, (8:2). It had violet color under UV turned to dark violet by I_2/ KI spray reagent.

UV: λ_{max} (MeOH): 274, 330.

EIMS: m/z 192 (M^+) corresponding to molecular formula $C_{10}H_8O_4$.

^{1}HNMR (DMSO- d_6): δ in ppm: 7.65 (s, H-7); 7.45 (s, H-4); 5.30 (s, H- 2); 3.60(s, OCH_3 at C-6).

Compound **IV:** It was isolated as white amorphous powder at R_f values (PC): 0.80 in (a) and 0.49 in (b). It appeared as a blue spot under UV and did not change after exposure to NH_3 vapours.

UV: λ_{max} (MeOH): 260 nm.

MS: m/z 152 (M^+ 10%), 115 (13%), 91 (22%), 77 (22%), 63 (45%), 55 (18%), 43 (40%), 27 (80%), 18 (80%) corresponding to molecular formula $C_8H_8O_3$.

^{1}H NMR(DMSO-d_6). δ ppm: 7.74 (d, *J*= 8.5 Hz, H- 2 and H-6); 6.78 (d, *J*= 8.5 Hz, H- 3 and H-5); 3.75 (s, OCH_3-4).

Investigation of cytotoxic activity of total ethanol extract of *Ehretia wallichiana* Hook.f. & Thomson ex Gamble by SRB assay

Potential cytotoxicity of the total ethanolic extract of the non flowering aerial part of the plant was tested using the method of (Skehan *et al*., 1990) SRB assay as follows:

A. The total ethanol extract of the plant was tested for cytotoxic activity against the following human tumor cell lines:

•U25l (brain tumor cell line) •MCF7 (breast carcinoma cell line)
•Hela (Cervix carcinoma cell line) •Hepg2 (Liver carcinoma cell line)

•H460 (Lung carcinoma cell line) •HCT116 (Colon carcinoma cell line)

Cells were plated in 96 - multi-well plate (10^4 cells / well) for 24 hours before treatment with the total ethanolic extract of the plant to allow attachment of the cell to the wall of the plate. Different concentrations of the extract under test (0, 1, 2.5, 5 and 10µg/mL DMSO) were added to the cell monolayer, triplicate wells being prepared for each individual dose. Monolayer cells were incubated with the total alcohol extract of the plant for 48 hours at 37°C and in atmosphere of 5% CO_2. After 48 hours cells were fixed, washed and stained with sulforhodamine B (SRB) stain (Sigma). Excess stain was washed with acetic acid and attached stain was recovered with tris-EDTA buffer (Sigma). Color intensity was measured in an ELISA reader. The relation between surviving fraction and the plant extract concentration was plotted to get the survival curve of each tumor cell line after treatment. The potency was compared with reference Cisplatin (Glaxo). The same method was repeated on the successive extracts using the cell line that showed lowest survival fraction.

RESULTS AND DISCUSSION

Identification of compounds

Compound **(I)** was isolated as light brown amorphous powder. It was found to possess chromatographic and color properties (dark spot on PC and UV light, intense blue $FeCl_3$ color reaction and a positive rose color with aqueous KIO_3 specific for galloyl esters (Barakat *et al*., 1999) and UV absorption maxima consistent with galloylated quercetin -3- glycoside (Markhams and Mohan Shari, 1982). On complete acid hydrolysis, (2N HCl at 100° C for 5 hours) yielded quercetin, gallic acid in the organic layer (CoPC, UV and ^{1}HNMR analysis) and glucose in the aqueous layer (CoPC). ^{1}HNMR spectrum in $(CD_3)_2CO$ of **(I)** exhibited the characteristic resonance pattern of quercetin, the anomeric glucose proton signal appeared as doublet (*J*= 7Hz) at δ 5.50 ppm and the galloyl protons appeared as doublet (*J*= 2 Hz) at δ 7.25 ppm. Attachment of the galloyl moiety to C- 6" of glucose has been deduced from the downfield shift of the two doublets of H- 6_a" and H- 6_b" at 5.27 and 5.20 respectively. The chemical shift values of **(I)** were in accordance with the structure of quercetin 3-*O*-*β*-(6"-galloyl glucopyranoside) (Sohretoglu *et al.*, 2009) (see Fig. 1). This represented the first report of this flavonoid galloylglucoside in *Ehretia wallichiana* Hook.f. & Thomson ex Gamble and even in the genus *Ehretia*.

Compound **(II)** was isolated as dark yellow amorphous powder, dark spot on PC, under UV light, turned orange yellow upon exposure to NH_3 vapour, and blue with $FeCl_3$ reagent. UV absorption maxima consistent with quercetin-3-*O*-glycoside (Mabry *et al.*, 1970). On complete acid hydrolysis, it yielded quercetin (CoPC, UV and ^{1}HNMR) and glucose (CoPC). ^{1}HNMR spectrum in DMSO- d_6 and UV with different shift reagents confirmed its structure as quercetin- 3-*O*-*β*-glucopyranoside (Ibrahim *et al.*, 2007) (see Fig. 2).

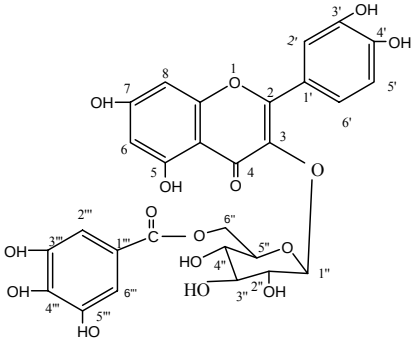

Fig. 1. quercetin 3-*O*-*β*-(6"-galloyl glucopyranoside).

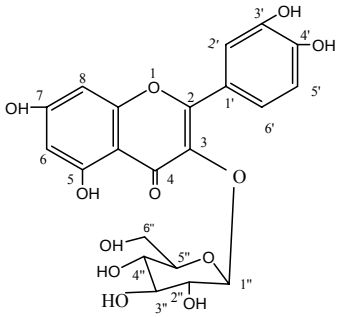

Fig. 2. quercetin- 3-*O*- *β*-glucopyranoside.

Compound (**III**): It was isolated as white powder, with violet color under UV turned to dark violet by I_2 / KI spray reagent and exhibited an UV spectrum characteristic of 5-hydroxy-6-methoxybenzofuran-3-carbaldehyde, with maxima at 274 and 330 nm^{-1}. The EIMS of the compound exhibited a molecular ion peak at m/z 192 (M^+), and its molecular formula $C_{10}H_8O_4$. The downfield signal was observed in the ^{1}HNMR spectrum at δ 7.65 ppm and was allocated to H-7 and the singlet signal at δ 7.45 ppm is for proton H-4, while H-2 appeared as singlet at δ 5.30 ppm and the methoxy group was confirmed at C-6 a singlet at δ 3.6 ppm signal. The structure of compound **(III)** has been established on the basis of its chemical, chromatographic and spectral analysis and found to be identical with 5-hydroxy-6-methoxybenzofuran-3-carbaldehyde (Fig. 3). It is a precursor of coumarin.

Compound **(IV):** The structure of compound **(IV)** was identified on the basis of its spectral data (UV, ^{1}HNMR and EI-MS) which were identical with *p*- methoxybenzoic acid (Shabana *et al.*, 2013). ^{1}HNMR proved 1, 4-disubstituted benzene structure as could be concluded from the recognized mode of splitting of the recorded proton resonances. These resonances appeared as doublet (*J*=8.5 Hz) at δ7.74 and 6.78 ppm attributed to H-2, 6 and H-3, 5, respectively. The methoxy group at position 4

Table 1. Cytotoxic activity of total 90% ethanol extract of *Ehretia wallichiana* Hook.f. & Thomson ex Gamble.

Cell line	Conc μg/mL	90% Ethanol extract		Cisplatin	
		SF	MSE	SF	MSE
Brain	10.000	0.866	0.006	0.494	0.051
Breast	10.000	0.538	0.008	No effect	-----
Cervix	10.000	0.692	0.005	0.059	0.024
Colon	10.000	0.737	0.002	No effect	-----
Liver	10.000	0.780	0.004	0.518	0.054
Lung	10.000	0.896	0.005	0.401	0.007

*SF: Survival fraction. *MSE: Mean standard error

Table 2. Cytotoxic activity of successive extracts (10 μg/mL) of Ehretia *wallichiana* Hook.f. & Thomson ex Gamble on breast cell line.

Extract	Petroleum Ether	Chloroform	Ethyl Acetate	Ethanol
Survival Fraction	0.630	0.634	0.602	0.670

appeared as singlet at δ 3.75 ppm. The positive EI-MS confirmed the structure and gave signal at m/z 153 (M^+ +H) corresponding to molecular weight (M^+) 152 and molecular formula ($C_8H_8O_3$) of 4-methoxy benzoic acid (Fig.4). Compound **(IV)** was found to be 4-methoxy benzoic acid (*p*-anisic acid).

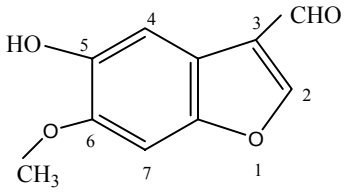

Fig. 3. 5-hydroxy-6-methoxybenzofuran-3-carbaldehyde.

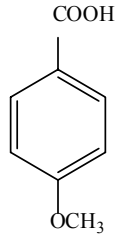

Fig. 4. *p*-methoxybenzoic acid.

Cytotoxic activity of *Ehretia wallichiana* Hook.f. & Thomson ex Gambleby SRB assay

The total ethanol extract showed strong cytotoxic activity against breast cancer cell line (IC_{50}=10 μg/mL) when compared to cisplastin as reference drug (Table 1), which was not sensitive to this cancer cell line. As the preliminary cytotoxic screening indicates that the total ethanol extract inhibited breast cancer cell line, potential cytotoxicity of the successive extracts of *Ehretia wallichiana* leaves was carried out against breast cancer cell line by the same SRB assay (Table 2). The four successive extracts (petroleum ether, chloroform, ethyl acetate and ethanol) showed nearly the same cytotoxic activity against breast cancer cell line (surviving fraction 0.630, 0.634, 0.602 and 0.670/10μg mL^{-1}), respectively. The strong *in vitro* cytotoxic activity of petroleum ether and chloroform extracts on breast carcinoma cell line may be attributed to its hydrocarbon, steroidal and terpenoidal contents. The significant cytotoxic activity of polar extracts (ethyl acetate and ethanol) could possibly attribute to their flavonoidal and phenolic contents.

CONCLUSION

Cytotoxic activity of *Ehretia wallichiana* was investigated by SRB assay against 6 cell lines. Total ethanol extract showed strong cytotoxic activity against breast cancer cell line followed by ethyl acetate extract. Phytochemical investigation of ethanolic extract resulted in isolation of four phenolic compounds which may be responsible for this cytotoxic activity. *Ehretia wallichiana* could be considered a good candidate for protection of breast cancer.

REFERENCES

Agarwal, SK., Rastogi, RP., Van Koningsveld, H., Goubitz, K. and Olthof, GJ. 1980. The molecular structure of 4a,5,8, 8a-tetrahydro-11,14-dimethoxy-7-methyl-4a-(3-methyl-2-butenyl)-5,8a-*O*-benzeno-1,4-naphthoquinone. Tetrahedron. 36:1435-1438.

Anjaneyulu, B., Roa, VB., Ganguly, AK., Govindachari, TR., Joshi, BS., Kamat, VN., Manmade, AH., Mohamed, PA., Rahmatulia, AD., Saksena, AK., Varde, DS. and Viswanathan, N. 1965. Chemical Investigation of Some Indian Plants. Indian J. Chem. 3:237.

Barakat, HH., Souleman, AM., Hussein, AM., Ibrahim, OA. and Nawwar, MAM. 1999. Flavonoid

galloylglucosides from the pods of *Acacia fornesiana*. Phytochemistry. 51:139-142.

Ibrahim, LF., El-Senousy, WM. and Hawas, UW. 2007. NMR spectral analysis of flavonoids from *Chrysanthemum coronarium*. Chem. Nat. Compd.43:659-662.

Iqbal, K., Nawaz, SA., Malik, A., Riaz, N., Mukhtar, N., Mohammad, P. and Choudhary, MI. 2005. Isolation and lipoxygenase-inhibition studies of phenolic constituents from *Ehretia obtusifolia.* Chem. Biodivers. 2:104-111.

Kleiman, R., Earle, FR. and Wolff, IA. 1964. Search for New Industrial Oils.XI. Oils of Boraginaceae. J. Am. Oil Chemistry Soc. 41:459.

Koyama. 1953. T. J. Pharm. Soc. Japan. 73:411.

Mabry, TJ., Markham, KR. and Thomas, MB. 1970. The Systematic Identification of Flavonoids. Springer, Verlag, New York, USA.

Markham, JR. 1982. Techniques of Flavonoids Identification. Academic Press, London.

Markham, KR. and Mohan Shari, V. 1982. In: Flavonoids Advances in Research. Eds. Harbone, JB. and Mabry, TJ. Chapman and Hall, London.

Selvanayagam, ZE., Gnanavendham, SG., Balakrishna, K., Rao, RB., Sivaraman, J., Subramanian, K., Puri, R. and Puri, RK. 1996. Ehretianone, a novel quinonoid xanthene from *Ehretia buxifolia* with antisnake venom activity. J. Nat. Prod. 59:664.

Shabana, MH., Hashem, FAM., Singab, AN., Khaled, S. and Farrag, AR. 2013. Protective and therapeutic activities of *Mayodendron igneum* Kurz against paracetamol induced liver toxicity in rats and its bioactive constituents. Journal of Applied Pharamaceutical Science. 3:147-155.

Simpol, LR., Otsuka, H., Ohtani, K., Kasai, R. and Yamasaki, K. 1994. Nitrile glucosides and rosmarinic acid, the histamine inhibitor from *Ehretia philippinensis*. Phytochemistry. 36:91-95.

Skehan, P., Storeng, R., Scudiero, D., Monks, A., McMahon, J., Vistica, D., Warren, JT., Bokesch, H., Kenney, S. and Boyd, MR. 1990. New colourimetric cytotoxicity assay for anticancer drug screening. J. Natl. Cancer Inst. 82:1107-1112.

Sohretoglu, D., Sakar, MK., Sabunguoglu, SA., Ozgunes, H. and Sterner, O. 2009. Antioxidant galloylated flavonoids from *Geranium tuberosum* L. sub sp. *Tuberosum*. Turkish J Chem. 33:685-692.

Suri, OP., Jamwal, SJ., Suri, KA. and Atal, CK. 1980. Ehretinine, a novel pyrrolizidine alkaloid from *Ehretia aspera*. Phytochemistry. 19:1273.

Yamamura, S., Simpol, LR., Ozawa, K., Ohtani, K., Otsuka, H., Kasai, R., Yamasuki, K. and Padolina, WG. 1995. Antiallergic dimeric prenylbenzoquinones from *Ehretia microphylla*. Phytochemistry. 39:105-110.

Received: June 2, 2014; Accepted: July 1, 2014

SENRA Academic Publishers, British Columbia
Vol. 8, No. 3, pp. 3005-3009, October 2014
Online ISSN: 1920-3853; Print ISSN: 1715-9997

Canadian Journal of pure&applied sciences

SYNTHESIS AND CHARACTERIZATION OF BIS(5-DIISOPROPYLAMINO-1,2,3,4-TETRAZOLATO)-TRIS(DIMETHYLAMIDO)DIGALLIUM: THE FIRST EXAMPLE OF A GALLIUM TETRAZOLATE COMPLEX

Issam Kobrsi
Department of Chemistry, The Petroleum Institute
PO. Box 2533, Abu Dhabi, UAE

ABSTRACT

GaN continues to be an important material for thin films and can be deposited by CVD or ALD using single source precursors that preferentially avoid Ga–C bonds. In this report, the complex bis(5-diisopropylamino-1,2,3,4-tetrazolato)tris(dimethylamido)digallium (**1**) was synthesized to potentially serve as a precursor to GaN. **1** is the first example of a Ga-tetrazolate complex, and was prepared by protonolysis of tris(dimethylamido)gallium using an equimolar amount of 5-diisopropylamino-1*H*-1,2,3,4-tetrazole. The complex was characterized spectroscopically and structurally. It exhibits a Ga_2N_2 4-membered ring, with a very close Ga–Ga distance of 2.8917(5) Å. The coordination to the tetrazolate ligand occurs at N^2, which is unusual due to N^1 being more basic. This unusual coordination is due to the steric hindrance provided by the very bulky substituent, the diisopropylamino group.

Keywords: Gallium, nitride, tetrazolate, tetrazole, bulky.

INTRODUCTION

There is continued interest in the development of gallium nitride thin films (Quah and Cheong, 2013). One of the many uses of gallium nitride and related III–V semiconductor alloys include blue and white light emitting diodes and laser diodes, electronic devices such as field effect transistors, and high-power, high-efficiency optoelectronic devices (Luo *et al*., 2004; Puchingera *et al*., 2002). The thin film deposition processing has focused on chemical vapor deposition (CVD) and molecular beam epitaxy (MBE) (Puchingera *et al*., 2002; Uhl*et al*., 2011). Approaches to GaN based on single-source precursors offer the potential for significant improvement in the growth process and film quality (Luo *et al*., 2005; Kouvetakis *et al*., 2000). For the CVD of gallium-containing films, there is interest in developing non-pyrophoric, alternative precursors to trimethyl or triethyl gallium. It is also desirable for these precursors to minimize carbon contamination. This can be achieved by the use of complexes that do not contain direct gallium–carbon bonds (Luo *et al*., 2005; Kouvetakis *et al*., 2000). Complexes can be stabilized with bulky ligands to eliminate the formation of oligomers (Luo *et al*., 2005). Tetrazoles are a group of compounds that can serve as ligands for several metal centers. They have the potential to reduce the possibility of carbon contamination when used in CVD due to the potential to form N–Ga bonds and also due to the relatively low percentage of carbon atoms in the molecule. For this reason I was interested in exploring the synthesis of gallium tetrazolate complexes.

Corresponding author email: ikobrsi@pi.ac.ae

MATERIALS AND METHODS

General Considerations
All reactions other than ligand syntheses were performed under an inert atmosphere of argon using either glovebox or Schlenk line techniques. Toluene was distilled from sodium. Tris(dimethylamido)gallium was purchased from Sigma-Aldrich and used as received.

^{1}H and ^{13}C NMR were obtained at 500 MHz and 125 MHz, respectively, in benzene-d_6. Infrared spectra were obtained using Nujol as the medium. Elemental analyses were performed in-house. Melting points were obtained on a Haake-Buchler HBI digital melting point apparatus and were uncorrected.

*Preparation of bis(5-diisopropylamino-1,2,3,4-tetrazolato)tris(dimethylamido)digallium (**1**).*
A 100 mL Schlenk flask equipped with a stir bar and a rubber septum was charged with 5-diisopropylamino-1*H*-1,2,3,4-tetrazole (tetzH) (0.516g, 3.05 mmol) and tris(dimethylamido)gallium (0.614 g, 3.04 mmol). Toluene (50 mL) was added and the resulting mixture was refluxed for 18 hours. The solvent was removed by vacuum and the identity of the crude product was verified by NMR. The product was then extracted with toluene (30 mL), filtered through a pad of Celite, and recrystallized by storing at –20°C. Complex **1** (0.687g, 69.2%) was isolated as air sensitive pale yellow crystals. Mp 132°C dec.; ^{1}H NMR (C_6D_6, 18°C, δ) 4.06 (septet, 4 H, $(CH_3)_2CH$), 2.44 (s, 24 H, $(CH_3)_2N$), 1.27 (d, 24H, $(CH_3)_2CH$); ^{13}C NMR (C_6D_6, 18°C, δ) 166.81 (s, CN_4), 47.41 (s, $(CH_3)_2CH$), 32.20 (s, $(CH_3)_2N$), 21.32 (s,

$(CH_3)_2CH$). Anal. calcd for $C_{22}H_{52}Ga_2N_{14}$: C, 40.51; H, 8.04; N, 30.07. Found: C, 41.51; H, 7.88; N, 30.67.

RESULTS AND DISCUSSION

Synthetic Aspects

I hereby report the reaction of tris(dimethylamido)gallium with 5-diisopropylamino-1*H*-1,2,3,4-tetrazole (tetzH) to produce bis(5-diisopropylamino-1,2,3,4-tetrazolato)tris (dimethylamido)digallium (**1**). TetzH was prepared from diisopropylcyanamide and sodium azide following a modified literature procedure (Fig. 1) (Koguro *et al*., 1998). **1** was synthesized by reacting 1 equivalent of tetzH with $Ga[N(CH_3)_2]_3$ in toluene under an atmosphere of argon (Fig. 2). **1** has been characterized by spectral analysis and X-ray measurements.

X-ray Crystal Structures

The X-ray crystal structure of **1** was obtained to establish the solid state configuration. Experimental crystallographic data are summarized in table 1 and selected bond lengths and angles are presented in tables 2 and 3. Representative perspective views of **1** are shown in figure 3 and figure 4. The molecular structure of **1** displays two Ga centers bridged by two dimethylamido ligands forming a Ga_2N_2 ring. The Ga–N bond distances are 1.993(2) Å and 2.012(2) Å. The N–Ga–N and Ga–N–Ga bond angles are 87.58(10)° and 92.42(10)° respectively making it almost a perfect square. Each gallium center also bears a terminal dimethylamido ligand and a terminal η^1-tetz ligand bonded through N^2.

Table 1. Experimental crystallographic data for **1**.

	1
Empirical formula	$C_{22}H_{52}Ga_2N_{14}$
Fw	652.22
Space group	P-1
a (Å)	7.2450(7)
b (Å)	8.1574(8)
c (Å)	13.7304(14)
α (deg)	94.658(2)
β(deg)	93.198(2)
γ (deg)	101.082(2)
V ($Å^3$)	791.59(14)
Z	1
λ	0.71073
Calcd (g cm^{-3})	1.368
μ (mm^{-1})	1.738
R	0.0448
Rw	0.1335

Complex **1** exhibits several interesting features. Firstly it is the first structurally characterized tetrazolato complex of gallium. The chemistry of pyrazolato and triazolato ligands with main group metallic elements is very well established (Kobrsi *et al*., 2006; Saly and Winter, 2010; Sirimanne *et al*., 2005; El-Kaderi *et al*., 2005a; El-Kaderi *et al*., 2005b; Zheng *et al*., 2004) and for no gallium tetrazolato complexes to be present in the literature

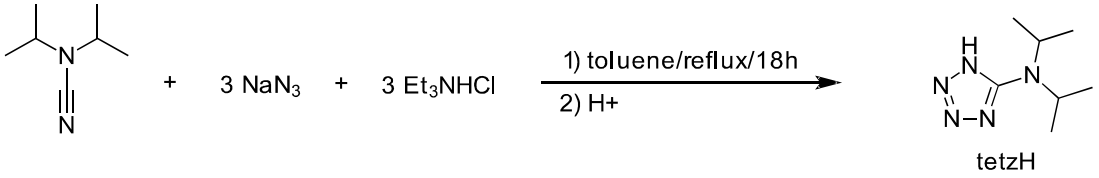

Fig. 1. Synthesis of tetzH from diisopropylcyanamide.

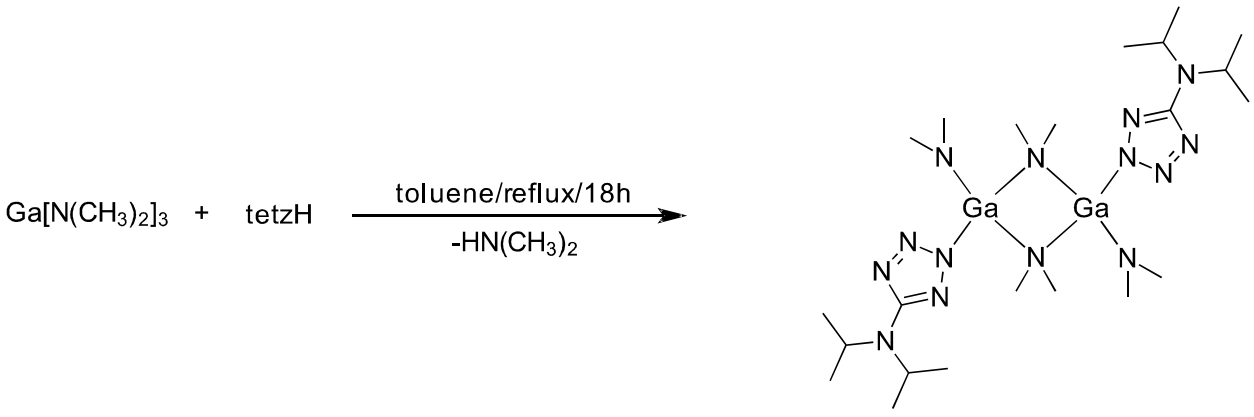

Fig. 2. Synthesis of **1**.

indicates that their synthesis is very difficult. Secondly, the Ga–Ga bond distance is 2.8917(5) Å, which puts it at the borderline of Ga–Ga covalent bond distances, generally ranging from about 2.3598(3) Å to about 2.5298(10) Å (Sanden *et al*., 2012). Thirdly, the tetrazolato ligand is coordinated through N^2 and not the more basic N^1. This is rarely observed since if sterically undemanding, the tetrazolato core would generally coordinate through N^1 or N^4 due to their higher basicity (Kobrsi *et al*., 2006; Kobrsi *et al*., 2005). When these two more basic N's are difficult to bond to due to steric hindrance such as that provided by the diisopropylamino group, the tetrazolato core will coordinate through the less basic but more accessible N^2 and N^3 (Kobrsi *et al*., 2005; Kobrsi and Bassioni, 2011). This complex has been synthesized at a scale of tens of grams, and can be purified easily by recrystallization, making it a favorable candidate for assays as a molecular precursor for CVD and/or ALD.

Table 2. Selected bond lengths (Å) for **1**.

Ga(1)–N(2)	1.814(2)	N(3)–N(4)	1.324(3)
Ga(1)–N(3)	1.948(2)	N(3)–N(6)	1.348(3)
Ga(1)–N(1)	1.993(2)	N(4)–N(5)	1.325(4)
Ga(1)–N(1)	2.012(2)	N(5)–C(5)	1.357(4)
Ga(1)–Ga(1)	2.8917(5)	C(5)–N(6)	1.339(4)
N(1)–C(1)	1.483(4)	C(5)–N(7)	1.376(4)
N(1)–C(2)	1.495(4)	N(7)–C(6)	1.473(4)
N(2)–C(3)	1.440(4)	C(6)–C(7)	1.520(5)

CONCLUSION

A gallium tetrazolato complex can be synthesized by protonolysis of tris(dimethylamido)gallium by tetzH. The complex is molecular and does not form oligomers or polymers as is common with azole-type ligands. This is due in part to the bulkiness of the diisopropylamino group, which makes the ligand sterically demanding and blocks further coordination. This steric bulk also provides for coordination at the N^2 site and not the expected N^1 site. This complex will be further studied to determine its thermal behavior, volatility, and suitability as GaN precursor.

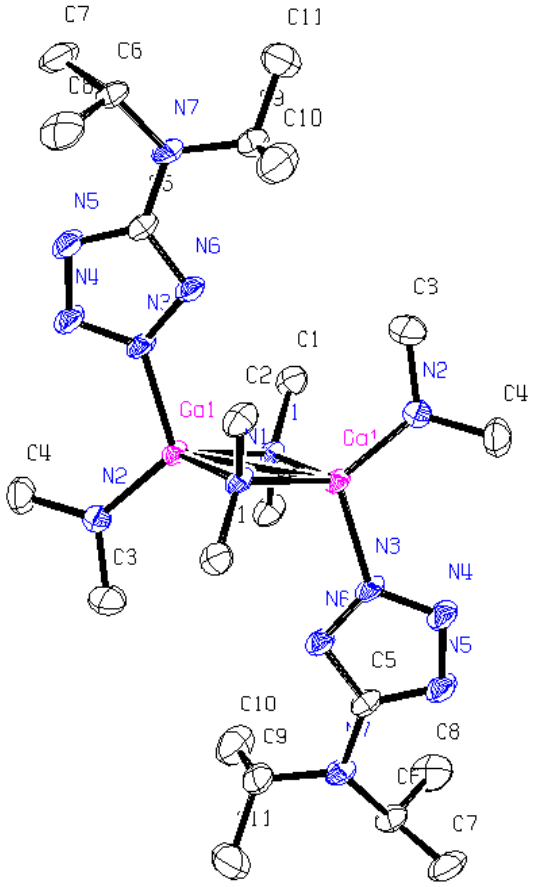

Fig. 3. Molecular structure of **1** (50% probability thermal ellipsoids).

Table 3. Selected bond angles (deg) for **1**.

N(2)–Ga(1)–N(3)	113.66(11)	C(3)–N(2)–C(4)	110.7(3)
N(2)–Ga(1)–N(1)	121.13(12)	N(4)–N(3)–N(6)	112.1(2)
N(3)–Ga(1)–N(1)	108.24(10)	N(4)–N(3)–Ga(1)	126.3(2)
N(1)–Ga(1)–N(1)	87.58(10)	N(3)–N(4)–N(5)	107.8(2)
Ga(1)–N(1)–Ga(1)	92.42(10)	N(4)–N(5)–C(5)	105.5(2)
C(1)–N(1)–Ga(1)	115.22(18)	N(6)–C(5)–N(5)	112.2(3)
C(3)–N(2)–Ga(1)	123.9(2)	N(6)–C(5)–N(7)	123.8(3)
C(1)–N(1)–C(2)	106.8(2)	C(5)–N(7)–C(6)	119.1(3)

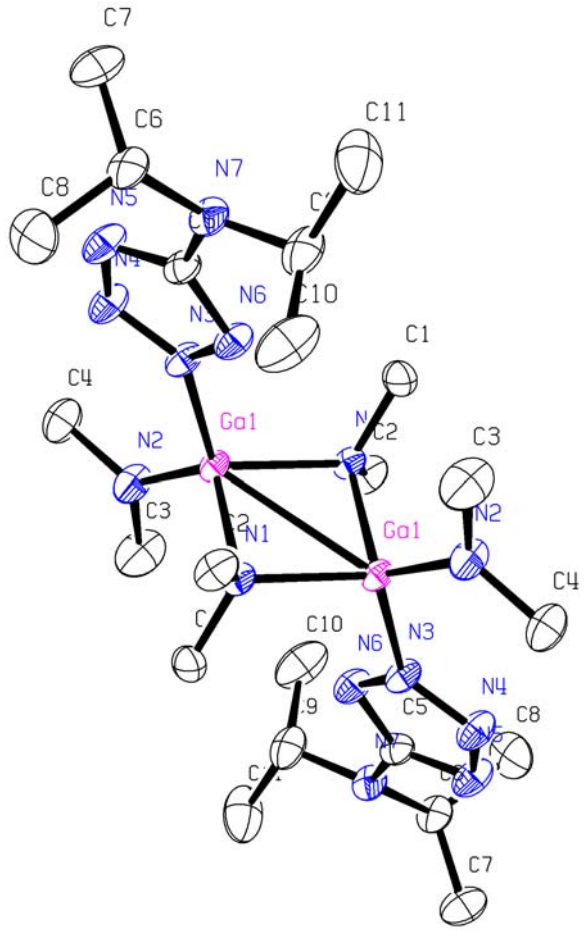

Fig. 4. Molecular structure of **1** with a clear view of the Ga_2N_2 diazametallacyclobutane (50% probability thermal ellipsoids).

ACKNOWLEDGMENTS

The author is grateful for funding from the Petroleum Institute (RIFP Grant No. 13329).

REFERENCES

El-Kaderi, HM., Heeg, MJ. and Winter, CH. 2005. Synthesis, Structure, and Ligand Redistribution Equilibria of Mixed Ligand Complexes of the Heavier Group 2 Elements Containing Pyrazolato and β-Diketiminato Ligands. European Journal of Inorganic Chemistry. (11):2081-2088.

El-Kaderi, HM., Heeg, MJ. and Winter, CH. 2005. Synthesis, structure and properties of monomeric strontium and barium complexes containing terminal η^2-3,5-di-tert-butylpyrazolato ligands. Polyhedron. 24(5): 645-53.

Kobrsi, I. and Bassioni, G. 2011. Bis(l,5-diisopropylamino-1,2,3,4-tetrazolido-K^2N^2:N^3)bis[(triiso propylphosphane)copper(I)]. Acta Crystallographica. E67:975-976.

Kobrsi, I., Knox, JE., Heeg, MJ., Schlegel, HB. and Winter, CH. 2005. Weak Carbon-Hydrogen-Nitrogen Interactions Affect the Heterocyclic Ligand Bonding Modes in Barium Complexes Containing η^2-Tetrazolato and η^2-Pentazolato Ligands. Inorganic Chemistry. 44(14):4894-4896.

Kobrsi, I., Zheng, W., Knox, JE., Heeg, MJ., Schlegel, HB. and Winter, CH. 2006. Experimental and Theoretical Study of the Coordination of 1,2,4-Triazolato, Tetrazolato, and Pentazolato Ligands to the $[K(18\text{-crown-}6)]^+$ Fragment. Inorganic Chemistry. 45(21):8700-8710.

Koguro, K., Oga, T., Mitsui, S. and Orita, R. 1998. Novel Synthesis of 5-Substituted Tetrazoles from Nitriles. Synthesis. (6):910-914.

Kouvetakis, J., McMurran, J., Steffek, C., Groy, TL. and Hubbard, JL. 2000. Synthesis and Structures of Heterocyclic Azidogallanes $[(CH_3)ClGaN_3]_4$ and $[(CH_3)BrGaN_3]_3$ en Route to $[(CH_3)HGaN_3]_x$: An Inorganic Precursor to GaN. Inorganic Chemistry. 39:3805-3809.

Luo, B., Kucera, BE. and Gladfelter, WL. 2005. Mono- and digallane complexes of a tridentate amido-diamine ligand. Chemical Communications. (27):3463-3465.

Luo, B., Lee, SY. and White, JM. 2004. Adsorption, Desorption, and Reaction of a Gallium Nitride Precursor, $(H_2GaNHNMe_2)_2$, on HfO_2. Chemistry of Materials. 16:629-638.

Puchingera, M., Kisailusb, DJ., Langeb, FF. and Wagner, T. 2002. Microstructural evolution of precursor-derived gallium nitride thin films. Journal of Crystal Growth. 245:219-227.

Quah, HJ. and Cheong, KY. 2013. Surface Passivation of Gallium Nitride by Ultrathin RF-Magnetron Sputtered Al_2O_3 Gate. ACS Applied Materials and Interfaces. 5:6860-6863.

Saly, MJ. and Winter, CH. 2010. Highly Distorted K^3-N,N,H Bonding of Bis(3,5-di-tert-butylpyrazolyl)borate Ligands to the Heavier Group 2 Elements. Organometallics. 29:5472-5480.

Sanden, T., Gamer, MT., Fagin, AA., Chudakova, VA., Konchenko, SN., Fedushkin, IL. and Roesky, PW. 2012. Synthesis of Unsupported Ln-Ga Bonds by Salt Metathesis and Ga-Ga Bond Reduction. Organometallics. 31:4331-4339.

Sirimanne, CT., Zheng, W., Yu, Z., Heeg, MJ. and Winter, CH. 2005. Synthesis, Structure, and Bridge-Terminal Exchange Kinetics of Pyrazolate-Bridged Digallium and Diindium Complexes Containing Bridging Phenyl Groups. Organometallics. 24:6184-6193.

Uhl, W., Layh, M. and Rezaeirad, B. 2011. Aluminum, Gallium, and Indium Hydrazides and the Generation of Oligonuclear Element-Nitrogen Cages: Molecular Intermediates on the Way to Element Nitrides. Inorganic Chemistry. 50:12275-12283.

Zheng, W., Heeg, MJ. and Winter, CH. 2004. Synthesis and Characterization of Potassium Complexes Containing Terminal η^2-Pyrazolato Ligands. European Journal of Inorganic Chemistry. (13):2652-2657.

Received: May 24, 2014; Accepted: July 4, 2014

SENRA Academic Publishers, British Columbia
Vol. 8, No. 3, pp. 3011-3018, October 2014
Online ISSN: 1920-3853; Print ISSN: 1715-9997

Canadian Journal of pure&applied sciences

LEVELS OF HEAVY METALS (CADMIUM, CHROMIUM, COPPER AND LEAD) ON WATER AND SELECTED TISSUES OF *OREOCHROMIS MOSSAMBICUS* FROM DIFFERENT LOCATIONS OF MALIR RIVER, KARACHI

*Raheela Sharmeen, M Zaheer Khan, Ghazala Yasmeen and Syed Ali Ghalib
Department of Zoology (Wildlife Section), University of Karachi, Karachi-75270

ABSTRACT

Heavy metals (Cd, Cr, Cu and Pb) concentrations were determined in surface and deep water samples along with their accumulation in tissues of the fish *Oreochromis mossambicus* from Malir River. Water and fish samples were collected from four locations (Murad Memon Goth, Malir City, Shah Faisal Colony and Qayumabad) of Malir River. Heavy metals concentrations in water and the fish were analyzed by using atomic absorption spectrophotometer. Heavy metal concentration in surface and deep water samples were found in order Cr>Cu>Pb>Cd and in the fish these were in the order Pb>Cu>Cr>Cd. In fish, Cd and Pb concentrations were found higher in gill samples while Cr and Cu concentrations were higher in liver samples, whereas gonads appeared to be the least preferred site for the bioaccumulation of metals. The concentrations of water samples were found to be above the values recommended by FAO/WHO (1993), NEQS (1993) and JECFA (2000) and in fish samples the concentrations of Cr, Cu and Pb were found to be higher than those recommended by WHO (1985), FEPA (2003) and FAO (1983) in fish food.

Keywords: Malir River, heavy metals, bioaccumulation, *Oreochromis mossambicus*.

INTRODUCTION

Freshwater contamination has become a matter of concern over the last few decades (Canli and Kalay, 1998; Dirilgen, 2001; Vutukuru, 2005; Vinodhini and Narayanan, 2008). Among most of the pollutants discharged into the aquatic environment, heavy metals are regarded as one of the most serious pollutants due to their environmental persistence and tendency to accumulate in aquatic environment (Schüürmann and Markert, 1998; Edem *et al*., 2008; Amisah *et al*., 2009; Benzer *et al*., 2013). Heavy metals are known as high density metallic elements or stable metals with density greater than 5.00 to 6.00 g/cm³, which may have hazardous effects on plant and animal ecosystems when present in high concentrations than found naturally (Keepax *et al*., 2011). Heavy metals can be categorized as potentially toxic (aluminiun, arsenic, cadmium, antimony, lead and mercury), semi-essential (nickel, vanadium, cobalt) and essential [copper, zinc, selenium, manganese, iron, etc] (Szentmihalyi and Then, 2007). These essential metals can also cause toxic effects when taken in excessive amounts (Tüzen, 2003; Ellias, 2009). Fishes are most important organisms in the aquatic food chain, which are sensitive to heavy metals contamination, thus fish not only indicate the pollution status of aquatic ecosystem but have significant impact on the food web (Chi *et al*., 2007). Fishes are one of the main sources of protein-enriched food all over the world (Mansour and Sidky, 2002). Consumption of fish contaminated with heavy metals can have hazardous effects on human health (Mai *et al*., 2006). Various studies have been conducted on heavy metal bioaccumulation in the muscle tissues of fish collected from different freshwater aquatic systems in relation to their concentrations in water (Ebrahimpour and Mushrifah, 2008; Batvari *et al*., 2008; Raja *et al*., 2009; Biswas *et al*., 2011).

The objective of the present study was to determine the occurrence and levels of some selected heavy metals (cadmium, chromium, copper and lead) in surface and deep water samples including their accumulation in selected tissues i.e. gills, gonads, liver and muscles of the fish, *Oreochromis mossambicus* collected from four different locations of Malir River (Murad Memon Goth, Malir City, Shah Faisal Colony and Qayumabad) within Karachi.

MATERIALS AND METHODS

Sampling Sites

For the collection of samples four different locations of Malir River were selected viz. (1) Murad Memon Goth (2) Malir City (3) Shah Faisal Colony and (4) Qayumabad.

Preservation of the Samples

The water samples (both surface and deep) and the samples of the fish, *Oreochromis mossambicus* were collected monthly from all four locations during the whole study period from January to December 2010. The water samples were collected with the help of ruttner

*Corresponding author email: raheela_sharmeen@yahoo.com

Table 1. Average concentrations (ppm) of Cd, Cr, Cu and Pb in surface water samples at Locations 1-4.

Locations	Data Analysis	Cadmium	Chromium	Copper	Lead
Murad Memon Goth	Average Values (ppm) ± SD	0.027 ± 0.005	0.706 ± 0.010	0.286 ± 0.010	0.396 ± 0.014
	Max. and Min. conc.(ppm)	0.030 - 0.020	0.720 - 0.690	0.300 - 0.260	0.420 - 0.380
	95 % Confidence Limit	0.024 - 0.030	0.700 - 0.712	0.281 - 0.300	0.387 - 0.405
Malir City	Average Values (ppm) ± SD	0.029 ± 0.003	1.059 ± 0.011	0.675 ± 0.018	0.755 ± 0.005
	Max. and Min. conc.(ppm)	0.030 - 0.020	1.080 - 1.050	0.700 - 0.650	0.760 - 0.750
	95 % Confidence Limit	0.030 - 0.031	1.052 - 1.110	0.664 - 0.690	0.752 - 0.758
Shah Faisal Colony	Average Values (ppm) ± SD	0.054 ± 0.005	1.245 ± 0.010	0.995 ± 0.005	0.646 ± 0.005
	Max. and Min. conc.(ppm)	0.060 - 0.050	1.260 - 1.220	1.000 - 0.990	0.650 - 0.646
	95 % Confidence Limit	0.051 - 0.060	1.241 - 1.251	0.992 - 1.000	0.643 - 0.649
Qayumabad	Average Values (ppm) ± SD	0.056 ± 0.007	0.937 ± 0.012	0.579 ± 0.012	0.523 ± 0.005
	Max. and Min. conc.(ppm)	0.070 - 0.050	0.950 - 0.920	0.590 - 0.560	0.530 - 0.520
	95 % Confidence Limit	0.052 - 0.060	0.931 - 0.944	0.568 - 0.583	0.520 - 0.526

water sampler and were kept into separate 1 liter tightly packed clean and previously washed rubber bottles (after acidification) and labeled for metals analysis. Fish were captured with the help of gill net and hand net and were kept in clean polythene bags and kept chilled in an ice box.

Preparation and Analysis of Samples

The Whattman filter paper No. 40 was used to filter water samples and the fish were washed with plenty of cold water and taken to laboratory to dissect gills, gonads, liver and muscles for metal analysis. All the tissues were wrapped in aluminum foil separately for complete dryness in a heating oven at 40-50°C upto constant weight. These dried samples and filtered water samples were digested as follows:

Acid digestion of water samples was done according to EPA (1976). 100ml of homogenized samples were taken in a beaker. Three ml of concentrated Analar grade HNO_3 was added. The beaker was placed on hot plate and evaporated to dryness. It was made sure that sample should not boil, then it was cooled and further addition of 3 ml of concentrated HNO_3 was made. Again, the beaker was put on a hot plate. The temperature of hot plate was increased for the occurrence of gentle reflux action. Heating was continued with addition of some more acid as when needed, until the digestion was completed (indicated by light colored residue). Sufficiently distilled 1:1 HCl was added and warmed to dissolve the residue and the sample was filtered to remove silicates and other insoluble materials which may clog the capillary of atomizer. Finally, volumes were adjusted on the basis of expected metal concentration.

Acid digestion of tissue samples was performed according to Benton (1988). Around 0.500 g of dried tissues were transferred to a beaker and 2.5 ml concentrated HNO_3 was added, and it was allowed to stand overnight while covered, then it was placed on hot plate at 80°C for one hour again, then cooled and 2.5 ml perchloric acid ($HClO_4$) was added. Covered beaker was placed on hotplate and digested at 180-200°C for 2-3 hours or till clear solution was obtained. The beaker was uncovered and heated at 80°C till removal of fumes. Then it was taken off hotplate and cooled. Little amount of deionized water was added and transferred to volumetric flask. Final volume was made up with distilled water.

Preparation of Standard Solutions

All working standards were prepared by subsequent dilution of available stock reference solution having 1000ppm metal in 5N HNO_3.

Procedure

Standards and samples were analyzed by aspirating into Atomic absorption spectrophotometer (Perkin Elmer AA 3100) for Cd, Cr, Cu and Pb using Hollow Cathode lamps at air acetylene flame.

RESULTS AND DISCUSSION

Analysis of Water Samples

In the surface water samples from Location No. 1 (Murad Memon Goth), the average concentrations of Cd, Cr, Cu and Pb were 0.027±0.005, 0.706±0.010, 0.286±0.010 and 0.396±0.014 ppm, respectively (Table 1). While the average concentrations of Cd, Cr, Cu and Pb in deep water samples were 0.018±0.004, 0.640±0.013, 0.308±0.009 and 0.398±0.013 ppm, respectively (Table 2).

It was measured that in surface water samples from Location No. 2 (Malir City), the average concentrations of Cd, Cr, Cu and Pb were 0.029±0.003, 1.059±0.011, 0.675±0.018 and 0.755±0.005 ppm, respectively (Table 1), while in deep water samples, the average concentrations of Cd, Cr, Cu and Pb were 0.028±0.005, 1.003±0.014, 0.575±0.016 and 0.818±0.006 ppm, respectively (Table 2).

Table 2. Average concentrations (ppm) of Cd, Cr, Cu and Pb in deep water samples at Locations 1-4.

Locations	Data Analysis	Cadmium	Chromium	Copper	Lead
Murad Memon Goth	Average Values (ppm) ± SD	0.018 ± 0.004	0.640 ± 0.013	0.308 ± 0.009	0.398 ± 0.013
	Max. and Min. conc.(ppm)	0.020 - 0.010	0.650 - 0.620	0.320 - 0.300	0.420 - 0.380
	95 % Confidence Limit	0.016 - 0.021	0.632 - 0.648	0.302 - 0.313	0.389 - 0.406
Malir City	Average Values (ppm) ± SD	0.028 ± 0.005	1.003 ± 0.014	0.575 ± 0.016	0.818 ± 0.006
	Max. and Min. conc.(ppm)	0.030 - 0.020	1.020 - 0.980	0.600 - 0.550	0.820 - 0.800
	95 % Confidence Limit	0.025 - 0.030	0.994 - 1.011	0.565 - 0.585	0.814 - 0.821
Shah Faisal Colony	Average Values (ppm) ± SD	0.053 ± 0.005	1.208 ± 0.008	1.001 ± 0.029	0.695 ± 0.008
	Max. and Min. conc.(ppm)	0.060 - 0.050	1.220 - 1.200	1.050 - 0.950	0.710 - 0.680
	95 % Confidence Limit	0.050 - 0.055	1.203 - 1.214	0.983 - 1.019	0.690 - 0.700
Qayumabad	Average Values (ppm) ± SD	0.052 ± 0.007	0.961 ± 0.033	0.584 ± 0.014	0.618 ± 0.006
	Max. and Min. conc.(ppm)	0.060 - 0.040	1.010 - 0.900	0.600 - 0.560	0.620 - 0.600
	95 % Confidence Limit	0.047 - 0.056	0.940 - 0.982	0.575 - 0.593	0.614 - 0.621

It was calculated that in surface water samples from Location No. 3 (Shah Faisal Colony), the average concentrations of Cd, Cr, Cu and Pb were 0.054±0.005, 1.245±0.010, 0.995±0.005 and 0.646±0.005 ppm, respectively (Table 1), while the average concentrations of Cd, Cr, Cu and Pb in deep water samples were 0.053±0.005, 1.208±0.008, 1.001±0.029 and 0.695±0.008 ppm, respectively (Table 2).

In surface water samples from Location No. 4 (Qayumabad), the average concentrations of Cd, Cr, Cu and Pb were 0.056±0.007, 0.937±0.012, 0.576±0.012 and 0.523±0.005 ppm, respectively (Table 1), while the average concentrations of Cd, Cr, Cu and Pb in deep water samples were 0.052±0.007, 0.961±0.033, 0.584±0.014 and 0.618±0.006 ppm, respectively (Table 2).

In freshwater, cadmium is generally present in concentrations of between 0.1 and 10µg/l (Friberg *et al*., 1974). The maximum acceptable concentration of cadmium in drinking water is 0.005 mg/l (5 µg/l) (FAO/WHO, 1993) this value was lowered to 0.003 mg/l in the 1993 Guidelines, based on the PTWI set by JECFA (JECFA, 2000). While in the present work, the highest cadmium concentration in surface water samples was found 0.056±0.007 ppm at Qayumabad followed by 0.054±0.005 at Shah Faisal Colony whereas the lowest concentration were observed as 0.027±0.005 at Murad Memon Goth. Thus, the values recorded at all study areas in surface and deep water samples were found above the acceptable limits of cadmium in drinking water prescribed by FAO/WHO (1993) and JECFA (2000).

Chromium (Cr) is a relatively scarce metal, the occurrence and amounts in aquatic ecosystems is generally very low i.e. 0.001 to 0.002 mg/l (Moore and Ramamoorthy, 1984; Kupchella and Hyland, 1993; DWAF, 1996). The concentration of Cr was found in the ranges of 0.0001-0.0082 µg/l and 3.62-41.81 µg/l in industrial effluents of NWFP and ground water of Korangi industrial area (KIA) Karachi, respectively (Iqbal *et al*., 1998; Mahmood *et al*., 1998). While in present study, chromium had high concentration level in surface and deep water samples i.e. 1.245±0.010 ppm and 1.208±0.008 ppm, respectively at Shah Faisal Colony. The chromium concentrations were found higher i.e. 0.961±0.033 ppm in deep water samples and 0.937±0.012 ppm in surface water samples at Qayumabad. The values observed as 1.059±0.011 ppm and 1.245±0.010 ppm at Malir City and Shah Faisal Colony exceed the permissible limits of chromium i.e. 1.00 mg/l set by NEQS (1993). Thus the values of all samples at all study areas were found above the prescribed range of chromium in drinking water i.e. 0.05 mg/l set for Cr (WHO, 1996).

Copper is one of the most abundant trace metal and an essential micronutrient for almost all organisms (Duffus, 1980). Natural concentrations of copper in surface water are at <5 mg/l (Alabaster and Lloyd, 1980). In the present work, the concentration of copper in surface and deep water samples had high concentrations level i.e. 0.995±0.005 and 1.001±0.029 ppm at Shah Faisal Colony whereas in deep water samples the copper concentration levels of 0.584±0.014 ppm were recorded higher as compared to surface water samples i.e. 0.579±0.012 at Qayumabad. Thus the samples obtained from all study areas were found under the permissible concentration of copper in drinking water i.e. 2 mg/l set by WHO (1996), whereas the copper concentrations in deep water samples at Shah Faisal Colony i.e. 1.001±0.029 ppm were found above the desirable level i.e. 1.0 mg/l recommended by NEQS (1993).

Lead (Pb) is a general toxicant and a cumulative poison which is present in water to some extent as a result of its dissolution from natural sources, but the excessive lead may be primarily from house hold plumbing. Several

Table 3. Average concentrations (ppm) of Cd, Cr, Cu and Pb in the gills of *Oreochromis mossambicus* at Locations 1-4.

Locations	Data Analysis	Cadmium	Chromium	Copper	Lead
Murad Memon Goth	Average Values (ppm) ± SD	0.368 ± 0.011	0.803 ± 0.011	0.942 ± 0.009	3.082 ± 0.009
	Max. and Min. conc.(ppm)	0.380 - 0.350	0.820 - 0.780	0.950 - 0.920	3.090 - 3.060
	95 % Confidence Limit	0.360 - 0.374	0.795 - 0.810	0.936 - 0.948	3.076 - 3.088
Malir City	Average Values (ppm) ± SD	0.650 ± 0.010	1.220 ± 0.013	2.696 ± 0.010	4.096 ± 0.011
	Max. and Min. conc.(ppm)	0.680 - 0.640	1.240 - 1.200	2.710 - 2.680	4.110 - 4.080
	95 % Confidence Limit	0.643 - 0.666	1.211 - 1.229	2.690 - 2.702	4.089 - 4.102
Shah Faisal Colony	Average Values (ppm) ± SD	0.818 ± 0.008	1.472 ± 0.011	3.979 ± 0.013	3.935 ± 0.016
	Max. and Min. conc.(ppm)	0.830 - 0.800	1.480 - 1.450	4.000 - 3.960	3.950 - 3.900
	95 % Confidence Limit	0.813 - 0.823	1.464 - 1.479	3.971 - 3.998	3.925 - 3.945
Qayumabad	Average Values (ppm) ± SD	0.277 ± 0.010	1.079 ± 0.010	2.478 ± 0.017	2.289 ± 0.016
	Max. and Min. conc.(ppm)	0.290 - 0.200	1.090 - 1.060	2.500 - 2.450	2.310 - 2.260
	95 % Confidence Limit	0.270 - 0.283	1.073 - 1.085	2.467 - 2.488	2.279 - 2.299

Table 4. Average concentrations (ppm) of Cd, Cr, Cu and Pb in the gonads of *Oreochromis mossambicus* at Locations 1-4.

Locations	Data Analysis	Cadmium	Chromium	Copper	Lead
Murad Memon Goth	Average Values (ppm) ±SD	0.023 ± 0.005	0.204 ± 0.014	0.071 ± 0.009	0.286 ± 0.011
	Max. and Min. conc.(ppm)	0.030 - 0.020	0.220 - 0.180	0.080 - 0.060	0.300 - 0.260
	95 % Confidence Limit	0.020 - 0.025	0.195 - 0.213	0.065 - 0.0766	0.279 - 0.292
Malir City	Average Values (ppm) ±SD	0.027 ± 0.005	0.243 ± 0.008	0.096 ± 0.007	0.506 ± 0.010
	Max. and Min. conc.(ppm)	0.030 - 0.020	0.250 - 0.230	0.100 - 0.080	0.520 - 0.489
	95 % Confidence Limit	0.0235 - 0.030	0.238 - 0.248	0.0916 - 0.100	0.500 - 0.512
Shah Faisal Colony	Average Values (ppm) ±SD	0.032 ± 0.006	0.243 ± 0.020	0.112 ± 0.006	0.389 ± 0.011
	Max. and Min. conc.(ppm)	0.040 - 0.020	0.300 - 0.220	0.120 - 0.100	0.400 - 0.370
	95 % Confidence Limit	0.028 - 0.035	0.230 - 0.255	0.108 - 0.115	0.382 - 0.396
Qayumabad	Average Values (ppm) ±SD	0.028 ± 0.004	0.168 ± 0.013	0.088 ± 0.005	0.308 ± 0.006
	Max. and Min. conc.(ppm)	0.030 - 0.020	0.180 - 0.150	0.090 - 0.080	0.320 - 0.300
	95 % Confidence Limit	0.026 - 0.031	0.160 - 0.176	0.085 - 0.090	0.305 - 0.312

scientists reported the concentration of Pb in the following ranges, 0.0-0.52, 0.0-0.6, 0.013-0.16, 0.0-0.00083 mg/l and 6.97-30.73 µg/l, respectively (Ipinmoroti, 1993; Khan *et al*., 1995; Tariq *et al*., 1996; Iqbal *et al*., 1998; Mahmood *et al*., 1998). While in present study the highest concentrations level of lead in surface water samples were recorded as 0.755±0.005 ppm at Malir City. In the deep water samples the lead concentrations were recorded higher as compared to surface water samples from all study areas. All the samples collected from all study areas exceeded the guideline value of cadmium in drinking water i.e. 0.01mg/l set by WHO (1996) and the desirable level i.e. 0.5 mg/l set by NEQS (1993).

Analysis of Heavy Metals in Fish Tissues

Heavy metal contamination has been reported in aquatic organisms and considered to be serious pollutants inducing their toxic effects on aquatic fauna (Farkas *et al*., 2002).

The present work was carried out on fish *Oreochromis mossambicus* because this indigenous South African species is relatively easy to manage, accessible throughout the year, inexpensive and serves as an excellent indicator of water quality and on large scale serves by local inhabitants.

In the samples from Location No. 1 (Murad Memon Goth), the average concentrations of Cd, Cr, Cu and Pb in gills samples were 0.368±0.011, 0.803±0.011, 0.942±0.009 and 3.082±0.009 ppm, respectively (Table 3), while the average concentrations of Cd, Cr, Cu and Pb in gonads samples were 0.023±0.005, 0.204±0.014, 0.071±0.009 and 0.286±0.011 ppm, respectively (Table 4). The average concentrations of Cd, Cr, Cu and Pb in liver samples were 0.160±0.010, 0.999±0.008, 5.073±0.010 and 1.713±0.008 ppm, respectively (Table 5), while the average concentrations of Cd, Cr, Cu and Pb in muscles samples were 0.045±0.005, 0.193±0.009, 0.224±0.008 and 0.452±0.007 ppm, respectively (Table 6).

Table 5. Average concentrations (ppm) of Cd, Cr, Cu and Pb in the liver of *Oreochromis mossambicus* at Locations 1-4.

Locations	Data Analysis	Cadmium	Chromium	Copper	Lead
Murad Memon Goth	Average Values (ppm) ±SD	0.160 ± 0.010	0.999 ± 0.008	5.073 ± 0.010	1.713 ± 0.008
	Max. and Min. conc.(ppm)	0.180 - 0.150	1.010 - 0.990	5.080 - 5.050	1.720 - 1.700
	95 % Confidence Limit	0.153 - 0.167	0.994 - 1.004	5.066 - 5.079	1.708 - 1.717
Malir City	Average Values (ppm) ±SD	0.175 ± 0.008	2.095 ± 0.011	3.643 ± 0.014	3.012 ± 0.008
	Max. and Min. conc.(ppm)	0.190 - 0.160	2.120 - 2.080	3.660 - 3.620	3.020 - 3.000
	95 % Confidence Limit	0.170 - 0.180	2.088 - 2.101	3.633 - 3.652	3.006 - 3.017
Shah Faisal Colony	Average Values (ppm) ±SD	0.222 ± 0.007	2.358 ± 0.005	5.076 ± 0.012	2.096 ± 0.007
	Max. and Min. conc.(ppm)	0.230 - 0.210	2.360 - 2.350	5.090 - 5.050	2.110 - 2.090
	95 % Confidence Limit	0.217 - 0.226	2.354 - 2.360	5.068 - 5.083	2.091 - 2.100
Qayumabad	Average Values (ppm) ±SD	0.113 ± 0.008	1.333 ± 0.013	2.063 ± 0.010	1.816 ± 0.007
	Max. and Min. conc.(ppm)	0.120 - 0.100	1.350 - 1.320	2.080 - 2.050	1.820 - 1.800
	95 % Confidence Limit	0.109 - 0.118	1.324 - 1.341	2.056 - 2.069	1.812 - 1.820

Table 6. Average concentrations (ppm) of Cd, Cr, Cu and Pb in the muscles of *Oreochromis mossambicus* at Locations 1-4.

Locations	Data Analysis	Cadmium	Chromium	Copper	Lead
Murad Memon Goth	Average Values (ppm) ±SD	0.045 ± 0.005	0.193 ± 0.009	0.224 ± 0.008	0.452 ± 0.007
	Coefficient of Variation (%)	0.050 - 0.040	0.200 - 0.180	0.230 - 0.210	0.460 - 0.440
	95 % Confidence Limit	0.042 - 0.048	0.187 - 0.198	0.219 - 0.229	0.447 - 0.456
Malir City	Average Values (ppm) ± SD	0.056 ± 0.005	0.353 ± 0.011	0.337 ± 0.008	0.958 ± 0.005
	Coefficient of Variation (%)	0.060 - 0.050	0.360 - 0.330	0.350 - 0.320	0.960 - 0.950
	95 % Confidence Limit	0.053 - 0.059	0.345 - 0.360	0.332 - 0.342	0.955 - 0.960
Shah Faisal Colony	Average Values (ppm) ± SD	0.063 ± 0.005	0.546 ± 0.005	0.367 ± 0.017	0.818 ± 0.006
	Coefficient of Variation (%)	0.070 - 0.060	0.550 - 0.540	0.400 - 0.350	0.830 - 0.810
	95 % Confidence Limit	0.060 - 0.065	0.543 - 0.549	0.356 - 0.377	0.815 - 0.822
Qayumabad	Average Values (ppm) ± SD	0.048 ± 0.009	0.177 ± 0.008	0.197 ± 0.005	0.517 ± 0.009
	Coefficient of Variation (%)	0.060 - 0.030	0.180 - 0.160	0.200 - 0.190	0.530 - 0.500
	95% Confidence Limit	0.0424 - 0.054	0.172 - 0.182	0.194 - 0.200	0.511 - 0.522

In the samples from Location No. 2 (Malir City), the average concentrations of Cd, Cr, Cu and Pb in gill samples were 0.650±0.010, 1.220±0.013, 2.696±0.010 and 4.096±0.011 ppm, respectively (Table 3), while the average concentrations of Cd, Cr, Cu and Pb in gonads samples were 0.027±0.005, 0.243±0.008, 0.096±0.007 and 0.506±0.010 ppm, respectively (Table 4). The average concentrations of Cd, Cr, Cu and Pb in liver samples were 0.175±0.008, 2.095±0.011, 3.643±0.014 and 3.012±0.008 ppm, respectively (Table 5), while the average concentrations of Cd, Cr, Cu and Pb in muscles samples were 0.056±0.005, 0.353±0.011, 0.337±0.008 and 0.958±0.005 ppm, respectively (Table 6).

In the samples from Location No. 3 (Shah Faisal Colony), the average concentrations of Cd, Cr, Cu and Pb in gills samples were 0.818±0.008, 1.472±0.011, 3.979±0.013 and 3.935±0.016 ppm, respectively (Table 3), while the average concentrations of Cd, Cr, Cu and Pb in gonads samples were 0.032±0.006, 0.243±0.020, 0.112±0.006 and 0.389±0.011 ppm, respectively (Table 4). The average concentrations of Cd, Cr, Cu and Pb in liver samples were 0.222±0.007, 2.358±0.005, 5.076±0.012 and 2.096±0.007 ppm, respectively (Table 5), while the average concentrations of Cd, Cr, Cu and Pb in muscles samples were 0.063±0.005, 0.546±0.005, 0.367±0.017 and 0.818±0.006 ppm, respectively (Table 6).

In the samples from Location No. 4 (Qayumabad), the average concentrations of Cd, Cr, Cu and Pb in gill samples were 0.277±0.010, 1.079±0.010, 2.478±0.017 and 2.289±0.016 ppm, respectively (Table 3), while the average concentrations of Cd, Cr, Cu and Pb in gonads samples were 0.028±0.004, 0.168±0.013, 0.088±0.005 and 0.308±0.006 ppm, respectively (Table 4). The average concentrations of Cd, Cr, Cu and Pb in liver samples were 0.113±0.008, 1.333±0.013, 2.063±0.010 and 1.816±0.007 ppm, respectively (Table 5), while the average concentrations of Cd, Cr, Cu and Pb in muscles samples were 0.048±0.009, 0.177±0.008, 0.197±0.005 and 0.517±0.009 ppm, respectively (Table 6).

Cadmium (Cd) is a non-essential and toxic element. It can easily cause chronic toxicity even when present in low

amount, below 1.00µg/g. The permissible limit set for cadmium (Cd) is 2.00µg/g (FAO, 1983). In the present work, cadmium concentrations were found higher in gills 0.818±0.008 ppm, gonads 0.032±0.006 ppm, liver 0.222±0.007 ppm and muscles 0.108±0.155 ppm at Shah Faisal Colony. The levels of Cd (0.023 – 0.818 ppm) recorded in fish samples were lower than the maximum recommended limits of 2.00ppm (WHO, 1985; FEPA, 2003) in fish food.

Chromium (Cr) is an essential trace element and plays an important role in fish metabolism (Sthanadar *et al.,* 2013). Chromium concentrations in gills, liver and muscles tissues were found higher i.e. 1.472±0.011 ppm, 2.358±0.005 and 0.546±0.005 ppm at Shah Faisal Colony. The gonads had same concentration of chromium i.e. 0.243±0.020 ppm and 0.243±0.008 ppm at Shah Faisal Colony and Malir City, respectively. Presently the mean concentration of chromium (Cr) in the gills and liver tissue were found higher than the permissible limit (1.00 µg/g) of FAO (1983). Vinodhini and Narayanan (2008) have reported a low level of chromium (Cr) deposition in the fish liver with a mean value of 0.863 ± 0.015 (µg/g.d.wt). Contrarily, Yousafzai (2004) recorded a high level of chromium (Cr) in *Tor putitora* liver with a mean value of 3.2± 0.05 µg/wet weight of the body. This was in fact a high level of chromium (Cr) in the fish liver. Similarly, Rauf *et al*. (2009) have recorded a high level of Chromium in the liver of fish species, *Catla catla*, *Labeo rohita* and *Cirrhina mrigala* caught from the River Ravi in Pakistan.

Copper had high concentrations in gills, muscles and gonads i.e. 3.979±0.013, 0.367±0.017 and 0.112±0.006 ppm at Shah Faisal Colony, whereas approximately the same concentrations of copper were found 5.076±0.012 and 5.076±0.010 ppm in liver samples at Murad Memon and Shah Faisal Colony, respectively. Cu can induce respiratory distress in fish, and it is striking that the most hypoxia sensitive species are also the most Cu sensitive. The levels of Cr (0.177–2.358 ppm) recorded in fish samples were higher than the maximum recommended limits of 0.15-1.0ppm (FAO, 1983; WHO, 1985; FEPA, 2003) in fish food.

The increased level of industrialization is continuously increasing the risk and damages of lead (Pb) to humans via different types of food chains. It is quite considerable that industrial effluents and domestic sewage should approach the main flow after its proper treatment (Sthanadar *et al*., 2013). Lead had high level concentrations in the gills, gonads, liver and muscles i.e. 4.096±0.011, 0.506±0.010, 3.012±0.008 and 0.958±0.005 ppm at Malir City. The levels of Pb (0.286-4.096 ppm) recorded in fish samples were lower than the maximum recommended limits of 2.0 ppm (FAO, 1983; WHO, 1985; FEPA, 2003) in fish food.

The overall concentrations of cadmium, chromium and copper in gills, gonads, liver and muscles tissues of *Oreochromis mossambicus* were found higher in this pattern Shah Faisal Colony> Malir City> Qayumabad> Murad Memon Goth, whereas the concentration of lead in gills, gonads, liver and muscles of *Oreochromis mossambicus* were found higher in this pattern Malir City> Shah Faisal Colony> Qayumabad> Murad Memon Goth.

The concentration of heavy metals i.e. cadmium and lead were found higher in gills tissues whereas chromium and copper concentrations were found higher in liver tissues. The lowest concentrations of all selected heavy metals were found in gonads. However, the muscle had the least concentration of the heavy metals compared with gills and liver in the fish samples. This is in agreement with previous study by Ishaq *et al.* (2011) which showed that muscle is not an active organ in the accumulation of heavy metals. Gills, on the other hand, has been reported as metabolically active site and can accumulate heavy metals in higher level.

STATISTICAL ANALYSIS

Minitab (version 15) has been used for the analysis of trace metals concentration. It was observed that the concentrations of Cd, Cr, Cu and Pb in surface water samples were not significantly higher ($p>0.05$) than those of deep water samples. The concentrations of metals i.e. Cd, Cr and Cu were significantly higher at Shah Faisal Colony ($p<0.05$) whereas the concentrations of Pb was significantly higher at Malir City ($p<0.05$).

CONCLUSION

This study revealed that the concentrations of selected heavy metals cadmium, chromium, copper and lead in water samples were found higher than the values recommended in drinking water by FAO/WHO (1993), NEQS (1993), WHO (1996) and JECFA (2000). But fortunately the water of Malir River is not used for drinking purposes. It has highly polluted water due to the effects of incoming drains and effluents. In fish organs, the concentrations of cadmium and lead were found higher in gills samples, whereas the concentrations of chromium and copper were found higher in liver tissues. The levels of Cd, Cr and Cu in fish organs were found higher than the maximum recommended limits set by WHO (1985), FEPA (2003) in fish food, whereas the concentrations of lead were found lower than the recommended values set by WHO (1985), FAO (1983) and FEPA (2003). The total metals accumulation were found highest in liver and gills whereas the lowest concentrations were found in muscles and gonads. During the study period, the water samples and fishes collected from Shah Faisal Colony were found highly contaminated

with studied heavy metals as compared to other sampling locations. The results of this research should be brought to the notice of the Fisheries Department for proper actions to be taken about consumption of river fishes. There is also a need to study the overall fish fauna of Malir River to record the edible species and the level of their exploitation for human use. The relevant agencies should find ways for managing the quality of water resources.

REFERENCES

Alabaster, JS. and Lloyd, R. 1980. Water Quality Criteria for Freshwater Fish. Butterworth and Co. Ltd., London, Great Britain. pp297.

Amisah, S., Adjei-Boateng, D., Obirikorang, KA. and Quagrainie. 2009. Effects of clam size on heavy metal accumulation in whole soft tissues of *Galatea paradoxa* (Born, 1778) from the Volta estuary. Ghana. Inter. J. Fisher. Aquacul. 1(2):14-21.

Batvari, BPD., Kamala, KS., Shanthi, K., Krishnamoorthy, R. and Lee, KJ. 2008. Heavy metals in two fish species (*Carangoide malabaricus* and *Belone stronglurus*) from Pulicat Lake, North of Chennai, Southeast Coast of India. Environ Monit Assess. 145:167-175.

Benton, J. JR. 1988. Official methods of analysis: Procedure and use. Food Fertilizer Technology Centre. Tech. Bull. No. 109.

Benzer, S., Arslan, H., Uzel, N., Gül, A. and Yılmaz, M. 2013. Concentrations of metals in water, sediment and tissues of *Cyprinus carpio* L., 1758 from Mogan Lake (Turkey). Iranian Journal of Fisheries Sciences. 12(1):45-55.

Biswas, S., Prabhu, RK., Hussain, KJ., Selvanayagam, M. and Satpathy, KK. 2011. Heavy metals concentration in edible fishes from coastal region of Kalpakkam, Southern part of India. Environ. Monit. Assess. 184:5097-5104.

Canli, M. and Kalay, M. 1998. Levels of heavy metals (Cd, Pb, Cu, Cr and Ni) in tissue of *Cyprinus carpio*, *Barbus capito* and *Chondrostoma regium* from the Seyhan River, Turkey. Turkish Journal Zoology. 22:149-157.

Chi, QQ., Zhu, GW. and Langdon, A. 2007. Bioaccumulation of Heavy Metals In fishes from Taihu Lake, China. Journal of Environmental Sciences. 19(12):1500-1504. doi:10.1016/S1001-0742(07)60244-7.

Dirilgen, N. 2001. Accumulation of heavy metals in fresh water organisms: Assessment of toxic interactions. FAO. Fischer. Technology. 212:1-13.

Duffus, JH. 1980. Environmental Toxicology. Edward Arnold Publishers Ltd., London, Great Britain. pp164.

DWAF (Department of Water Affairs and Forestry). 1996. South African water quality guidelines *(*2nd edi.). Aquatic Ecosystems. 7:159.

Ebrahimpour, M. and Mushrifah, I. 2008. Heavy metal concentrations in water and sediments in Tasik Chini, a freshwater lake, Malaysia. Environ Monit Assess. 141:297-307.

Edem, CA., Akpan, B. and Dosunmu, MI. 2008. A comparative assessment of heavy metals and hydrocarbon accumulation in *Sphyrena afra, Orechromis niloticus* and *Lops lacerta* from Anantigha Beach market in Calabar-Nigeria. Afr. J. Environ. Pollut. and Health. 6:61-64.

Ellias, LD. 2009. Chemical and toxicological studies on hazardous waste sites in Harris country. M.Sc. Thesis. Faculty of Science, Texas Solution University, USA.

EPA (US Environmental Protection Agency). 1976. Quality Criteria for Water. Washington, DC. 440 (9):76-123.

FAO (Food and Agriculture Organization) 1983. Compilation of Legal Limits for Hazardous Substances in Fish and Fishery Products. FAO Fisheries Circular No. 464:5-100.

FAO/WHO. 1993. Evaluation of certain food additives and contaminants: Forty-first report of the Joint FAO/WHO Expert Committee on Food Additives. WHO Technical Report Series, WHO, Geneva. Vol. 837.

Farkas, A., Salanki J. and Specziar, A. 2002. Relation between growth and the heavy metal concentration in organs of bream, *Abramis brama* L. populating lake Balaton. Arch. of Environ. Contam. Toxicol. 43(2):236-243.

FEPA (Federal Environmental Protection Agency) 2003. Guidelines and standards for environmental pollution control in Nigeria. pp238.

Friberg, L., Piscator, M., Nordberg, GF. and Kjellstrom, T. 1974. Cadmium in the environment. (2nd edi.). Chemical Rubber Company Press, Cleveland, Ohio. pp248.

Ipinmoroti, KO. 1993. Water quality of shallow wells located close to dump sites in Akure, Nigeria. Pak. J. Sci. Ind. Res. 36(4):137-141.

Iqbal, M., Haq, IU. and Berns, JAS. 1998. The Leather Sector, Environmental Report. Environmental Technology Program for Industry. (ETPI), Federation of Pakistan Chambers of Commerce & Industry (FPPCI).1-27.

Ishaq, ES., Rufus, SA. and Annune, PA. 2011. Bioaccumulation of Heavy Metals in Fish (*Tilapia zilli* and *Clarias gariepinus*) organs from River Benue, North-Central Nigeria. Pak. J. Anal. Environ. Chem.12(1&2): 25-31.

JECFA. 2000. Summary and conclusions of the fifty-fifth meeting. World Health Organization, Joint FAO/WHO Expert Committee on Food Additives.

Keepax, RE., Moyes, LN. and Livens, FR. 2011. Speciation of heavy metals and radioisotopes. In: Environmental and Ecological Chemistry vol II. Encyclopedia of Life Support Systems (EOLSS). available from http://www.eolss.net/Sample-Chapters/C06/E6-13-03-05.pdf

Khan, MA., Akhtar, M., Nazli, A. and Khan, MA. 1995. Evaluation of public health quality of vegetables, fishes and water. Presented in 2nd conf. on the impact of Food Research on New Product Development, Pakistan.

Kupchella, CE. and Hyland, MC. 1993. Environmental Science, Living within the System of nature. (3rd edi.). Prentice Hall International, Englewood Cliffs, New Jersey, USA. 1-579.

Mahmood, SN., Naeem, S., Siddiqui, I. and Khan, FA. 1998. Metal contamination in ground water of Korangi Industrial Area, Karachi. J. Chem. Soc. Pakistan. 20, 125.

Mai, HX., Zhang, YW., Si, R., Yan, ZG., Sun, LD., You, LP. and Yan, CH. 2006. High-Quality Sodium Rare-Earth Fluoride Nanocrystals: Controlled Synthesis and Optical Properties. Journal of the American Chemical Society. 128(19):6426-6436.

Mansour, SA. and Sidky, MM. 2002. Ecotoxicological Studies Heavy Metals Contaminating Water and Fish from Fayum Governorate, Egypt. Food Chemistry. 78(1):15-22. doi:10.1016/S0308-8146(01)00197-2

Moore, JW. and Ramamoorthy, S. 1984. Heavy Metals in Natural Waters: Applied Monitoring and Impact Assessment. Springer-Verlag, New York, USA. 268.

NEQS, 1993. National Environmental Quality Standards. Gazette of Govt. of Pakistan.

Raja, P., Verasingam, S., Suresh, G., Marichamy, G. and Venkatachalapathy, R. 2009. Heavy metal concentration in four commercially valuable marine edible fish species from Parangipettai coast, south east coast of India. Int. J. Anim. Vet. Adv. 1:10-14.

Rauf, A., Javed, M. and Ubaidullah, M. 2009. Heavy metal levels in three major carps (*Catla catla*, *Labeo rohita* and *Cirrhina mrigala*) from the River Ravi, Pakistan. Pakistan Veterinary Journal. 29(1):24-26.

Schüürmann, G. and Markert, B. 1998. Ecotoxicology: Ecological Fundamentals, Chemical Exposure, and Biological Effects. John Wiley & Sons, Inc., New York, and Spektrum Akademischer Verlag, Heidelberg. pp936.

Sthanadar, AA., Sthanadar, IA., Muhammad, A., Ali, PA., Shah, M., Zahid, M., Begum, B. and Yousaf, M. 2013. Bioaccumulation profile of heavy metals in the liver tissues of *Wallago attu* (Mulley) from Kalpani River Mardan, Khyber Pakhtunkhwa, Pakistan. International Journal of Biosciences. 3(11):92-103.

Szentmihalyi, K. and Then, M. 2007. Examination of microelements in medicinal plants of the carpathian basin. Acta Alimentaria. 36:231-236.

Tariq, J., Ashraf, M., Jaffer, M. and Afzal, M. 1996. Pollution status of Indus River, Pakistan through heavy metals and macronutrient contents of fish, sediment and water. Water Res. 30(6):1337-1344.

Tüzen, M. 2003. Determination of heavy metals in fish samples of the MidDam Lake Black Sea (Turkey) by graphite furnace atomic absorption spectrometry. Food Chemistry. 80:119-123.

Vinodhini R. and Narayanan, M. 2008. Bioaccumulation of heavy metals in organs of fresh water fish *Cyprinus carpio* (common carp). International Journal of Environment Science and Technology. 2(5):179-182.

Vutukuru, SS. 2005. Acute effects of Hexavalent chromium on survival, oxygen consumption hematological parameters and some biochemical profiles of the India major carp, *Labeo rohita*. International Journal of Environmental Research and Public Health. 2(3):456-462.

WHO (World Health Organization). 1985. Guidelines for Drinking Water Quality (Recommendations). WHO, Geneva.

WHO (World Health Organization). 1996. Guidelines for drinking water quality. (2nd edi.), Vol. 2. Australia. Geneva.

Yousafzai, AM. 2004. Toxicological Effects of Industrial Effluents Dumped in River Kabul on Mahaseer, *Tor putitora* at Aman Garh Industrial Area Nowshera, Peshawar, Pakistan. Ph.D. Thesis. University of the Punjab, Lahore.

Received: June 15, 2014; Revised and Accepted: July 25, 2014

SENRA Academic Publishers, British Columbia
Vol. 8, No. 3, pp. 3019-3028, October 2014
Online ISSN: 1920-3853; Print ISSN: 1715-9997

Canadian Journal of pure&applied sciences

TOXIC EFFECTS OF HEAVY METALS POLLUTION ON BIOCHEMICAL ACTIVITIES OF THE ADULT BRINE SHRIMP, *ARTEMIA SALINA*

Azza H Mohamed, *Sherin K Sheir, Gamalat Y Osman and Hoda H Abd-El Azeem
Department of Zoology, Faculty of Science, Menoufia University, Egypt

ABSTRACT

Toxic metals are widely spread in aquatic ecosystems and aquatic invertebrates are continuously subjected to it. In this study, adult brine shrimp, *Artemia salina* was collected from El Hamra Lake, Wadi El Natrun and acclimated in lake water. They were exposed to sublethal concentrations of $CdCl_2$ (5 mg/l), $FeCl_3$ (30 mg/l) and Cd + Fe (5+30 mg/l) for 7 days. A control group was exposed to lake water only. Antioxidant enzymes activity (Superoxide Dismutase; SOD, Catalase; CAT and Glutathione Peroxidase; GPx), metallothioniens (MTs) and total protein patterns using SDS-PAGE were estimated after exposure to the previous heavy metals for 1, 3 and 7 days. Cd increased the activity of the antioxidants CAT, GPX and SOD significantly (ANOVA/Kruskal Wallis, $P \leq 0.02$) than Fe and Cd + Fe, which increased but insignificantly. Results indicated that concentration of metallothioneins was the significantly higher after Cd exposure (23.9 ± 0.9 ng/100 mg, ANOVA, $P \leq 0.001$) followed by Cd + Fe (14.9 ± 2.4 ng/100 mg) and the lowest was after the Fe exposure (10.8 ± 0.3 ng/100 mg). The total proteins profile of *A. salina* tissue was analyzed after the treatment with Cd and Fe. The total proteins intensity increased in all treatments at the beginning of the experiment then decreased gradually than the control by the end of exposure. In conclusion, Cd exposure alone influenced *A. salina* biological responses than Fe alone or Cd + Fe. *A. salina* is an excellent biomonitor for metals pollution; antioxidant enzymes, metallothioniens and total proteins electrophoresis are good biomarkers to measure *A. salina* biological responses to specific metal exposure.

Keywords: *Artemia*, metals, antioxidants, metallothioneins, total proteins.

INTRODUCTION

Heavy metals enter aquatic environments through different pathways. These can be mainly through natural sources such as weathering of rocks and soil in the catchment and anthropogenic sources like agricultural, urban, domestic, and industrial wastes (Demirak *et al*., 2006 and Cevik *et al*., 2009). During the last century, chemical pollution from human activities has become one of the most important stressors of continental aquatic ecosystems. Aquatic heavy metal pollution usually represents high levels of Hg, Cr, Pb, Cd, Cu, Zn, Ni in water systems (Aoyama *et al*., 1987). Heavy metals are often present in the environment in mixtures, making the assessment of environmental hazards even more difficult due to the antagonistic or synergistic actions that may occur. The investigation of the joint toxic effects of chemicals in a mixture is generally based on comparison of the actual toxic effect of the mixture with the toxic effects of the individual chemicals. In field, the organisms are not safeguarded from the effects of combined toxicants. So, there is a need to quantify and understand the mechanisms of multiple toxicity of metals (Verriopoulos *et al*., 1987; Kungolos *et al*., 1999; Mowat and Bundy, 2002).

Artemia is one of the most valuable test organisms available for ecotoxicity testing and is one of the most sensitive groups to stressors. Its natural tolerance may be faced as an advantage, in comparison to other test organisms. Almost all of tests focused on *Artemia*-based testing which involve cyst-based assays or animals cultured in the laboratory (Nunes *et al*., 2006; Ates *et al*., 2013). Another study, Dhont and Sorgeloos (2002) found that *Artemia franciscana* was chosen as a test organism to investigate the influence of Cadmium (Cd) and Zinc (Zn) exposure on the accumulation of the metals in the tissue. The brine shrimp, *Artemia sinica* possesses a high degree of tolerance, enabling it to cope with various challenging conditions including temperature fluctuations, drought, variable food resources, changes in aeration, and accumulation of heavy metals (Blust *et al*., 1988). After one-year of biomonitoring study, elevated concentrations of metals (Cd, Cu, and Zn) in water of the Arkansas River were paralleled by higher concentrations in benthic macroinvertebrates (Clements, 1994).

Of the various toxic heavy metals, cadmium (Cd), lead (Pb), mercury (Hg) and Zinc (Zn) occur frequently in the environment due to their relatively high industrial use. The toxicity of these elements depend on their interactions with essential elements that are necessary for

*Corresponding author email: sherin.sheir@yahoo.com

the nutrition of live organisms, such as calcium, iron, selenium, copper, chromium and manganese (Pechová *et al*., 1998). Cadmium (Cd) is a non-essential metal that can displace essential metal ions and interfere with the functional characteristics of proteins because of its high affinity for sulphydryl groups (Nieboer and Richards, 1980; Rainbow, 1985). Cadmium belongs to heavy metals widely distributed in the environment. In nature, it is found together with zinc at a ratio of 1:100, or even 1:1000. Relatively high quantities of cadmium are present in phosphate fertilizers which increase the concentration of cadmium in soil and plants. The chemical speciation of cadmium in saline waters is dominated by the formation of complexes with chloride. Only a small fraction of the cadmium exists as free metal ion while most of the cadmium found in chloride complexes. The concentration of the free metal ions increases with decreasing salinity (Turner *et al*., 1981; Nriagu, 1988; Blust et *al*., 1992; Korénekova *et al*., 2002). Iron (Fe) is innocuous to the aquatic organisms but toxic at high concentration (Pandy *et al*., 1988).

Metallothioneins were a potential biomarker for metal stress in invertebrates. Crustacean metallothioneins (MTs) were shown to be markedly similar to vertebrate metallothioneins on molecular weights, UV absorption spectra, isoelectric points and amino acid compositions (Olafson *et al*., 1979). The biological functions for metallothioneins are; firstly; these proteins comprise non-toxic zinc and copper reservoir available for the synthesis of metallo enzymes, allowing the homeostasis of many cellular processes. Secondly, MTs can prevent the binding of non-essential metals (Cd, Hg or Ag) within cells, and so restrict their toxic potential (Zaroogian and Jackim, 2000). Cadmium-binding metallothionein proteins have been isolated from many invertebrates after exposure to Cd. These invertebrates include the crab *Cancer magister* and *Scylla serrata*, adult and nauplii larvae of *Artemia,* the planktonic shrimp *Acetes sibogae* and the chiton *Cryptochiton stelleri* (Olafson *et al*., 1979; Acey *et al*., 1989; Del Ramo *et al*., 1995; Martínez *et al*., 1996).

Exposure to free radicals from a variety of sources has led organisms to develop a series of defence mechanisms (Cadenas, 1997). Defence mechanisms against free radicals-induced oxidative stress involve: (i) preventive mechanisms, (ii) repair mechanisms, (iii) physical defences, and (iv) antioxidant defences. Enzymatic antioxidant defences include superoxide dismutase (SOD), catalase (CAT) and glutathione peroxidase (GPx). Non-enzymatic antioxidants are represented by ascorbic acid (Vitamin C), tocopherol (Vitamin E), glutathione (GSH), carotenoids, flavonoids, and other antioxidants. Under normal conditions, there is a balance between both activities and the intracellular levels of these antioxidants. This balance is essential for the survival of organisms and their health (Valko *et al*., 2007). The various roles of enzymatic antioxidants (SOD, CAT and GPx) in the protection against oxidative stress have been proved in numerous reviews (Kojo, 2004; Schrauzer, 2006).

This work was designed to study the toxic effect of heavy metals (Cd and Fe single/in combination) on antioxidant enzymes activity, metallothioneins concentration and total protein patterns of adult *Artemia salina* collected from El Hamra Lake, Wadi El Natrun, Egypt.

MATERIALS AND METHODS

Experimental animal

Artemia salina used in the present investigation were collected from El Hamra Lake, Wadi El Natrun, Egypt. Individuals were placed in plastic box contained Lake water. The animals were maintained under laboratory conditions (17± 2ºC) and mild aeration was applied (El-Bermawi *et al*., 2004).

Experimental materials

Cadmium as $CdCl_2$ was prepared in solution at sublethal concentration 5 mg/l (Nováková *et al*., 2007). Iron as $FeCl_3$ was prepared in solution at sublethal concentration 30 mg/l (Gajbhiye and Hirota, 1990).

Experimental design

Adult *Artemia salina* (360 individual) were divided into 4 groups, each group contained three replicates (30 individual/ replicate). The 1st group (control) was kept in filtered Lake water, the 2nd group treated with $CdCl_2$ (5 mg/l), the 3rd group treated with $FeCl_3$ (30 mg/l), and the 4th group treated with mixed solution of $CdCl_2$ (5 mg/l) + $FeCl_3$ (30 mg/l). Animals were fed mixed diet of yeast, wheat flour, soybean meal, squid and *spirulina*. 3 hrs before the semistatic change of the treatments/water. The experimental time intervals were 1, 3 and 7 day (Dvořák *et al*., 2005).

Determination of metallothionein proteins

Metallothioneins was measured using ELISA according to (Viarengo *et al*., 1997) with minor modifications. Breifly, 0.1 g of whole *Artemia salina* tissue was homogenized with 200 µl of Phosphate buffered saline (PBS). Samples were centrifuged at 10,000 rpm for 30 min. The supernatant was collected and diluted with 100 µl of PBS. Chemicals were obtained from Frontier Institute company, LTD, Hokkaido, Japan.

The Phosphate buffer, standard (Metallothioneins), samples and antibody solution (PBS containing MTs antibody) were kept at 10˚C. Then the strips were washed with washing buffer, 96 well plates were turned upside-down and taped out on a paper towel until the remaining buffer has been removed. 50 µl of assay sample and standard were added into each well and the antibody solution was added to the same wells. The contents in the

wells were stirred then the plate was covered and incubated at 4˚C for 1 hr. After incubation, the solution was discarded from the well then washed 3 times with washing solution (350 µl). 100 µl of the 2nd antibody solution was added in each well and incubated for 1 hr at room temperature then the contents in the wells were stirred. 100µl of the substrate and 50 µl of stop solution were added to each well and incubated for 10 min at room temperature. The optical density (OD) was measured at 450 nm using the spectrophotometer.

Total Proteins analysis

The protein analysis was assayed by SDS- PAGE according to Laemmli (1970) method. 0.02 g of the tissue was homogenized with 200 µl of Tris buffer saline (50 mM tris- HCl, pH 7.5, containing 75 mM NaCl), 1:10 (w/v) ratio. The homogenate was centrifuged at 10,000 rpm for 10 min at 4˚C. The pellet was discarded and the supernatant was aliquoted (Bradford, 1976). Total tissue proteins of *Artemia salina* were separated on 12% resolving gel with 4% stacking gel using. The protein bands were visualized by staining the gel with Coomassie Brilliant Blue (CBB) stain (De-Moreno *et al*., 1985). The gel was photographed and analyzed using gel docu advanced program.

Antioxidant enzymes assays

0.1 g of *Artemia salina* tissue was homogenized in 0.2 ml cold assay buffer, centrifuged at 10,000 g for 15 min at 4 °C. The supernatant was collected for the assay.

Superoxide dismutase (SOD)

SOD activity in *Artemia salina* tissue was measured according to Rest and Spitznagel (1977) using Superoxide Dismutase Assay kit (CAB-574601). One unit of SOD is defined as the amount of the enzyme in 20 µl of sample solution that inhibits the reduction reaction of WST-1 with superoxide anion by 50%. The absorbance (A) was read at 450 nm using the following equation:

$$\text{SOD activity (Inhibition rate \%)} = \frac{[(\text{A blank 1} - \text{A blank 3}) - (\text{A sample} - \text{A blank 2})]}{(\text{A blank 1} - \text{A blank 3})} \times 100$$

Where: **blank 1** is the coloring without inhibitor, **blank 2** is the sample blank and **blank 3** is the reagent blank.

Catalase (CAT)

CAT activity in *Artemia salina* tissue was determined according to Aebi (1983) using Oxiselect ™ Catalase Activity assay kit (STA-341). One unit of catalase was expressed by the amount of catalase decomposes 1 µmol of H_2O_2 per min at pH 4.5 at 25°C. Samples were stored at (-30)°C. Optical density (OD) was measured at 570 nm using the following equation:

$$\text{Catalase Activity} = \frac{\text{B}}{30 \times \text{V}} \times \text{Sample dilution factor}$$

Where: **B** is the amount of decomposed H_2O_2, **V** is the pretreated sample volume added into the reaction well (in ml) and **30** is the reaction time (30 min).

Glutathione Peroxidase (GPx)

GPx activity in *Artemia salina* tissue was measured according to Prins and Loose (1969) using Total Glutathione Peroxidase Assay kit (ZMC-0805002). One unit GPx is defined as the amount of enzyme that will cause the oxidation of 1 µmol of NADPH to NADP per minute at 25 °C. Samples were kept at (-30)°C for storage. OD was measured at 340 nm at T1 to read A1, OD was measured at 340 nm again at T2 after incubating the reaction at 25 °C for 5 min to read A2 according to the following equation:

$$\text{GPx Activity} = \frac{(\text{B - B0})}{(\text{T2 - T1}) \times \text{V}} \times \text{Sample dilution}$$

Where: **B** is the amount of NADPH (in nmols) that was decreased between T1 and T2, **B0** is the background change (without Cumene Hydroperoxide) between T1 and T2, **T1** is the time of first reading (A1 in min), **T2** is the time of second reading (A2 in min) and **V** is the pretreated sample volume added into the reaction well (in ml).

Statistical analysis

All data were analysed using Statgraphics (v5.1 software). Data were expressed as mean ± SD. The statistical analysis was carried by One-way ANOVA was applied to set the difference between the control and treated groups of the experiment, setting the probability level to $P \leq 0.05$, where ANOVA could not be applied, Kruskal Wallis test was used.

RESULTS

Effect of heavy metals (Cd and Fe) exposure on the activity of antioxidant enzymes of *Artemia salina*

Exposure to Cd (5 mg/l) caused insignificant increase in the activity of Superoxide dismutase (SOD) on the 1st and 3rd days (ANOVA/ Kruskal Wallis, $P > 0.05$), and significant increase at day 7 (Kruskal Wallis, $P = 0.02$) when compared to the control. It recorded 89.7 ± 5.6 u/100 mg on the 1st day, 96.4 ± 4.3 u/100 mg on the 3rd day and 101.1 ± 3.6 u/100 mg on the 7th day, while the control value was 72.2 ± 0.3, 73.7 ± 1.3 and 73.8 ± 1.4 u/100 mg. Catalase (CAT) showed significant increase in its activity on the 1st and 3rd days (Kruskal Wallis, $P \leq 0.01$), and insignificant increase on the 7th day (Kruskal Wallis, $P > 0.05$) when compared to the control. It was 23.6 ± 4.3 u/100 mg on the 1st day, 27.4 ± 1.9 u/100 mg on the 3rd day and 29.28 ± 1.1 u/100 mg on the 7th day when compared to the control value, 18.6 ± 0.5, 19.1 ± 0.4 and 19.2 ± 0.6 u/100 mg. Glutathione Peroxidase (GPx) showed significant increase in its activity during all time points of exposure. On the 1st day, it recorded 106.6

± 5.8 u/100 mg; on the 3rd day was 110.7 ± 5.8 u/100 mg and on the 7th day was 114.3 ± 0.4 u/100 mg (ANOVA / Kruskal Wallis, $P \leq 0.004$) when compared to the control value, 80.5 ± 0.8, 80.9 ± 0.8 and 81.2 ± 1.1 u/100 mg (Fig. 1).

Data showed in Fig. (1), indicated that exposure to Fe (30 mg/l) caused insignificant increase in the activity of SOD during all time points of exposure (ANOVA/ Kruskal Wallis, $P > 0.05$) when compared to the control. It was 85.6 ± 5.7 u/100 mg on the 1st day, 92.2 ± 0.6 u/100 mg

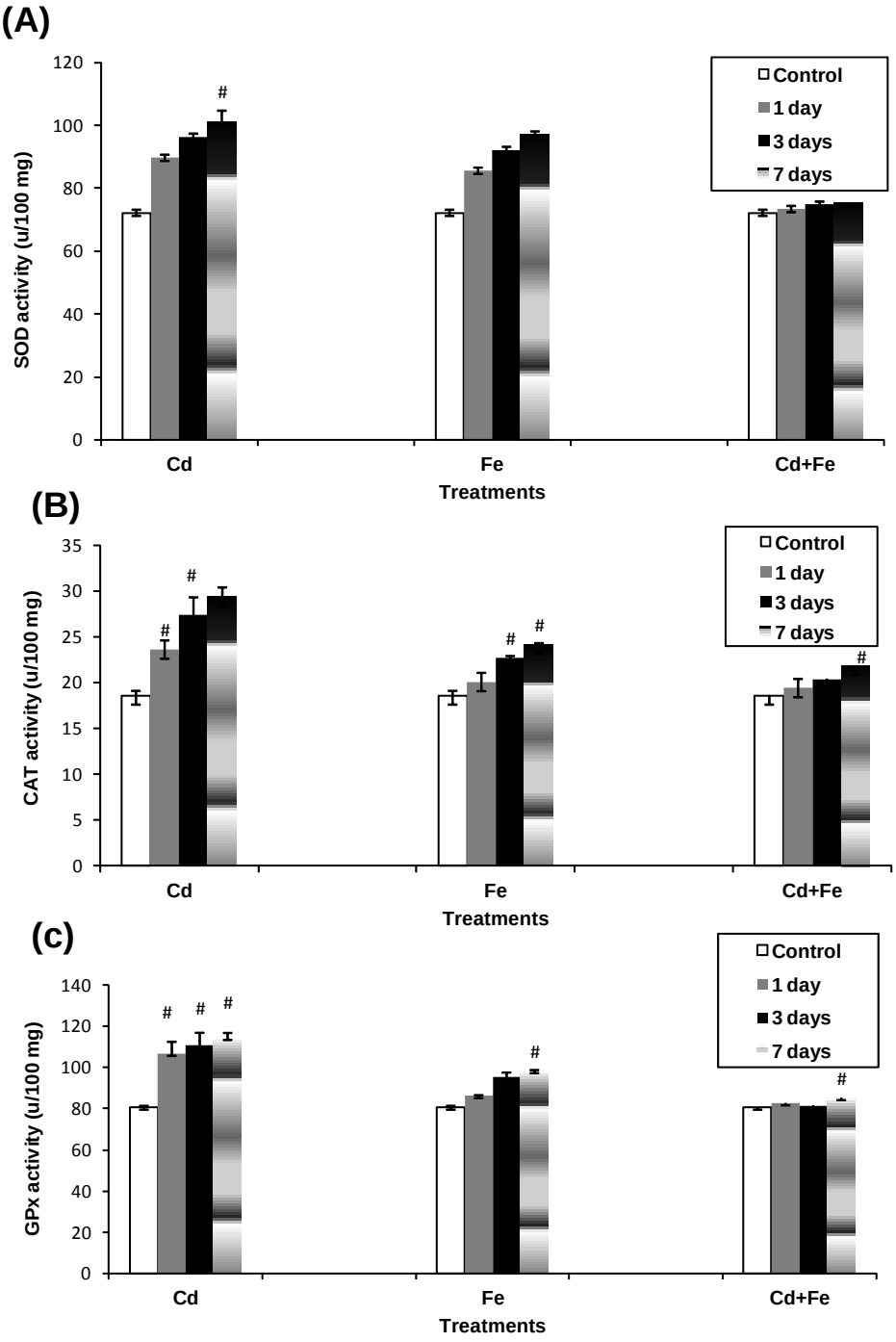

Fig. 1. Effect of Cd, Fe and Cd + Fe exposure on the activity of antioxidant enzymes **(A)** SOD, **(B)** CAT and **(C)** GPx of *Artemia salina* for 7 days, # indicates significant difference when $P < 0.05$ (ANOVA/ Kruskal Wallis).

on the 3rd day and 96.9 ±1u/100 mg on the 7th day when compared to the control value 72.2 ± 0.3, 73.7 ± 1.3 and 73.8 ± 1.4 u/100 mg. CAT showed insignificant increase in activity on the 1st day (Kruskal Wallis, $P > 0.05$), significant increase on the 3rd and the 7th days (ANOVA / Kruskal Wallis, $P \leq 0.01$) when compared to the control. It was 20.06 ± 0.5 u/100 mg on the 1st day, 22.7 ± 0.6 u/100 mg on the 3rd day and 24.1 ± 0.7 u/100 mg on the 7th day when compared to the control value 18 ± 0.5, 19.1 ± 0.4 and 19.2 ± 0.6 u/100 mg. GPx showed insignificant increase in its activity on the 1st and the 3rd days (ANOVA/ Kruskal Wallis $P > 0.05$) and significant increase on the 7th day (Kruskal Wallis, $P = 0.0005$) when compared to the control. It was 86.1 ± 6.04 u/100 mg on the 1st day, 95.5 ± 0.6 u/100 mg on the 3rd day and 98.2 ± 2 u/100 mg on the 7th day when compared to the control value 80.5 ± 0.8, 80.9 ± 0.8 and 81.2 ± 1.1 u/100 mg.

As showed in figure 1, exposure to Cd+Fe caused insignficant increase in the activity of SOD during all time points of exposure (ANOVA/ Kruskal Wallis, $P > 0.05$) when compared to the control. It recorded 73.4 ± 1.1 u/100 mg on the 1st day, 74.8 ± 0.5 u/100 mg on the 3rd day and 75.2 ± 1.2 u/100 mg on the 7th day when compared to the control value 72.2 ± 0.3, 73.7 ± 1.3 and 73.8 ± 1.4 u/100 mg. CAT showed insignficant increase of activity on the 1st and the 3rd days (Kruskal Wallis, $P > 0.05$) and significant increase on the 7th day (ANOVA, $P = 0.0001$) when compared to the control. It was 19.4 ± 0.4 u/100 mg on the 1st day, 20.4 ± 0.2 u/100 mg on the 3rd

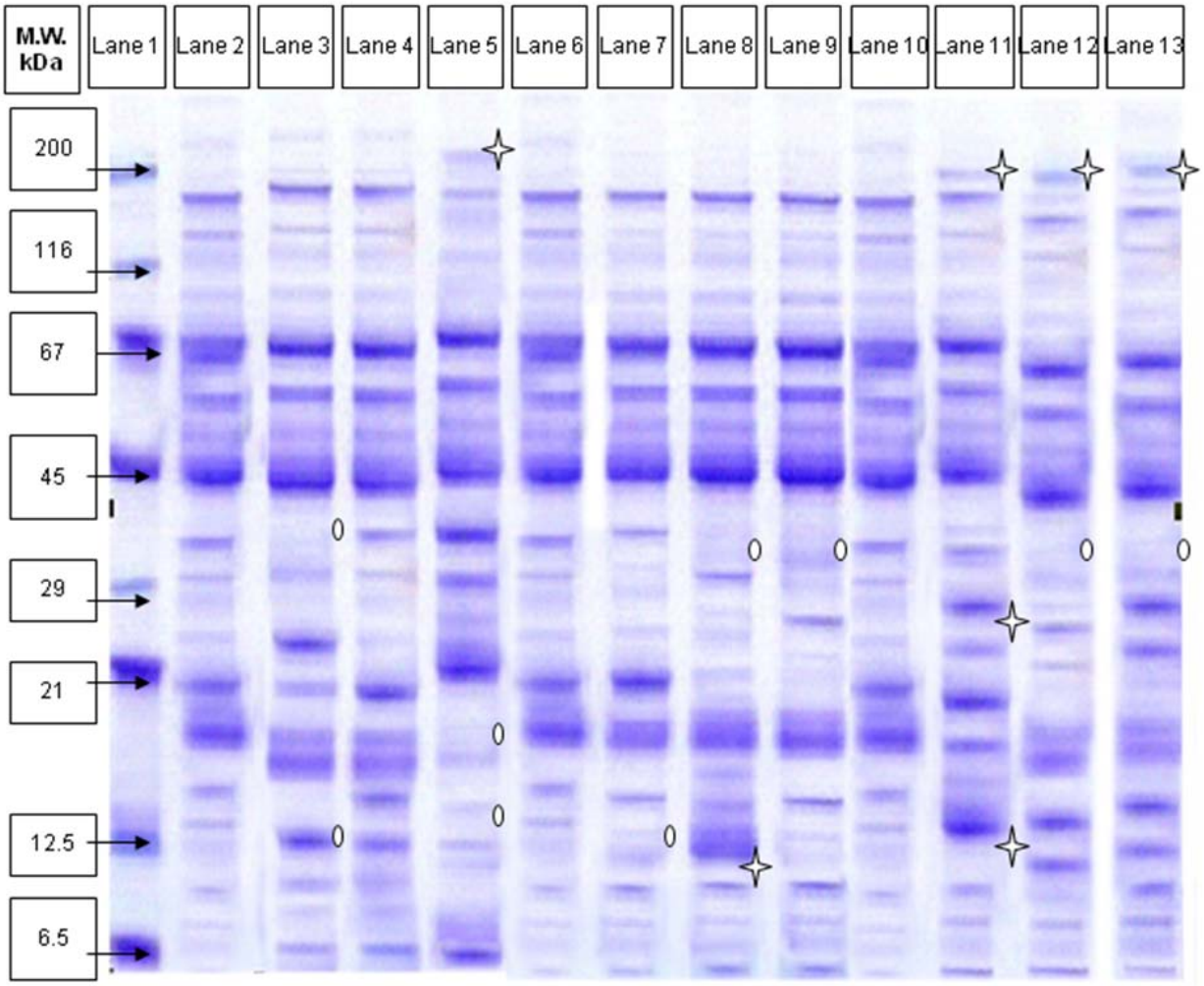

Fig. 2. SDS-PAGE profile of total proteins of *Artemia salina* stained with CBB treated with Cd and Fe for 7 days of exposure. Lane 1, marker, Lane 2, 3, 4 and 5, control and treated with Cd, Fe and Cd + Fe for 1 day, respectively; Lane 6, 7, 8 and 9, control and treated with Cd, Fe and Cd + Fe for 3 day, respectively; Lane 10, 11, 12 and 13, control and treated with Cd, Fe and Cd + Fe for 7 day, respectively and represent appearance and disappearance of bands, respectively. ✦ and O represent appearance and disappearance of bands, respectively.

Table 1. Effect of heavy metals (Cd + Fe) on metallothioneins concentration of *Artemia salina* for 7 days of exposure

Treatments / Time points	Control	Cd	Fe	Cd + Fe
1 day	3.1 ± 0.5	11.1 ± 0.8 #	6.3 ± 0.6	9.6 ± 0.3
3 days	3.2 ± 0.6	18.8 ± 0.5 #	9.4 ± 0.1 #	12.4 ± 2.7
7 days	3.4 ± 0.7	23.9 ± 0.9 #	10.8 ± 0.3 #	14.9 ± 2.4 #

Note; n = 3, data were expressed as means ± SD, ng/100 mg, # indicates significant difference when $P < 0.05$ (ANOVA/ Kruskal Wallis).

Table 2. Effect of heavy metals (Cd + Fe) on the intensity and profile of total proteins of *Artemia salina* for 7 days of exposure

Treatments / Time points	Control		Cd		Fe		Cd + Fe	
	Intensity	Bands No.	Intensity	Bands No.	Intensity	Bands No.	Intensity	Bands No.
1 day	16810,6784	17	272892,8800	14	38180,9223	20	27998,1197	14
3 days	26257,0989	16	4403,0011	16	46432,7554	15	36274,1365	14
7 days	49380,2113	16	24491,4061	18	34671,7158	15	15459,3467	16

day and 21.8 ± 0.2 u/100 mg on the 7th day when compared to the control value 18.6 ± 0.5, 19.1 ± 0.4 and 19.2 ± 0.6 u/100 mg. GPx showed insignificant increase in its activity on the 1st day, insignificant decrease on the 3rd day (ANOVA/ Kruskal Wallis $P > 0.05$) and significant increase on the 7th day (ANOVA, $P = 0.03$) when compared to the control. It was 82.6 ± 2.4u/100 mg on the 1st day, 81.4 ± 1.8 u/100 mg on the 3rd day and 85.1 ± 0.5 u/100 mg on the 7th day when compared to the control value 80.5 ± 0.8, 80.9 ± 0.8 and 81.2 ± 1.1 u/100 mg.

Effect of heavy metals (Cd and Fe) on metallothioneins concentration of *Artemia salina*

Treatment with Cd significantly increased the concentration of metallothioneins on the 1st, 3rd and 7th day (ANOVA, $P \leq 0.001$) when compared to the control. It was 11.1 ± 0.8 ng/100 mg on the 1st day, 18.8 ± 0.5 ng/100 mg on the 3rd day and 23.9 ± 0.9 ng/100 mg on the 7th day while the control values were 3.1 ± 0.5, 3.2 ± 0.6 and 3.4 ± 0.7 ng/100 mg at 1, 3 and 7 days, respectively. Fe caused insignificant increase in the concentration of metallothioneins at 1st day (Kruskal Wallis, $P > 0.05$), significant increase on the 3rd and 7th days (ANOVA/Kruskal Wallis, $P \leq 0.002$) when compared to the control. It was 6.3 ± 0.6 ng/100mg on the 1st day, 9.4 ± 0.1 ng/100 mg on the 3rd day and 10.8 ± 0.3 ng/100 mg on the 7th day compared to control values 3.1 ± 0.5, 3.2 ± 0.6 and 3.4 ± 0.7 ng/100 mg, respectively. Cd + Fe recorded insignificant increase in the concentration of metallothioneins on the 1st and 3rd days (ANOVA/ Kruskal Wallis, $P > 0.05$), significant increase on the 7th day (ANOVA, $P = 0008$) when compared to the control. It was 9.6 ± 0.3 ng/100 mg on the 1st day, 12.4 ± 2.7 ng/100 mg on the 3rd day and 14.9 ± 2.4 ng/100 mg on the 7th day when compared to the control values 3.1 ± 0.5, 3.2 ± 0.6 and 3.4 ± 0.7 ng/100 mg, respectively (Table 1).

Effect of heavy metals (Cd and Fe) on the intensity and profile of total proteins of *Artemia salina*

On the 1st day of treatment, Cd (5 mg/l) exposure caused disappearance of the bands with molecular weight 32.08 and 14.47 kDa, increased protein intensity (272892,8) and decreased band numbers to 14 bands. Fe (30 mg/l) increased in the number of protein fractions to 20 with intensity (38180,9) with appearance of low molecular weight bands (6, 7 and 8 kDa). Cd + Fe showed decreased in the number of protein fractions to 14 with increased intensity to 27998, 1 when compared to the control (17 and 16810,6), respectively. The protein bands 16.69 and 13.41disappeared under the effect of treatment with Cd + Fe (Fig. 2 and Table 2).

On the 3rd day of treatment, Cd caused decrease in the protein intensity (4403,0) and no change in the number of protein fractions as the control (16). The band with molecular weight 12.35 kDa disappeared under the effect of treatment with Cd. Fe treatment caused increase in the protein intensity (46432,7) and decrease in the number of bands to 15. The protein band 32.16 kDa disappeared under the effect of treatment with Fe. Cd + Fe showed decrease in the number of protein fractions to 15 with increased intensity to 36274 when compared to the control (16 and 26257,1), respectively. The protein band 34.02 kDa disappeared under the effect of treatment with Cd + Fe (Fig. 2 and Table 2).

On the 7th day of treatment, Cd caused increase in the number of protein fractions to 18 but decreased intensity to 24491,4. The bands with molecular low weight as 7.2 and 6.2 kDa appeared under the effect of treatment with Cd. Fe treatment decreased both protein bands and intensity (15 and 34671,7), with appearance of 180.79 kDa and disappearance of 33.48 kDa bands. Cd + Fe caused decreased in the protein intensity 15459,3 with the same number of fractions 16, when compared to the control (16 and 49380,2), respectively. The protein band 181.28 kDa appeared and the band 34.23 kDa disappeared under the effect of treatment with Cd + Fe (Fig. 2 and Table 2).

DISCUSSION

Effect of heavy metals Cd and Fe exposure on the activity of antioxidant enzymes of *Artemia salina*

The present results indicated that sublethal concentrations of Cd and Fe single or in combination caused increase of antioxidant enzymes (SOD, CAT and GPx) activity in the treated tissue of *Artemia salina*. This supported by Cadenas (1997), who stated that antioxidant enzymes considered one of defence mechanisms after exposure to free radicals from a variety of sources. Cd significantly induced stimulation in SOD, CAT and GPx activities after 0.5 day at concentrations 0.025 and 0.05 mg/l in the gills and hepatopancreas of the crab *Charybdis japonica* (Pan and zhang, 2006). Ercal *et al*. (2001) stated that redox-active metals such as Fe, Cu and Cr or redox-inactive metals such as Pb, Cd and Hg, may cause an increase in production of reactive oxygen species (ROS) such as hydroxyl radical (HO), superoxide radical (O_2^-) or hydrogen peroxide (H_2O_2). Enhanced generation of ROS can result in a condition known as "oxidative stress". Cells under oxidative stress display various dysfunctions due to lesions caused by ROS to lipids, proteins and DNA. Kojo (2004) and Schrauzer (2006) stated that the enzymatic antioxidant defences include SOD, CAT and GPx are considered one of the defence mechanisms against oxidative stress and may play an important role in reducing some hazards of heavy metals.

Effect of heavy metals Cd and Fe exposure on metallothioneins concentration and the total proteins profile of *Artemia salina*

The present results indicated that Cd exposure highly increased concentration of metallothioneins of *A. salina* followed by Cd + Fe and finally the lowest recorded after Fe exposure. This supported by the findings that invertebrates exposed to elevated metal concentrations respond to this stress by metal-induced synthesis of metal-binding proteins, metallothioneins (Roesijadi *et al*., 1982; Dallinger, 1994). In addition, laboratory experiments showed significant rise in metallothioneins concentrations after exposure to heavy metals (Bodar *et al*., 1988 on *Daphnia magna*; Martínez *et al*., 1996 on *Echinogammarus echinosetosus* and Barka *et al*., 2001 on copepod, *Tigriopus brevicornis***)**. Increase in the concentration of metallothioneins may relate to its biological role, where these proteins can prevent the binding of non-essential metals (Cd, Hg or Ag) within cells, and so restrict their toxic potentials (Viarengo and Nott, 1993; Roesijadi, 1996). In the present work, decreased metallothioneins concentration under the effect of Cd + Fe exposure is supported by Nováková *et al*. (2007) who found that higher concentration of Cd and Zn caused synergistic effects on *A. franciscana*. They explained that the low concentration of zinc and cadmium bound to metallothioneins and after blocking all binding sites on this protein, the metals pass to the blood and tissues as free ions and cause toxicity. However, if the time for metallothioneins synthesis is insufficient due to parallel administration of zinc and cadmium, the influence of zinc on the prevention of cadmium toxicity can`t be observed.

The analysis of SDS- PAGE profile of proteins of treated *Artemia* revealed changes in total protein intensity and fractions number. Variations in protein content reflect the enzymatic changes in *Artemia* tissue. The level of enzymes changes in response to infection or stressors (Cheng *et al*., 1978). Tolba *et al*. (1997) stated that the reduction in the total protein content caused by heavy metals might suggest disturbance in functions of the internal organs as a sequence of structural damage that may lead to inhibition of protein synthesis. An occasional appearance of protein bands indicated that *Artemia* produces additional proteins in response to the heavy metals. Many invertebrates exposed to elevated metal concentrations respond to this stress by metal-induced synthesis of metallothioneins (Rainbow, 1985). In the present study, some low molecular weight proteins appeared as a response to metals exposure, especially Cd. In a recent study, Seebaugh and Wallace (2004) recorded expression of metal-binding proteins (MTs) in response to the exposure to Cd and Zn in *Artemia franciscana*. Ubiquitin (Ub)/proteasome-dependent proteolytic systems that break down proteins to reduce muscle mass of the claw in land crab, *Gecarcinus lateralis*, and american lobster, *Homarus americanus* increased to facilitate withdrawal of the appendage at ecdysis (Koenders *et al*., 2002). Because ubiquitin is a low molecular weight protein (8.5 kDa) appeared under stress, like inflammation, which is characteristic to Cd exposure, *Artemia* expressed low protein intensity under treatment.

CONCLUSION

It is concluded that, *A. salina* is an excellent biomonitor for heavy metals toxicity. Antioxidant enzymes, metallothioniens and total proteins electrophoresis are good biomarkers to measure *A. salina* specific biological responses to specific metal exposure.

REFERENCES

Acey, RA., Yoshida, BN. and Edep, ME. 1989. Metalloproteins in developing *Artemia*. In: Cell and Molecular Biology of *Artemia* Development. Eds. Warner, AH., MacRae, TH. and Bagshaw, JC. Plenum Press, New York, USA. 203-219.

Aebi, H. 1983.´Catalase´. In: Methods of Enzymatic Analysis. Ed. Bergmeyer, H. Verlag Chemie, Weinheim. 273-277.

Aoyama, I., Okamura, H. and Yagim, H. 1987. The interaction effect of toxic chemical combinations on *Chlorella ellipsoidea*. Toxicity Assessment. 2(3):341-355.

Ates, M., Daniels, J., Hilsamar, F., Rivera, E., Arslan, Z. and Farah, I. 2013. Comparative evaluation of impact of Zn and ZnO nanoparticles on brine shrimp *Artemia salina* larvae: effects of particle size and solubility on toxicity. Environmental Science. Processes and Impacts. 15:225-229.

Barka, S., Pavillon, JF. and Amiard, JC. 2001. Influence of different essential and non-essential metals on MTLP levels in the copepod *Tigriopus brevicornis*. Comparative Biochemistry and Physiology Part C. 128:479-493.

Blust, R., Kockelbergh, E. and Baillieul, M. 1992. Effect of salinity on the uptake of cadmium by the brine shrimp *Artemia franciscana*. Marine Ecology Progress Series. 84:245-254.

Blust, R., Linden, A., Verheyen, E. and Decleir, W. 1988. Evaluation of microwave heating digestion and graphite furnace atomic absorption spectrometry with continuum source background correction for the determination of Fe, Cu and Cd in brine shrimp. Journal of Analytical Atomic Spectrometry. 3:387-393.

Bodar, CM., Kluytmans, Van., Montfort, JC., Voogt, PA. and Zandee, DI. 1988. Cadmium resistance and the synthesis of metallothionein-like proteins in *Daphnia magna*. Proceedings of the Third International Conference of Environmental Contamination. CEP. Edinburg. 79-81.

Bradford, MM. 1976. A rapid and sensitive method for the quantitation of microgram quantities of protein utilizing the principle of protein-dye binding. Analytical Biochemistry. 72(1):248-254.

Cadenas, E. 1997. Production of superoxide radicals and hydrogen peroxide in Mitochondria. Molecular Aspects of Medicine. 25(1):17-26.

Cevik, T., Buzgan, H. and Irmak, H. 2009. An assessment of metal pollution in surface sediments of Seyhan dam by using enrichment factor, geoaccumulation index and statistical analyses. Environmental Monitoring and Assessment. 152(1-4):309-319.

Cheng, TC., Lie, KJ., Heyneman, D. and Richard, CS. 1978. Elevation of aminopeptide activity in *Biomphalaria glabrata* (Mollusca) parasitized by *Echinostoma lindoense* (Trematoda). Journal of Invertebrate Pathology. 31:57-62.

Clements, WH. 1994. Benthic invertebrate community responses to heavy metals in the Upper Arkansas River Basin, Colorado. Journal of the North American Benthological Society. 30-44.

Dallinger, R. 1994. Invertebrate organisms as biological indicators of heavy metal pollution. Applied Biochemistry and Biotechnology. 48(1):27-31.

Del Ramo, J., Torreblanca, A., Martínez, M., Pastor, A. and Díaz- Mayans, J. 1995. Identification of cadmium-induced metallothionein in crustaceans by the silver-saturation method. Marine Environmental Research. 39:121-125.

Demirak, A., Yilmaz, F., Tuna, AL. and Ozdemir, N. 2006. Heavy metals in water, sediments and tissues of *Leuciscus cephalus* from a stream in southwestern Turkey. Chemosphere. 63(9):1451-1458.

De- Moreno, MR., Smith, JF. and Smith, RV. 1985. Silver staining of proteins in polyacrylamide gels: increased sensitivity through a combined Coomassie Blue-silver stain procedure. Analytical Biochemistry. 151(2):466-470.

Dhont, J. and Sorgeloos, P. 2002. Applications of *Artemia*. In: *Artemia*: Basic and Applied Biology. Eds. Abatzopoulos, TJ., Eardmore, JA., Clegg, JS. and Sorgeloos, P. Kluwer Academic Publishers, Dordrecht. 251-277.

Dvorak, P., Sucmane, E. and Benova, K. 2005. The development of a ten-day biotest using *Artemia salina* nauplii. Biologia. 60:593-597.

El- Bermawi, N., Baxevanis, A., Abatzopoulos, T., Stappen, G. and Sorgeloos, P. 2004. Salinity effects on survival, growth and morphometery of four Egyptian *Artemia* populations (International study on *Artemia*. LXVII). Hydrobiology. 523:175-188.

Ercal, N., Gurer- Orhan, H. and Aykin- Burns, N. 2001. Toxic metals and oxidative stress part-1: mechanisms involved in metals oxidative damage. Environmental Health Perspectives. 1:529-539.

Gajbhiye, SN. and Hirota, R. 1990. Toxicity of heavy metals to brine shrimp *Artemia*. Journal of the Indian Fisheries Association. 20:43-50.

Koenders, A., Yu, X., Chang, ES. and Mykles, DL. 2002. Ubiquitin and actin expression in claw muscles of land crab, *Gecarcinus lateralis*, and american lobster, *Homarus americanus*: Differential expression of ubiquitin in two slow muscle fiber types during molt-induced

atrophy. Journal of Experimental Zoology. 292(7):618-632.

Koréneková, B., Skalická, M. and Nad, P. 2002. Cadmium exposure of cattle after long-term emission from polluted area. Trace Elements and Electrolytes. 19:97-99.

Kojo, S. 2004. The various roles of enzymatic antioxidants (Superoxide dismutase, Catalase and glutathione peroxide) and non-enzymatic antioxidants (Vitamin C, Vitamin B and Carotenoids). The International Journal of Biochemistry and Cell Biology. 39(1):44-84.

Kungolos, A., Samaras, PG., Kipopoulous, A. and Zoumboulis, A. 1999. Interactive toxic effects of agrochemicals on aquatic organisms. Water Science and Environmental Saftey. 40(1):357-364.

Laemmli, UK. 1970. Cleavage of structural proteins during the assembly of the head of bacteriophage T_4. Nature. 227-680.

Martínez, M., Del Ramo, J., Torreblanca, A. and Diaz-Mayans, J. 1996. Cadmium toxicity, accumulation and metallothionein induction in *Echinogammarus echinosetosus*. Journal of Environmental Science and Health Part A. 31(7):1605-1617.

Mowat, F. and Bundy, K. 2002. Experimental and mathematical computational assessment of the acute toxicity of chemical mixtures from the Microtox assay. Advances in Environmental Research. 6:547-558.

Nieboer, E. and Richardson, DHS. 1980. The replacement of the nondescript term 'heavy metals' by a biologically and chemically significant classification of metal ions. Environmental Pollution Series B, Chemical and Physical. 1:3-26.

Nováková, J., Daňová, D., Trišková, KS., Hromada, R., Mičková, H. and Bišková, M. 2007. Zinc and cadmium toxicity using a biotest with *Artemia franciscana*. Acta Veterinaria Brno. 76:635-642 .

Nriagu, JO. 1988. A silent epidemic of environmental metal poisoning. Environmental Pollution. 50:139-161.

Nunes, BS., Carvalho, FD., Guilhermino, LM. and Van Stappen, G. 2006. Use of the genus *Artemia* in ecotoxicity testing. Environmental Pollution. 144:453-462.

Olafson, RW., Sim, RG. and Boto, KG. 1979. Isolation and chemical characterization of the heavy metal-binding protein metallothionein from marine invertebrates. Comparative Biochemistry and Physiology. 62(4):407-416.

Pan, I. and Zahang, H. 2006. Metallothionein, antioxidant enzymes and DNA strand breaks as biomarkers of Cd exposure in a marine crab, *Charybdis japonica*. Comparative Biochemistry and Biology. 144(1):67-75.

Pandy, AS., Go, EC. and Macrae, TH. 1988. Effect of inorganic mercury on the emergence and hatching of the brine shrimp *Artemia francisana*. Marine Biology. 50:31-38.

Pechova, A., Illek, J., Pavlata, L., Sindelar, M. and Horky, D. 1998. Effects of chronic exposure to cadmium on state of health and accumulation in tissues of calves. Acta Veterinaria Brno. 67:167-174.

Prins, HK. and Loose, JA. 1969. Glutathione. In: Biochemical Methods in Red cell genetics. Edited Academic Press. London. 126-129.

Rainbow, PS. 1985. The biology of heavy metals in the sea. International Journal of Environmental Studies. l 78:169-181.

Rest, RF. and Spitznagel, JK. 1977. Subcellular distribution of superoxide dismutases in humen neutrophils. Influence of myeloperoxidase on the measurement of superoxide dismutase activity. Biochemistry Journal. 166:145-153.

Roesijadi, G. 1996. Metallothionein and its role in toxic metal regulation. Comparative Biochemistry and Physiology Part C. 113(2):117-123.

Roesijadi, G., Drum, AS., Thomas, JM. and Fellingham, GW. 1982. Enhanced mercury tolerance in marine mussels and relationship to low weight, mercury-binding proteins. Marine Pollution Bulletin. 13(7):250-253.

Schrauzer, GN. 2006. Selenium yeast: composition, quality, analysis, and safety. Pure and Applied Chemistry. 78(1):105-109.

Seebaugh, D. and Wallace, W. 2004. Importance of metal-binding proteins in the partitioning of Cd and Zn as trophically available metal (TAM) in the brine shrimp *Artemia franciscana*. Marine Ecology Progress Series. 272:215-230.

Tolba, MR., Mohamed, B. and Mohamed, M. 1997. Effect of some heavy metals on respiration, mean enzyme activity and total protein of the pulmonate snails *Biomphalaria alexandrina* and *Bulinus truncates*. Journal of Egyptian German Society of Zoology. 24 (D):17-35.

Turner, DR., Whitifield, M. and Dickson, AG. 1981. The equilibrium speciation of dissolved components in freshwater and seawater at 25°C and 1 atm pressure. Geochimica et Cosmochimica Acta. 45:855-881.

Valko, M., Leibfritz, D., Moncol, J., Cronin, MT., Mazur, M. and Telser, J. 2007. Free radicals and antioxidants in normal physiological functions and human disease. International Journal of Biochemistry and Cell Biology. 39(1):44-84.

Verriopoulos, G., Moraitou, M. and Millious, E. 1987. Combined toxicity of four toxicants (Cu, Cr, Oil, and Oil dispersant) to *Artemia salina*. Bulletin Environmental Contamination and Toxicology. 38:483-490.

Viarengo, A. and Nott, JA. 1993. Mechanisms of heavy metal cation homeostasis in marine invertebrates. Comparative Biochemistry and Physiology Part C. 104(3):355-372.

Viarengo, A., Ponzano, E. and Dondero, F. 1997. A simple spectrophotometric method for metallothionein evaluation in marine organisms: an application to Mediterranean and Antarctic Molluscs. Marine Environmental Research. 44(1):69-84.

Zaroogian, G. and Jackim, E. 2000. In vivo metallothionein and glutathione status in an acute response to cadmium in *Mercenaria mercenaria* brown cells. Comparative Biochemistry and Physiology Part C. 127:251-261.

Received: July 11, 2014; Accepted: Aug 28, 2014

SENRA Academic Publishers, British Columbia
Vol. 8, No. 3, pp. 3029-3033, October 2014
Online ISSN: 1920-3853; Print ISSN: 1715-9997

Canadian Journal of pure&applied sciences

SERUM SIALIC ACID (TOTAL SIALIC ACID AND LIPID ASSOCIATED SIALIC ACID), B-CAROTENE AND SUPER OXIDE DISMUTASE (SOD) LEVELS IN IRAQI PATIENTS WITH KNEE OSTEOARTHRITIS

Mohammed I Hamzah, *Mohammed AM Al-Bayati and Faisal Gh. Al-Rubaye
[1]Department of Chemistry and Biochemistry, Al-Nahrain University, Al-Kadhmiya, Baghdad, 14222, Iraq

ABSTRACT

Osteoarthritis (OA) is a degenerative joint disease, occurring primarily in older persons, characterized by erosion of the articular cartilage, hypertrophy of bone at the margins (i.e., osteophytes), subchondral sclerosis, and a range of biochemical and morphological alterations of the synovial membrane and joint capsule. In osteoarthritis free radicals may act as triggering factor for degenerative changes seen in cartilage. Oxidative stress leads to increased risk for osteoarthritis but the precise mechanism remains unclear. Sialic acid concentration varies physiologically with age, but its level may also be influenced by such condition as inflammation. The aim of this study was to investigate the changes in the serum sialic acid levels (TSA and LSA), β-Carotene and super oxide dismutase (SOD) in patients with knee osteoarthritis. In this study 96 subjects divided into four groups, 33 patients with obese Knee OA and 25 patients non obese Knee OA, their age range (32-78). The other 38 subjects age and sex matched healthy subjects were studied as controls include 23 obese and 15 non obese. This study was conducted in AL-Kadhemiya Teaching Hospital during the period from October 2011 to April 2012. Serum total sialic acid level, lipid sialic acid, serum β-Carotene and serum SOD were determined. A significant increase in serum sialic acid (TSA & LSA) levels were observed, while there were a significant decrease in serum β-Carotene and SOD levels in patients with knee osteoarthritis when compared to healthy controls. The results of our study suggest higher oxygen free radical production, evidenced by decreased SOD and β-Carotene levels support to the oxidative stress in knee osteoarthritis. The increase of serum TSA and LSA levels is associated positively with the presence of inflammation and could be suggested as one of the many markers for Knee osteoarthritis.

Keywords: Sialic acid, super oxide dismutase (SOD), knee osteoarthritis (KOA).

INTRODUCTION

Osteoarthritis (OA) is a chronic degenerative disorder of multifactorial etiology, characterized by a gradual loss of articular cartilage, thickening of the subchondral bone, bony outgrowths (osteophytes) at the joint margins, and mild, chronic nonspecific synovial inflammation (Berenbaum *et al*., 2001; Morehead, 2003). Sialic acid (N-acetyl neuraminic acid NANA) is acetylated derivative of neuraminic acid. It is attached to non-reducing residues of the carbohydrate chains of glycoproteins and glycolipids. The suggested biological functions of sialic acid are as following: (a) stabilizing the conformation of glycoproteins and cellular membranes, (b) assisting in cell to cell recognition and interaction, (c) contributing to membrane transport, (d) affecting the function of membrane receptors by providing binding sites for ligand, (e) influencing the function stability and survival of blood glycoproteins, and (f) regulating the permeability of the basement membrane of glomeruli (Schauer *et al*., 1995). Sialic acid concentration varies physiologically with age, but its level may also be influenced by such a condition as inflammation (Novak *et al*., 2005). Neoplastic tumors or inborn genetic disorder which cause abnormal sialic acid metabolism (Fang-Kirsher, 1997). Sialic acid and its derivatives were used in the treatments of several diseases, including neuropathic and inflammatory diseases as well as certain tumors (Witczak and Nieforth, 1997). Lipid-associated sialic acid (LSA) is a useful adjunct in the management of a variety of malignancies (Mahmood and Ahmed, 2008). Elevation in blood LSA level was reported in patients with mammary (63%), gastroenteric (65%), pulmonary (79%) and ovarian (94%) neoplasms as well as those with leukemia (91%), lymphoma (87%), melanoma (84%), and Hodgkin disease (91%) (Bhargava *et al*., 1984; Dinstrian and Schwartz, 1983; Erbil *et al*., 1985; Katopodis *et al*., 1982; Khanderia *et al*., 1983; Dwivedi *et al*., 1990). Sialic acid levels do not appear to be a good marker for discriminating malignant from nonmalignant disease of the Lung (Turgut *et al*., 2001). Higher levels of total sialic acid were found in women with metabolic gestation syndrome (Srihana *et al*., 2002) and during periodontal disease.

In osteoarthritis free radicals may act as triggering factor for degenerative changes seen in cartilage. Oxidative

*Corresponding author email: mohammedchina@gmail.com

stress leads to increased risk for osteoarthritis but the precise mechanism remains unclear. Body has a host of protective mechanism to prevent the tissue damage caused by reactive oxygen species (ROS). These include both enzymatic and non enzymatic mechanism. Enzymatic mechanism includes Super oxide dismutase (SOD), catalase and glutathione peroxidase (GPX). Vitamins A (β-carotene), vitamin C (Ascorbic acid), vitamin E (α- tocopherol) and glutathione are some of the major non enzymatic antioxidant in the body (18). Although an area much less studied, free radicals may also play a role in the pathogenesis of Osteoarthritis and in particular, via the effects upon lipids and cartilage. Observational and epidemiological studies suggest that diets deficient in antioxidants may be associated with an increased incidence of Osteoarthritis or faster disease progression. Antioxidant supplements and diets have long been advocated for the treatment of oesteoarthritis (OA) and other inflammatory arthritis. Some investigators support the hypothesis that free radicals from oxygen metabolism destroy antioxidant system (Ascorbic acid and sulphydryl group) (Situnayake, 1991). The present study aims to assess serum levels of sialic acid (TSA and LSA), super oxide dismutase (SOD) and β-Carotene, levels in Iraqi patients with knee osteoarthritis.

MATERIALS AND METHODS

The present study was conducted in AL-Kadhemiya Teaching Hospital, Baghdad during the period from October 2011 to April 2012. Study population consisted of 96 subjects divided into four groups, 58 subjects with age range (32-78) 33 were obese KOA (O-KOA) and25 patients non obese KOA (NO-KOA). The other 38 age and sex matched healthy subjects were included as a controls consisted of 23 obese and 15 non obese individuals. Complete clinical and personal histories of the subjects were also recorded. Inclusion criteria for knee osteoarthritis were on the basis of clinical and radiological evidence. Patients with asymptomatic knee osteoarthritis or association of any other chronic debilitating disease were excluded from the study; 5 ml venous blood was aspirated from a suitable vein. Samples were collected between 8:00-9:00 am after 12 hours fast. Serum total sialic acid level was determined using the assay method described by Svenerholm methods (1957). Estimation of serum lipid sialic acid level was determined using the assay method described by Katopodis *et al*. (1982) in mg/dl. Estimation of SOD was done by method described by Varley, Expressed in U/g Hemoglobin, estimation of Serum Beta-carotene was done by Carr and Price (1988) and expressed as μg/dl.

STATISTICAL ANALYSIS

All data were expressed as mean ± SD. The statistical significance was evaluated by Student's t- test using Statistical Package for the Social Sciences (SPSS Cary, NC, USA) version 15.0.p value were expressed as significant if the values of $p < 0.005$.

RESULTS AND DISCUSSION

Serum sialic acid (TSA & LSA), Oxidative stress marker (SOD) and serum β-Carotene levels were estimated in 96 patients with knee osteoarthritis patients, (33 O-KOA&25 NO-KOA) 38 patients were females and 20 were males in knee osteoarthritis group, compared with 38 healthy control group, age and sex matched, include 24 obese and 14 non obese. Control group consist of 20 females and 18 males. Mean studied age of Knee osteoarthritis patients was range (32-78 years) and that of control was also of same range. By using students t test there was no significant difference seen in mean age, between control group and knee osteoarthritis group. A significant difference was seen according to body mass index (BMI) between the two groups (obese and non obese) in KOA and control as shown in tables 1 and 2. A significant statistical difference was observed in LSA, SOD and β-Carotene in KOA patients between two groups (O-KOA and NO-KOA) as shown in table 2. The levels of serum total sialic acid (TSA) and lipid sialic acid (LSA) indicate significant increase in the Knee osteoarthritis patients group compared with healthy control group as shown in table 3. The levels of antioxidant enzymes SOD and βcarotene were significantly decrease in patients with knee osteoarthritis compared to controls as shown in table 3. The mean ± SD of sialic acid (TSA & LSA), Oxidative stress (SOD) and β-Carotene in healthy control and knee osteoarthritis patients are depicted in tables 1, 2 and 3.

Osteoarthritis is a mechanically induced disorder in which the consequences of abnormal joint mechanics provoke biological effects that are mediated biochemically through local or systemic factors (Brandt *et al*., 2006). Many studies on KOA have focused more on evaluation of biochemical markers in serum and/or synovial fluid of knee joint; such as, adipokines, MMPs, TIMPs, toxic oxygen radicals, and others (Crofford *et al*., 2004; Dumond *et al*., 2003; Hurter *et al*., 2005; Pottie *et al*., 2006). The present data show that TSA and LSA are significantly higher in patients with knee osteoarthritis (KOA). KOA causes inflammation of joints and surrounding tissues, but also it can affect other organs, TSA and LSA may, thus be able to differentiate inflammatory knee osteoarthritis from adehydrative, non-inflammatory osteoarthritis. Our results are supported with previously published work (Alturfan *et al*., 2007). These results can suggest that increased levels of total sialic acid and lipid sialic acid levels might be considered as a defense molecule against the increased oxidative stress in KOA. Antioxidant property of Sialic acid as a H_2O_2 scavenger has been reported by Tanaka *et al*. (1997). In this study, different antioxidant levels were

Table 1. Statistical Data of Control Group.

Parameters	Obese control	Non-obese control	P value
Number %	24	14	……
Age (years)	58.11±9.51	57.91±8.91	NS
BMI (kg/m^2)	34.64±4.35	23.68±1.19	<0.001
TSA(mg/dl)	65.53±14.31	61.88±11.23	NS
LSA(mg/dl)	17.64±1.62	18.86±1.02	NS
SOD (U/gm)	1458.66±117.33	1317.36±133.87	NS
β-Carotene (µg/dl)	90.36±3.81	86.14±2.82	NS

Table 2. Statistical Data of KOA Group.

Parameters	Obese KOA	Non-obese KOA	P value
Number %	33	25	…….
Age (years)	59.89±7.9	58.65±8.8	NS
BMI (kg/m^2)	34.26±4.55	22.82±2.15	<0.001
TSA(mg/dl)	87.22±12.23	80.87±13.15	NS
LSA(mg/dl)	43.95±2.31	29.83±2.18	<0.001
SOD (U/gm)	866.86±102.31	1053±111.46	<0.001
β-Carotene (µg/dl)	36.81±9.72	27.34±2.11	<0.001

Table 3. Comparison of mean S. Total sialic acid(TSA),lipid sialic acid (LSA) ,super oxide dismutase(SOD) and β Carotene in controls and patients with knee osteoarthritis studied by Students 't' test.

Parameters	Total control	Total KOA	P value
Number %	38	58	……
Age (years)	56.55±11.36	58.35±12.95	NS
BMI (kg/m^2)	24.16±2.82	26.84±2.68	□0.001
TSA(mg/dl)	64.39±9.58	83.46±14.95	□0.001
LSA(mg/dl)	17.46±1.35	36.87±2.86	□0.001
SOD (U/gm)	1439.71±127.18	922.4±123.84	□0.001
β-Carotene (µg/dl)	88.78±5.79	31.09±3.86	□0.001

compared between the control group and knee Osteoarthritis groups. One of the most important antioxidant is the enzyme superoxide dismutase, which in the present study, have been decreased significantly in patients with knee osteoarthritis compared with healthy control. Our findings were consistent with a study done by Surapaneni *et al*. (2007) and Surapaneni and Venkataramana (2007) as they demonstrated a significant increase in erythrocyte MDA levels; superoxide dismutase (SOD), glutathione peroxidase (GPX) and plasma glutathione - S - transferase (GST) activities; and a significant decrease in erythrocyte glutathione (GSH), ascorbic acid, plasma vitamin E levels and catalase activity in patients with osteoarthritis when compared to controls, indicating that oxidative stress in OA is much higher than the ability of protective reducing system to overcome (Surapaneni and Venkataramana, 2007). SOD is an important antioxidant enzyme having an antitoxic effect against superoxide anion. The body's overall vascular and neural functions are closely related (Motilal *et al*., 2012). Statistical analysis, of mean serum β-Carotene levels among the two groups (Table 3), indicate significant difference between control group and knee Osteoarthritis group ($p<0.001$). These results are in agreement with previous study done by Peter *et al*. (2001), who found that Serum β-carotene and α-tocopherol concentrations have different associations with diet, smoking, and general and central adiposity. BMI showed statistically difference between obese and non obese in healthy control and knee osteoarthritis patients, these result goes with study demonstrated by Hotamisligil (2006), who demonstrate that Metabolic inflammation associated with obesity is believed to exacerbate the condition by contributing to metabolic inflexibility and the sustained production of pro-inflammatory mediators, Metabolic inflammation also appears to increase osteoarthritis risk, although the mechanisms for this association are not yet well understood. Several recent studies suggest that metabolic inflammation and hyperlipidemia increase the susceptibility of chondrocytes to biomechanically-induced cellular stress, as occurs following joint injury (Aspden, 2011; Mooney *et al*.,

2011). The elucidation of the exact role of biochemical factors that regulate the behavior of the chondrocytes and other cells in the joint will lead to identification of new targets for osteoarthritis therapy (Van der Kraan, 2006). In conclusion, the increase of plasma TSA and LSA levels is associated positively with the presence of inflammation and appears to be a consequence of the disease itself, and could be suggested as one of the newly discovered marker for KOA. While the decrease in the levels of SOD and β-Carotene parameters may be due to the increased turnover for preventing oxidative damage in these patients, suggesting an increased defense against oxidant damage in knee osteoarthritis.

REFERENCES

Alturfan, AA., Uslu, E., Alturfan, EE., Hatemi, G., Fresko, I. and Kokoglu, E. 2007. Increased serum sialic acid levels in primary osteoarthritis and inactive rheumatoid arthritis. Tohoku J Exp Med. 213:241-248.

Aspden, RM. 2011. Obesity punches above its weight in osteoarthritis. Nat. Rev. Rheumatol. 7(1):65-8.

Berenbaum, F., Hochberg, MC. and Cannon, GW. 2001. Osteoarthritis. In: Primer on the Rheumatic diseases. Eds. Klippel, JH., Crofford, LJ., Stone, JH. and Weyand, CM. (12th edi.). Arthritis Foundation. 13:285-97.

Bhargava, AK., O'Donnell, AM., Birl, T., *et al*. 1984. Plasma Lipid-Bound Sialic Acid (LSA) in Cancer and Noncancer Patients. Clin Chem. 30:940.

Brandt, KD., Radin, EL., Dieppe, PA. and Van de Putte L. Yet. 2006. More evidence that OA is not a cartilage disease. Ann Rheum Dis. 65:1261-1264.

Carr, FH. and Price, EA. 1988. Practical Clinical Biochemistry. (6th edi.). Varley Harold.

Crofford, LJ., Metha, HH., Roessler, BJ. and Mancuso, P. 2004. Leptin induces production of eicosanoids and proinflammatory cytokines in human synovial fibroblasts. Arthritis Res Ther. 6(3):64.

Dwivedi, C., Dixit, M. and Hardy, RE, 1990. Plasma lipid-bound sialic acid alterations in neoplastic diseases. Cellular and Molecular Life Sciences. 46(1):91-94.

Dinstrian, AM. and Schwartz, MK. 1983. Ann Clin Lab Sci. 13(2):137-1342.

Dumond, H., Presle, N., Terlain, B., Mainard, D., Loeuille, D., Netter P., Loeuille, D., Netter, P. and Pottie, P. 2003. Evidence for the key role of leptin in osteoarthritis. Arthritis Rheum. 48:3118-29.

Erbil, KM., Jones, JD. and Klee, GG. 1985. Cancer. 55(2):404-409.

Fang-Kircher, SG. 1997. Comparison of sialic acids excretion in spot urines and 24-hour-urines of children and adults. Eur. Journal Clin. Chem. Clin. Biochem. 35:47-52.

Hotamisligil, GS. 2006. Inflammation and metabolic disorders. Nature. 444(7121):860-867.

Hurter, K., Spreng, D., Rytz, U., Schawalder, P., Ott-Knüsel, F. and Schmökel, H. 2005. Measurements of CRP in serum and LDH in serum and synovial fluid of patients with osteoarthritis. The Veterinary Journal. 169:281-285.

Katopodis, N., Hirshaut, Y. and Geller, NL. 1982. Lipid–associated sialic acid test for the detection of human cancer. Cancer Res. 42:5270-5275.

Khanderia, U., Keller, JH. and Barton, HG. 1983. Serum sialic acid is a biologic marker for malignant disease. Journal of Surgoncol. 23(3):163-166.

Mahmood, TJ. and Ahmed, SA. 2008. JMCZ, Hawler Medicinal University.

Mooney, RA., Sampson, ER., Lerea, J., Rosier, RN. and Zuscik, MJ. 2011. High-fat diet accelerates progression of osteoarthritis after meniscal/ligamentous injury. Arthritis Res Ther.13 (6):R198.

Morehead, K. and Sack, KE. 2003. Osteoarthritis: What therapies for this disease of many causes? Postgrad Med. 114(5):11-17.

Motilal, C., Tayade, N. and Kulkarni, B. 2012. Effect of smoking on nerve conduction velocity in young healthy individuals. International Journal of Current Research and Review. 4(15):59-63.

Novak, J., Tomana, M., Shah, GR., Brown, R. and Mestecky, J. 2005. Heterogeneity of IgG glycosylation in adult periodontal disease**.** J. Dent. Res. 84(10):897-901.

Peter, W., Elisabet, W., Petra, HL., Bo, G., Lars, J. and Göran, B. 2001. Serum concentrations of β-carotene and α-tocopherol are associated with diet, smoking, and general and central adiposity1,2,3. American J. Clin. Nutr. 73(4):777-785.

Pottie, P., Presle, N., Terlain, B., Netter, P., Mainard, D. and Berenbaum, F. 2006. Obesity and osteoarthritis: More complex than predicted. Ann Rheum Dis. 65:1403-1405.

Schauer, R., Kelm, S., Reuter, G., Roggentn, P. and Shaw, L. 1995. In: Biology of the Sialic Acids. Ed. Rosenberg, A. Plenum Publ. Corp. New York, USA. pp7-67.

Situnayake, RD. 1991. Chain-breaking antioxidant status in rheumatoid arthritis: and laboratory correlates. AnnRheum Dis. 50(2):81-6.

Srihana, M., Reichelt, AJ., Lúcia R., *et al.* 2002. Total Sialic Acid and Associated Elements of the Metabolic Syndrome in Women With and Without Previous Gestational Diabetes. Diabetes Care. 25:1331-1335.

Surapaneni, KM. and Venkataramana, G. 2007. Status of lipid peroxidation, glutathione, ascorbic acid, vitamin E and antioxidant enzymes in patients with osteoarthritis. Indian Journal of medical science. 61(1):9- 14.

Svenneehlom, L. 1957. Quantitative estimation of sialic acids. II. A colorimetric resorcinol-hydrochloric acid method. Biochimica et Biophysica Acta. 7:24(3):604-611.

Tanaka, K., Tokumaru, S. and Kojo, S. 1997. Possible involvement of radicalreactions in desialylation of LDL. FebsLett. 413:202-224.

Turgut, I., Gulbu, I., Yasemin, B., Recep, A. and Mehmet, KC. 2001. Comparison of serum and bronchoalveolar lavage fluid sialic acid levels between malignant and benign lung diseases. BMC Plum Med. 1:4.

Van der Kraan. 2006. Growth Factors and Cytokines in OA Pathogenesis. Annals of the Rheumatic Diseases, Amsterdam. The EULAR Journal Scientific Abstract. 9.

Witczak, ZJ. and Nieforth, K. 1997. Carbohydrates: New and Old Targets for Rational Drug Design. Carbohydrates in Drug Design, Marcel Dekker Inc., New York, USA. pp1-37.

Received: May 2, 2014; Revised and Accepted: Aug 4, 2014

SENRA Academic Publishers, British Columbia
Vol. 8, No. 3, pp. 3035-3042, October 2014
Online ISSN: 1920-3853; Print ISSN: 1715-9997

Canadian Journal of pure&applied sciences

INDUCED EFFECTS OF LEAD, CHROMIUM AND CADMIUM ON *GALLUS DOMESTICUS*

*Karim Gabol[1], M Zaheer Khan[1], M Umair A Khan[1], Peer Khan[1], Farina Fatima[3], Saima Siddiqui[1],Tanveer Jabeen[1], Nadeem Baig[1], M Asif Iqbal[1], M Usman A Hashmi[2] and Muhammad Tabish[1]
[1]Department of Zoology, Faculty of Science, University of Karachi, Karachi75270
[2]Department of Zoology, Govt Dehli Science College, Karachi
[3]1372 Freeport Drive, Mississauga, ONT L5C 1S6, Canada

ABSTRACT

The objective of this study was to investigate the induced effects of three selected heavy metals lead, chromium, and cadmium on poultry bird *Gallus domesticus* which are widely consumed in Karachi. Lead caused decrease in level of blood parameters whereas chromium and cadmium increased level of blood parameters. Red Blood Corpuscles (RBCs) decreased due to cadmium and lead whereas White Blood Corpuscles (WBCs) decreased with exposure to lead and chromium. Lead also decreased the life span of RBCs. After administration of high dose (20µg /body weight) of lead Hemoglobin (Hb) was 13.42 g/dL, R.B.C 3.33 (x10E12/L), Mean Corpuscular Volume (M.C.V) 160.30 (fL), Mean Corpuscular Hemoglobin (M.C.H) 40.74 (pg), Mean corpuscular hemoglobin concentration (M.C.H.C) 29.18 g/dl and W.B.C 189 (x10E9/L), respectively whereas for low dose (10 µg /body weight) Hb was 12.52 g/dL, R.B.C 3.18 (x10E12/L), M.C.V 155.72 (fL), M.C.H 39.44pg, M.C.H.C 27.99 g/dl and W.B.C 207.50 (x10E9/L), respectively. At high dose of cadmium (20 µg /body weight) concentration of Hb was 14.87g/dL, R.B.C 3.19 (x10E12/L), M.C.V 129.69 (fL), M.C.H 48.38 (pg), M.C.H.C 37.56 g/dl, W.B.C 135.24 (x10E9/L) whereas at low dose (10 µg/body weight) concentration of Hb was 14.21g/dL, R.B.C 3.11 (x10E12/L), M.C.V 127.51 (fL), M.C.H 47.54 (pg), M.C.H.C 36.70 g/dl and W.B.C 145.75 (x10E9/L), respectively. At high dose of chromium (20 µg /body weight) Hb as 9.35g/dL, R.B.C 2.03 (x10E12/L), M.C.V 142.40 (fL), M.C.H 37.20 (pg), M.C.H.C 23.95 g/dl and W.B.C 235.02 (x10E9/L) whereas at low dose (10 µg/body weight) Hb as 10.40 g/dL, R.B.C 2.37 (x10E12/L), M.C.V 148.02 (fL), M.C.H 39.42 (pg), M.C.H.C 25.60 g/dl and W.B.C 207.31 (x10E9/L), respectively. In histo-pathological study, induction of a high dose of heavy metals (Pb, Cr and Cd) showed abnormalities of cells size and function, damage to cells and tissue of liver, kidney, intestine and brain.

Keywords: Toxic effects, heavy metals, lead, chromium, cadmium, poultry bird.

INTRODUCTION

Quality of food and its safety is a most important community concern all over the world. The risks associated with consumption of food stuffs contaminated by pesticides, heavy metals and/or toxins have stimulated research in this field (D'Mello, 2003). Heavy metals are found naturally in an ecosystem with varying concentrations but a large amount of heavy metalsare introduced into the ecosystem due to anthropogenic activities. The occurrence of heavy metals in the environment is of great ecological importance due to their toxicity at certain level, translocation through food chains and which are considered as persistent (Abdul-Jameel *et al*., 2012). Hence contamination with heavy metals is a serious threat to humans because of their toxicity, bioaccumulation and biomagnifications in the food chain (Demirezen Uruç, 2006). Karachi is the industrial city and economic hub of Pakistan and about 70% of the total industry of the country is sited there. The chief industry consist of textile, chemicals, pharmaceuticals, biocides, electronic goods, food, beverages, vegetable oils, fishing, plastics, paints, dyes, cement, asbestos, glass, ceramics, oil refinery, tanneries, soap and detergents, tobacco, ship building and breaking, iron and steel, metal finishing, auto assembling and manufacture, thermal power generation, paper and printing and also forge and foundry. The sub-lethal effects of lead nitrate on hematological profile of *Clarias batrachus* studied and various hematological changes noticed. In exposed fishes RBC counts, hemoglobin percentage and serum protein levels were decreased significantly in comparison to control groups (Mastan *et al*., 2009). Strong amount of lead damages the RBC and cell membranes (Shaheen and Akhtar, 2012). Chromium shrinks the blood cells and the change in shape affects the binding of oxygen to RBC (Mazon *et al*., 2002). Chromium induced in animals showed affects on intestine tissues (Sharma and Satyanrans, 2011). Cadmium chloride at teratogenic dose induced significant alterations in the detoxification enzymes of the liver and the kidney which lead to hepatica injuries, lung damage, kidney disinfection, and

*Corresponding author email: kgabol.gabol@gamil.com

hypertension (Reddy and Yellamma, 1996). The effects of cadmium on hematologic values of Broiler chicken showed that the values of RBC, Hb, PCV, MCHC and MCH were significantly lower and their anemia was hypo-chromic and normocytic (Caiying *et al*., 2005). The effects of heavy metal $CdCl_2$ on survival and hematology parameters of Rock pigeon *Columbia livia* showed that the treatment with 150µg of $CdCl_2$ reduces the survival time and increases the value of hematological parameters hemoglobin content, RBC, WBC, MCHC and MCH whereas PCV and MCV decreased. The low dose (50 µg) produced nominal effects on these parameters except WBC and MCH (Gabol *et al*., 2003).

Heavy metals act as environmental stressors and may alter serum biochemical parameters in fresh water fish *Oreochromis niloticus* from prolonged exposure to heavy metals such as Ag, Cd, Cr, Cu, and Zn (Öner *et al*., 2008). Trough anthropogenic activities a large amount of heavy metals are introduced into the ecosystem of the Karachi which has now great environmental importance due to their toxicity at certain intensity. The objective of this study was to investigate the induced effects of three heavy metals lead, chromium, and cadmium on poultry bird *Gallus domesticus*.

MATERIALS AND METHODS

The experiment was carried on *Gallus domesticus* (chicks) which were bought from the local market of Karachi. Birds were kept in room tempture for 5 to 7 days before experimental work, and then were divided into three groups:
(a) Lab Control
(b) Low dose (10 µg/body weight) and
(c) High dose (20 µg/body weight).

Metals used

Chromium, cadmium, and lead were used in the form of salts, chromium sulphate ($CrSO_4$), cadmium chloride ($CdCl_2$), and lead nitrate ($PbNO_3$). These were used as a low dose (10 µg /body weight) and high dose (20 µg/body weight).

The hematological parameters were measued in the following units:
Hemoglobin: g/dL
R.B.C: Red Blood Corpuscles : x10E12/L
M.C.V: Mean corpuscular volume: fL
M.C.H: Mean corpuscular hemoglobin: pg
M.C.H.C: Mean corpuscular hemoglobin concentration: g/dl
W.B.C : White Blood Corpuscles: x10E9/L

Dacie and Lewis (1977) methods were applied for estimation of following parameters:
Erythrocytes count (R.B.C.)
Leukocytes count (W.B.C.)
Mean corpuscular volume (M.C.V.)
Mean corpuscular haemoglobin concentration (M.C.H.C)
Mean corpuscular haemoglobin (M.C.H).

RESULTS AND DISCUSSION

Hematological parameters were carried out from March to December of 2013. Pathological changes and toxic effects were also observed in this study. Comparison of various hematological parameters such as Hb, RBC, WBC, MVC, MCH and MCHC after treatment with high and low dose of heavy metal lead, chromium and cadmium is shown in tables 1, 2, 3. The mean variance value of blood parameters for lead ranged between 0.10 - 1790 (Table 1) whereas mean variance value for chromium ranged between 0.03 - 123.23 (Table 2), similarly mean variance

Table 1. Toxic effects of lead on blood parameters of *Gallus domesticus*.

Blood Parameters	Doses	March	April	May	June	July	Aug.	Sep.	Oct.	Nov.	Dec.	Mean	Var.	S.D
Hb g/dL	Control	12.8	13.1	12.4	11.7	13.7	12.1	10.8	11.1	12.1	9.6	11.94	1.44	1.20
	Low	12.9	13.9	12.9	12.8	14.1	13.1	11.1	11.7	12.6	10.1	12.52	1.52	1.23
	High	13.8	14.7	13.8	13.9	15.8	13.9	11.8	11.9	13.8	10.8	13.42	2.22	1.49
RBC (10E12/L)	Control	3.2	3.4	3.0	2.9	3.4	3.3	2.9	3.0	2.8	2.4	3.03	0.10	0.31
	Low	3.1	3.6	3.1	3.6	3.5	3.4	3.1	3.1	2.9	2.4	3.18	0.14	0.37
	High	3.9	3.8	3.4	3.2	3.6	3.6	3.2	3.1	3.0	2.5	3.33	0.18	0.42
WBC (x10E9/L)	Control	248	250	220	208	261	323	199	201	200	180	229.00	1790	42.31
	Low	241	239	209	180	241	209	191	195	200	170	207.50	654.28	25.58
	High	220	210	191	150	208	181	184	190	188	168	198.00	424.44	20.60
MCV (fL)	Control	161	168	165	152	170	164	141	142	138	135	153.60	183.82	13.56
	Low	160	170	169	158	172	167	143	143	140	135.2	155.72	198.65	14.09
	High	168	175	178	164	177	171	145	143	146	136	160.30	258.23	16.07
MCH (pg)	Control	46	47	42	39	42	40	37	37	35	24	38.90	42.32	6.51
	Low	44	47.8	43	40	43	42	38.1	35.5	36	25	39.44	40.06	6.33
	High	46.5	48.1	45	42	45	44	39.0	35	37	25.8	40.74	45.45	6.74
MCHC (g/dl)	Control	28	31	29	25	28	26	25	25	27	27	27.10	3.88	1.97
	Low	27	32	30	27	29	28	26.2	25.7	27.8	27.2	27.99	3.58	1.89
	High	28.1	33	32	28.1	31	30	27	25.8	29	27.8	29.18	5.22	2.28

Table 2. Toxic effects of Chromium on blood parameters of *Gallus domesticus*.

Blood Parameters	Doses	March	April	May	June	July	Aug.	Sep.	Oct.	Nov.	Dec.	Mean	Var.	S.D
Hb g/dL	Control	11.2	12.1	11.8	9.1	11.8	9.8	11.9	11.1	9.8	12.1	11.7	1.22	1.11
	Low	10.2	11.1	11.1	8.8	11.1	9.1	11.1	10.7	9.1	11.7	10.40	1.08	1.04
	High	8.2	9.4	10	8	9.8	8.4	10.2	9.9	8	11.6	9.35	1.40	1.18
RBC (10E12/L)	Control	2.5	3.2	1.3	2.4	2.8	2	2.9	2.4	1.8	3	2.34	0.35	0.59
	Low	2.1	2.8	2.8	2.2	2.7	1.8	2.7	2.2	1.6	2.8	2.37	0.20	0.45
	High	1.1	2.2	2.4	1.9	2.6	1.5	2.5	2	1.4	2.7	2.03	0.30	0.55
WBC (x10E9/L)	Control	220.4	228	180	170	197	144	210	208	148	240	194.54	1090.56	33.20
	Low	300.1	255	205	188	208	158	231	214	152	162	207.31	2156.96	46.44
	High	360.2	262	244	200	210	162	247	226	162	277	235.02	3442.45	58.67
MCV (fL)	Control	160.1	170.3	155	144	150	137	148	141	132	162	149.94	144.12	12
	Low	162.1	168	152	139	148	135	146	139	130	161.1	148.02	160.60	12.67
	High	142	160	148	134	144	134	144	136	128	154	142.40	96.71	9.83
MCH (pg)	Control	44.2	47.1	40	40	43.10	37	39	40	32	48	41.04	22.76	4.77
	Low	48.1	44	39.1	38	42	34	35	38.1	29.1	46.8	39.42	35.19	5.39
	High	44.1	40	38	36	40	32	33	37	26.8	45.1	37.20	31.18	5.58
MCHC (g/dl)	Control	28.7	30.1	30.8	27	26.1	22	28	25	20	30	26.77	12.80	3.58
	Low	30.1	28	29.2	26.1	25.2	20.1	26.1	24	18.4	28.8	25.60	14.95	3.87
	High	24.1	26.1	29	24.9	24.2	19.7	24.8	23.7	16.9	26.1	23.95	11.95	3.4

Table 3. Toxic effects of Cadmium on blood parameters of *Gallus domesticus*.

Blood Parameters	Doses	March	April	May	June	July	Aug.	Sep.	Oct.	Nov.	Dec.	Mean	Var.	S.D
Hb g/dL	Control	12.3	17.2	16.8	14.1	11.7	10.7	18.1	15.1	11.8	14.1	14.19	6.63	2.57
	Low	12.4	17.0	16.79	14.1	11.72	10.72	18.12	15.2	11.81	14.2	14.21	6.46	2.54
	High	13.4	18.1	17.8	14.7	11.99	10.2	18.77	16.8	12.1	14.80	14.87	8.66	2.94
RBC (10E12/L)	Control	3.35	3.13	3.04	3.30	2.80	2.77	3.03	3.31	2.90	3.03	3.07	0.04	0.21
	Low	3.37	3.13	3.04	3.30	3.01	2.94	3.03	3.31	2.90	3.03	3.11	0.03	0.16
	High	3.47	3.34	3.08	3.32	3.21	3.0	3.22	3.32	2.95	3.03	3.19	0.03	0.17
WBC (x10E9/L)	Control	111.28	143.9	129	111.3	102.1	122.2	95.0	350	150	200	151.48	5782.7	76.04
	Low	109.44	138.9	119.9	110.0	99.98	119	85.10	330	146.	199	145.75	5175.5	71.94
	High	99.94	127.9	115.4	108.9	97	100	84.2	300	139	180	135.24	4095.7	64
MCV (fL)	Control	114.22	136.6	131.5	118.2	114.2	112.2	137.8	138.8	129.11	137.8	127.05	123.73	11.12
	Low	117.21	136.9	131.4	118.2	114.2	112.2	137.9	138.9	129.17	138.9	127.51	119.76	10.94
	High	121.22	137	132.1	120.1	115.8	114.3	138.4	149.1	129.81	139.1	129.69	132.74	11.52
MCH (pg)	Control	36.77	54.88	52.81	37.77	36.77	35.71	57.8	59.81	50.28	51.81	47.45	92.46	9.62
	Low	37.78	53.81	52.99	37.99	36.79	35.88	57.9	59.99	50.31	51.99	47.54	88.53	9.41
	High	39.11	54.8	58	38.01	37	36	58.22	59.88	50.81	52	48.38	95.34	9.76
MCHC (g/dl)	Control	32.19	40.18	39	33.21	32.21	31.2	40.2	41.18	37.08	39.17	36.56	15.40	3.92
	Low	32.28	39.1	40.01	33.24	32.28	31.28	40.2	42.0	37.31	39.28	36.7	16.07	4.01
	High	34.22	41.2	41.08	34.81	33.81	32	41.22	41.0	37.2	39.1	37.56	13.01	3.61

value of blood parameters for cadmium ranged between 0.20 - 2156.96 (Table 3).

Deposition of heavy metals in chickens is due to feeding and drinking of contaminated feed and water as well as through exposure to different manufacturing processes of factories and industries; this in addition to the air pollution with some heavy metals that may be found around the poultry raising areas. Accumulation of heavy metals within the body may take place by contaminated food and water. Effects of environmental pollution on food items has been a matter of great concern. It was observed that in ecosystem heavy metals found naturally with variations in concentrations but major source of heavy metals which are introduced into the ecosystem are due to anthropogenic activities such as combustion of fossil fuels, mining industries, domestic sewage, and wastedisposal, use of pesticide, insecticides and herbicides etc. The occurrences of heavy metals in the environment is considered persistent and is of great concern to health of humans (Friberg *et al*., 1979).

A recent study Khan *et al*. (2012) reported that all chickens samples collected from Karachi, Hyderabad and Thatta city were contaminated with Cadmium (Cd), Nickel (Ni), Copper (Cu) and Lead (Pb). Whereas Copper contamination was found to be the highest level as compared to other metals tested.

During the present study it was found that metal ($CdCl_2$, $PbNO_3$, and $CrSO_4$) concentrations in blood of *Gallus domesticus* caused enormous variation in blood parameters (Hb, RBC, WBC, MCV, MCH and MCHC level) at primarily stage of our work. However, from the research of ten months it is observed that the levels of blood parameters decreased with lead where as chromium

and cadmium treated samples showed increased in blood parameters. RBC counts decreased with cadmium where as WBC count decreased with chromium.

Katavolos *et al*. (2007) reported that lead causes hemolysis in swan birds, which can lead to anemia. It was also observed that lead caused osmotic changes in blood hence osmotic fragility is the reason for hemolysis (Legget, 1993). Lead damages the RBC and cell membranes (Ashan *et al*., 2006). In the present study the treatment of high dose of lead nitrate showed that RBCs counts decreased from 3.9 to 2.5 (x10E12/L) during March to December 2012, where as variation were observed June and August. The numbers of WBC were decreased from 220 to 168 (x10E9/L) but number WBC count was increased during 5^{th}, 7^{th} and 8^{th} months. After complete period WBCs count greater than before. MCV level was decreased from 168 to136 (fL) but level was increased during 2^{nd}, 3^{rd}, 5^{th} and in 9^{th} whereas MCH level was decreased from 46.50 to25.80 (pg) but during 2^{nd}, 5^{th} and 9^{th} month, level was increased. MCHC level was decreased from 28.10 to 27.80 g/dl but during 2^{nd}, 5^{th} and 9^{th} months showed increase in level.

Cadmium produces toxic effects and can also cause kidney dysfunction, hypertension, hepatic injury and lung damage (John and Jeanne, 1994). It is reported that cadmium affects the cells of kidney in mammals (Johri *et al*., 2010). The size of brain cells as well as neuron and neurotranmetrs are also effected by cadmium (Gerspacher, 2009). Effects of cadmium on the hematologic value of poultry birds have been reported. The blood film showed hypo-chromic and normocytic and the blood parameters RBC, Hb, PCV, MCHC and MCH were higher when cadmium was introduced in poultry birds (Caiying *et al*., 2005). It is reported that after applying the high dose of cadmium on Rock pigeon the level of blood parameters increased (Gabol *et al*., 2003). In the resent study treatment of high dose of cadmium chloride showed that RBCs counts were decreased from 3.47 to 3.03 (x10E12/L) after first month to last month i.e. March to December. The numbers of WBC sincreased from 99.94 to 180 (x10E9/L) but during 3^{rd}, 4^{th} , 5^{th} and 7^{th} months showed decline in WBCs count. MCV levels increased from 121.22 to139.10 (fL) but level decreased during 3^{rd}, 4^{th}, 5^{th} and 6^{th} and in 9^{th} month. MCH levels increased from 39.11 to 52 (pg) but during 4^{th}, 5^{th} and 9^{th} months level was decreased. MCHC level was increase from 34.22 to 39.10 g/dl but during 3^{rd} to $6^{th,}$ 8^{th} and 9^{th} months showed decline in level.

Cui *et al*. (2005) reported that high of chromium in chick increased the blood parameters Hb, RBC, PCV. Another study, Dartsch *et al*. (1998) found that high dose of chromium affects liver epithelial cells and damages the kidney cells. Chromium sulfate CrSO4 causes great fluctuation in blood parameters. RBCs counts were increase from 1.10 to 2.70 (x10E12/L) during month of March to December, but level was decreased during 4^{th}, 6^{th} and 9^{th} months. The numbers of WBC decreased from 360.20 to 277 (x10E9/L) but during 5^{th}, 7^{th} and 8^{th} and 10^{th} months showed increase in WBCs count. MCV level was increased from 142 to154 (fL), but level was decreased during 3^{rd}, 4^{th}, 6^{th}, 8^{th} and in 9^{th} months. MCH level was increase from 44.10 to 45.10 (pg) but during month of 2^{nd}, 3^{rd}, 4^{th}, 6^{th} and 9^{th} months level was decreased. MCHC level was increase from 24.10 to 26.10 g/dl whereas during 4^{th}, 5^{th}, 6^{th},8^{th} and 9^{th} months observed decrease in level.

The high and low doses of chromium and cadmium showed increase in the level of Hb where as lead showed decline in Hb level. The high doses of Pb, Cd and Cr showed mean concentration value of Hb as13.42, 14.87 and 9.35 g/dL, respectively. Hb level decreased with lead from 13.80 to10.80 g/dL whereas chromium and cadmium showed increase level of Hb from 8.20to11.60 g/dL and 13.40 to 14.80 g/dL, respectively.

High doses of lead caused highest rates of hemolysis. The highest concentration showed maximum hemolysis as well as it destroyed the red blood cells and caused anemia. Legget (1993) obtained similar results, while Foulkes (2011) and Evoy (2012) reported that lead damages the tissue of intestine and also affects the gut function. A recent study, Khaki and Khaki (2010) reported that lead damages the kidney cells and shrinks the collection tubules in rats. It was reported that lead damages the liver cells (Petersipos and Blazovics, 2003).

Two other studies Goldstein (1990) and Brochin *et al*. (2008) reported that lead affects the brain cells and also affects the neurotransmitter and brain function affected due to toxic heavy metals lead.

High dose of lead showed that hepatic cells, blood vessels and smooth muscle are damaged. Some area show high number of cells death in the liver after applying strong doses. Figure 1 showed that induced strong dose of lead damaged the kidney cells known as nephropathy. Figure 2 shows that high dose of lead damages intestinal lining and outer covering epithelium tissues.

Figure 3 shows that lead damages brain cells. Some black spots showed that these areas cells were damage where s some sides' myelin coasts also lost. Another study Johri *et al*. (2010) also reported that cadmium affects the cell of kidney in mammals. Some studies already reported that cadmium affects the brain cell neuron size decayed and function of brain and neurotranmetrs was also influence due to cadmium (Gerspacher, 2009).

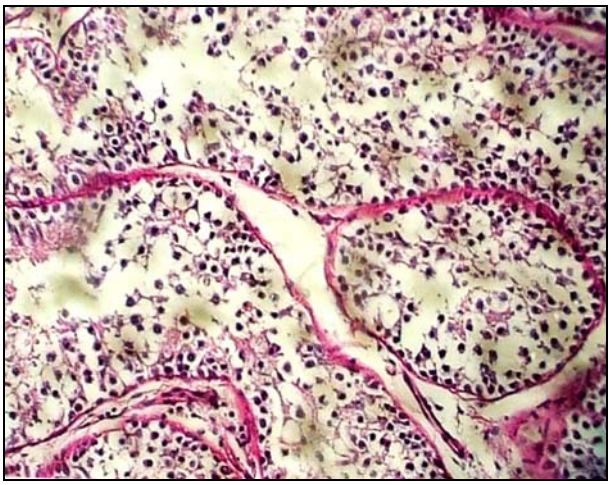

Fig. 1. Kidney induced dose of Lead.

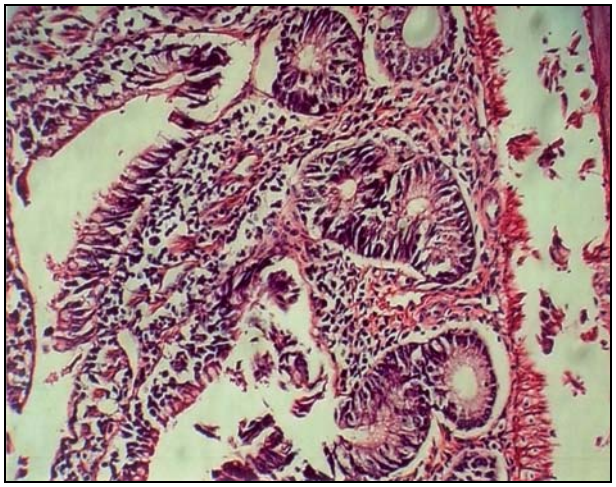

Fig. 2. Intestine induced dose of Lead.

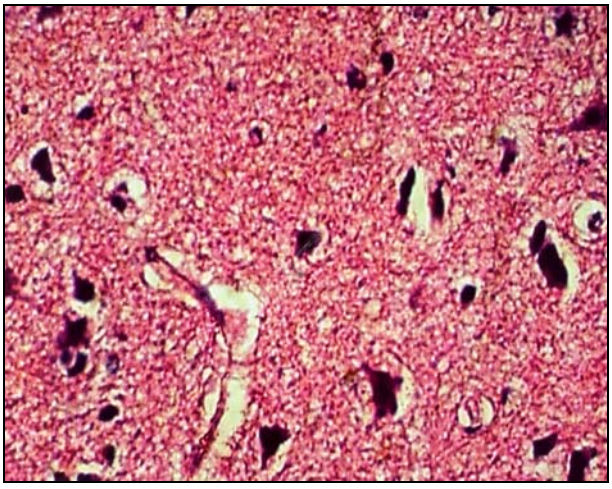

Fig. 3. Brain induced dose of Lead.

Figure 4 cadmium has detritus effects on cell functions. Figure 5 showes normal size of liver cells in control experiment. It is clear from figures 6 and 7 that the size of liver cell Melanomarcophes in small size but the induced effect of cadmium (20mg) the cell size increased. Figure 8 showes that the intestinal lymphoid tissues are major haemopoietic tissues. Kidney consists of lymphoid tissues and many nephropores with intestinal lymphoid tissues.

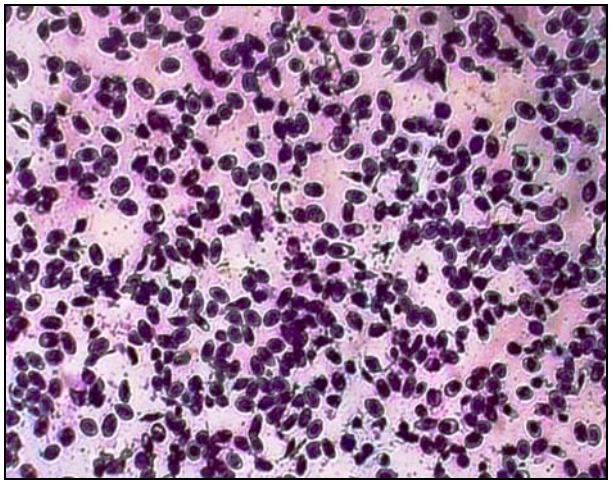

Fig. 4. Blood of *Gallus domesticus* (control).

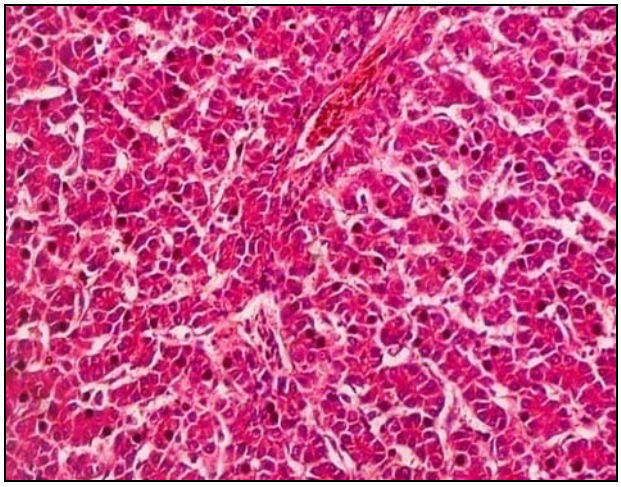

Fig. 5. Liver of *Gallus domesticus* (control).

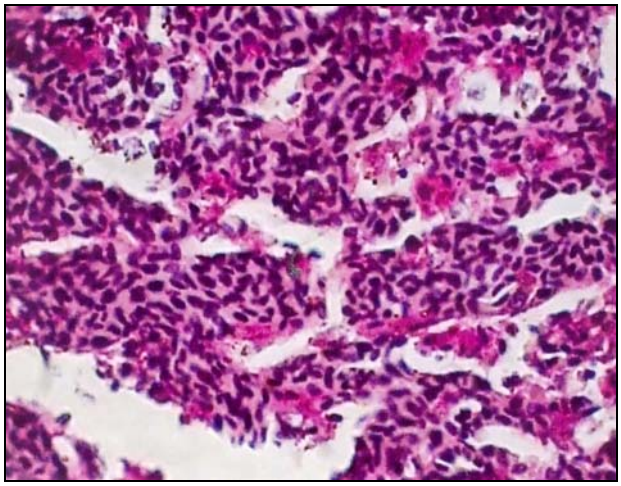

Fig. 6. Liver induced dose of Cadmium (h x e).

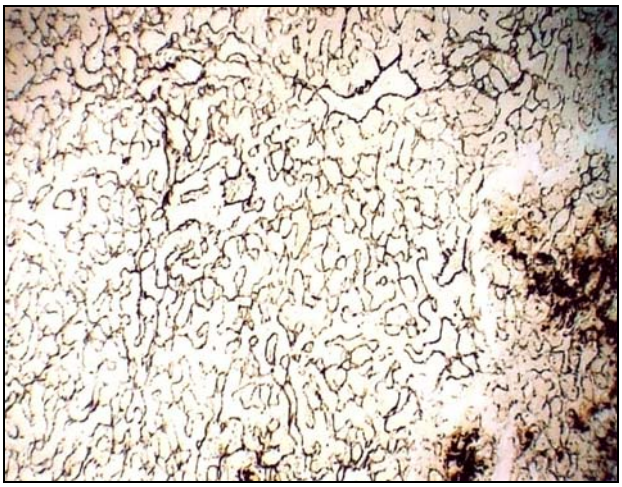

Fig. 7. Liver induced dose of Cadmium (silver).

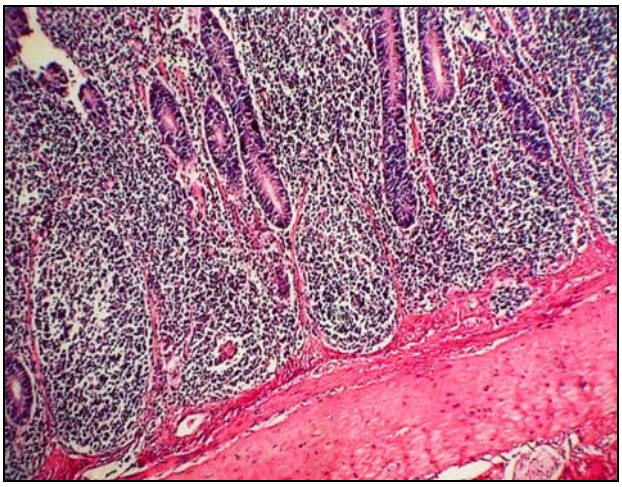

Fig. 8. Intestine induced dose of Cadmium.

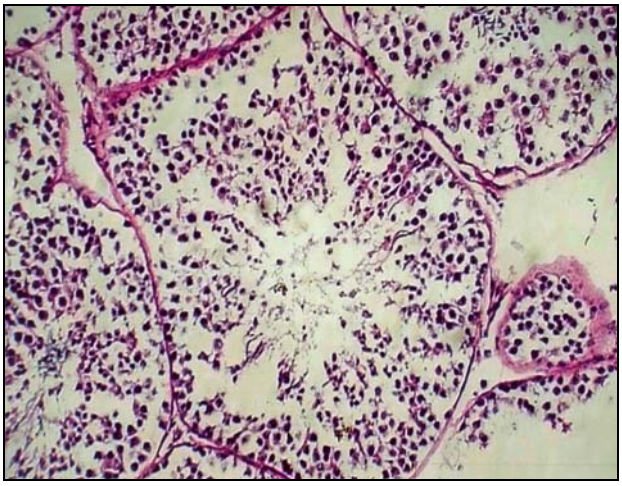

Fig. 9. Kidney induced dose of Cadmium.

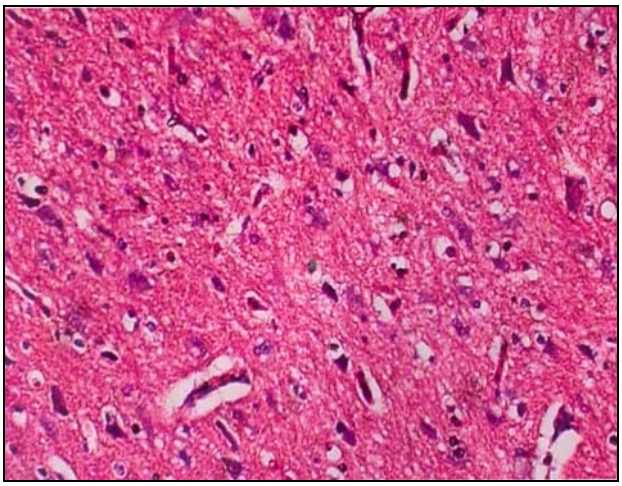

Fig. 10. Brain of *Gallus domesticus* (control).

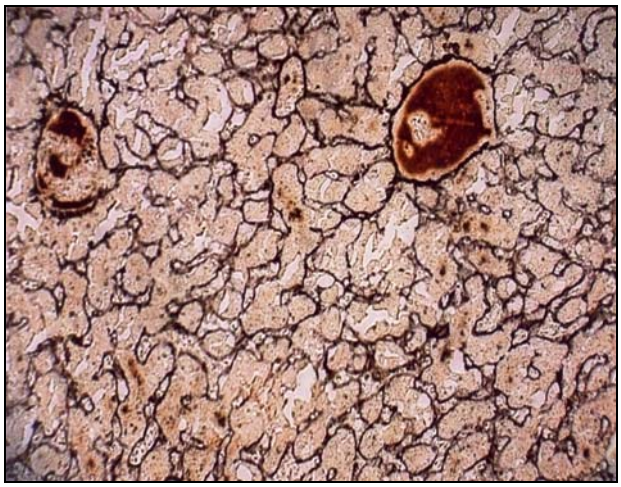

Fig. 11. Liver induced dose of Chromium (silver).

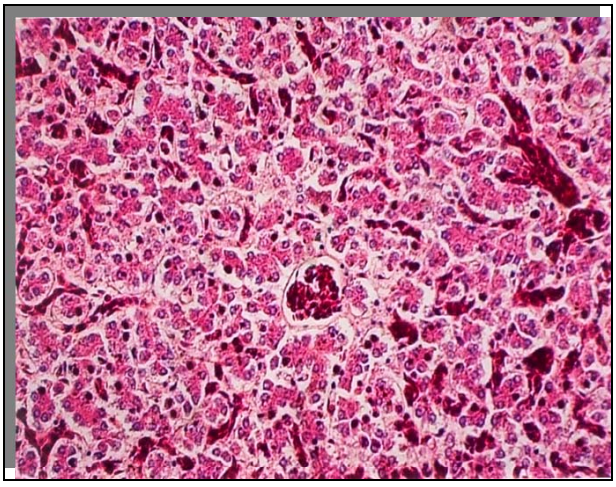

Fig. 12. Liver induced dose of Chromium (h x e).

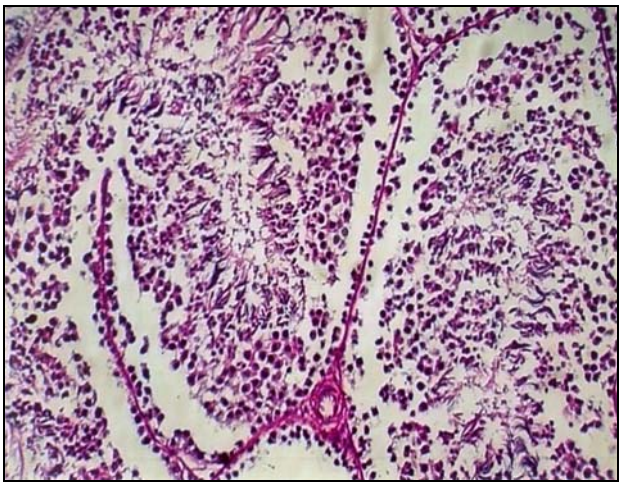

Fig.13. Kidney induced dose of Chromium.

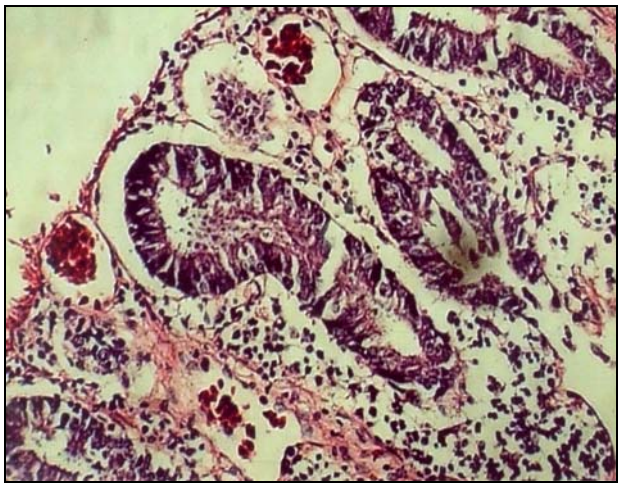

Fig. 14. Intestine induced dose of Chromium.

Figure 9 showes that the lethal concentration of $CdCl_2$ caused deteriorative changes in haemopoietic tissues and degeneration of kidney. The present study showes that large number of macrophages in liver and kidney were capable of taking up the debris in haemopoietic tissues. Figure 10 shows high dose of cadmium enlarges the size of brain cells. High doses of chromium affected cells size and the liver epithelial cells (Dartsch *et al*., 1998). It is also observed that chromium caused hepatic cells damage and necrosis. Sharma and Satyanrans (2011) reported that the intestine tissue of animal was damaged and effect due to high amount of chromium which was induced in animals.

Figures 11 and 12 compared the control cells size was normal but strong dose chromium affected on cells size increased and the liver epithelial cells affected due to which hepatic cells damage and necrosisoccurred. In figure 13 kidney epithelium cells increased and some nephrons were damaged. At higher concentration the cell volume increased figure 14 showes that high dose of chromium affected the cellular levels of intestinal tissue.

CONCLUSION

The level of blood parameters decreased with lead where as chromium and cadmium showed increased level of blood parameters. RBC level decreased with cadmium and lead whereas WBC level was decreased with lead and chromium. The present study showed that large number of macrophages in liver and kidney were capable of taking up the debris in haemopoietic tissues. It was noted that cadmium has detritus effects on cell functions and cause abnormality in cell size. It caused degenerative changes in haemopoietictissues as well as swelling in renal tubules, cellular hypertrophy and kidney cells was damaged and enlarged. It also affects on the size of neuron of brain and cause abnormality in neurotranmetrs. It was observed that high dose of cadmium enlarges size of brain cells where as high dose of chromium affected the liver epithelial cells and hepatic cells and caused damages of hepatica cells and necrosis. Kidney epithelium cells increased and some nephrons were damaged and at higher concentration the cell volume increased cellular levels of intestinal tissue was affected. It was also observed that high doses of lead cause highest rates of hemolysis, decrease haemoglobin synthesis and reduced the life span of RBC as well as changes in brain cells and loss of myelin coat of brain. It was also found that lead can damage the tissue of intestine, kidney cells, liver cells and also affect the gut function.

REFERENCES

Abdul-Jameel, A., Sirajudeen, J. and Abdul-vahith, R. 2012. Studies on heavy metal pollution of ground water sources between Tamilnadu and Pondicherry, India. Advances in Applied Science Research. 3 (1):424-429.

Ahsan, MM., Shakoori, FR. and Shakoori, AR. 2006. Biochemical and hematological abnormalities in factory workers exposed to hexavalent Chromium in Tanneries of Kasur district. Pak. J. Zool. 38(3):239-253.

Brochin, R., Leone, S., Phillips, D., Shepard, N., Zisa, D. and Angerio, A. 2008. The cellular effect of lead poisoning and its clinical picture. The Georgetown Undergraduate J Health Sci. 5:1-8.

Caiying, Z., Guoliang, H. and Xiaoquan, G. 2005. Effect of Cadmium on hematologic values of Broiler chicken. Acta Agriculturae Universitatis Jiangxiensis. 27(2):279-281.

Cui, H., Yang, G., Pen, X., Junliangm D. and Debing, L. 2005. Effect of Copper Toxicity on Blood Biochemical Parameters in Broilers. ActaVeterneria E.T. Zootechnica Sinica. 36(12):1329-1333.

Dacie, JA. and Lewis, SM. 1977. Practical haematology. (5th edi.). J.A. Churchil Ltd, London.

Dartsh, PC., Hildenbrand, S., Kimmel, R. and Schmahl, FW. 1998. Investigations on the nephrotoxicity and hepatotoxicity of trivalent and hexavalent chromium compounds. International Archives of Occupational and Environmental Health. 71:40-45.

Demirezen, D. and Uruç, K. 2006. Comparative study of trace elements in certain fish, meat and meat products. Meat Sci. 74:255-260.

D'Mello, JPF. 2003. Food Safety: Contaminants and Toxins. CABI Publishing, Wallingford, Oxon, Cambridge. pp480.

Evoy, MM. 2012. Lead damage Gut function. Jou.Toxic. Res. 8(2):28-32.

Foulkes, EC. 2011. Transport of toxic metal lead across the intestinal tissue. Jour. Env. Health. 2 (1):1428-1438.

Friberg, L., Gunnar, F., Nordberg. and Velimer, B. 1979. Handbook on Toxicology of Metals, Elsevier/Northe Holland Biomedical Press.

Gabol, K., Tabassum, R. and Khan, MZ. 2003. Induced effect of Cadmium chloride on Rock pigeon (*Columbia livia*). J. Nat. Hist. Wild. 2(1):39-43.

Gerspacher, C. 2009. The effect of cadmium on brain cells. Int. J. Mol. Med. 24(3):311-8.

Goldslein, GW. 1990. Lead poisoning and brain cell damage. Envir. Health Perspect. 89:91-94.

John, HH. and Jeanne, IR. 1994. Food Additives, Contaminants and Natural Toxins. In: Modern Nutrition in Health and Disease. (8th edi.). Eds. Maurice, ES., James, AO. and Moshe, SL. Febiger. 2:1597-1598.

Johri, N., Jacquillet, G. and Unwin, R. 2010. Heavy metal poisoning: The effects of cadmium on the kidney. J. Env. Re. 23(5):783-92.

Katavolos, P., Staempfli, S., Sears, W., Gancz, AY., Smith, DA. and Beinzle, D. 2007. The effect of lead poisoning on hematologic and biochemical values in Trumpeter Swans and Canada Geese. Vet. Clin. Pathol. 36(4):341-7.

Khaki, AA. and Khaki, A. 2010. Lead effects the liver tissue and kidney of rat. Journal of Medical Plant Res. 8 (4):1492-1495.

Khan, MZ., Gabol, K., Yasmeen, R., Siddiqui, S., Fatima, F., Mehmood, N., Parveen, P., Hussain, H., Begum, B. and Jabeen, T. 2012. Determination of Heavy Metals in Brain, Liver and Heart Muscles of Poultry Chicken *Gallus domesticus* in three Cities of Sindh. CJPAS. 6(3):2089-2104.

Leggett, RW. 1993. Environ. Health Perspect. 101. 598.

Mastan, S., Indu-priya, G. and Babu, EG. 2009. Haematological profile of *Clarias batrachus* (Linn.) Exposed to sub-lethal doses of lead nitrate. Intl. J. Hematol. 6(1):35-42.

Mazon, AF., Monteiro, EAS., Pinheiro, GHD. and Fernandes, MN. 2002. Hematological and physiological changes induced by short-term exposure to copper in the freshwater fish, *Prochilodus scrofa*. Braz. J. Biol. 62(4):621-631.

Öner, M., Atli, G. and Canli, M. 2008. Changes in serum biochemical parameters of freshwater fish *Oreochromis niloticus* following prolonged metal (Ag, Cd, Cr, Cu, Zn) exposures. Environmental Toxicology and Chemistry. 27(2):360-366.

Petersipos. and Blazovics, A. 2003. Some effect of lead on liver. Actabiologicaszegediensis. 47(1):139-142.

Reddy, ATV. and Yellamma, K. 1996. Cadmium chloride induced alteration in the detoxification enzymes of rat liver and kidney. Pollut. Res. 15:371-373.

Shaheen, T. and Akhtar, T. 2012. Assessment of Chromium in *Cyprinus carpio* through hematological and bio chemical blood markers.Turk. J. Zool. 36(5):682-690.

Sharma, VJ. and Satyanrans. 2011. Effect of selected heavy metals on the histopathology of different tissue of earth worm *Eudrilus eugeniae*. Env Mont Ass 180:257-267.

Received: June 2, 2014; Revised: July 9, 2014; Accepted: July 11, 2014

SENRA Academic Publishers, British Columbia
Vol. 8, No. 3, pp. 3043-3050, October 2014
Online ISSN: 1920-3853; Print ISSN: 1715-9997

Canadian Journal of pure&applied sciences

ONTOLOGY DRIVEN ANALYSIS AND PREDICTION OF PATIENT RISK IN DIABETES

Sherimon PC[1],*Vinu PV[1], Reshmy Krishnan[2] and Youssef Saad[3]
[1]Department of Computer Science, M. S University, India
[2]Department of Computing, Muscat College, Oman
[3] Faculty of Computer Studies, Arab Open University, Oman

ABSTRACT

In any health care system, the patient medical history is crucial to help the doctors for further patient diagnosis. History of the patient is collected mainly through face-to-face interaction when the patient visits the hospital. If the medical staff is not well experienced, it results in failure of collecting the patient history. So in most of the cases, effective patient risk analysis cannot be done. This paper proposes an ontology based system to collect the patient history and to assess the patient risk factorsdue to smoking history, alcohol history, erectile dysfunction history, and cardiovascular history. According to the patient history, a total score is calculated for each of the above factors. According to the score, the ontology performs the risk assessment on a patient profile and predicts the potential risks and complications of the patient.Ontology is among the most powerful tools to encode medical knowledge semantically.

Keywords: Patient profile, risk assessment, ontology, clinical guidelines.

INTRODUCTION

The conventional health care information collection systems address the issues of interoperability, flexibility and scalability. Patient's information is an important component in any health care system. At the time of emergency, the previous medical history of the patient is crucial, so that appropriate attention and treatment can be given immediately on any place at any time (Sanjay and Anand, 2010). The main commitment for any health care system is to improve the quality and privacy of patient's information. Currently, patient information is collected mainly through static questionnaires, patient information collection systems (hard coded systems) or through face-to-face interaction when patient visits the hospital. Normally, when a patient visits a hospital, a nurse will first diagnose the patient and will record the preliminary observations such as readings of blood pressure, height, weight, body and temperature (Ahmadian *et al*., 2010). Then doctors carry out physical examination and gather further information about the patient. Here, in most of the cases, the patient medical history will be incomplete. There are many reasons for this incompleteness such as lack of experience of the medical staff in collecting relevant patient details, patient does not want to disclose certain sensitive and personal health problems, patient is not able to communicate many medical details related to family (family history) because of shortage of time, etc. Also in some cases, doctors may not be able to ask the exact questions to each and every patient. In effect, effective risk analysis cannot be done in most of the cases.

*Corresponding author email: vinusherimon@yahoo.com

In many health centers, the information is also obtained through a computerized database system, supporting the doctors. In this case, every patient is required to answer the same set of questions. Also in such systems, it is difficult to change the order of questions or to add extra questions without major programming work. So in order to avoid these shortcomings, we propose an ontology based system to collect the history of patients and to analyze and predict the patient risk factors. The proposed system generates the patient profile, apply clinical guidelines on the profile, examine the patient risk associated with different factors and predict the risk. Instead of a normal database system, a knowledge based approach is used. The intelligence of the system depends on its knowledge base and reasoning algorithm. Ontology based systems are easy to update without any additional cost or work. Ontology languages allow users to write explicit, formal conceptualizations of domain models (Vinu *et al*., 2014). They help to explicitly define the existing information about the domain and formally encode that information (Ashburner *et al*., 2000). W3C has developed a language, called OWL that can be used to describe the ontology (Huiqun *et al*., 2012). OWL is based on description logics (Sherimon *et al*., 2013a). OWL represents ontology by building hierarchies of classes that describe the concepts in a domain and the properties which relate these classes to each other (Kawazoe and Ohe, 2008). In OWL, data are represented as individuals of OWL classes and are manipulated by the inference mechanism realized by Semantic Web Rule Language (SWRL) that provides an accessible method for expression of domain information as a rule set of an antecedent-consequent pair (Kawazoe and Ohe, 2008).

MATERIALS AND METHODS

Currently available patient information gathering systems use static questionnaires. Sometimes, some of the questions in the questionnaire are irrelevant to a majority of the patients. Most of the systems are hard coded, so it is not easy to alter a question or to introduce new questions. Our approach is to use an ontology based questionnaire to gather the medical history of patients and to analyse the patient risk associated with many factors such as smoking, cardiac history, alcohol history, etc.

Ontology is a formal specification of the concepts within a domain and their interrelationships (Subhashini and Akilandeswar, 2011). It is a methodology which describes the domain knowledge structure in the area of specialty, which promotes its various kinds of data processing intended to provide systematic, semantic links among groups of related concepts (Mojgan *et al*., 2009). They are well known for many years in the Artificial Intelligence and Knowledge representation communities (Rajendra, 2009). Ontologies are used to represent knowledge. Domain knowledge is contained in the form of concepts, individuals belonging to these concepts and relationships between the concepts and, between concepts and individuals (Sherimon *et al*., 2013b). It was initially proposed to model declarative knowledge for knowledge-based systems (Haya, 2011). It is an abstract model which represents a common and shared understanding of a domain (Sherimon *et al*., 2013b). Gruber (1993) proposed the most popular definition of ontology which is defined as "…a formal, explicit specification of a shared conceptualization." The W3C has developed a language, called OWL that can be used to describe the ontology (Huiqun *et al*., 2012). It is built on W3C standards XML, RDF/RDFS and extends these languages with richer modelling primitives (Vinu *et al*., 2014).

Methodology

An ontology driven approach is utilized here to model the medical history of the patient and to assess the patient risk. Ontologies are the backbone of Semantic Web and they include the descriptions of classes, properties and their instances (Vinu *et al*., 2012). Ontology is among the most powerful tools to encode medical knowledge semantically. The ontology's structure facilitates the organization, retrieval, and analysis of the encoded knowledge, including database design and merging of databases (Andreas *et al*., 2009). Ontology Reasoners are used to checking the consistency of the ontology and to automatically compute the ontology class hierarchy (Sherimon *et al*., 2013a). The reasoner will find out any hidden relationship in the ontology (Sherimon*et al*., 2013c). The use of ontologies is well suited for applications in medicine. When certain relations are asserted in the ontology, an ontology reasoner can infer more relations, which is not explicitly asserted in the ontology (Sherimon *et al*., 2011). They are renowned for their flexible architectures, easy to share and reuse knowledge modelling structures and inexpensive maintenance operations (Kamran *et al*., 2012). So ontology based adaptive system are used to generate the profile of the patient.

Initially, a questionnaire was designed with the help of medical experts. The questions related to patient's family history, diabetic history, smoking history, etc. are included as ontological classes. Accordingly sub-classes, data properties and object properties were also defined. The user interfaces are created in Java. Jena API is used to read the questions from the ontology. The user input is analysed and the semantic profile is generated. Later the clinical guidelines are applied to the semantic profile and patient risk is analysed.

Implementation

Ontology Development

Questionnaire ontology is created in Protégé. All the main concepts are created as parent classes in Questionnaire ontology. They are *Question_Bank*, *Question*, *Answered Questionnaire*, *Patient*, etc. *Question-Bank* is an abstract class. It consists of different subclasses according to the category. These sub-classes contain instances that correspond to that particular category. For example, the instances of *Diatecian-QuestionBank* class are questions coming under nutritional history. The *Question* class consists of subclasses to hold each type of question. For example, instances of *MultipleChoiceQuestion* class are multiple choice type questions. The object property *contains* is used to associate the class *Question_Bank* with *Question* class. Data properties *questionno* and *question-part* are used to keep the question number and the question text. The object properties *hasChoice*, and *subQuestion* keeps a set of choices and one or more sub-questions, if any. The class *AnsweredQuestionnaire* is created to store the instances of patient records. The instances of the class *Patient* are used to store the risk factor score of the patient. Figure 1 represents the class hierarchy of Questionnaire ontology.

Creation of Semantic Profile

Java application developed using Jena APIs provides different interfaces for patient, nurse, doctor, lab technician and dietician. It reads the questions from the ontology and displays it to the user. Patient is required to answer a set of questions on diabetic history, family history, smoking history, alcohol history, physical-activity history, etc. Nurse will enter some vital information about the patient such as body temperature, blood pressure, height, etc. The dietician enters information about the nutritional history of the patient. The lab technician enters the results of different lab tests conducted and finally the doctor examines the patient and enters his/her observations. For every new patient, the system stores the

values entered by the users. Jena aims to provide a consistent programming interface for ontology application development, independent of which ontology language we are using in programs. Figure 2 shows the interface provided for the patients to enter his/her personal information.

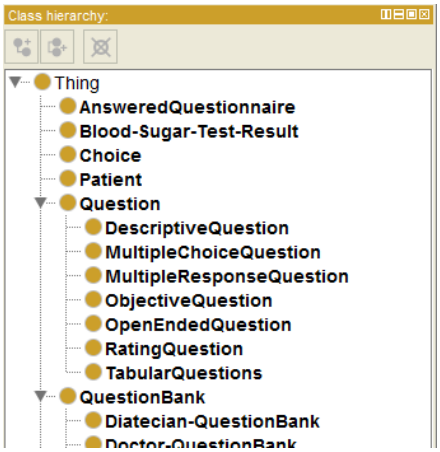

Fig. 1. Ontological Classes.

When the users complete filling the questionnaire, a new instance of *AnsweredQuestionnaire* class is automatically generated with patient ID as the instance name. For each instance, the values entered by the users are asserted into different data properties. For example, *questionnaire Answer-Cigarette-Count-Per-Day* is a data property to represent the number of cigarettes smoked by a patient per day. The domain of this class is *Answered Questionnaire* and the range is {10 or less, 11-20, 21-30 , 31 or more}. If a patient with ID 100 has chosen that he smokes 10 or fewer cigarettes a day, then the value of the property *questionnaireAnswer-Cigarette-Count-Per-Day* is "10 or less" for that particular instance.

Patient Risk Assessment

By performing the risk assessment on semantic profile, the potential risks and complications of a patient are predicted. The patient risk is assessed for five factors, according to smoking history, alcohol history, erectile dysfunction history, and cardiovascular history. It is done by checking the input provided by the users to different questions related to the above factors. A score is associated with each answer choice. So according to the user input, a total score is calculated for each category.

The clinical guidelines are hard coded in Java and the values generated are written back to the ontology. Figure 3 shows a section of the clinical guidelines implemented in Java. The risk/ risk level as per the score for each category is available in the clinical guidelines. Accordingly, the score, risk/ risk level, and suitable treatment are suggested by the system.

Here we are describing the estimation of cardiac score and the risk according to Framingham Heart Study, a risk assessment tool to predict a person's chance of having a heart attack in the next 10 years. According to Framingham heart study, the cardiovascular risk is calculated based on factors such as Gender, Age, Total Cholesterol, HDL, Systolic Blood Pressure, Smoking habit, and Hypertension. Table 1 represents the cardiovascular risk points associated with each factor in the case of Women.

According to the user input to the questionnaire, the total cardiovascular risk points are calculated and then the cardiovascular risk is calculated according table 2.

Table 1. CardioVascular Risk Points – Women.

Points	Age, years	HDL	Total Cholesterol	SBP (Not Treated)	SBP (Treated)	Smoker	Diabetic
−3				<120			
−2		>1.56					
−1		1.30–1.55			<120		
0	30–34	1.17–1.29	<4.14	120–129		No	No
1		0.9–1.16	4.14–5.15	130–139			
2	35–39	<0.9		140–149	120–129		
3			5.16–6.19		130–139	Yes	
4	40–44		6.20–7.24	150–159			Yes
5	45–49		>7.25	160+	140–149		
6					150–159		
7	50–54				160+		
8	55–59						
9	60–64						
10	65–69						
11	70–74						
12	75+						

Table 2. CardioVascular Risk – Women.

Points	Risk, %
≤−2	<1
−1	1.0
0	1.2
1	1.5
2	1.7
3	2.0
4	2.4
5	2.8
6	3.3
7	3.9
8	4.5
9	5.3
10	6.3
11	7.3
12	8.6
13	10.0
14	11.7
15	13.7
16	15.9
17	18.5
18	21.5
19	24.8
20	28.5
21+	>30

According to the risk calculated, the treatment is suggested as per the clinical guidelines. Figure 4 represents the part of the guidelines related to cardiovascular risk. The medicine *Aspirin* is recommended by considering the risk calculated in the above step and the risk factors such as age, smoking, hypertension, etc.

RESULTS AND DISCUSSION

Patient Medical History

The class *AnsweredQuestionnaire* is created to store the instances of patient records. It consists of all patient records stored in the form of ontology. Each patient is considered as an individual (instance) of this class and is automatically generated from Questionnaire Ontology using Property Insertion (OWL 2) and Individual Insertion (OWL 1 & 2) mechanisms. The *questionnaire Answer-Typical-Result* is the object property used to link the individuals of the classes *AnsweredQuestionnaire* and *Blood-Sugar-Test-Result*. *Blood-Sugar-Test-Result* class creates instances when a patient enters his/her blood results. When a patient enters his medical history, an instance of *AnsweredQuestionnaire* is asserted in the ontology. The name of the instance will be the patient Id. The values entered by the patient are stored in the concerned sub-data properties of the main data property *questionnaireDataTypeAnswers*.

The system instantiates the Questionnaire ontology and stores the corresponding answers in it. The System processes this information and automatically generates a Patient Ontology instance in the server. Patient Medical Profile is an OWL file which encapsulates patient details as entered by the patient, nurse and other users in a Web/Mobile Application. This file is initially generated as soon as the patient enters and submits the questionnaire through the application. Later, the same is updated by the Clinical officials (e.g. nurse). Figure 5 shows the semantic profile generated in OWL.

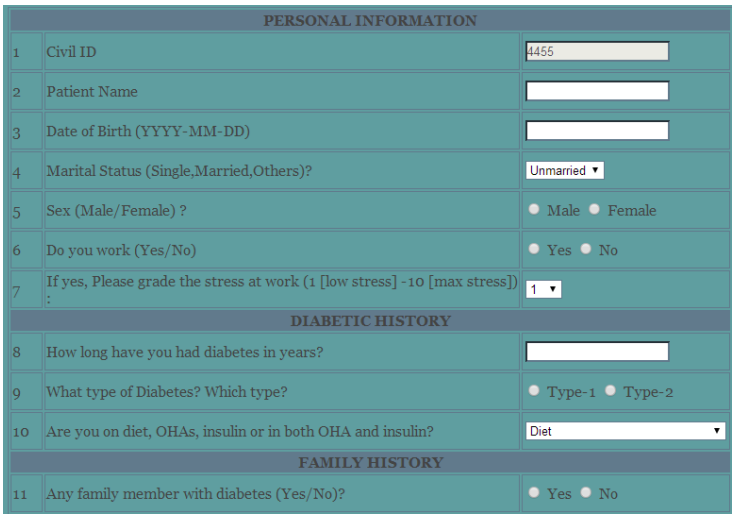

Fig. 2. Patient Interface.

```
if(uneasyGiveupTime.equalsIgnoreCase("First in the morning"))total_smoking_score++;
if(smokeSickTime.equalsIgnoreCase("Yes"))total_smoking_score++;
ontology.addDataPropertyValue("p_"+civil_id,"smoking-Score",OWL2Datatype.XSD_NON_NEGATIVE_INTEGER
if(total_smoking_score>=0&&total_smoking_score<=3){
    ontology.addDataPropertyValue("p_"+civil_id,"smoking-Risk-Level",OWL2Datatype.XSD_STRING,"Low
    ontology.addObjectPropertyValue("p_"+civil_id, "smoking-Treatment", "Score_Level-0-3");
}
if(total_smoking_score>=4&&total_smoking_score<=6){
    ontology.addDataPropertyValue("p_"+civil_id,"smoking-Risk-Level",OWL2Datatype.XSD_STRING,"Med
    ontology.addObjectPropertyValue("p_"+civil_id, "smoking-Treatment", "Score_Level-4-6");
}
if(total_smoking_score>=7&&total_smoking_score<=10){
    ontology.addDataPropertyValue("p_"+civil_id,"smoking-Risk-Level",OWL2Datatype.XSD_STRING,"Hig
```

Fig. 3. Clinical Guidelines in Java.

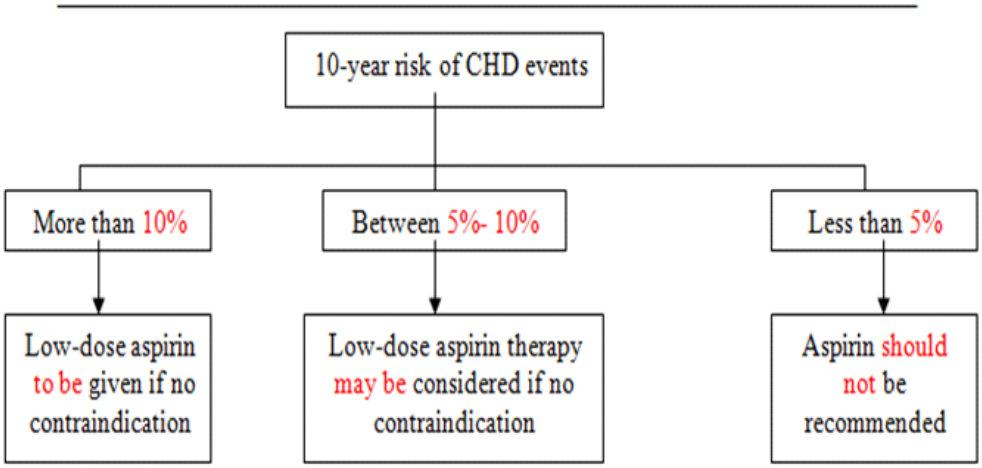

Fig. 4. Suggested Treatment as per the Risk %.

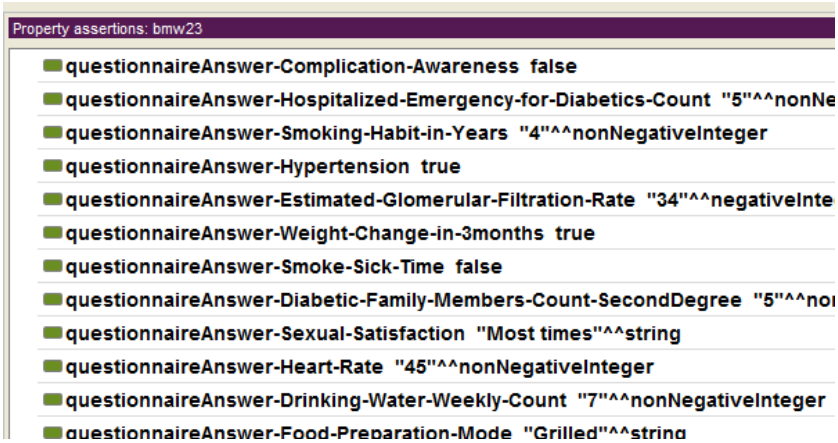

Fig. 5. Patient Profile: OWL View.

Doctor needs to view the history of the patient before suggesting treatment. The profile format created in OWL cannot be understood by a Doctor. So after the data is entered by patient, nurse, lab technician and dietician, the doctor can view the complete history of the patient in a tabular format. Figure 6 represents the view of Doctor.

Patient Risk Analysis

Apart from viewing the history of the patient, doctor can also view the risk of the patient associated with several factors. Every answer to a question carries a particular point. So according to the user input, the points will be allocated and total score is calculated for each and every

PATIENT PHYSICAL ACTIVITY HISTORY		
1	Type of Work & Related Physical Activity	My work involves definite physical effort including handling of heavy objects and use of tools
2	Physical Exercise Duration	Some but less than one hour
3	Cycling Time	Three hours or more
4	Walking Time	One hour but less than 3 hours
5	Child Care Time	Some but less than one hour
6	Gardening Time	One hour but less than 3 hours
7	Walking Pace	Slow Pace
PATIENT MEDICAL HISTORY		
1	Hospitalized for Diabetics?	Yes
2	No. of times hospitalized	5
3	Hospitalized in Emergency for Diabetics?	Yes

Fig. 6. Patient Profile: Doctor View.

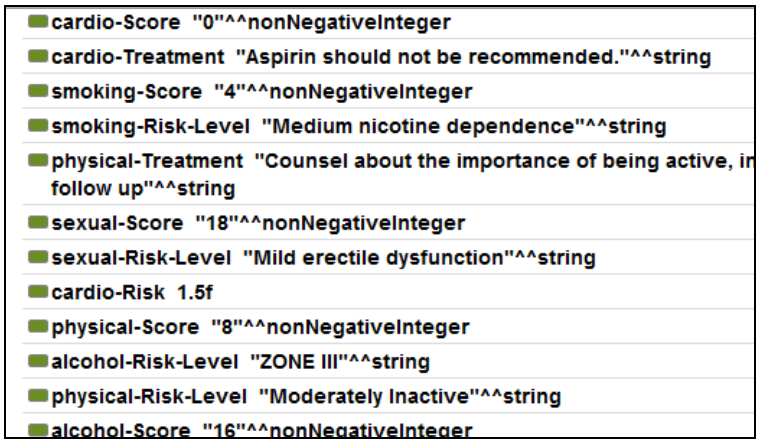

Fig. 7. Patient Score, Risk and Treatment asserted as Data Property values.

category. For example, according to the user input to all the questions included in the Smoking History Category, a score is calculated and it provides the risk of the patient due to smoking. The system will analyze the risk of the patient according to the history in five important aspects, Smoking, Alcohol, Sexual, Cardio Vascular and Physical and displays it.

Data properties are used to store the scores, risk level and the treatment of each of the above factors. For example, *cardio-score*, *cardio-risk* and *cardio-Treatment* are the data properties related to cardiac history. As per the clinical guidelines, the score, risk and treatment are calculated, an instance of Patient class is asserted in the ontology and the above calculated values are stored as data property values of the instance. Figure 7 shows the score, risk and treatment of a patient with ID P_789, for each of the parameters discussed earlier.

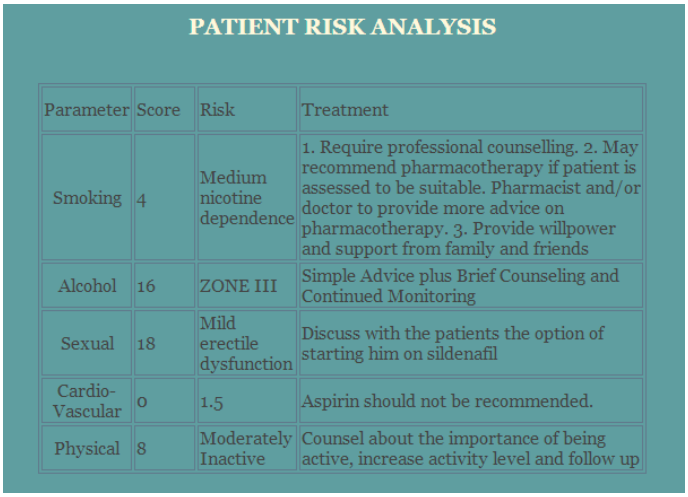

PATIENT RISK ANALYSIS

Parameter	Score	Risk	Treatment
Smoking	4	Medium nicotine dependence	1. Require professional counselling. 2. May recommend pharmacotherapy if patient is assessed to be suitable. Pharmacist and/or doctor to provide more advice on pharmacotherapy. 3. Provide willpower and support from family and friends
Alcohol	16	ZONE III	Simple Advice plus Brief Counseling and Continued Monitoring
Sexual	18	Mild erectile dysfunction	Discuss with the patients the option of starting him on sildenafil
Cardio-Vascular	0	1.5	Aspirin should not be recommended.
Physical	8	Moderately Inactive	Counsel about the importance of being active, increase activity level and follow up

Fig. 8. Patient Risk Analysis.

The patient risk analysis is also displayed in the form of a table for doctors to decide about further specific treatment to the patients. The system suggests treatment as per the risk associated with each factor. It is represented in figure 8.

CONCLUSION

Knowing Patient history is vital for a doctor to perform a proper patient risk assessment and to suggest appropriate treatment. We have used ontology based approach in generating the health history of patients. These systems gather better medical history than nurse/ dietician/ other hospital staff. The questionnaire is not static, it is adaptive in nature, so only relevant questions according to patient context will be asked. System reduces the number of questions, thus saving the time of patients. Since the questions are read from the ontology, if we want to add or update or delete any questions, we need to do it only in the questionnaire ontology. The information about each patient is generated as a separate OWL file. It can be viewed from Protégé in OWL format and also from the system in the tabular format. The patient risk associated with different factors is also generated. These risk values (score) will help the doctor to understand about the current situation of a patient. Ontology based reasoning makes a way to discover new knowledge, which can lead to new directions in research. The future scope of our research is to update the rules hard coded in Java to SWRL (Semantic Web Rule Language) to implement the Clinical Guidelines and to use the reasoning power of OWL to support the doctors in suggesting specific medicines and further detailed treatment.

REFERENCES

Ashburner, M., Ball, CA., Blake, JA., Botstein, D., Butler, H., Cherry, JM., Davis, AP., Dolinski, K., Dwight, SS., Eppig, JT., Harris, MA., Hill, DP., Issel-Tarver, L., Kasarskis, A., Lewis, S., Matese, JC., Richardson, JE., Ringwald, M., Rubin, GM. and Sherlock, G. 2000. Gene ontology: Tool for the unification of biology. The Gene Ontology Consortium. Nat Genet. 25(1):25-29.

Gruber, 1993. A translation approach to portable ontologies, Knowledge Acquisition. 5(2):199-220.

Haya, El-Ghalayini. 2011. E-Course Ontology for Developing E-Learning Courses. Developments in E-Systems Engineering (DeSE). 245-249.

Huiqun, Z., Shikhan, Z. and Junbao, Z. 2012. Research of using Protégé to Build Ontology. In: Proceeding(s) of the IEEE/ACIS 11th International Conference in Computer and Information Science. 697-700.

Kamran, FAH., Stephen, L., Chris, E., Calum, MR. and Warner, S. 2012. An Ontology Driven and Bayesian Network Based Cardiovascular Decision Support Framework, Advances in Brain Inspired Cognitive Systems. Lecture Notes in Computer Science. 7366:31-41.

Mojgan, H., Michihiko, K., Takako, T. and Hiroshi, T. 2009. Development of clinical ontology for mood disorder with combination of psychomedical information. Journal of Medical and Dental Sciences. 56(1):1-15.

Rajendra, A. 2009. Foundations of the Semantic Web. Narosha Publishing House.

Subhashini, R. and Akilandeswar, J. 2011. A Survey on Ontology Construction Methodologies, International Journal of Enterprise Computing and Business Systems. 1(1):60-72.

Sanjay, A. and Akshat, V. 2010. Development of Ontology for Smart Hospital and Implementation using UML and RDF. IJCSI International Journal of Computer Science. 7(5):206-212.

Sherimon, PC.,Vinu, PV., Reshmy, K. and Youssef Takroni. 2013[a]. Developing Survey Questionnaire Ontology for the Decision Support System in the Domain of Hypertension. IEEE South East Conference, Florida, USA.

Sherimon, PC., Reshmy, K., Vinu, PV. and Youssef Takroni. 2013[b]. Ontology Based System Architecture to Predict the Risk of Hypertension in Related Diseases. International Journal of Information Processing and Management. 4(4)doi:10.4156/ijipm.

Sherimon, PC., Reshmy, K., Vinu, PV. and Youssef, T. 2013[c]. Exhibiting Context Sensitive Behavior in Gathering Patient Medical History in Diabetes Domain using Ontology. International Journal of Advancements in Computing Technology. IJACT. 5(13):41-47.

Vinu, PV., Sherimon, PC. and Reshmy, K. 2014. Development of Ontology for Sea food Quality Assurance System. Journal of Convergence Information Technology. 9(1):25-32.

Vinu, PV., Sherimon, PC. and Reshmy, K. 2012. Knowledge - Base Driven Framework for Assuring the Quality of Marine Seafood Export. International Journal of Artificial Intelligence and Knowledge Discovery. 2(3): 6-10.

Kawazoe, Y. and Ohe, K. 2008. An Ontology-based Mediator of Clinical Information for Decision Support Systems: A Prototype of a ClinicalAlert System for Prescriptions. Methods Inf Med. 47:549-559 doi:10.3414/ ME9126.

Received: April 19, 2014; Accepted: June 26, 2014

SENRA Academic Publishers, British Columbia
Vol. 8, No. 3, pp. 3051-3055, October 2014
Online ISSN: 1920-3853; Print ISSN: 1715-9997

Canadian Journal of pure&applied sciences

AN OVERVIEW OF THE STATUS AND DISTRIBUTION OF THE MANGROVE FORESTS AND THEIR WILDLIFE IN SINDH

*Said A Damhoureyeh[1] and Syed Ali Ghalib[2]
[1]Department of Biology, Faculty of Science, University of Jordan, Amman, 11942, Jordan
[2]Department of Zoology, University of Karachi, Karachi-75270, Pakistan

ABSTRACT

Globally some of the largest mangrove forests are found in Asia. The shoreline of Pakistan is approximately 990 km long and 40-50 km wide. It is dominated by the Mangroves *Avicennia marina*. In Pakistan, eight species of mangroves was reported in the coastal areas, out of which, now only 4 species survive in the Indus Delta. Total area covered by mangroves in 32,000 ha, of which 129,000 ha lies in Indus Delta and approximately 3,000 ha on the coast of Balochistan including the areas of Miani Hor, Kalmat Khor and Gwatar Bay. In Sindh Province, major mangrove plantations and associated ecosystems have been found in Indus Delta, Karachi Coast and Keti Bunder areas. In this paper, we reviewed status and distribution of the mangrove forests and their important wildlife.

Keywords: Indus delta, mangroves, distribution, status.

INTRODUCTION AND DISCUSSION

There is growing empirical and theoretical evidence that ecosystem functions and services are linked with biodiversity (Cardinale *et al.*, 2012; Hooper *et al.*, 2012; Tilman *et al*., 2001). Coastal habitats such as mangroves, sea grass beds, salt marshes and shellfish reefs continue to decline in extent, threatening highly valuable ecosystem services including the removal of significant quantities of carbon dioxide from the atmosphere. Coastal ecosystems and near shore marine areas are among the most productive yet highly threatened systems in the world (Wilkinson, 2004). Globally, a 25% reduction in mangrove area has been observed since 1980, categorizing mangroves as one of the most threatened and vulnerable ecosystems of the world (Abbas *et al*., 2013). Currently, Asia has the largest mangrove area of any region, and the mangroves are exceptional for their high biodiversity. Pakistan harbours the largest mangrove forest cover over the world in an arid climate. Historically, more than 160,000 ha of the Indus Delta were covered with mangroves which have now significantly reduced. The Indus Delta constitutes 97% of the total mangrove forests found in Pakistan. The survival of mangrove forests is largely associated with perennial freshwater supply from the River Indus that flows through the delta before reaching the Arabian Sea (WWF-Pakistan, 2006).

The mangroves provide a habitat and breeding ground for a variety of marine life (particularly fish, shrimps and crabs). They also provide suitable habitats for migratory birds, protect the coastline and the seaports from erosion, meet fuel wood and fodder requirements of the local communities and support the livelihood of the coastal population of over 10 millions in Sindh (IFAP, 2008a,b).

In Pakistan, the total area covered by mangroves is 32,000 ha, of which 129,000 ha lies in Sindh (Indus Delta) and approximately 3,000 ha on the coast of Balochistan including the areas of Miani Hor, Kalmat Khor and Gwatar Bay (Memon, 2000). The Sindh coastline is characterized by mudflats, delta wetlands, estuary systems and a wide and almost flat continental shelf (www.mangrovesforthefuture.org).

Mangrove Species of Pakistan

Mangrove forests are highly-productive ecosystems in the inter-tidal zones of tropical and sub-tropical coastlines. In the coastal areas of Pakistan, eight species of mangroves have been reported (UNESCAP, 1996). Out of which, now only four species have survived in the Indus Delta (Table 1).

Table 1. Mangrove Species of Pakistan.

Family Rhizopharaceae
1. *Bruguiera conjugate*
2. *Ceriops tagal**
3. *Ceriops roxburghiana*
4. *Rhizophora apiculata*
5. *Rhizophora mucronata**

Family Myrcinaceae
6. *Aegiceras corniculata**

Family Avicenniaceae
7. *Avicennia marina**

Family Sonneratia
8. *Sonneratia caseolaris*

*Species still surviving

*Corresponding author email: saidd@ju.edu.jo

Important Sites
The important sites in Sindh with mangrove plantations and associated ecosystems have been found in Indus Delta, Karachi Coast and Keti Bunder.

Indus Delta
The Indus delta mangrove forests are unique in being the largest area of arid climate mangroves in the world. The Indus Delta is a vast complex of tidal river channels and creeks, low-lying sandy islands, mangrove swamps and inter tidal mudflats stretching from near Korangi Creek in the north east to Sir Creek on the Indian Border. There are 17 major creeks in the original Indus Delta. These include: Korangi Creek, Gharo / Phitti Creek System, Chann Waddo Creek, Khuddi Creek, Khai Creek, Patiani Creek, Dabbo Creek, Sisa Creek, Bhuri Creek, Hajamro Creek, Tursian Creek, Khobar Creek, Qalandri Creek, Kahr Creek, Wari Creek, Kajhar Creek and Sir Creek. Due to reduced flows from Kotri only the area between the Hajamro Creek and Kharak Creek now receives water from the Indus, and there is only one main outlet to the Sea the Khobar Creek.

The mangroves forest of Indus delta is found only in estuaries between mean sea level and high water spring tides. Mangroves covering an area of about 600,000 hectares, constitute an important ecosystem in the coastal deltaic region formed by the River Indus (Saifullah, 1997). Presently, there are four mangrove species in the Indus delta with areas covered in brackets: *Avicennia marina* (90%), *Rhizophora mucronata* (8%), *Aegiceras corniculatum* (1.5%) and *Ceriops tagal* (0.5%) (Sindh Forest Department, 2014; http://sindhforests.gov.pk/mangroves).

Currently, *Avicennia marina* is dominant and occurs as an almost monotypic stand throughout the delta. The Indus Delta was designated a Ramsar Site on 5 November 2002.

The area is rich in wildlife and hence it has been declared as a Wildlife Sanctuary, mainly for water birds. The migratory birds include Pelicans, Herons and Egrets, Waders and Raptors. Among Mammals, Wild Boar, Indian Jackal and Cetaceans (Humpback Dolphin and Bottlenosed Dolphin) have been recorded, while Indian Cobra, Vipers, and Sea Snakes are recorded as common reptiles.

Karachi Coast
It forms a complex of tidal areas and marshes with extensive mangrove swamps and inter tidal mudflats, near the southeastern outskirts of Karachi. This is an important site for water birds. Due to its important biological features, it has been included in Global 200 Ecoregions (North Arabian Sea). It contains the following two important sites:

The Sandspit Backwaters Area
It is located 18 km southwest of Karachi, stretching about 20 km along the Arabian Sea Coast with extensive intertidal mudflats and 1640 ha of mangrove swamps behind the beach (Fig. 1).

Karachi Harbour Backwaters
It includes Chinna Creek and the Boat Basin Area. It has a wide enclosed wetland area with mangroves. It is a good area for gulls and terns. It is potentially a very good area for recreational development.

Keti Bunder
Keti Bunder lies about 200 km southeast of Karachi, constituting part of the Indus Delta (Fig. 2). The settlements are built on the mudflats between the channels/ creeks. The location of Keti Bunder has changed thrice during the past 70 years due to intrusion of the sea. The Keti Bunder reduced natural resource, most notably a decline in freshwater flows due to anthropogenic activities, so that the community is almost totally reliant on fishing in the surrounding sea and creeks and poverty remains high despite some infrastructure development (Asian Development Bank, 2008). The mangrove forests along Keti Bunder have suffered due to diversion of Indus River water for agriculture and hydropower generation through construction of dams and barrages over it. The area is rich in wildlife and hence it has been declared as a Wildlife Sanctuary, mainly for water birds.

In 2008 WWF Pakistan reported that 69 bird species including 25 resident and 44 migratory species. 21 species of reptiles, 2 species of amphibians, 63 species of finfish and 24 species of shellfish were observed. The migratory birds include Pelicans, Herons and Egrets, Waders and Raptors. Among Mammals, Wild Boar, Indian Jackal and Cetaceans (Humpback Dolphin and Bottlenosed Dolphin) have been recorded, while Indian Cobra, Vipers, and Sea Snakes are recorded as common reptiles (Hasnain, 2005).

Fauna of the Mangrove Forests
The mangrove forests provide important habitat for invertebrates and vertebrate species and serve as critically important spawning grounds and nurseries for fishes and aquatic crustaceans. The wildlife of the mangroves of Sindh comprises of the following important mammals, birds and reptiles (Ahmed *et al.*, 1989).

The mammalian species recorded from the mangrove areas include Humpbacked Dolphin (*Sousa plumbea*), Bottlenosed Dolphin (*Tursiops truncatus*), Finless Porpoise (*Neophocaena phoceanoides*), Indian Jackal (*Canis aureus*), Fishing Cat (*Prionailurus viverrinus*), Wild Boar (*Sus scrofa*) and Small Indian Mongoose (*Herpestes javanicus*).

Fig. 1. Mangroves Forest at Sandspit Backwaters Area, Karachi.

Fig. 2. A view of Mangroves Forest at Keti Bunder.

Among the birds, a wide variety of birds has been recorded, comprising of waterbirds, birds of prey, passerines and others. As many as 78 species have been recorded. The key/widespread species include: Kentish Plover (*Charadrius alexandrinus*), Terek Sandpiper (*Tringa terek)*, Common Sandpiper *(Tringa hypoleucos)*, Grey Heron (*Ardea cinerea*), Bartailed Godwit *(Limosa lapponica)*, Little Stint (*Calidris minutus*), Dunlin (*Calidris alpina*), Herring Gull (*Larus argentatus*), Slenderbilled Gull (*Larus genei*), Blackheaded Gull (*Larus ridibundus*), Caspian Tern (*Hydroprogne caspia*), Sandwich Tern (*Sterna sandvicensus*), Brahminy Kite *(Haliastur indus*), Common Kite (*Milvus migrans*), Cinereous Vulture (*Aegypius monachus*), Common Crow (*Corvus splendens*) and White – eye (*Zosterops palpebrosa*).

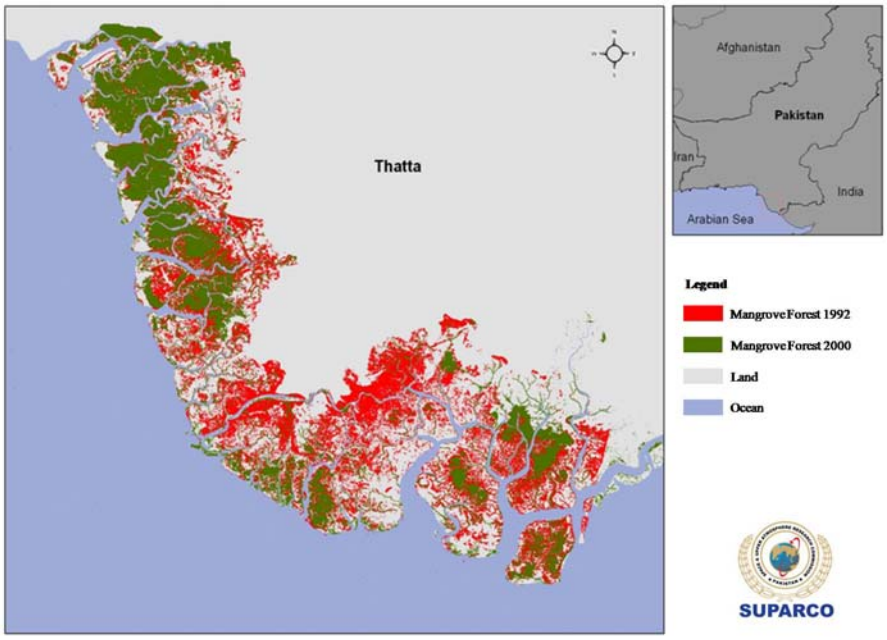

Fig. 3. Mangrove Forest Cover along Indus Delta Thatta, Sindh – 1992 and 2000 (Source: SUPARCO).

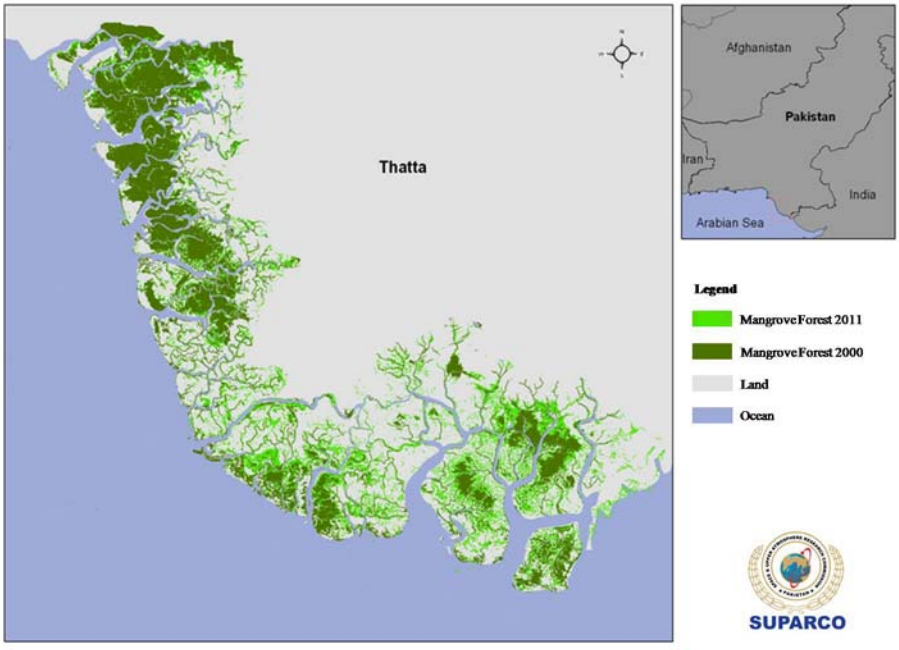

Fig. 4. Mangrove Forest Cover along Indus Delta Thatta, Sindh – 2000 and 2011 (Source: SUPARCO).

Among the reptiles, Beaked Sea Snake, (*Enhydrina schistose*), Annulated Sea Snake, (*Hydrophis cyanocinctus*), Yellow Sea Snake (*Hydrophis spiralis*), Blue-green Sea Snake (*Hydrophis caerulescens*), Small-headed Sea Snake (*Hydrophis fasciatus*) and Pelagic Sea Snake (*Pelamis platurus*) have been recorded.

Threats

The main threats to the mangrove ecosystem on the Sindh Coast include habitat destruction, land reclamation for housing schemes, coastal and industry development, wood cutting for fuel wood, overgrazing by camels, salt water intrusion, lack of freshwater in the Indus,

construction of various dams, Canals and barrages and Pollution. Currently due to human interventions climate change and environmental degradation the mangrove forests of the Indus Delta region are under stress.

The analysis of satellite images and measurements of the spatial extents made by Pakistan Space and Upper Atmosphere Research Commission (SUPARCO) have estimated that the mangrove forest cover has changed from 1992 to 2000 with loss of approx. 50000 ha forest cover and for years 2000 to 2011 (see Figs. 3 and 4)

Due to several threats**,** as a result, there has been a marked degradation in the mangrove forest cover in Pakistan, as given in table 2 (IUCN, 2005).

Table 2. Coverage of Mangrove Forests along the Coast of Pakistan (Source: IUCN, 2005).

Mangrove Categories	Year	Area in Hectares
Dense, normal and sparse Mangrove vegetation	1932	604,870
	1986	440,000
	1996	160,000
	2005	86,000

Conservation

A lot of afforestation initiatives have been taken to plant *Avicennia* and *Rhizophora* species in the Indian Delta particularly at Korangi / Phitti / Kadero Creeks (Karachi Coast) and at Shahbander (Thatta District) by IUCN and the Sindh Forest Department. In 1990 a collaboration between the Government of Pakistan and the World Conservation Union (IUCN) facilitated the rehabilitation of 19 000 ha of *Avicennia marina* and *Rhizophora mucronata*.

Recently, the Provincial Forest Department set a new Guinness Book of World Records on June 23rd of 2013 by planting 750,000 mangrove saplings at Kharochhan, district Thatta, in just over 12 hours. This is the highest number of saplings planted within a day (Rafiul Haq, Pers. Comm).

In 2009, the Sindh Forest Department had set a record by planting 541,176 saplings at Keti Bunder. The record was toppled later that year by India.

REFERENCES

Abbas, S., Mueen, QF., Ghaffar, ANKT., Khurram, SRS. and Gilani, H. 2013. An Assessment of status and distribution of mangrove forest cover in Pakistan. J. Bio. E. Env. Sci. 3(6):64-78.

Ahmad, MF., Ghalib, SA., Niazi, MS., Perveen Z. and Hassan, A. 1989. Study of the Vertebrate Fauna of Mangrove Swamps of Sindh Coast. PARC Final Report Zoological Survey Department, Karachi. (Unpublished Report).

Asian Development Bank. 2008. ADB Annual Report 2008. ISSN. 306-8370

Cardinale, BJ., Duffy, JE., Gonzalez, A., Hooper, DU., Perrings, C., *et al*. 2012. Biodiversity loss and its impact on humanity. Nature 486:59-67.

Hasnain, SA. 2005. Keti Bunder Village Development Plan. WWF-Pakistan, Karachi. pp30.

Hooper, DU., Adair, EC., Cardinale, BJ., Byrnes, JEK., Hungate, BA., *et al*. 2012. A global synthesis reveals biodiversity loss as a major driver of ecosystem change. Nature. 486:105–U129.

Indus For All Program (IFAP). 2008[a]. Indus Delta-A vanishing Ecosystem. WWF-Pakistan, Karachi.

Indus For All Program (IFAP). 2008[b]. Mangroves of Pakistan WWF- Pakistan, Karachi, pp16.

IUCN Pakistan. 2005. Mangroves of Pakistan-Status and Management.pp 110.

Memon, N. 2000. Damming the Delta. LEAD, Pakistan.

Pakistan Space and Upper Atmosphere Research Commission (SUPARCO).

Saifullah, SM. 1997. Management of the Indus Delta Mangrove. In: Coastal Zone Management Imperative for Maritime Developing Nations. Eds. Haq, BU., *et al*. Kluwer Academic Publishers, Netterlands. 333-346.

Sindh Forest Department. 2014. Mangrove. http://sindhforests.gov.pk/mangroves .

Tilman, D., Reich, PB., Knops, J., Wedin, D., Mielke, T., *et al*. 2001. Diversity and productivity in a longterm grassland experiment. Science 294:843–845.

UNESCAP. 1996. Coastal Environmental Management Plan for Pakistan.

Wilkinson, C. 2004. Status of Coral Reefs of the World. Australian Institute of Marine Science (AIMS), Townsville, Australia.

WWF Pakistan. 2006. Mangrove Ecosystem of Pakistan. pp4.

www.mangrovesforthefuture.org

World Wildlife Fund Pakistan. 2008. Detailed Ecological Assessment of Fauna Including Limnology Studies at Keti Bunder. Indus for All Program, WWF Pakistan.

Received: July 1, 2014; Revised and Accepted: Aug 15, 2014

SENRA Academic Publishers, British Columbia
Vol. 8, No. 3, pp. 3057-3060, October 2014
Online ISSN: 1920-3853; Print ISSN: 1715-9997

Canadian Journal of pure&applied sciences

Short Communication

RISK FACTOR OF METABOLISM ALTERATION IN BURN PATIENTS

Fatin F Alkazaz[1],*Sura A Abdulsattar[2], Farred MA Farred and Shahad J Mahmood
Department of Chemistry, College of Science, Al-Mustansyria University, Iraq

ABSTRACT

Severe burn causes a catabolic response with profound effects on glucose and muscle protein metabolism. Our aim is to determine whether a changes of metabolism and inflammatory protein like serum albumin and CRP and if their level can predict mortality in burn patients.Twenty seven burn patients were included in this study and compared with twenty seven healthy donors. A significant differences ($p<0.001$) between burn patients and control group were observed in total protein, albumin, globulin, high sensitive C reactive protein, urea, and uric acid. While a non significant increase ($p>0.05$) in glucose level was observed in burn patients. On the other hand a non significant difference ($p>0.05$) between burn degrees in same parameters were observed. We conclude from the present study that the metabolic changes occur in patients with varying degrees of burns and its values didn't depended on burn degree, although its values can be use to predict the mortality of burn patients.

Keywords: Burn, hypermetabolism, albumin, risk factor, glucose.

INTRODUCTION

Burn injuries are among the most destructive of all injuries and a major global public health problem (Peck *et al*., 2008). The changes in patient metabolism following a major burn may be seen for more than 12 months after the initial injury (Norbury *et al*., 2006). Hypermetabolism is occur in response to severe burns patient (Williams *et al*., 2009; Machado*et al*., 2011). It is characterized by hyperdynamic circulatory, physiology, catabolic, immune system responses, and increased risk for infection (Hart *et al.,* 2000). These changes are responsible for much of the morbidity and mortality seen with such an injury (Norbury *et al*., 2006). The use of prognostic factors has been attempted in burn patients, such as sex, age, total burned body surface area (BSA), full-thickness injuries, and serum albumin levels (Tobiasen *et al*., 1982; Hörbrand*et al*., 2003). However early identification of patients with the greatest risk is essential for their management, and their overall treatment (Colleen, 1998). Severe burn causes a catabolic response with profound effects on glucose and muscle protein metabolism. This response is characterized by hyperglycemia and loss of muscle mass, both of which have been associated with significantly increased morbidity and mortality (Ballian *et al*., 2010). Plasma C-reactive protein (CRP) is a biomarker commonly used to assess the inflammatory response, and increases are associated with increased inflammation, infection, or sepsis (Lavrentieva *et al.,* 2007). Hypoalbuminemia is a common clinical deficiency in burn patients and is associated with complications related to increased extravascular fluid, including edema, abnormal healing, and susceptibility to sepsis (Aguayo-Becerra *et al.,* 2013). Urea is a measure of the major end product of protein metabolism (Grove *et al*., 1995). Uric acid is an end product of purine metabolism . Uric acid is more toxic to tissue than xanthine or hypoxanthine (Yadav, 2010).

Some prognostic tools do not include biochemical parameters, whereas others consider them together with comorbidities it would be ideal to have a biomarker to predict the risk of developing severe infection.The purpose of this study was to determine whether a changes of metabolism and the inflammatory protein like serum albumin and CRP and if their level can predict mortality in burn patients.

MATERIALS AND METHODS

A total of 27 patients with burn attending Al-Kindy Hospital in Baghdad city were participated in this study. We obtained general information about each patient, including age, sex, etiology, location of burns and degree burn. As a control of 27 healthy individual with matches were included in this study. Five ml were collected from healthy donors and patients. The blood sample was centrifuged at 3000 rpm for 5 min after allowing the blood to clot at room temperature. Serum separated and transferred into test tube,and stored at -20^0C until being used. Total protein was measured by Biuret method, and albumin levels were measured by (Bromo Cresol Green) BCG method. High sensitive CRP and IL10 were measured using Enzyme Linked Immuno Assay (ELISA) kits.

*Corresponding author email: sura742003@yahoo.com

The statistical software (SPSS v 15; Chicago, IL, USA) was used. The data were analyzed using unpaired *t*-test and person correlation coefficients. differences were considered significant when $P< 0.05$.

RESULTS AND DISCUSSION

Demographic study of burn patients presented that among 27 burn patients 66.6% were female, 33.3% were male of 14-66 years age. Including 40.7% of burn patients were second degree, 40.7% were third degree, and 18.5% were mixed of second and third degree. Burn wounds were caused by flame in 23 cases, by hot water in 2 cases, by electricity in 2 cases (Table 1).

Hypermetabolic response in burn patients occurs by altering the physiological and biochemical environment characterized by increased metabolic rates, multi-organ dysfunction, muscle protein degradation, blunted growth, insulin resistance (Atiyeh*et al*., 2008).

Total protein concentration was measured in the sera of control and burn patients according to biuret method. The results in table 2 showed the presence of a highly significant decrease in protein concentration in sera of burn patients in comparison to that of the control group and this decrease was due to the overwhelming protein losses by bleeding, where with bleeding the protein is lost along with the blood so the more deeper the burn is, the more bleeding and more protein-rich fluid leaks from the open burn wounds causes a high decrease in protein concentration (Lehnhardt *et al*., 2005). This result was agreement with the results obtained by Manelli *et al*. (1998) who showed that low values of protein observed in burn patients are caused by several factors including microvascular hyper-permeability and inflammatory processes. Also the result was agreement with the results obtained by Lenhardrat *et al.* (2005) who found that protein levels in serum were significantly lower as compared to physiological levels.

A highly significant decrease of albumin level ($p \square 0.001$) was observed in the present study in sera of burn patients compared to control group. This result in line with the fact that skin is the major storage for albumin so whenever the skin got burned the albumin level will decrease (Aguayo-Becerra *et al*., 2013). Burns affecting >20% of the body surface cause a major loss of extracellular fluids, thereby inducing shock by increasing vascular permeability and reducing plasma albumin from the wound exudations (Lehnhardt *et al*., 2005). The results of the present study was agreement with Aguayo-Becerra *et al*. (2013) who suggests that hypoalbuminemia has a deleterious effect on patient survival but does have some limitations. Miquet-Rodríguez *et al*. (2013) reported a mortality rate of <10% in severely burn patients (2/23) in whom hypoalbuminemia was frequently observed, demonstrating a significant association between the extent of the burn and the serum albumin level.

Globulin level in this study showed a highly significant decrease ($p<0.001$) in sera of burn patients compared to control group. This decrease is due to blood loss via damaged skin (Steven *et al*., 2008). This result was agreement with Muhammad and Hayder (2011) who found that the total serum protein, albumin and globulin of male and female burn patients shows significant decrease ($p<0.01$).

Table 1. Demographic study of burn patients.

Category	Number (%)
Age in year	
0-19	6(22.2)
20-39	13(48.1)
40-59	7(25.9)
≥60	1(3.7)
Gender	
Male	9(66.6)
Female	18(33.3)
Burn degree	
Second II	11(40.7)
Third III	11(40.7)
Mix(II &III)	5(18.5)
Etiology	
Thermal	23(85.1)
Hot water	2(7.4)
Electricity	2(7.4)

The acute phase response develops in a wide range of acute and chronic inflammatory conditions. The physiological role of CRP is to bind to phosphocholine expressed on the surface of dead or dying cells in order to activate the complement system. Measuring CRP level is a screen for infectious and inflammatory diseases (Du Clos, 2000). A highly significant increase in hsCRP level ($p<0.001$) was observed in the present study in sera of burn patients compared to control group. This result was agreement with Jeschke *et al*. (2013) who found that significantly higher levels of CRP were found in large burns, and CRP values significantly correlated with burn size, survival and gender. Pileri *et al*. (2009) showed in their study that CRP levels were higher in septic than in non septic patients ($p < 0.05$), but until day 15 day CRP values did not distinguish survivor from non survivor septic patients.

For many years a condition of hyperglycemia among patients suffering major burn injury was considered as a normal and desired response (Holm *et al*., 2004; Hemmila *et al*., 2008; Chatham *et al*., 2008). However the present study showed a non significant increase of glucose level in sera of burn patients in compared to control group. This result may be due to insulin administration as therapy

Table 2. Mean values of serum total protein, albumin, globulin, hsCRP, glucose, urea, and uric acid.

Parameters	Control Mean± SD	Burn patient Mean± SD	P Value
Total protein(g/dl)	8.0484±1.1927	4.990±1.1783	p<0.001
Albumin(g/dl)	3.7413±0.73	2.552±0.6977	p<0.001
Globulin(g/dl)	4.3067±1.539	2.394±1.178	p<0.001
hsCRP(µg/dl)	87.0792±121.05	337.8393±134.163	p<0.001
Glucose(mg/dl)	96.7248±18.555	109.25±34.329	p<0.05
Urea(mg/dl)	15.197±3.5743	35.7363±16.1967	p<0.001
Uric acid(mg/dl)	5.7933±0.7573	2.9233±1.4191	p<0.001

Table 3. Mean values of different parameters in sera of burn patients at II,III, and mix (II&III) degrees.

Parameters	II degree Mean± SD	III degree Mean± SD	Mix(II&III)degree Mean± SD
Total protein(g/dl)	5.0765±1.124	4.7216±.962	5.423±1.8965
Albumin(g/dl)	2.6151±0.8068	2.4134±0.6809	2.725±0.464
Globulin(g/dl)	2.4614±0.3172	2.3082±0.2811	2.698±1.432
hsCRP(µg/dl)	299.829±164.96	350.646±141.28	366.35±86.12
Glucose(mg/dl)	98.758±32.843	112.80±39.48	124.548±20.88
Urea(mg/dl)	37.819±21.22	35.00±10.60	32.77±16.52
Uric acid(mg/dl)	3.1045±1.63	2.901±1.53	2.575±0.518

where it is well known that insulin has anti-hyperglycemic action,reduction in infections, promotes muscle anabolism and regulates the systemic inflammatory response (Ballian *et al*., 2010).

Burns cause a reduces of blood flow to the kidney which lead to, build up of nitrogen waste products, such as creatinine and urea in the body (azotemia). Prerenal azotemia is the most common form of kidney failure in hospitalized patients (Yu ASL 2007). Sabry *et al*. (2009) conclude from their study that acute renal failure complicates burn patients and is related to the size and depth of burn and occurrence of septicemia. A highly significant increase in urea level ($p< 0.001$) was observed in the present study in sera of burn patients compared to control group.

Uric acid results of the present study showed a highly significant decrease ($p< 0.001$) in their levels in sera of burn patients in compared to control group. This decrease is due to increase the fractional excretion of uric acid (Peretz *et al*., 1983). Conflicting results for uric acid level in burns were observed where Nagane *et al.* (2003) indicated in their study significant increase of uric acid in burn patients due to increased activity of xanthine oxide. While Yadav (2010) showed in his study a significant decrease in seum uric acid of burn patients in compared to control group.

The overall analysis of different parameters study in sera of burn patients at degree II, degree III, and mixture degree (II & III) were presented in table 3. As shown from the Mean values there were a fluctuation in total protein, albumin, and globulin between these degrees. While a non significant increase in hsCRP and glucose levels ($p>0.05$), and a non significant decrease ($p>0.05$) in urea and uric acid levels were observed.

CONCLUSION

We conclude from the present study that the metabolic changes occur in patients with varying degrees of burns and its values did not depended on burn degree, suggesting that its value can be used to predictthe mortality of burn patients.

REFERENCES

Aguayo-Becerra, OA., Torres-Garibay, C., Macías-Amezcua, MD., Fuentes-Orozco, C., Chávez-Tostado Mde, G., Andalón-Dueñas, E., Espinosa Partida, A., Alvarez-Villaseñor, Adel S., Cortés-Flores, AO. and González-Ojeda, A. 2013. Serumalbuminlevel as a riskfactor for mortality in burnpatients. Clinics (Sao Paulo). 68(7):940-945.

Atiyeh, BS., Gunn, SW. and Dibo, SA. 2008. Metabolic implications of severe burn injuries and their management: a systematic review of the literature. World J Surg. 32(8):1857-69.

Ballian, N., Rabiee, A., Andersen, DK., Elahi, D. and Gibson, BR. 2010. Glucose metabolism in burn patients: the role of insulin and other endocrine hormones. Burns. 36(5):599-605.

Chatham, JC., Nöt, LG., Fülöp, N. and Marchase, RB. 2008. Hexosamine biosynthesis and protein O-glycosylation: the first line of defense against stress, ischemia, and trauma. Shock. 29(4):431-440.

Colleen, M. 1998. Objective estimates of the probability of death from burn injuries. N Engl J Med. 335(5):362-7.

Du Clos, TW. 2000. Function of C-reactive protein. Ann Med. 32(4):274-8.

Grove, G. and Jackson, AA. 1995. Measurement of protein turnover in normal man using the end-product method with oral [15N]glycine: comparison of single-dose and intermittent-dose regimens. Br J Nutr.74(4):491-507.

Hart, DW., Wolf, SE., Mlcak, R., Chinkes, DL., Ramzy, PI., Obeng, MK., Ferrando, AA., Wolfe, RR. and Herndon, DN. 2000. Persistence of muscle catabolism after severe burn. Surgery. 128(2):312-9.

Hemmila, MR., Taddonio, MA., Arbabi, S., Maggio, PM. and Wahl, WL. 2008. Intensive insulin therapy is associated with reduced infectious complications in burn patients. Surgery. 144(4):629-635.

Holm, C., Hörbrand, F., Mayr, M., von Donnersmarck, GH. and Mühlbauer, W. 2004. Acute hyperglycaemia following thermal injury: friend or foe? Resuscitation. 60(1):71-77.

Hörbrand, F., Schrank, C., Henckel-Donnersmarck, G. and Mühlbauer, W. 2003. Integration of preexisting diseases and risk factors in the Abbreviated Burn Severity Index (ABSI) Anasthesiol Intensivmed Notfallmed Schmerzther. 38(3):151-7.

Jeschke, MG., Finnerty, CC., Kulp, GA., Kraft, R. and Herndon, DN. 2013. Can we use C-reactive protein levels to predict severe infection or sepsis in severely burned patients? Int J Burns Trauma. 8(3):137-43.

Lavrentieva, A., Kontakiotis, T., Lazaridis, L., Tsotsolis, N., Koumis, J., Kyriazis, G. and Bitzani, M. 2007. Inflammatory markers in patients with severe burn injury. What is the best indicator of sepsis? Burns. 33:189-194.

Lehnhardt, M., Jafari, H.J, Druecke, D., Steinstraesser, L., Steinau, HU., Klatte, W., Schwake, R. and Homann, HH. 2005. A qualitative and quantitative analysis of protein loss in human burn wounds. Burn. 31(2):159-167.

Mendonça Machado, N., Gragnani, A. and Masako Ferreira, L. 2011. Burns, metabolism and nutritional requirements. Nutr Hosp. 26(4):692-700.

Manelli, JC., Badetti, C., Botti, G., Golstein, MM., Bernini, V. and Bernard, D. 1998. A reference standard for plasma proteins is required for nutritional assessment of adult burn patients. Burn. 24(4):337-345.

Miquet-Rodríguez, LM., Rodríguez-Garcell, R., Santana-Porben, S. and Cervantes-Flores, R. 2013. Valor Pronóstico del nivel de albúmina sérica inicial en los pacientes quemados. http://www.portalesmedicos.com/publicaciones/articles/1108/2/Valor-pronostico-del-nivel-de-albumina-serica-inicial-en-los-pacientes-quemados.

Muhammad, O. and Hayder, AH. 2011. Some Physiological Changes in Burn Patients. Medical Journal of Babylon. 8(3):303-319.

Nagane, NS., Bhagwat, VR. and Subramanium, M. 2003. Increased free radical activity in burns. Indian J Med Sci. 57(1):7-11.

Norbury, WB., Jeschke, MG. and Herndon, DN. 2006. Metabolic Changes Following Major Burn Injury: How to Improve Outcome. Intensive Care Medicine. 514-524.

Peck, MD., Kruger, GE., van der Merwe, AE., Godakumbura, W. and Ahuja, RB. 2008. Burns and fires from non-electric domestic appliances in low and middle income countries Part I. The scope of the problem. Burns. 34:303.

Peretz, A., Decaux, G. and Famaey, JP. 1983. Hypouricemia and intravenous infusions. J Rheumatol. 10(1):66-70.

Pileri, D., Accardo-Palumbo, A., D'Amelio, L., D'Arpa, N., Arnone, G., Grisaffi, C., Amico, M., Brancato, R., Lombardo, C. and Conte F. 2009. Serum Levels of Cortisol, Immunoglobulin, and C-reactive Protein in Burn Patients. Ann Burns Fire Disasters. 22(1):3-5.

Prerenal azotemia| niversity of Maryland Medical Center. https://umm.edu/Health/.../Prerenal-azotemia.

Sabry, A., Wafa, I., El-Din, AB., El-Hadidy, AM. and Hassan, M. 2009. Early markers of renal injury in predicting outcome in thermal burn patients. Saudi J Kidney Dis Transpl. 20(4):632-8.

Steven, L., Stockham, SL. and Scott, MA. 2008. Fundamentals of Veterinary Clinical Pathology. (2nd edi.).

Tobiasen, J., Hiebert, JM. and Edlich, RF. 1982. The Abbreviated Burn Severity Index. Ann Emerg Med. 11(5):260-2.

Williams, FN., Herndon, DN. and Jeschke, MG. 2009. The Hypermetabolic Response to Burn Injury and Interventions to Modify This Response. Clin Plast Surg. 36(4):583-596.

Yadav, MK. 2010. A Study On Levels Uric Acid In Burn Patients. MS Thesis. Rajiv Gandhi University of Health Sciences, Karnataka, Bangalore, India.

Received: June 6, 2014; Accepted: June 27, 2014

SENRA Academic Publishers, British Columbia
Vol. 8, No. 3, pp. 3061-3080, October 2014
Online ISSN: 1920-3853; Print ISSN: 1715-9997

Canadian Journal of pure&applied sciences

MULTI-OBJECTIVE EVOLUTIONARY COMPUTATION HEURISTIC FOR TRAFFIC GROOMING IN WDM OPTICAL NETWORKS

Pakorn Leesutthipornchai[1], Chalermpol Charnsripinyo[2] and *Naruemon Wattanapongsakorn[3]
[1]Department of Computer Science, Faculty of Science and Technology
Thammasat University, Rangsit Campus, Pathumthani, Thailand
[2]National Electronics and Computer Technology Center, Pathumthani, Thailand
[3]Department of Computer Engineering, Faculty of Engineering
King Mongkut's University of Technology Thonburi, Bangkok, 10140, Thailand

ABSTRACT

Traffic grooming, which is the combination of traffic demands into a single wavelength channel is a well-known issue in Wavelength Division Multiplexing (WDM) optical networks. Grooming allows wavelength channels with high transmission capacity to serve many low-rate traffic demands simultaneously. In this paper, we address the traffic grooming, routing and wavelength assignment (GRWA) problem for WDM optical networks by considering multiple design objectives: maximizing the number of demands (commodities) served, minimizing the number of wavelength channels assigned, and minimizing number of transmission ports required. We use a hybrid multi-objective evolutionary computation approach consisting of Genetic Algorithm for routing allocation, Extended Traffic Grouping for traffic grooming and Maximum Degree First for wavelength assignment (GA-ETG-MaxDF). Then we apply the Fast Non-dominated Sorting Genetic Algorithm (NSGA-II) to search for the set of non-dominated candidate solutions in multi-objective space. We compare the simulation results obtained from our approach (GA-ETG-MaxDF) with the alternative approaches (MST and MRU) published in the literature. We also examine standard performance metrics for multi-objective optimization solutions such as Hyper-volume, Spread, and Inverted Generational Distance. Based on our results, we conclude that the proposed technique is effective for solving the multi-objective GRWA problem in WDM optical networks.

Keyword: Multi-Objective Genetic Algorithm, multi-objective optimization, traffic grooming, routing and wavelength assignment, WDM optical network.

INTRODUCTION

In new generation optical networks, wavelength division multiplexing (WDM) technology will be widely used. Each optical fiber link can be divided into multiple channels which are identified by the length of light waves, called "wavelength channels". Dense wavelength division multiplexing (DWDM) technology can support over a hundred wavelength channels per fiber (Awwad *et al*., 2007). The transmission speed of each channel can be several Gigabits per second (Gbps). Speeds of 2.488 Gbps (OC-48), 10 Gbps (OC-192) and 40 Gbps (OC-768) have been proposed (Dutta and Rouskas, 2002) for commercial use. Most traffic demands (connections) typically have lower data rates than the full capacity of a wavelength channel. In order to fully utilize the network resources, multiple low-speed traffic streams need to be efficiently multiplexed or "groomed" into high-speed light-paths for data transmission between sources and destinations. This procedure is known as Traffic Grooming. Traffic grooming consists of three sub-problems which are Grooming, Routing and Wavelength Assignment (GRWA). We denote a source-destination node pair with traffic demand as a "commodity" (Jaekel *et al*., 2008). Grooming combines multiple low-data-rate commodities into a higher transmission rate channel. Routing allocates a light-path to each traffic flow in a given set of commodities. Finally, a group of commodities is assigned to an available wavelength channel. Grooming, routing and wavelength assignment are interrelated. Optimal routing depends on effective grouping, and effective wavelength assignment requires optimal routing. The GRWA problem tries to find optimal solutions for routing, and wavelength assignment with multi-commodity flows. The traffic grooming or GRWA problem is an NP complete problem (Shalom *et al*., 2007).

Previous research has considered the GRWA problem with various different design objectives. Another study, Zhu and Mukherjee (2002, 2003) have considered the GRWA problem to improve network throughput and reduce the network cost and to reduce the grooming device cost while serving all traffic demands. While, Awwad *et al*. (2007) considered GRWA to minimize total cost of grooming and conversion equipment, Shen and

*Corresponding author email: naruemon@cpe.kmutt.ac.th

Tucker (2009) considered GRWA to maximize the served traffic demand and minimize the wavelength capacity. Given many different potential design objectives, the GRWA problem can be formulated as a multi-objective optimization problem. In such problems, multiple evaluation functions influence the decision of which option to select.

This paper considers the GRWA problem with three objective functions. We attempt to simultaneously maximize the number of accepted commodities, minimize the number of wavelength channels and minimize the number of switching ports. Each of these objectives can conflict with the others such that when one is optimized, the other functions may get worse (Coit and Konak, 2006). For instance, maximizing accepted commodities normally requires a large number of wavelengths and switching ports. Minimizing the number of switching ports could cause a large number of commodities to be blocked or fewer commodities to be accepted. Several Multi-objective Evolutionary Algorithms such as Strength Pareto Evolutionary Algorithm: SPEA2 (Zitzler *et al*., 2001) and Fast Non-dominated Sorting Genetic Algorithm: NSGA-II (Deb *et al*., 2002) has been previously proposed for general multi-objective optimization problems. To solve the multi-objective GRWA problem, we propose a new evolutionary computation heuristic called "GA-ETG-MaxDF" and use it with NSGA-II. We construct potential routes by using a Genetic Algorithm (GA), combine multiple low rate traffic demands by using Extended Traffic Grouping (ETG) algorithm and assign the wavelength channel by using the Maximum Degree First (MaxDF) algorithm. We then apply the NSGA-II to search for non-dominated solutions in the three dimensional space of accepted commodities, required wavelength channels and required switching ports. The results are provided as non-dominated candidates.

After implementing our approach in a simulation, we compare the results from GA-ETG-MaxDF with those from the alternative approaches (MST and MRU). We also compare the approaches in terms of indicators of multi-objective solution quality.

MATERIALS AND METHODS

Traffic Grooming, Routing and Wavelength Assignment Problem

Traffic grooming, routing and wavelength assignment (GRWA) problems have been previously studied by a number of researchers. Traffic grooming has been applied to both ring network topology (Wang *et al*., 2001; Dutta and Rouskas, 2002; Zhu and Mukherjee, 2003) and mesh network topology (Zhu and Mukherjee, 2002; Hu and Leida, 2004; Prathombutr *et al*., 2005). Traffic grooming in mesh networks is usually difficult to solve optimally (Zhu and Mukherjee, 2003). The evolution, challenges and future vision of traffic grooming and all-optical network are proposed by Saleh and Simmons (2012).

Zhu and Mukherjee (2002) proposed grooming, routing and wavelength assignment techniques to improve the network throughput subject to a limited number of transmitters, receivers and available wavelength channels. They used the Maximizing Single-hop Traffic (MST) heuristic algorithm to assign multiple requested connections to a new light path. If the network has enough network resources (i.e., wavelength channels, transmitters, receivers, grooming devices and wavelength converters), all requested connections can traverse on a single light path and the traffic delay will be minimized. If there are not enough network resources to support a new light path, the method assigns connections that can complete in a single hop light path before connections that require multiple light paths. Zhu and Mukherjee (2002) used a Maximizing Resource Utilization (MRU) heuristic algorithm to allocate limited network resources. The MRU approach sets up a light path using available spare wavelength channels in the logical network links, possibly assigning connection requests to multiple light paths, then multiplexes the remaining connection requests with the existing light paths. The connection that uses the fewest established light paths will be groomed first. Hu and Leida (2004) proposed a GRWA technique to minimize the total number of transponders required in the network, subject to a limited number of wavelength channels in each fiber and requiring that each light path use the same wavelength channel for every link that it traverses (i.e., wavelength continuity constraint). In their work, they assumed a transponder is required at each end of the light path. Thus minimizing the number of transponders also minimized the number of wavelengths. They solved their GRWA problem using a commercial tool called CPLEX 7.0. In a recent study, Awwad *et al*. (2007) proposed a GRWA in a WDM mesh network with sparse resources (i.e., some logical network nodes are able to groom while others are not). Their objective was to minimize the total costs for traffic grooming and wavelength conversion devices. The traffic grooming device has more functions and higher cost than the wavelength conversion device. Both types of devices are deployed on the nodes based on the decision variables of the optimization model. Because their GRWA implementation allows a light path to use different wavelength channels, it significantly increases blocking probability. They applied a Genetic Algorithm (GA) to solve their GRWA problem and compared the results with their previous approaches including Most-contiguous (MC) heuristic algorithm, and Fixed Alternated Routing and First Fit Wavelength Assignment (FAR-FF) algorithm.

Shen and Tucker (2009) proposed an algorithm to select the best locations for opaque nodes (a kind of grooming

device). They aimed to maximize served traffic demands under a limited network capacity and minimize the required wavelength channel while all traffic demands are served. Chatterjee *et al*. (2012) proposed a priority based routing and wavelength assignment with traffic grooming mechanism (PRWATG) to reduce blocking probability. The blocking probability increases when the number of connections is increased. In their algorithm, which enforces the wavelength continuity constraint, connections with the same source and destination are combined first to avoid optical to electrical conversions. Then, the set of routes and wavelength channels are assigned to the groomed connections according to their priority. A groomed connection with a direct path had higher priority than one with an indirect path. Zhao *et al*. (2013) considered the GRWA problem with the goal of satisfying quality of transmission requirements (QoT). The QoT Guaranteed (QoT-G) algorithm accommodates a set of traffic demands with heterogeneous bandwidth requirements in order to minimize the blocking probability. Their paper used the shortest path algorithm for routing. In the grooming step, the connection requiring the most bandwidth is considered first. If multiple connections have the same bandwidth requirement, the connection with the shorter path is selected. Most studies in the literature (Dutta and Rouskas, 2002; Zhu and Mukherjee, 2003; Hu and Leida, 2004; Awwad *et al*., 2007; Chatterjee *et al*., 2012; Zhao *et al*., 2013) have concentrated on traffic grooming with a single objective function. Research work on traffic grooming with multiple objectives has been proposed (Prathombutr *et al*., 2005).

Prathombutr *et al*. (2005) proposed an algorithm for traffic grooming in WDM optical mesh networks with the objectives of maximizing the traffic throughput, minimizing the number of transceivers and minimizing the average propagation delay. They considered the GRWA problem with and without a wavelength converter. They applied the SPEA approach to search a set of non-dominated solutions. They offered superior results than those from MST and MRU (Zhu and Mukherjee, 2002). The results from MST and MRU are also used to compare with the obtained solutions from the Multi Objective Evolutionary Algorithm (MOEA) as proposed in (De *et al*., 2008). MST and MRU algorithms are easy to follow and implement. Traffic grooming is a network design problem that the network topology affects the obtained results. MST and MRU are developed on the basis of the shortest path algorithm and well known as efficient traffic grooming algorithms.

Multi-Objective Network Design

Multi-objective network design evolved from a network model that seeks to optimize only one objective function, but with many design constraints such as network design cost, limitation of maximum delay and network survivability requirement (Hsu *et al*., 2008). Assis *et al*. (2008) proposed a true multi-objective network design model that minimizes total link length and total number of hops, while maximizing link load simultaneously. This research combined all objective functions into one function and then optimized the single objective function while maintaining the design constraints. A mixed integer programming tool (CPLEX 10.0) was used to find the optimal solution. Kavian *et al*. (2008) also proposed a network design model with multiple objective functions. Their network model minimized bandwidth consumption and end-to-end delay. They used a genetic algorithm to minimize each function individually and then combine the obtained results from both objectives. Finally, Banerjee and Kumar (2007) proposed a network design to minimize total network cost (from nodes, links, and amplifier) and also minimize average delay. Their research also found a set of optimal solutions using an advanced genetic algorithm but they evaluated each solution with both objective functions at the same time. Some papers Cahon *et al*. (2006) and Ribeiro *et al*. (2007) have suggested that multi-objective network design can solve all objectives simultaneously by using parallel computing to find the best solution from all possible sets. Parallel computing distributes the possible sets into clusters and then combines the distributed results to get the best solution. De *et al*. (2008) proposed the Multi Objective Evolutionary Algorithm (MOEA) for optimizing traffic grooming problem by considering multiple objectives, i.e., throughput, transceiver requirement and intermediate propagation delay simultaneously. The obtained results are compared with those of MST and MRU algorithms. Roa *et al*. (2009) proposed a Multi Objective Evolutionary Algorithm by considering two design objectives, i.e., minimizing blocking number and the number of wavelength converters. The results are compared with the solutions from SPEA algorithm. Lin *et al.* (2012) suggested two heuristics algorithms, Multicast Trail Grooming (MTG) and Multiple Destination Trail-based Grooming (MDTG) to minimize the network cost in terms of the number of higher layer electronic ports and number of wavelengths used. The solutions obtained by two heuristics are compared with the ILP optimal solution. In a most recent study, Chen *et al.* (2013) proposed the bi-objective ILP for maximizing the throughput and then minimizing the energy consumption for the obtained maximized throughput. The obtained results are compared with the single objective optimization. In this paper, we use a true multi-objective optimization algorithm which maintains separate objective functions for each criterion. There are many multi-objective optimization approaches as described in the next section.

Multi-Objective Genetic Algorithms

Genetic Algorithm (GA) approaches have been used to solve multi-objective optimization problems in several

areas. The efficient multi-objective GA provides an encouraging approach for searching toward the true Pareto front while maintaining diversity in the population (Konak *et al*., 2006). Various Multi-Objective Genetic Algorithms have been previously discussed in (Konak *et al*., 2006; Leesutthipornchai *et al*., 2009). Examples of Multi-Objective Genetic Algorithms are Weight-Based GA: WBGA (Hajela and Lin, 2005), Random Weighted GA: RWGA (Murata and Ishibuchi, 1995), Vector Evaluated GA: VEGA (Schaffer, 1985), Niched Pareto GA: NPGA (Horn *et al*., 1994), Multi-Objective GA: MOGA (Fonseca and Fleming, 1993), Nondominated Sorting GA: NSGA (Srinivas and Deb, 1994), Fast Non-dominated Sorting GA: NSGA-II, Strength Pareto Evolutionary Algorithm: SPEA (Zitzler and Thiele, 1999), enhanced SPEA: SPEA2 (Zitzler *et al*., 2001) and Pareto-Archived Evolution Strategy: PAES (Knowles and Corne, 1999).

In our previous work (Leesutthipornchai *et al*., 2009), we evaluated NSGA-II with all optimal and non-dominated solutions (i.e., the Pareto-front) using a well-known combinatorial problem (i.e., Knapsack problem with 2 objective functions and 100 decision variables). The experiment showed that NSGA-II can provide excellent results.

Problem Definition and Model Formulation

In this section, we describe our multi-objective GRWA problem and present the GRWA model formulation.

We assume that the WDM optical networks have hybrid optical-electronic switching devices to support grooming. In an all-optical network (Huang and Copeland, 2003), the signals can pass through network nodes in the optical domain. An all-optical network reduces the transmission delay at intermediate nodes by avoiding the OEO (Optical-Electrical-Optical) conversion between the optical and the electrical domains. Each node requires one optical port for receiving and another optical port for transmitting, with electrical ports required only at the source and destination of the connection. However, electrical ports are also needed at some intermediate nodes, wherever multiple commodities are groomed into the same wavelength channel. The number of transmission ports and wavelength channels required for traffic grooming are different from the case when the traffic connections are not groomed. Wavelength channels and switching ports are network resources that must be efficiently used. Grooming makes it possible to combine multiple traffic streams in a single wavelength channel. The so-called wavelength continuity constraint states that a wavelength channel can be assigned only to one light path connection, so that the wavelength channel does not change along the light path from the source to the destination node.

In this paper, we consider the GRWA problem in WDM optical networks to serve a given set of commodities. Each commodity has many possible routings and each routing has several choices for aggregation with other connections and various choices of wavelength channel assignment. A percentage of commodities is allowed to be blocked if this is necessary to optimize wavelength channels and switching ports. A commodity that has been successfully assigned with a wavelength channel is called "accepted commodity". Our GRWA problem aims to maximize the number of accepted commodities, to minimize the number of wavelength channels and to minimize the number of switching ports. We consider these three design objectives simultaneously, while preserving the wavelength continuity constraint. The next section presents our notation for this problem formulation.

Set of Notations: **Network Topology Properties**

Let N be the set of network nodes. E denotes the set of edges or links in the network. $E(i,*)$ is the set of edges that leave from node $i \in N$. $E(*, i)$ is the set of edges that go to node $i \in N$. D is the set of network edge distances where D_e represents the length of network edge $e \in E$. Each network edge has $|K|$ wavelength channels. K is the set of available wavelength channels. G is the set of aggregated groups in which multiple commodities are merged together. Each accepted commodity must belong to a group (which might have only a single member). Q is the set of given commodities, expressed as a source-destination node pair with a bandwidth requirement. In this paper, the bandwidth is a fraction of the wavelength capacity. $P_{\max}$ is the maximum number of switching ports in the network. P_A is the required number of switching ports. Q_A is the number of accepted commodities. K_A is the number of required/assigned wavelength channels. L is the maximum acceptable path length (in kilometer). H is an upper-bound hop counts.

Let ω_g^e be the number of commodities in the group $g \in G$ on network edge $e \in E$. ω_g^e is a positive integer number. $\psi(o)_g^e$ is the number of optical ports. $\psi(e)_g^e$ is the number of electrical ports. The electrical port count is calculated as the sum of the electrical transmitting units $\varphi(s)_g^e$ and electrical receiving units $\varphi(d)_g^e$. $\varphi(s)_g^e$ is the number of electrical transmitting units of the group on the network edge. $\varphi(d)_g^e$ is the number of electrical receiving units of the group on the network edge. $\varphi(o)_g^e$ is the number of optical units of the group on the network edge. T_{acc} is the minimum threshold value representing the ratio of accepted commodities that are required over the total

number of commodities, where $0 \le T_{acc} \le \frac{Q_A}{|Q|} \le 1$. $|K| \le K_{max}$ which is an upper-bound number of wavelengths. t_q is the bandwidth requirement of the commodity.

Set of Notations: **Decision Variables**

Let $\delta_{q,g}{}^{e,k}$ denotes the decision variable of a commodity q that decides whether to occupy a wavelength channel k on network edge e with group g, or not. Note that $\delta_{q,g}{}^{e,k}$ is equal to 1 if the wavelength channel on the edge is occupied by the commodity and it belongs to a group; otherwise it is equal to 0.

Given

Network topology

Set of source-destination node pairs with bandwidth requirements

Assumption

The combination of commodities can be performed in the electrical domain only.

Design Objectives

Minimize:

$$f_{obj} = \min\left(f_c, f_w, f_p\right) \tag{1}$$

$$f_c = \frac{|Q| - Q_A}{|Q|} \tag{2}$$

$$f_w = \frac{K_A}{K_{\max}} \tag{3}$$

$$f_p = \frac{P_A}{P_{\max}} \tag{4}$$

Design Constraints

Subject to:

$$\sum_{g\in G}\sum_{e\in E(*,i)}\sum_{k\in K}\delta_{q,g}^{e,k} - \sum_{g\in G}\sum_{e\in E(i,*)}\sum_{k\in K}\delta_{q,g}^{e,k} = \begin{cases} -\beta_q, i = Source_q \\ \beta_q, i = Dest_q \\ 0, otherwise \end{cases} ;\forall q \in Q, i \in N \tag{5}$$

$$\sum_{q\in Q}\sum_{k\in K}\delta_{q,g}^{e,k}\cdot t_q \le \Re_g^e \quad ;\forall g \in G, \forall e \in E \tag{6}$$

$$\Re_g^e \le 1 \quad ;\forall g \in G, \forall e \in E \tag{7}$$

$$\delta_{q,g}^{e,k} \le \gamma_q^k \quad ;\forall q \in Q, \forall g \in G, \forall e \in E, \forall k \in K \tag{8}$$

$$\sum_{k\in K}\gamma_q^k \le 1 \quad ;\forall q \in Q \tag{9}$$

$$\sum_{g\in G}\sum_{k\in K}\delta_{q,g}^{e,k} \le \beta_q \quad ;\forall q \in Q, \forall e \in E \tag{10}$$

$$\delta_{q,g}^{e,k} \le \Lambda_{q,g} \quad ;\forall q \in Q, \forall g \in G, \forall e \in E, \forall k \in K \tag{11}$$

$$\sum_{g\in G}\Lambda_{q,g} \le 1 \quad ;\forall q \in Q \tag{12}$$

$$\delta_{q,g}^{e,k} \le y_g^k \quad ;\forall q \in Q, \forall g \in G, \forall e \in E, \forall k \in K \tag{13}$$

$$\sum_{k\in K} y_g^k \le 1 \quad ;\forall g \in G \tag{14}$$

$$Q_A = \sum_{q\in Q}\beta_q \tag{15}$$

$$K_A = \sum_{k\in K}\phi_k \tag{16}$$

$$\omega_g^e \ge \sum_{q\in Q}\sum_{k\in K}\delta_{q,g}^{e,k} \quad ;\forall g \in G, \forall e \in E \tag{17}$$

$$\varphi(s)_g^e \ge \begin{cases} \sum_{g\in G}\sum_{k\in K}\delta_{q,g}^{e,k}, e \in E(Source_q,*) \\ \sum_{g\in G}\sum_{k\in K}\delta_{q,g}^{e,k}, e \in E(*,Dest_q) \\ \sum_{g\in G}\sum_{k\in K}\delta_{q,g}^{e,k}, e \notin E(Source_q,*) \wedge e \notin E(*,Dest_q) \wedge \omega_g^{e'(*,Source_e)} \le 1 \\ \sum_{g\in G}\sum_{k\in K}\delta_{q,g}^{e,k}, e \notin E(Source_q,*) \wedge e \notin E(*,Dest_q) \wedge \omega_g^{e'(Dest_e,*)} \le 1 \\ 0, \quad otherwise \end{cases}$$

where $\forall q \in Q, \forall e \in E$ (18)

$$\varphi(d)_g^e \ge \begin{cases} \sum_{g\in G}\sum_{k\in K}\delta_{q,g}^{e,k}, e \in E(*,Dest_q) \\ \sum_{g\in G}\sum_{k\in K}\delta_{q,g}^{e,k}, e \in E(Source_q,*) \\ \sum_{g\in G}\sum_{k\in K}\delta_{q,g}^{e,k}, e \notin E(*,Dest_q) \wedge e \notin E(Source_q,*) \wedge \omega_g^{e'(Dest_e,*)} \le 1 \\ \sum_{g\in G}\sum_{k\in K}\delta_{q,g}^{e,k}, e \notin E(*,Dest_q) \wedge e \notin E(Source_q,*) \wedge \omega_g^{e'(*,Source_e)} \le 1 \\ 0, \quad otherwise \end{cases}$$

where $\forall q \in Q, \forall e \in E$ (19)

$$\psi(e)_g^e = \varphi(s)_g^e + \varphi(d)_g^e \quad ;\forall g \in G, \forall e \in E \tag{20}$$

$$\varphi(o)_g^e \ge \sum_{g\in G}\sum_{k\in K}\delta_{q,g}^{e,k} \quad ;\forall q \in Q, \forall e \in E \tag{21}$$

$$\psi(o)_g^e = 2\cdot\varphi(o)_g^e \quad ;\forall g \in G, \forall e \in E \tag{22}$$

$$P_A = \sum_{g\in G}\sum_{e\in E}\left(\psi(o)_g^e + \psi(e)_g^e\right) \tag{23}$$

$$y_g^k \le \phi_k \quad ;\forall g \in G, \forall k \in K \tag{24}$$

$$\frac{Q_A}{|Q|} \ge T_{acc} \tag{25}$$

$$\sum_{e\in E}\delta_{q,g}^{e,k} \le H \quad ;\forall q \in Q, \forall g \in G, \forall k \in K \tag{26}$$

$$\sum_{e\in E}(D_e\cdot\delta_{q,g}^{e,k}) \le L \quad ;\forall q \in Q, \forall g \in G, \forall k \in K \tag{27}$$

$$\beta_q \in \{0,1\} \quad ;\forall q \in Q \tag{28}$$

$$\phi_k \in \{0,1\} \quad ;\forall k \in K \tag{29}$$

$$\gamma_q^k \in \{0,1\} \quad ;\forall q \in Q, \forall k \in K \tag{30}$$

$$\Lambda_{q,g} \in \{0,1\} \quad ;\forall q \in Q, \forall g \in G \tag{31}$$

$$y_g^k \in \{0,1\} \quad ;\forall g \in G, \forall k \in K \tag{32}$$

$$\varphi(s)_g^e \in \{0,1\} \quad ;\forall g \in G, \forall e \in E \tag{33}$$

$$\varphi(d)_g^e \in \{0,1\} \quad ;\forall g \in G, \forall e \in E \tag{34}$$

$$\varphi(o)_g^e \in \{0,1\} \quad ;\forall g \in G, \forall e \in E \tag{35}$$

$$\delta_{q,g}^{e,k} \in \{0,1\} \quad ;\forall q \in Q, \forall g \in G, \forall e \in E, \forall k \in K \tag{36}$$

Note that a commodity can have several possible routes from source to destination but only one route is considered at a time and the available wavelength channel is considered to be occupied for the selected route. Our proposed network model considers grooming, routing and wavelength assignment, attempting to maximize the number of accepted commodities (Q_A), to minimize the number of required wavelengths (K_A) and to minimize the number of required switching ports (P_A), as shown in Eq. (1)-(4). The objective function in Eq. (2) transforms the maximization of accepted commodities to a minimization function. When Q_A is maximized to reach the total number of commodities ($|Q|$), the value of Eq. (2) will be minimized to 0.

The objective functions are normalized by dividing with their total range of values (or magnitudes), so that all will have values in the interval [0,1].

The set of constraints Eq. (5)-(27) are described below.

Eq. (5) is the network flow constraint. The flow of traffic that enters and leaves from node must equal 0. The traffic demand at the source node is $-\beta_q$ and the traffic demand at the termination node is β_q. Decision variable β_q represents the existence of a network commodity. β_q=1, if the commodity has a network flow on the node. Otherwise, it is 0.

Eqs. (6) and (7) are the wavelength bandwidth constraints. The wavelength bandwidth on the network edge for all commodities in the group must be less than or equal to one unit of the wavelength channel bandwidth. Since multiple commodities can be assigned to the group on network edge, in Eq. (6), the $\Re_g^e$ is the maximum bandwidth required to support all commodities in group on the network edge. Eq. (7) ensures that each group must have a total bandwidth requirement less than or equal to 1.The bandwidth granularities of all commodities are less than or equal to 1 wavelength.

Eqs.(8) and (9) are the wavelength continuity constraints. Only one wavelength channel is used for the commodity throughout multiple (connected) edges. Since multiple edges can be used for the commodity with a wavelength, in Eq.(8), if the commodity occupies a wavelength channel on any edge, then $\gamma_q^k = 1$. If $\gamma_q^k = 0$, there is no assignment of wavelength channel for the commodity on any edge. Eq.(9) ensures that each commodity must have a number of assigned wavelength channels less than or equal to 1.

Eq.(10) is the commodity assignment constraint. The commodity variable β_q is equal to 1, if there exists one or more edge(s) occupied by the commodity with one wavelength channel.

Eqs.(11) and (12) are the single group assignment constraints. A particular commodity can be assigned to only one group. In Eq.(11), if the commodity is assigned to a group, then $\Lambda_{q,g} = 1$. Otherwise, $\Lambda_{q,g} = 0$. Eq.(12) ensures that each commodity must have the number of assigned groups less than or equal to 1.

Eqs.(13) and (14) are the wavelength continuity constraints for the group. Only one wavelength channel is used for the group throughout multiple (connected) edges. Since multiple edges can be used for the commodity in group with a wavelength, in Eq.(13), if the group occupies a wavelength channel on any edge, then $y_g^k = 1$. If $y_g^k = 0$, there is no assignment of wavelength channel for the group on any edge. Eq.(14) ensures that each group must have the number of assigned wavelength channels less than or equal to 1.

In Eq.(15), the number of accepted commodities (Q_A) is equal to the count of all commodities which can be routed (on one or multiple edges) from their source to destination and assigned with a wavelength channel throughout the route.

In Eq. (16), the number of required wavelength channels (K_A) is equal to the count of all assigned wavelength channels where each assigned wavelength channel is occupied by at least one accepted commodity.

Eq. (17) is the number of commodities in the group on a network edge.

Eq. (18) is the number of electrical transmitting units of the group on the network edge. If a network edge is the source of some commodity in a group, an electrical transmitting unit is required for adding the new commodity to the existing group. Note that if more than one commodity in the group has its source on the network edge, only one transmission unit is required for group on the network edge. For the group of multiple commodities, it is possible to drop the existing light path to remove a commodity from the group when the commodity reaches its destination. Therefore, in the second condition, for each network edge if there exists a commodity in the group that reaches its destination, a transmitting unit is required for adding the remaining connections after the commodity is split out of the group. In our model, it is possible to groom two commodities that do not have the same source and/or destination into the same wavelength channel. This gives rise to two additional conditions. For example in figure 1, commodities 1 and 2 are groomed into the same wavelength at edge 2→3. The network edge 2→3 is neither the source nor the destination of commodities 1 and 2. However, an electrical port is required at node 2, in order to groom commodity 2 into the light path. Furthermore, an electrical port is required at node 3, where commodity 2 leaves the common light path, to add the remaining communications after commodity 2 is split out.

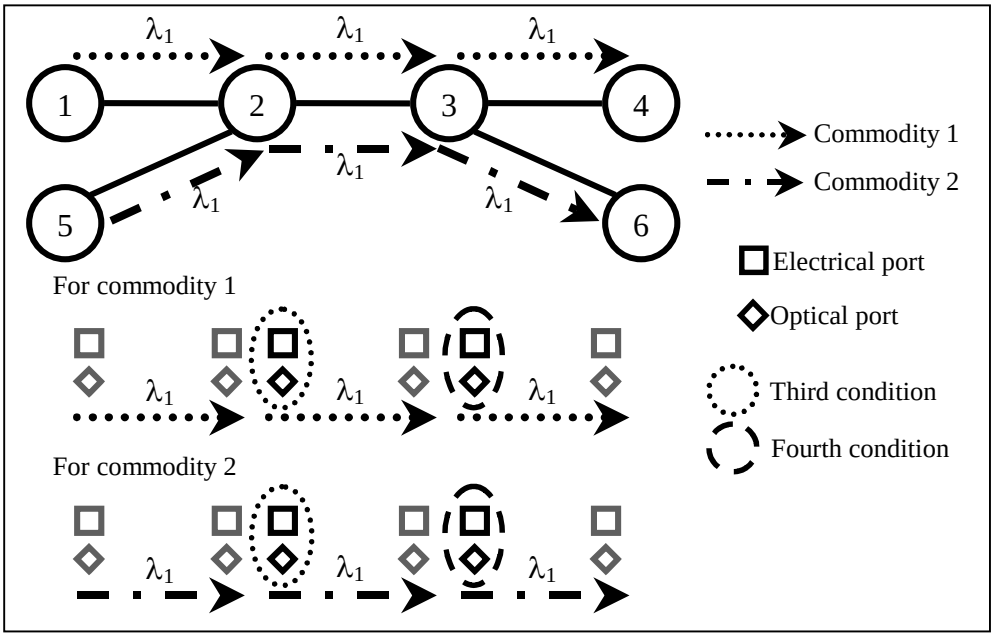

Fig. 1. The grooming condition in MP2MP for the electrical transmitting unit.

Eq. (19) is the number of electrical receiving units of the group on the network edge. As is the case with transmitting units, a unit is needed at each location where a commodity joins or leaves a path.

Eq. (20) is the number of electrical ports for a group on a network edge. The number of electrical ports is calculated as the sum of electrical transmitting units $\varphi(s)_g^e$ and electrical receiving units $\varphi(d)_g^e$. The number of electrical ports for a group on a network edge may be 0 if none of the commodities in the group have their source or destination on the network edge.

Eq. (21) is the number of optical units for the group on the network edge. If a commodity in the group traverses on the network edge, an optical unit is required for retransmitting the optical signal. Note that if more than one commodity in the group traverses on the network edge, only one transmission unit is required for group on the network edge.

Eq. (22) is the number of optical ports for the group on the network edge. Twice as many optical ports as optical units are required for every network edge. One optical port is used for transmitting and another one for receiving.

Eq. (23) is the equation for calculating the number of switching ports. The number of all switching ports is the summation of optical and electrical ports in all groups traversing one or more network edges.

Eq. (24) is the wavelength utilization constraint. Each wavelength channel is selected if there is at least one commodity in the group which is set up. If there are two or more groups which are not overlapped, they can use the same wavelength channel (on different edges) subject to wavelength continuity constraint.

In Eq. (25), the number of accepted commodities must be greater than or equal to a threshold. For example, T_{acc}=0.8 means that 80% of all commodities must be accepted.

In Eq. (26), the hop distance of commodity traversing on multiple edges must not exceed the hop count limit.

In Eq. (27), the network link distance of commodity traversing on multiple edges must not exceed the length limit (in kilometers).

Eqs. (28)-(36) define the decision variables used in the model.

The routing of a commodity can be any of the possible routes that connect the specified source node to the specified destination node. Previously, the RWA (routing and wavelength assignment) problem has been shown to be NP-complete (Chlamtac *et al*., 1992). The GRWA problem considers not only routing and wavelength assignment but also combining multiple low rate traffic demands into the same wavelength channel. Our proposed network design model is solved heuristically using a hybrid evolutionary approach described in the next section.

Multi-Objective Evolutionary Computation Heuristic

In this section, we present heuristic algorithms to solve the multi-objective grooming, routing and wavelength assignment (GRWA) problem in optical network design. Our approach considers potential routes by using a Genetic Algorithm (GA), combines multiple low rate traffic demands with the Extended Traffic Grooming (ETG) algorithm, and assigns the wavelength channel by using the Maximum Degree First Wavelength Assignment (MaxDF) algorithm. Thus, we call our method GA-ETG-

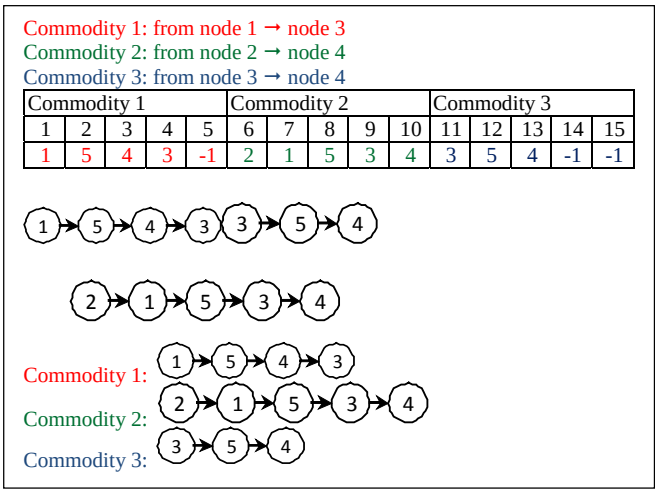

Fig. 2. An example of string encoding.

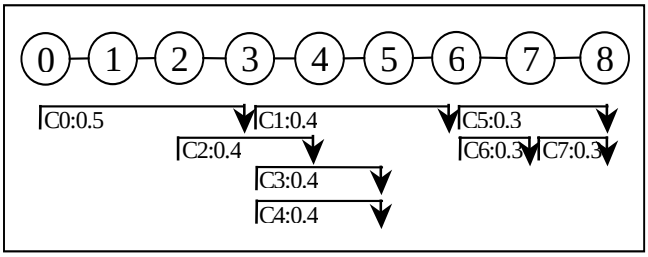

Fig. 3. Set of commodities with bandwidth requirement in an example network.

MaxDF. The Fast Non-dominated Sorting Genetic Algorithm (NSGA-II) is then applied to search for a set of non-dominated candidate solutions.

Genetic Algorithm for Routing

Banerjee and Sharan (2004) applied a Genetic Algorithm to solve a routing problem in WDM optical networks, based on a Fixed-Alternate Routing approach. Their algorithm limited the alternate routes of each commodity, considering only the K^{th} shortest routes. However, it is possible that some commodities require a longer route to avoid the congestion. In our research work, we propose a Genetic Algorithm for routing that allows most possible routes to be considered.

GA normally requires several sub-processes. The string encoding process represents each potential solution as a "chromosome" made up of genes, that is, as a vector of numeric values for each solution dimension or component. An initial set of chromosomes is generated. Then the algorithm iterates through a number of evolutionary cycles. In each cycle, the chromosomes may be modified by crossover (swapping values between chromosomes) and mutation (random modification of particular "gene" positions). A fitness function that measures solution quality is applied to the resulting chromosomes. Then the chromosomes with the highest fitness values are retained for the next iteration.

The string encoding used in this paper is a set of integers that indicates the route of each commodity. Suppose that we have a 5-node network (nodes labeled 1 through 5) and three commodities to be routed. The corresponding 15 position string encoding is displayed in figure 2. Each commodity has a separate region of the string, with a number of positions equal to the total number of nodes in the network. Each position p represents one node on a potential path for that commodity. If position p has the value n_p this represents a path segment connecting from n_p to n_{p+1}. A value of n_p= -1 indicates that the commodity's destination has been reached in previous connections. This string encoding scheme has the benefit that all possible routes can be considered.

Crossover is a process that generates new solutions from existing solutions. We pair up the chromosomes and use one-point crossover for each pair. In our work, 80% of the population will be interchanged. Each commodity pair swaps the route sections starting at the selected crossover point. Duplicated nodes or loops are detected and deleted. Mutation generates new solutions from existing solutions. We use one bit mutation for 25% of the population. One node position is randomly selected for mutation. The connection between that node and the following node is deleted, and the shortest alternative path between those nodes is calculated. If a new shortest path is found, the

intervening nodes will be inserted into the chromosome. Otherwise the previous path will be retained.

As discussed earlier, a GA usually evaluates the fitness of the individuals in the current population and chooses the fittest instances to survive into the next generation. In our work, the fitness testing and selection is part of the NSGA-II process.

Extended Traffic Grooming

In traffic grooming, commodities that have overlapping paths and whose total traffic demands are less than or equal to the channel capacity can be combined into a group using the same wavelength channel.

Previously, Zhu and Mukherjee (2002) proposed Maximizing Single-Hop Traffic (MST) and Maximizing Resource Utilization (MRU) techniques for traffic grooming. These grooming algorithms sort the set of commodities assorting to some criterion and then combine multiple overlapped commodities into the same group by following the ordering. Overlapped commodities early in the sequence are considered for grouping first.

In this paper, we propose that some non-overlapped commodities can be groomed into the same group if there exists a commodity which overlaps or bridges the routes between the non-overlapped commodities. Suppose that we have eight commodities with routings generated by using the GA, as shown in table 1 and figure 3. In Fig. 3, C0:0.5 represents a commodity C0 with 0.5 unit of wavelength requirement. We can see that the routes for C0 and C1 do not overlap. However, C0 and C1 can be combined together with C2 because C2 overlaps with both C0 and C1. By doing this, we can reduce the number of wavelength channels required in the optical network design.

Table 1. The route of each commodity obtained from GA.

Commodity	Routing	Commodity	Routing
0	0→1→2→3	4	3→4→5
1	3→4→5→6	5	6→7→8
2	2→3→4	6	6→7
3	3→4→5	7	7→8

Before we combine multiple commodities into groups, we create an auxiliary graph for the set of light paths to represent which commodities overlap. In the auxiliary graph shown in figure 4, which corresponds to the routings in table 1, each node represents a commodity. If a commodity's path overlaps with another commodity a link is created between these commodity nodes in the auxiliary graph.

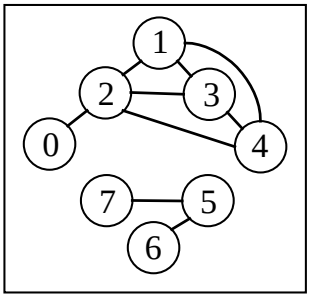

Fig. 4. The auxiliary graph of overlapped commodities.

In the traditional traffic grooming approach using MST, the commodities that overlap will be considered for grooming into a group. For example, in figure 4, commodities 3 and 4 are groomed first because they have the same source and destination. After that C0 and C1 are considered. C0 and C1 cannot be groomed together because they are not overlapped. C2 is groomed with C0 because high traffic demand is considered first. C1 cannot be groomed with C0 and C2 because their light paths overlap. Lastly, C5, C6 and C7 are groomed together in the same group.

In our extended traffic grooming (ETG) approach, we reexamine commodities in existing groups after this first phase. ETG will try to combine groups by searching for commodities in one group that overlap with commodities in another group, where the total bandwidth of the combined groups will not exceed the wavelength bandwidth constraint.

For example, C0 and C2 are first assigned into a group. C1 forms a second group on its own. We can add C1 to the group including C0 and C2 because C2 also overlaps with C1 and the summation of bandwidth on the path from 3 to 4 does not exceed the wavelength bandwidth constraint. Table 2 compares the set of commodities groomed in each group by using MST and ETG algorithms, for this example. The MST requires four groups while ETG requires only three.

The ETG algorithm sorts the commodities in descending order by the number of hops in their routes and their bandwidth requirements (traffic demand). Our experiments during algorithm development showed that when the bandwidth required by each commodity is small, the sequence of commodities should be sorted by bandwidth requirements first, and then by number of hops. In this paper, if the average bandwidth required is less than 0.4 wavelengths, we sort by bandwidth first, and then by number of hops. Otherwise we sort by number of hops first.

Table 2. The set of commodities and link bandwidth in the groomed groups.

MST			ETG		
Set of commodities	Joint edge	Link bandwidth	Set of commodities	Joint edge	Link bandwidth
C3 and C4	3→4	0.8	C0, C1 and C2	2→3	0.9
	4→5	0.8		3→4	0.8
C0 and C2	2→3	0.9	C3 and C4	3→4	0.8
C1		0.4		4→5	0.8
C5, C6 and C7	6→7	0.6	C5, C6 and C7	6→7	0.6
	7→8	0.6		7→8	0.6

In table 1, the set of commodities has the average traffic demand of 0.375 which is less than 0.4 wavelengths. Therefore, the sequence of commodities is sorted in descending order first by the bandwidth requirements and then by the hop count as shown in table 3.

Table 3. The groomed commodities.

Commodity	Traffic demand	Number of hops	Group ID.
0	0.5	3	0
1	0.4	3	0
2	0.4	2	0
3	0.4	2	1
4	0.4	2	1
5	0.3	2	2
6	0.3	1	2
7	0.3	1	2

Maximum Degree First (MaxDF) Wavelength Assignment

We propose the Maximum Degree First (MaxDF) algorithm to assign a limited number of wavelength channels to a set of commodities. After we combine multiple low-rate traffic demands into groups in the traffic grooming phase described previously, we create a second auxiliary graph to specify which groups of commodities overlap, as shown in figure 5. A traffic group overlaps with another group if it has at least one commodity whose route overlaps with a member of the other group. For example, Group 0 overlaps with Group 1 because commodity1 in the Group 0 overlaps with commodities 3and 4 in the Group 1. In the auxiliary graph, the circle symbol represents a group, while the rectangle shows members in the group. The link between a pair of nodes represents the existence of an overlap. In figure 5, for example, we have three groups. Groups 0 and 1 overlap (i.e., at network edge 3→4 and edge 4→5 in Fig. 3). Therefore, a link between overlapping groups is created. Any pair of auxiliary nodes that has a link cannot be assigned to the same wavelength.

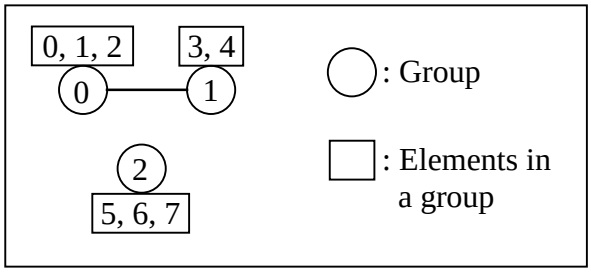

Fig. 5. The auxiliary graph of overlapped commodities in the group.

We modify the traditional First-Fit algorithm (Banerjee and Sharan, 2004) that assigns the wavelength from smallest channel index to the highest channel index. In our algorithm, we assign the wavelength according to the auxiliary graph. A node in the auxiliary graph that has a high degree represents a group that overlaps with others. Therefore, the maximum-degree node (group of commodities) in the auxiliary graph should be assigned first. If low degree nodes in the auxiliary graph are selected and assigned first, many other commodities in the group will be blocked. The MaxDF algorithm can be presented as follows.

Maximum Degree First (MaxDF) Algorithm

1. Sort all nodes (groups of commodities) by the number of degrees from the largest degree to the smallest degree.
2. At the first rank (largest number of degree, or highest overlapped group of commodities with the other), assign the first wavelength.
3. At the next group of commodities, if its commodity is not overlapped with the previous groups of commodities, assign the same wavelength channel as the previous group of commodities, else assign the next wavelength.
4. Repeat Step 3, until all groups of commodities are considered.

After the MaxDF process, we have the set of commodities in the group with wavelength channels as shown in figure 6. For instance, channel 0 is assigned to Groups 0 and 2

because none of the commodities in these groups overlap. The commodities in the group also have the same wavelength channel as shown in figure 7.

Group ID	0	1	2
Wavelength Channel	0	1	0

Fig. 6. The wavelength channel of the set of groups.

Commodity	0	1	2	3	4	5	6	7
Wavelength channel	0	0	0	1	1	0	0	0

Fig. 7. The wavelength channel of the set of commodities.

Our previous work (Leesutthipornchai *et al*., 2009) compared the performance of our routing algorithm with the traditional routing approach called Fixed Alternate Routing (FAR) and our wavelength assignment algorithm with the traditional wavelength assignment called First-Fit (FF). That study showed that our combined routing and wavelength assignment algorithms can assign the wavelength as fast as the First-Fit algorithm but with superior results in terms of accepted commodity requests.

NSGA-II Algorithm

Our GA-ETG-MaxDF algorithm generates many possible solutions, which tradeoff between our multiple objectives. We need to identify the best solution candidates in this large solution set. To do this, we employ the NSGA-II algorithm.

The Fast Non-dominated Sorting Genetic Algorithm (NSGA-II) proposed by Deb *et al*. (2002) is well-known as an efficient technique to search for the Pareto-optimal set in general multi-objective optimization problems. NSGA-II is a very fast algorithm that can rapidly converge to the Pareto-front. In this paper, we adapt the NSGA-II for the multi-objective grooming, routing and wavelength assignment (GRWA) problem as shown in figure 8.

The algorithm starts with population initialization. The five shortest paths for each commodity are created as a starting point. More possible paths are randomly generated, up to the specified population size, which was 200 in this study. The initialization stage produces multiple sets of routes, each of which represents a possible routing solution for the given set of commodities and bandwidth requirements.

In the next stage, which is used for traffic grooming, multiple low rate traffic demands are assigned to the same group to conserve wavelength channels and reduce the number of switching ports. We consider three traffic grooming algorithms which are Extended Traffic Grooming (ETG), Maximizing Resource Utilization (MRU) and Maximizing Single-hop Traffic (MST).

In the third stage which is used for wavelength assignment, non-overlapped groups are assigned to the same wavelength channel. After this wavelength assignment procedure, the number of accepted commodities, wavelength channels and switching ports are calculated. The number of required switching ports and wavelengths depend on whether a commodity is accepted or not. We consider three wavelength assignment methods which are First Fit (FF), Minimum Degree First (MinDF) and Maximum Degree First (MaxDF).

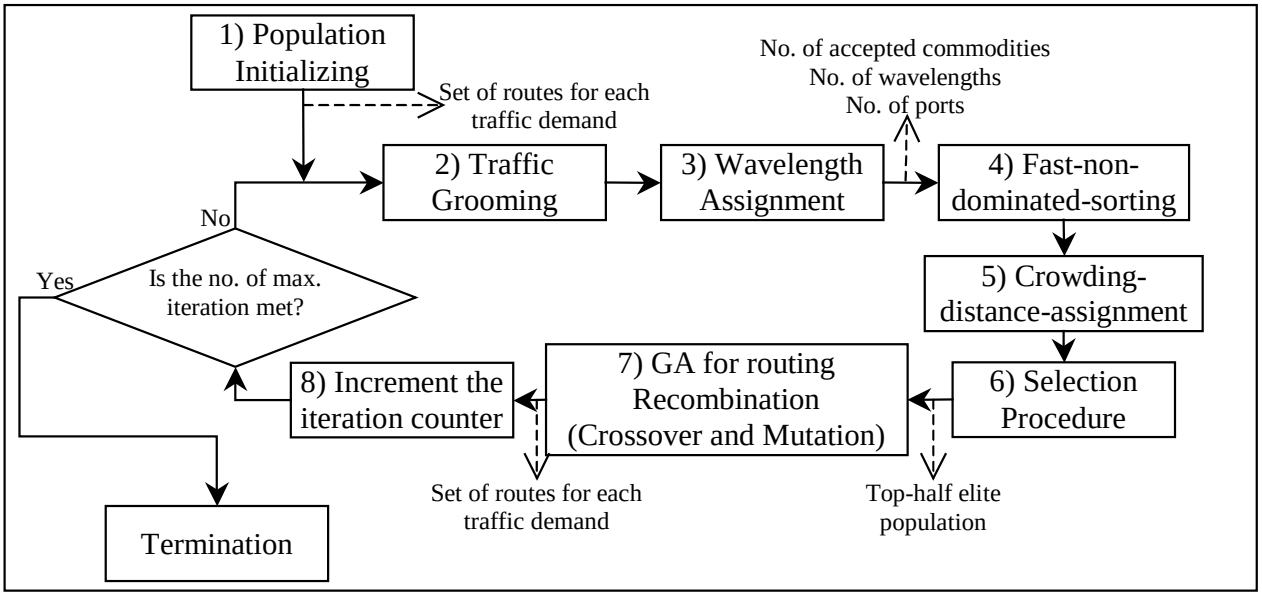

Fig. 8. The modified NSGA-II procedure.

Table 4. The features of various network topologies.

Network topologies	No. of (non-directional) edges	No. of nodes	No. of edges/ No. of nodes	Degree			
				Total deg.	Average deg. (Total Deg./ No. of nodes)	Min deg.	Max deg.
NSFNET	21	14	1.5	42	3	2	4
CHNNET	27	15	1.8	54	3.6	3	5
ARPANET	32	20	1.6	64	3.2	3	4

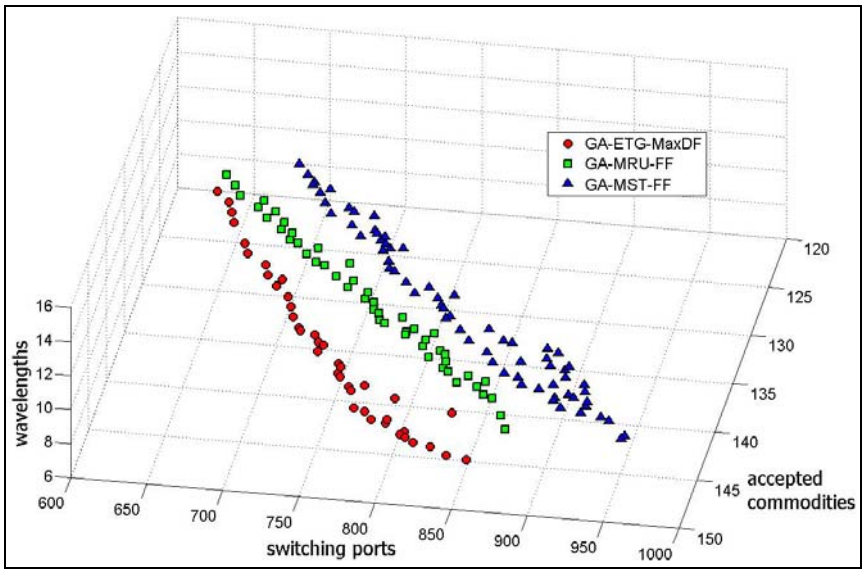

Fig. 9. The non-dominated solutions obtained from NSFNET.

Next, the potential solutions are sorted by solution quality and the best 50% are preserved for the next generation.

After sorting and selection, multiple sets of routes are exchanged and mutated in order to obtain new feasible routes that do not exist in the current population. Then the iteration counter is incremented. Lastly, the algorithm checks for the termination condition. In this paper, the algorithm is terminated when the maximum number of iterations is met, which in this case was 2,400.

RESULTS AND DISCUSSION

In our experiments, we considered the multi-objective GRWA problem with given network topologies, set of commodities and set of bandwidth requirements. We used a uniform distribution to randomly generate a set of test problems with various numbers of commodities and bandwidth requirements. We assumed that all edges have the same wavelength capacity. We limited the number of wavelength channels in each edge/link of the network and required at least 80% of the requested commodities must be accepted.

For our test network topologies, we adapted three different example networks which are National Science Foundation Network (NSFNET) with 14 nodes and 42 directional edges (Adhya and Datta, 2009), Chinese National Network (CHNNET) with 15 nodes and 54 directional edges (Guo *et al*., 2006) and Advanced Research Projects Agency Network (ARPANET) with 20 nodes and 64 directional edges. Table 4 summarizes the characteristics of these networks. CHNNET has the highest value of average degree (i.e., 3.6).

We implemented our algorithms with new own code in Java and ran our tests on a Pentium 4 PC (Core 2 Quad CPU 2.83 GHz, 3.25 GB of RAM).We compared our proposed GA-ETG-MaxDF heuristic with traditional traffic grooming algorithms and wavelength assignments methods which are 1) GA-MRU-FF (GA for routing, MRU for grooming and FF for wavelength assignment) and 2) GA-MST-FF (GA for routing, MST for grooming and FF for wavelength assignment). We used the same set of network configurations and traffic parameters for all traffic grooming algorithms. The obtained results were compared to each other as shown in figure 9-14.

In multi-objective optimization, the results are plotted as a front or set of non-dominated solutions. Table 5 also shows the multi-objective performance metrics and computation time obtained from each approach for various network configurations.

Our results show that the set of solutions from the GA-ETG-MaxDF is located in the area of high accepted commodities, few switching ports and few wavelengths, when compared with other algorithms. This is true for all network topologies as shown in figures 9-14. For the NSFNET topology, as shown in figures 9-11, the solutions from the GA-ETG-MaxDF require 626-860 switching ports while the solutions from the GA-MRU-FF and the GA-MST-FF require 632-886 and 680-962 ports, respectively. Figure 10 show that the GA-ETG-MaxDF technique can support 150 commodities within 860 ports. With the same number of ports, the GA-MRU-FF technique can support 145 commodities and the GA-MST-FF can support only 140 commodities. In other words, the GA-ETG-MaxDF requires a fewer number of switching ports compared with the GA-MRU-FF and the GA-MST-FF for satisfying all commodities.

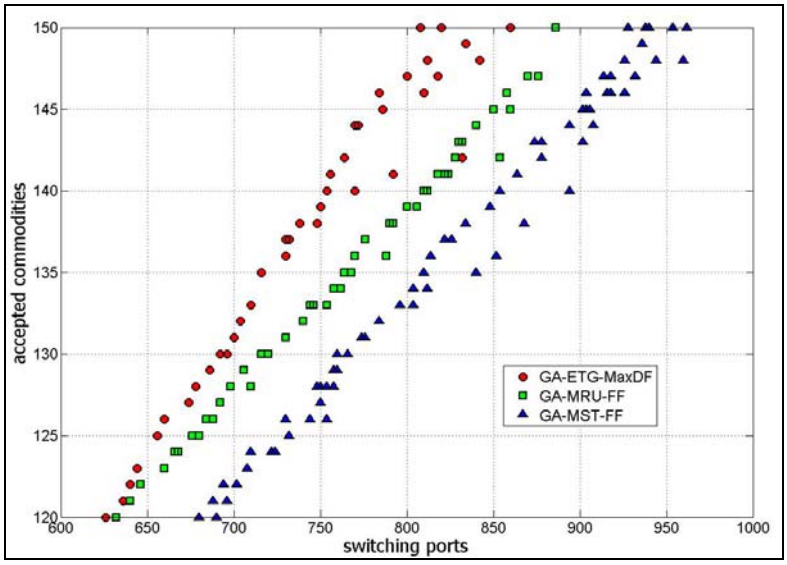

Fig. 10. The relation between accepted commodity and switching port obtained from NSFNET (with the number of wavelengths in the range of 6 to 15).

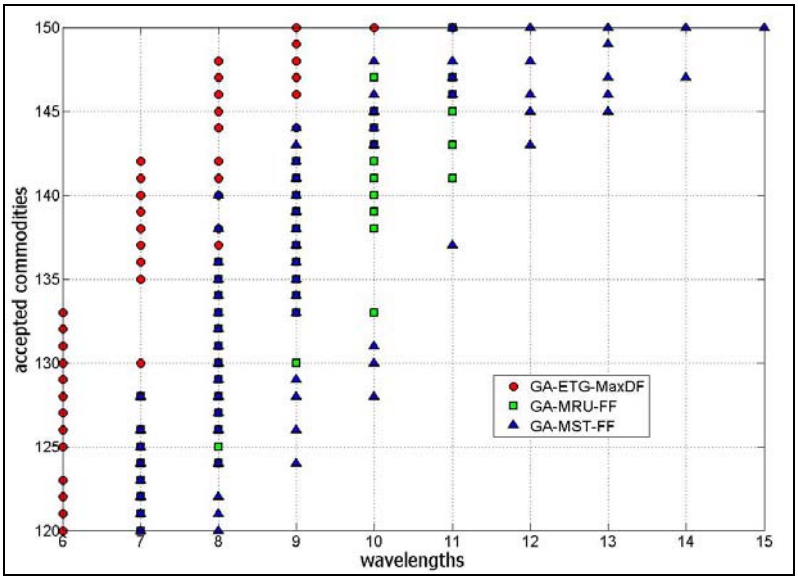

Fig. 11. The relation between accepted commodity and wavelength obtained from NSFNET (with the number of switching ports in the range of 626 to 962).

Figure 11 shows that the GA-ETG-MaxDF can support a larger number of accepted commodities than the GA-MRU-FF and the GA-MST-FF with the same number of wavelengths. To satisfy all commodities, the GA-ETG-MaxDF requires fewer wavelength channels than the GA-MRU-FF and the GA-MST-FF.

Similar patterns of results are obtained for the CHNNET topology as shown in figures 12 and 13, and the ARPANET topology as shown in figure 14.

In addition to the results shown in figures 9-14, we compared values of various multi-objective performance metrics (Zitzler, 1999; Tan *et al*., 2001; Nebro *et al*., 2009), namely Hyper-volume (HV), Spread, and Inverted Generational Distance (IGD). These metrics have been proposed to measure the "goodness" of a Pareto solution set, independent of the decision criteria functions.

Table 5 together with figures 15-17 show the obtained performance metrics of GA-ETG-MaxDF compared to GA-MST-FF and GA-MRU-FF.

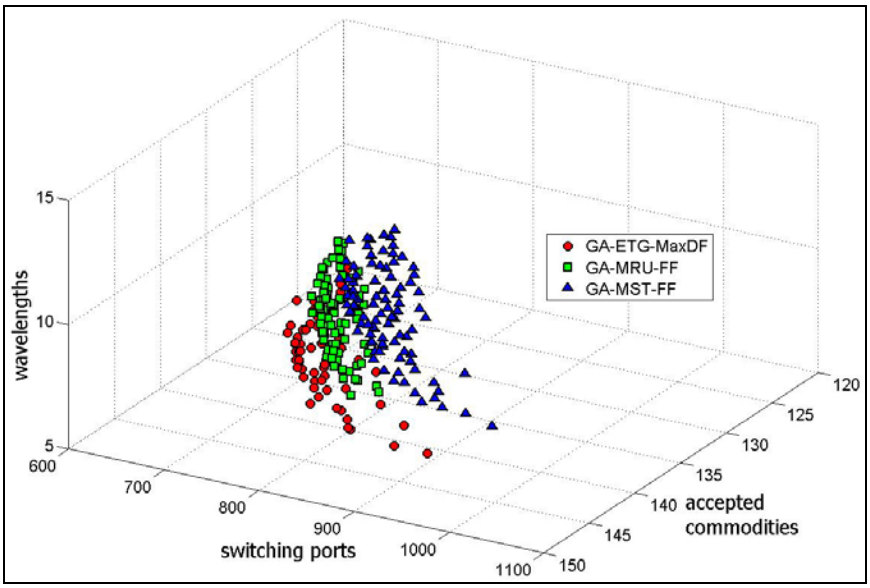

Fig. 12. The non-dominated solutions obtained from CHNNET.

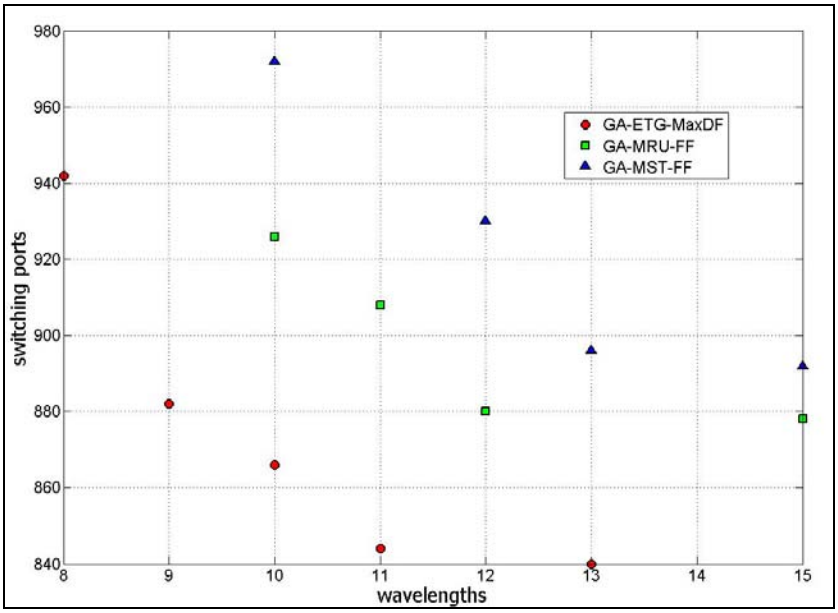

Fig. 13. The relation between switching port and wavelength obtained from CHNNET.

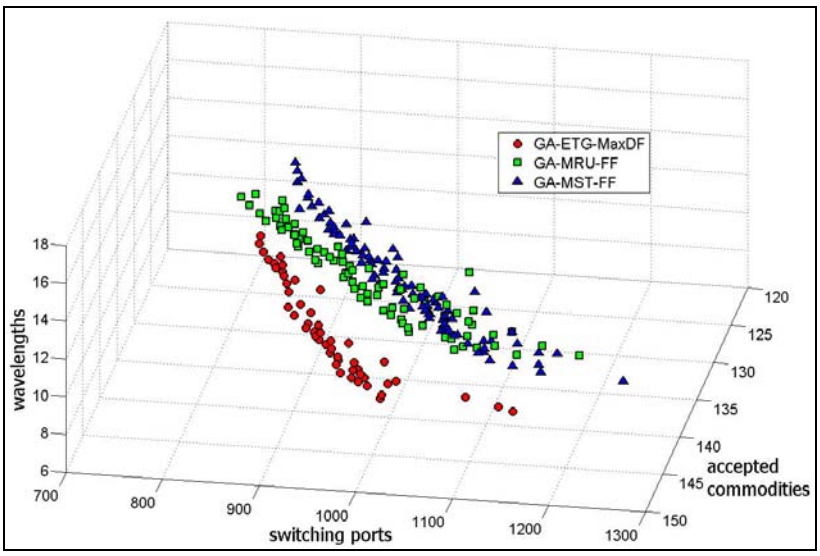

Fig. 14. The non-dominated solutions obtained from ARPANET.

Table 5. Multi-objective performance metrics of GA-ETG-MaxDF, GA-MST-FF and GA-MRU-FF in various network topologies.

Traffic demands (No. of source-destination pairs)	Network topologies	GRWA techniques	HV.	Spread	IGD.	CPU time (sec.)	
						Average*	Total
50	NSFNET	GA-ETG-MaxDF	**0.4701**	0.4262	**0.0000**	2,352.67	7,058.00
		GA-MST-FF	0.2684	0.4000	0.0556	2,320.00	6,960.00
		GA-MRU-FF	0.3333	0.3555	0.0317	2,300.33	6,901.00
	CHNNET	GA-ETG-MaxDF	**0.3677**	0.0692	**0.0000**	2,613.67	7,841.00
		GA-MST-FF	0.0129	0.8172	0.2411	2,561.00	7,683.00
		GA-MRU-FF	0.0839	0.6010	0.2308	2,548.00	7,644.00
	ARPANET	GA-ETG-MaxDF	**0.3825**	0.2685	**0.0000**	4,511.33	13,534.00
		GA-MST-FF	0.2235	0.4654	0.0494	4,433.00	13,299.00
		GA-MRU-FF	0.2497	0.4619	0.0487	4,428.33	13,285.00
100	NSFNET	GA-ETG-MaxDF	**0.5085**	0.4084	**0.0062**	8,606.33	25,819.00
		GA-MST-FF	0.1738	0.5213	0.0525	8,591.33	25,774.00
		GA-MRU-FF	0.3181	0.5411	0.0330	8,594.00	25,782.00
	CHNNET	GA-ETG-MaxDF	**0.5826**	0.4244	**0.0051**	9,713.67	29,141.00
		GA-MST-FF	0.4142	0.3532	0.0195	9,602.67	28,808.00
		GA-MRU-FF	0.5154	0.3482	0.0130	9,584.00	28,752.00
	ARPANET	GA-ETG-MaxDF	**0.4875**	0.4170	**0.0000**	16,860.33	50,581.00
		GA-MST-FF	0.2120	0.4557	0.0384	16,728.33	50,185.00
		GA-MRU-FF	0.3230	0.4238	0.0270	16,729.00	50,187.00
150	NSFNET	GA-ETG-MaxDF	**0.5064**	0.5124	**0.0000**	19,265.33	57,796.00
		GA-MST-FF	0.1522	0.5412	0.0502	19,249.67	57,749.00
		GA-MRU-FF	0.2704	0.4818	0.0369	19,269.00	57,807.00
	CHNNET	GA-ETG-MaxDF	**0.5884**	0.4832	**0.0051**	21,544.00	64,632.00
		GA-MST-FF	0.3420	0.4709	0.0245	21,400.00	64,200.00
		GA-MRU-FF	0.4955	0.4894	0.0127	21,254.33	63,763.00
	ARPANET	GA-ETG-MaxDF	**0.4859**	0.4830	**0.0098**	37,212.67	111,638.00
		GA-MST-FF	0.2106	0.4953	0.0346	37,218.67	111,656.00
		GA-MRU-FF	0.2558	0.4972	0.0288	37,187.67	111,563.00

*per 1 replication run

Hyper-Volume (HV) measures the coverage area of solutions. A high HV value is preferred, since this indicates that the non-dominated solutions cover the objective space more broadly. Table 5 and figure 15 show that the solutions from the GA-ETG-MaxDF give a higher HV value than those of GA-MRU-FF and GA-MST-FF in all network topologies and all cases of traffic demands.

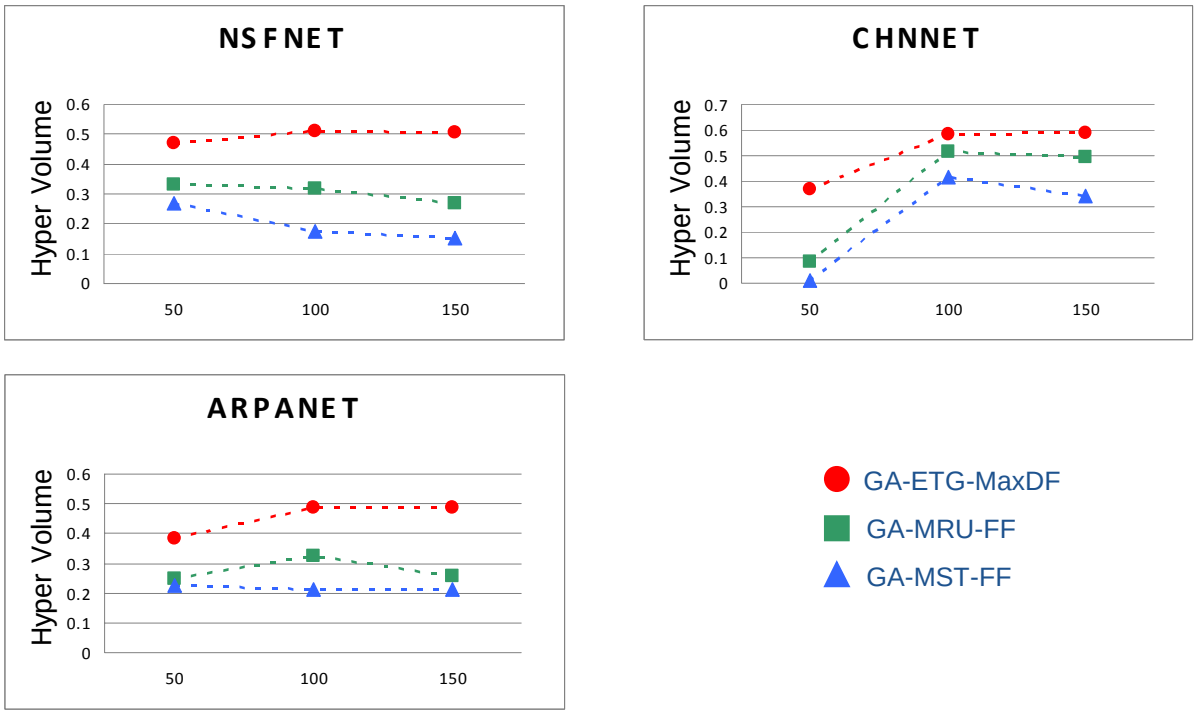

Fig. 15. Hyper-volume of traffic grooming algorithms with 50, 100 and 150 commodities for three network topologies.

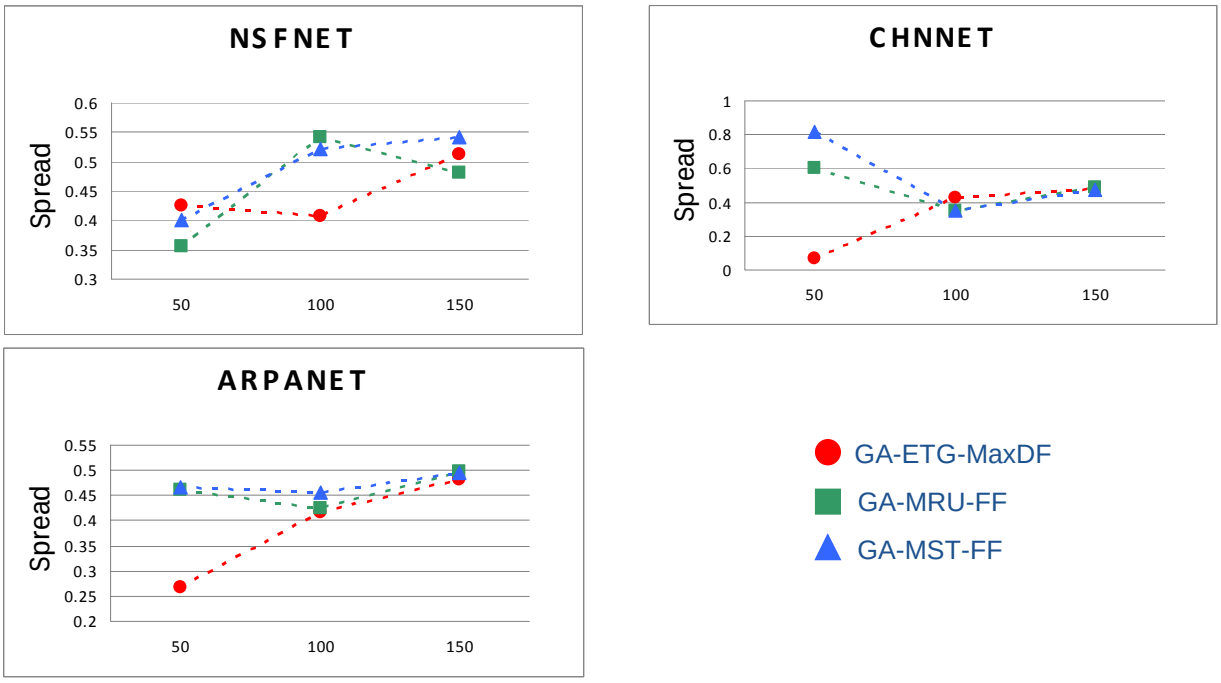

Fig. 16. Spread of traffic grooming algorithms with 50, 100 and 150 commodities for three different network topologies.

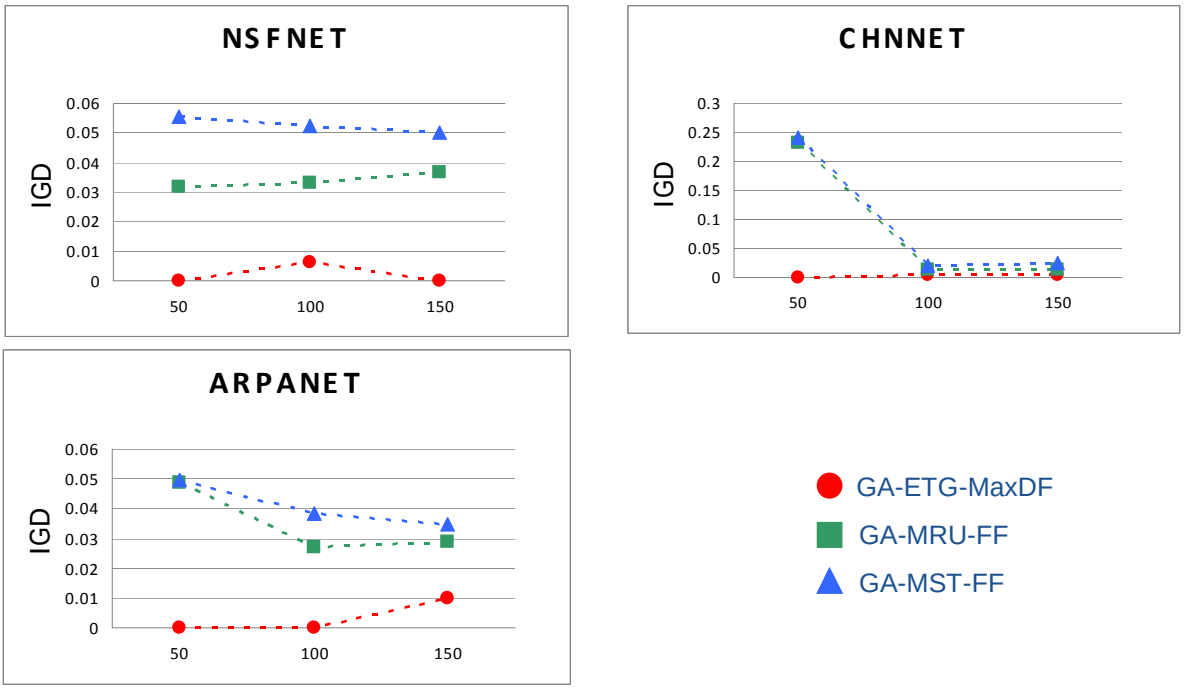

Fig. 17. IGD of traffic grooming algorithms with 50, 100 and 150 commodities for three different network topologies.

For the Spread metric, a low value is preferred. Low Spread values indicates that the solutions distribute into all objective areas equally (not crowding into one small objective area). In our experimental results, the Spread values from the three traffic grooming algorithms do not show any consistent patterns for NSFNET or CHNNET. However, for the ARPANET topology, the obtained results from our GA-ETG-MaxDF approach have lower Spread values than alternative approaches for all sizes of traffic demand as shown in figure 16.

Inverted Generational Distance (IGD is the distance from the obtained solutions to the Pareto optimal set. Lower IGD values indicate better solution quality. IGD is equal to zero when all elements are in the Pareto optimal set. Table 5 and figure 17 show that the results from our GA-ETG-MaxDF approach have lower IGD values than alternative approaches for all sizes of traffic demands and all network topologies. In some cases, such as for NSFNET topology with 150 commodities, the IGD value from GA-ETG-MaxDF is equal to 0. This means that all obtained solutions from GA-ETG-MaxDF are in the Pareto optimal set.

Finally, table 5 also shows the average and total CPU time of the three traffic grooming algorithms used to find solutions indifferent network topologies and traffic demands. The average and total CPU time of the three traffic grooming algorithms do not differ in any consistent way. These times are acceptable for offline computation.

In summary, the experimental results demonstrate that the GA-ETG-MaxDF heuristic outperforms both the GA-MST-FF and the GA-MRU-FF for solving the GRWA problem with a variety of network topologies and levels of demand. The solution sets produced by the algorithm also tend to score higher on measures of Pareto optimality.

CONCLUSION

In this paper, the Traffic Grooming, Routing and Wavelength Assignment (GRWA) problem in WDM optical network is addressed with a multi-objective network optimization approach. Our network design objectives are to maximize the number of accepted commodities, minimize the number of required wavelengths and minimize the number of switching ports. We propose a heuristic multi-objective solution procedure which combines GA-ETG-MaxDF and NSGA-II algorithms to solve the GRWA problem and search for a set of non-dominated solutions. The GA-ETG-MaxDF considers all potential routes by using Genetic Algorithm (GA), combines multiple low rate traffic demands with Extended Traffic Grooming (ETG) algorithm, and assigns the wavelength channel by using Maximum Degree First Wavelength Assignment (MaxDF) algorithm. The GA-ETG-MaxDF heuristic allows multiple non-overlapped commodities to be groomed into the same group which results in better utilization of network resources. We compared the performance of our proposed GA-ETG-

MaxDF approach with previously published traffic grooming algorithms, MST-FF and MRU-FF. All traffic grooming approaches used the same GA process for route generation and NSGA-II for searching non-dominated solutions. The results showed that the proposed GA-ETG-MaxDF heuristic together with NSGA-II algorithm outperforms the other two traffic grooming algorithms by providing a set of non-dominated solutions with a higher number of accepted commodities, fewer switching ports and fewer wavelength channels. We also compared all three traffic grooming algorithms by using the multi-objective performance metrics of Hyper-volume (HV), Spread and Inverted Generational Distance (IGD). We found that the results from the GA-ETG-MaxDF were generally superior to those from the existing traffic grooming approaches. Therefore, we are confident that the GA-ETG-MaxDF technique with NSGA-II algorithm is effective for solving the GRWA problem with multiple design objectives. Our research work makes several contributions as follows. 1) We have formulated the traffic grooming, routing and wavelength assignment (GRWA) problem in WDM optical networks as a multi-objective optimization model. 2) We have developed an effective technique called “GA-ETG-MaxDF” for solving the GRWA problem. 3) We have applied the state-of-the-art NSGA-II approach together with the GA-ETG-MaxDF technique as a multi-objective evolutionary computation heuristic to solve the multi-objective GRWA network design problem.

ACKNOWLEDGEMENT

This work was supported by the Thailand Research Fund through the Royal Golden Jubilee Ph.D. Program (Grant No. PHD 0045/2550), King Mongkut’s University of Technology Thonburi (KMUTT), National Research University Project of Thailand and Office of the Higher Education Commission.

REFERENCES

Adhya, A. and Datta, D. 2009. Design Methodology for WDM Backbone Networks using FWM-aware Heuristic Algorithm. Journal of Optical Switching and Networking. 6:10-19.

Assis, KDR., Santos, RMO., Freitas, M. and Waldman, H. 2008. Optical Networks Design with Multicriteria and Open Capacity Analysis. Proceedings of the 5th IFIP International Conference on Wireless and Optical Communications Networks (WOCN). 1-6.

Awwad, O., Al-Fuqaha, AI. and Rayes, A. 2007. Traffic Grooming, Routing, and Wavelength Assignment in WDM Transport Networks with Sparse Grooming Resources. International Journal of Computer Communications. 30(18):3508-3524.

Banerjee, N. and Sharan, S. 2004. An Evolutionary Algorithm for Solving the Single Objective Static Routing and Wavelength Assignment Problem in WDM Networks. Proceedings of the International Conference on Intelligent Sensing and Information Processing (ICISIP). 13-18.

Banerjee, N. and Kumar, R. 2007. Multiobjective Network Design for Realistic Traffic Models. Proceedings of the 9th Annual Conference on Genetic and Evolutionary Computation. 1904-1911.

Cahon, S., Talbi, EG. and Melab, N. 2006. A Parallel and Hybrid Multi-Objective Evolutionary Algorithm Applied to the Design of Cellular Networks. Proceedings of the International Conference on IEEE MELECON. 803-806.

Chatterjee, BC., Sarma, N. and Sahu, PP. 2012. Priority based routing and wavelength assignment with traffic grooming for optical networks. IEEE/OSA Journal of Optical Communications and Networking. 4(6):480-489.

Chen, B., Jiang, ZM., Teng, RKF., Lin, XH., Dai, MJ. and Wang, H. 2013. An Energy Efficiency Optimization Method in Bandwidth Constrained IP Over WDM Networks. The 9th International Conference on Information Communications and Signal Processing (ICICS). 1-4.

Chlamtac, I., Ganz, A. and Karmi, G. 1992. Lightpath Communications: An Approach to High Bandwidth Optical WANs. IEEE Transactions on Communications. 40(7):1171-1182.

Coit, DW. and Konak, A. 2006. Multiple Weighted Objectives Heuristic for the Redundancy Allocation Problem. IEEE Transactions on Reliability. 55(3):551-558.

De, T., Jain, P., Pal, A. and Sengupta, I. 2008. A Multi Objective Evolutionary Algorithm Based Approach for Traffic Grooming, Routing and Wavelength Assignment in Optical WDM Networks. IEEE Region 10 and the 3rd international Conference on Industrial and Information Systems (ICIIS). 1-6.

Deb, K., Pratap, A., Agarwal, S. and Meyarivan, T. 2002. A Fast and Elitist Multi-objective Genetic Algorithm: NSGA-II. IEEE Transactions on Evolutionary Computation. 6(2):182-197.

Dutta, R. and Rouskas, GN. 2002. Traffic Grooming in WDM Networks: Past and Future. IEEE Network. 16(6):46-56.

Fonseca, CM. and Fleming, PJ. 1993. Genetic Algorithms for Multiobjective Optimization: Formulation, Discussion and Generalization. Proceedings of the 5th International Conference in Genetic Algorithms. 416-423.

Guo, L., Cao, J., Yu, H. and Li, L. 2006. Path-based Routing Provisioning with Mixed Shared Protection in

WDM Mesh Networks. Journal of Lightwave Technology. 24(3):1129-1141.

Hajela, P. and Lin, CY. 2005. Genetic Search Strategies in Multi-criterion Optimal Design. Journal on Structural and Multidisciplinary Optimization. 4(2):99-107.

Horn, J., Nafpliotis, N. and Goldberg, DE. 1994. A Niched Pareto Genetic Algorithm for Multi-Objective Optimization. IEEE World Congress on Computational Intelligence. 1:82-87.

Hsu, CY., Wu, JLC., Wang, ST. and Hong, CY. 2008. Survivable and Delay-Guaranteed Backbone Wireless Mesh Network Design. Journal of Parallel and Distributed Computing. 68(3):306-320.

Hu, JQ. and Leida, B. 2004. Traffic Grooming, Routing, and Wavelength Assignment in Optical WDM Mesh Networks. Proceedings of the 23th Annual Joint Conference of the IEEE Computer and Communications Societies (INFOCOM). 1:495-501.

Huang, H. and Copeland, JA. 2003. Optical Networks with Hybrid Routing. IEEE Journal on Selected Areas in Communications. 21(7):1063-1070.

Jaekel, A., Bandyopadhyay, S. and Aneja, Y. 2008. A New Approach for Designing Fault-tolerant WDM Networks. International Journal of Computer and Telecommunications Networking. 52:3421-3432.

Kavian, YS., Rashvand, HF., Ren, W., Naderi, M., Leeson, MS. and Hines, EL. 2008. Genetic Algorithm Quality of Service Design in Resilient Dense Wavelength Division Multiplexing Optical Networks. Journal on IET Communications. 2(4):505-513.

Knowles, JD. and Corne, DW. 1999. The Pareto Archived Evolution Strategy: A New Baseline Algorithm for Pareto Multi-Objective Optimization. Proceedings of the 1999 Congress on Evolutionary Computation. 98-105.

Konak, A., Coit, DW. and Smith, AE. 2006. Multi-Objective Optimization Using Genetic Algorithms: A Tutorial. Proceedings of International Conference on Reliability Engineering and System Safety. 992-1007.

Leesutthipornchai, P., Wattanapongsakorn, N. and Charnsripinyo, C. 2009. Multi-Objective Design for Routing Wavelength Assignment in WDM Networks. Proceedings of the 1st International Workshop on Networks and Communications (NeCoM). 1315-1320.

Leesutthipornchai, P., Wattanapongsakorn, N. and Charnsripinyo, C. 2009. Multi-Objective Optimization Techniques Based on Genetic Algorithm. Proceedings of the National Computer Science and Engineering Conference (NCSEC). 276-281.

Lin, R., Zhong, WD., Bose, SK. and Zukerman, M. 2012. Multicast Traffic Grooming in Tap-and-Continue WDM Mesh Networks. IEEE/OSA Journal of Optical Communications and Networking. 4(11):918-935.

Murata, T. and Ishibuchi, H. 1995. MOGA: Multi-Objective Genetic Algorithms. Proceedings of the IEEE International Conference on Evolutionary Computation. 289-294.

Nebro, AJ., Durillo, JJ., Luna, F., Dorronsoro, B. and Alba, E. 2009. MOCell: A Cellular Genetic Algorithm for Multiobjective Optimization. International Journal of Intelligent Systems. 24(7):726-746.

Prathombutr, P., Stach, J. and Park, EK. 2005. An Algorithm for Traffic Grooming in WDM Optical Mesh Networks with Multiple Objectives. Journal of the INFORMS Section on Telecommunications. 369-386.

Ribeiro, CC., Martins, SL. and Rosseti, I. 2007. Metaheuristics for Optimization Problems in Computer Communications. Journal on Computer Communications. 30(4):656-669.

Roa, DP., Baran, B. and Brizuela, CA. 2009. Wavelength Converter Allocation in Optical Networks: An Evolutionary Multi-objective Optimization Approach. The 9th International Conference on Intelligent Systems Design and Applications (ISDA). 414-419.

Saleh, AAM. and Simmons, JM. 2012. All-Optical Networking - Evolution, Benefits, Challenges, and Future Vision. Proceedings of the IEEE. 100(5):1105-1117.

Schaffer, JD. 1985. Multiple Objective Optimization with Vector Evaluated Genetic Algorithms. Proceedings of the International Conference on Genetic Algorithm and Their Applications.

Shalom, M., Unger, W. and Zaks, S. 2007. On the Complexity of the Traffic Grooming Problem in Optical Networks. Lecture Notes in Computer Science: Fun with Algorithms. 4475:262-271.

Shen, G. and Tucker, RS. 2009. Sparse Traffic Grooming in Translucent Optical Networks. International Journal of Lightwave Technology. 27(20):4471-4479.

Srinivas, N. and Deb, K. 1994. Multiobjective Optimization using Nondominated Sorting in Genetic Algorithms. Journal of Evolutionary Computation. 2:221-248.

Tan, KC., Lee, TH. and Khor, EF. 2001. Evolutionary Algorithms for Multi-Objective Optimization: Performance Assessments and Comparisons. Proceedings of the IEEE Congress on Evolutionary Computation. 979-986.

Wang, J., Vemuri, VR., Cho, W. and Mukherjee, B. 2001. Improved Approaches for Cost-effective Traffic Grooming in WDM Ring Networks: ILP Formulations and Single-hop and Multihop Connections. IEEE/OSA Journal of Lightwave Technology. 19(11):1645-1653.

Zhao, J., Subramaniam, S. and Brandt-Pearce, M. 2013. QoT-aware Grooming, Routing, and Wavelength Assignment (GRWA) for Mixed-Line-Rate translucent optical networks. Journal of China Communications. 10(1):17-30.

Zhu, K. and Mukherjee, B. 2003. A Review of Traffic Grooming in WDM Optical Networks: Architectures and Challenges. SPIE Optical Networks Magazine. 4(2):55-64.

Zhu, K. and Mukherjee, B. 2002. Traffic Grooming in an Optical WDM Mesh Network. IEEE Journal on Selected Areas in Communications. 20(1):122-133.

Zitzler, E. 1999. Evolutionary Algorithms for Multiobjective Optimization: Methods and Applications. PhD dissertation. Swiss Federal Institute of Technology Zurich.

Zitzler, E., Laumanns, M. and Thiele, L. 2001. SPEA2: Improving the Strength Pareto Evolutionary Algorithm. Computer Engineering and Networks Laboratory (TIK), Department of Electrical Engineering, Swiss Federal Institute of Technology (ETH) Zurich, Switzerland. 1-21.

Zitzler, E. and Thiele, L. 1999. Multiobjective Evolutionary Algorithms: A Comparative Case Study and the Strength Pareto Approach. IEEE Transactions on Evolutionary Computation. 3(4):257-271.

Received: July 30, 2014; Accepted: Sept 5, 2014

SENRA Academic Publishers, British Columbia
Vol. 8, No. 3, pp. 3081-3089, October 2014
Online ISSN: 1920-3853; Print ISSN: 1715-9997

Canadian Journal of pure&applied sciences

SADDLEPOINT APPROXIMATION TO CUMULATIVE DISTRIBUTION FUNCTIONS FOR SOME DIFFICULT AND UNKNOWN LINEAR COMBINATIONS OF RANDOM VARIABLES

*Al Mutairi Alya O and Heng Chin Low
School of Mathematical Sciences, Universiti Sains Malaysia, 11800 Penang, Malaysia

ABSTRACT

Approximations are very important because it is sometimes not possible to obtain an exact representation of the probability distribution function (PDF) and the cumulative distribution function (CDF). Even when true (exact) representations are possible, approximations, in some cases, simplify the analytical treatments. In this paper, we extend the known saddlepoint tail probability approximations to univariate cases, including univariate conditional cases. Our first approximation (the weighted random sum $S_{N(c)}$) applies to unknown and very difficult statistics (we discuss the approximations within the random sum Poisson-Exponential random variables).We evaluate the performance of the saddlepoint approximation using simulations. Our second approximation (convolutions of Gamma random variables, L_N), are difficult to obtain. These computations are also compared with the exact and normal approximations. We find that the saddlepoint methods provide very accurate approximations for the CDFs probabilities that surpass other methods of approximation, such as normal approximation.The third approximation, including conditional saddlepoint approximations, uses the double saddlepoint. To demonstrate the methods of conditioning in statistical inference, we find a mid p-value using a conditionalsaddlepoint approximation for percentile modified linear rank tests. We show that in the double saddlepoint case, the saddlepoint approximations demonstrate better accuracy than the normal approximation while sharing the same accuracy.

Keywords: Saddlepoint approximation, weighted random sum, poisson-exponential random variables, convolutions of gamma random variables, percentile modified linear rank tests.

INTRODUCTION

The need to analyze distributions of linear combinations of random variables arises in many fields of research, such as biology, seismology, risk theory, insurance application and health science. A mathematical linear combination is expressed as

$$Lc_N = c_1X_1 + c_2X_2 + c_3X_3 + \cdots + c_NX_N, \quad (1)$$

where we have a set of coefficients, c_1 through c_N, that are multiplied by the corresponding variables,X_1 through X_N. During the first term, we have $c_1$times X_1, which is added to$c_2$times X_2, and so on, up to the variable X_N (Ali and Obaidullah, 1982).

This process can be expressed as the sum of the terms $c_i$times X_i, $i = 1,2,\ldots,N$. The selection of the coefficients c_1 through $c_N$very much depends on the application of interest and the types of scientific questions that we would like to address.

The present paper is organized as follows: in section 1, we establish the basic saddlepoint approximations for the linear combination of random variables. In section 2, we discuss Saddlepoint approximation and real numerical comparisons for the continuous Random Sum Poisson-Exponential Model. In section 3, we derive results for numerical examples for a linear combination of the Gamma distribution. The performance of the saddlepoint approximation for Percentile modified linear rank test is presented in section 4.

1. The linear combination of random variables

In this paper, we discuss saddlepoint approximations to cumulative distribution functions for the linear combination of random variables (Ali and Obaidullah, 1982) in three different cases, as presented:

*Corresponding author email: afaaq99@hotmail.com
*Permanent address:Applied Statistics Department, Faculty of Applied Science, Taibah University, AlMadinah, Kingdom of Saudi Arabia

The linear combination of the sum of independent random variables when N is a random variable

The distributions considered in this study results from the combination of two independent distributions in a particular way. When all $c_i = 1$, this process is termed

"generalization" by some authors (Johnson *et al*., 2005), though the term "generalized" is greatly overused in statistics. This distribution includes the sums of independent identically distributed (i.i.d.) random variables, $\{X_i\}$, with random index N, independent of

$X_i s$.

Definition 1

Let $X_1, X_2, X_3, \ldots$ be a sequence of independent identically distributed (i.i.d.) random variables with a common distribution $f_X(x)$. Let N be a discrete random variable that takes the value $1,2,3, \ldots$ and let $X_i s$ be independent of N, and c_i be non-negative real numbers. The sum

$$R_N = c_1X_1 + c_2X_2 + c_3X_3 + \cdots + c_NX_N \quad (2)$$

is called the weighted random sum (Kasparaviciute and Leonas, 2013).

Such sums have a wide range of applications in branching processes, damage processes and risk theory. A common application of the random sum is that a total claim amount is presented to an insurance company, where N is the number of claims and the X_is are the individual claims, which are assumed to be independent.

In general, random sums are extremely difficult to investigate; therefore, approximation techniques are frequently employed. Saddlepoint methods overcome this difficulty while providing us with an influential tool for obtaining precise expressions for distribution functions that are still unknown in the closed form. In addition, these methods roughly surpass other techniques in terms of calculating expenses, but exceed no other methods in terms of accuracy.

In this paper, approximations of the unknown difficult random sum Poisson-Exponential random variables which have a continuous distribution are discussed. The saddlepoint approximation method is shown to be not only quick, dependable, stable and accurate enough for general statistical inference, but it is also applicable without deep knowledge of probability theory.

The linear combination of the sum of independent random variables when N is constant

Linear combinations of convoluted random variables occur in a wide range of fields. In most cases, the exact distribution of these linear combinations is extremely difficult to determine, and the normal approximation usually performs very badly for these complicated distributions. A better method of approximating linear combination distributions involves the additional use of saddlepoint approximation.

Saddlepoint approximation is able to provide accurate expressions for distribution functions that are unknown in their closed forms. This method not only yields an accurate approximation, near the center of the distribution but also controls the relative error in the far tail of the distribution.

Definition 2

The probability distribution of the sum of two or more independent random variables is the convolution of their individual distributions. Consider the sum of two independent random variables, Z and Y. The distribution of their sum, $X = Z + Y$, is the convolution of these random variables. Now, let $X_1, X_2, \ldots, X_N$ be i.i.d. random variables and $c_1, c_2, \ldots, c_N$ be numbers. Thus, the random variable

$$L_N = c_1X_1 + c_2X_2 + c_3X_3 + \cdots + c_NX_N = \sum_{i=1}^{N} c_iX_i \quad (3)$$

is called the linear combination of the convolution random variable.

We derive the saddlepoint approximation of the convolution $aZ + bY$, where $a > 0$ and $b > 0$ are real constants and Z, Y denote Gamma random variables, respectively, while being distributed independently of each other. The associated saddlepoint approximations CDFs, exact and normal approximation are derived. The plots for the CDFs arealso given.

The linear combination of sum of independent Bernoulli random variables when N is constant and c_i are scores

The approximation for the distribution function of a test statistic is extremely important in statistics. Many statistical procedures that are applicable to the two sample problems are based on the rank order statistics for the combined samples, and many commonly used two-sample rank tests act as a linear combination of certain indicator Bernoulli random variables for the combined ordered samples.

For the approximation presented in this paper, a saddlepoint formula proposed are given constants called weights or scores, and $\{X_i\}$ are Bernoulli distributions, $i = 1,2,\dots,N$.

Definition 3

Let $X_1, X_2, \dots, X_m$ and $Y_1, Y_2, \dots, Y_n$ be two independent random samples drawn from populations with the continuous cumulative distribution functions, F_X and F_Y, respectively. Let $N = m + n$; then, the statistic

$T_N = \sum_{i=1}^{N} c_i Z_i$ (4)

is called a linear rank statistic, where the $\{c_i\}$ are given constants called weights or scores, $Z_i = 1$ if the i^{th} sampled value in the combined ordered sample is X and $Z_i = 0$ if it is Y (Gibbons and Chakraborti, 2003). It is noteworthy to mention that the statistic T_N is a linear combination of independent indicator Bernoulli random variables $\{Z_i\}$.

This paper examines mid p-values from the null permutation simulations distributions. The permutation simulations may lead to intractable computations apart from small values for the sample size, and the normal approximation may not result in the desired accuracy, particularly when the sample size is small. Saddlepoint approximation can be used to overcome this problem. This method results in a highly accurate approximation without placing constraints or guidelines on the values of the sample sizes.

In the three cases of linear combinations involving random variables given in Equations (2), (3) and (4), we used the saddlepoint approximation formula proposed by Daniels (1954, 1987) that has the type developed by Lugannani and Rice (1980) for the cumulative distribution function of a continuous random variable X with CDF F andcumulant generating function CGF K, with mean, μ. The saddlepoint approximation for $F(x)$, as introduced by Lugannani and Rice (1980), is

$$\hat{F}(x) = \begin{cases} \Phi(\hat{w}) + \phi(\hat{w})(1/\hat{w} - 1/\hat{u}) & if \\ \frac{1}{2} + \frac{K\square(0)}{6\sqrt{2\pi K''(0)^{3/2}}} & if \end{cases}$$

where Φ and □□ denote the standard normal density and CDF, respectively, and

$\hat{w} = sgn(\hat{s})\sqrt{2\{\hat{s}x - K(\hat{s})\}}, \quad \hat{u} = \hat{s}\sqrt{K''(\hat{s})}$ (6)

are functions of x and saddlepoint $\hat{s}$. In this case, $\hat{s}$ is the implicitly defined function of x given as the unique solution to $K'(\hat{s}) = x$, and $sgn(\hat{s})$ captures the sign ± for $\hat{s}$.

To approximate these unknown difficult statistics based on their moment generating functions, theorems related to these unknown statistics are employed. Then, we derived the saddlepoint equations that, in some cases, can be solved using numerical methods. By performing some calculations and applying saddlepoint formulas, we can obtain the CDF for these unknown difficult statistics. Subsequently, we find the exact distributions using simulation methods and the mean square error (MSE) as well as the absolute, relative error (RE) to investigate the performance of the saddlepoint approximation.

The Skovgaard (1987) approximation when Y is a continuous variable for which $F(y|x)$ admits a densityis

$\hat{F}(y|x) = \Phi(\hat{w}) - \phi(\hat{w})(1/\hat{w} - 1/\hat{u}), \quad \hat{t} \neq 0$ (7)

where

$\hat{w} = sgn(\hat{t})\sqrt{2[\{K(\hat{s}_0, 0) - \hat{s}_0{}^T x\} - \{K(\hat{s}, \hat{t}) - \hat{s}^T x - \hat{t}y\}]}$ (8)

$$\hat{u} = \hat{t}\sqrt{\frac{|K''(\hat{s}, \hat{t})|}{|K_{ss}''(\hat{s}_0, 0)|}}$$

The components s and t are associated with X and Y, respectively.For $(x, y) \epsilon \tau_\chi$ and τ_χ is the interior of the convex hull of the support $\chi = \{(x, y): f(x, y) > 0\}$. Here, the m-dimensional saddlepoint $(\hat{s}, \hat{t})$ solves the set of m equations $K'(\hat{s}, \hat{t}) = (x, y)$.Where $K'(\hat{s}, \hat{t})$ is the gradient with respect to both $s$and t. If $K''(\hat{s}, \hat{t})$ is the corresponding Hessian, the continuity corrections to CDF, as introduced by Skovgaard (1987) should be used to achieve the greatest accuracy.

First continuity correction

Suppose $(\hat{s}, \hat{t})$ is the solution to $K'(\hat{s}, \hat{t}) = (j, k)$ required for the numerator saddlepoint with $\hat{t} \neq 0$. Then,

$\hat{P}_{r1}(Y \geq k | X = j) = 1 - \Phi(\hat{w}) - \phi(\hat{w})(1/\hat{w} - 1/\tilde{u}_1), \quad \hat{t} \neq 0$ (9)

where $x \neq \mu$

$\hat{w} = sgn(\hat{t})\sqrt{2[\{K(\hat{s}_0, 0) - \hat{s}_0{}^T j\} - \{K(\hat{s}, \hat{t}) - \hat{s}^T j - \hat{t}k\}]}$ (10)

$x = \mu$

$$\tilde{u}_1 = (1 - e^{-\hat{t}})\sqrt{\frac{|K''(\hat{s}, \hat{t})|}{|K_{ss}''(\hat{s}_0, 0)|}} \quad (11)$$

and $\hat{s}_0$ solves $K_s'(\hat{s}_0, 0) = j$; see Skovgaard (1987).

Second continuity correction

If $k^- = k - 0.5$ is the offset value of k and $(\tilde{s}, \tilde{t})$ is the offset saddlepoint solving

$K'(\tilde{s}, \tilde{t}) = (j, k - 0.5)$ (12)

with $\tilde{t} \neq 0$, then

$$\hat{P}_{r2}(Y \geq k|X = j) = 1 - \Phi(\tilde{w}_2) - \phi(\tilde{w}_2)(1/\tilde{w}_2 - 1/\tilde{u}_2), \qquad \tilde{t} \neq 0 \quad (13)$$

where

$$\tilde{w}_2 = sgn(\tilde{t})\sqrt{2[\{K(\hat{s}_0, 0) - \hat{s}_0{}^T j\} - \{K(\tilde{s}, \tilde{t}) - \tilde{s}^T j - \tilde{t}k^-\}]} \quad (14)$$

$$\tilde{u}_2 = 2\sinh(\tilde{t}/2)\sqrt{\frac{|K^{''}(\tilde{s}, \tilde{t})|}{|K_{ss}{}^{''}(\hat{s}_0, 0)|}} \quad (15)$$

and the saddlepoint $\hat{s}_0$ is unchanged. Then, we find

$$\hat{F}_2(k|X = j) = 1 - \hat{P}_{r2}(Y \geq k + 1|X = j),$$

2. Saddlepoint approximation and real numerical comparisons for the continuous Random Sum Poisson Model

The random sum distribution plays a key role in both probability theory and its applications in biology, seismology, risk theory, meteorology and health science. The statistical significance of this distribution arises from its applicability to real-life situations, in which the researcher often observes only the total amount, say S_N, which is composed of an unknown random number N of random contributions, say Xs.

In health science, the random sum plays a very important role in many real-life applications. For example, let the number of hot spot of a contagious disease follow a Poisson distribution with a mean of Ψ, and let the number of sick people within the hotspotfollow a Negative Binomial distribution. If we want to find the probability that the total number of sick people is greater than 70, then the total number of sick people within the hotspotis

$$S_{N_1} = \sum_{i=1}^{N} X_i \quad (16)$$

where $X_i \backsim \text{Negative Binomial}\,(r, m)$ and $N \backsim \text{Poisson}(\psi)$.

Another practical application of the random sum is the number of times that it rains in a given time period, say N, which has a Poisson distribution with mean λ. If the amount of rain that falls has an Exponential distribution and if the rain fallsat that time period is independent of N, then the total rainfall in the time period is

$$S_{N_2} = \sum_{i=1}^{N} Y_i \quad (17)$$

where $Y_i \backsim \text{Exponential}(\phi)$ and $N \backsim \text{Poisson}\,(\lambda)$.

In fact, the total random sums S_{N_1} and S_{N_2} are composed of an unknown random number N of other random contributions, say X or Y which are very complex to analyze. In most cases, the distribution of the random sum is still unknown; in other cases, it is already known but is too complex for the computation of the distribution function, which often becomes too slow for many problems (Johnson *et al*., 2005). The saddlepoint approximation method can help us gain knowledge of these unknown difficult statistical behavior.

In this section, we suggest that the saddlepoint approximation and efficiency analysis should be compared to the true distribution over real data compared with other methods of approximation, such as normal approximations. Suppose that the number of times it rains in a given time period, N has a Poisson distribution with mean λ. Suppose,also when it rains, the amount of rain falling has an Exponential distribution. Let the rain falling and the time period be independent of one another and of N. Then, the total rainfall in the time period is as follows:

$$S_{N(t)} = \sum_{i=1}^{N(t)} R_i\,, \qquad t \geq 0 \quad (18)$$

where $\{R_i\}$are independent random variables with a distribution of R. Suppose now we observe the rainfall for Nin certain periods:$S_1, S_2, \ldots, S_N$.

Note that the probability of no rain in any such period is $P(S_{N(t)} = 0) = P_0 =$exp (λ)

Withers and Nadarajah (2011) considered the annual maximum daily rainfall data for the year 1907 to 2000 for fourteen locations in West Central Florida: Clermont, Brooksville, Orlando, Bartow, Avon Park, Arcadia, Kissimmee, Inverness, Plant City, Tarpon Springs, Tampa International Airport, St. Leo, Gainesville, and Ocala. The data were obtained from the Department of Meteorology in Tallahassee, Florida. Consider the distribution of $S_{N(t)}$, such that the unknown parameters are$\lambda$and α. The study conducted by Withers and Nadarajah (2011) found a distribution fit by these three methods, unconditional maximum likelihood estimation, conditional maximum likelihood estimation, and moments estimation. Remarkably, unconditional maximum likelihood estimation provided the best fit for each location; for example, in Orlando, the estimates were $\hat{\lambda}$= 9.565, $\hat{\alpha}$ = 2.373.

The numerical computations are plotted in figure 1 to show the 'exact' CDFs for a random sum Poisson (9.565)– $Exponential\,(2.373)$distribution $F(x)$ (the solid line), the saddlepoint $\hat{F}(x)$(the dotted line) and the normal approximation $F^{'}(x)$ (the dashed line).

The empirical distribution function is used to determine the 'exact' CDF for this model by simulating 10^6 independent values of S_N, where N is $\text{Poisson}(\lambda)$, and the $X_i{}'s$ are i.i.d random variables generated using

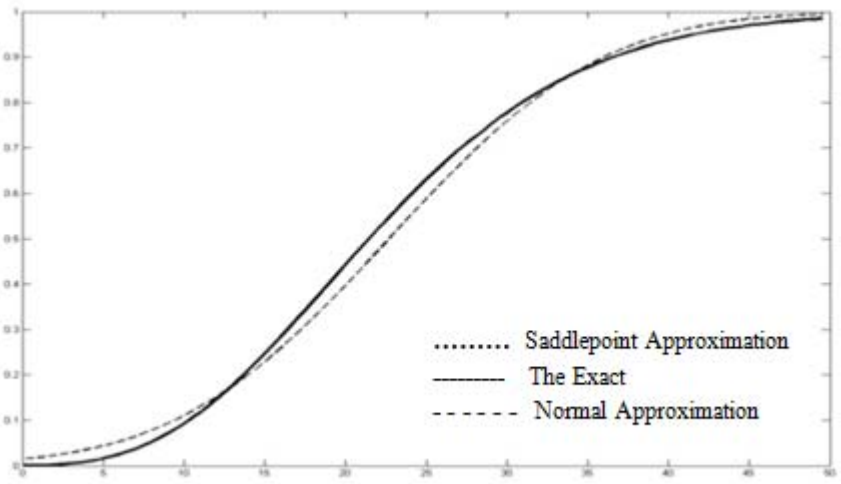

Fig. 1. The performance of the saddlepoint approximation $\hat{F}(x)$, the exact $F(x)$ and the normal approximation $F'(x)$for random sum Poisson (9.565)- Exponential (2.373) model.

Table 1. Approximate left tail of the saddlepoint approximation $\hat{F}(x)$ vs. exact $F(x)$and the normal approximation $F'(x)$, for random sum Poisson (9.565) Exponential (2.373) model.

x	$F(x)$	$\hat{F}(x)$	$F'(x)$	%RE1	%RE2
0.1	0.000100	8.96E-05	0.014731	1.04E-01	146.3100
0.2	0.000132	0.0001255	0.015094	4.94E-02	113.3485
0.3	0.000168	0.0001662	0.015464	1.07E-02	91.04762
0.4	0.000225	0.0002122	0.015843	5.70E-02	69.41333
0.5	0.000260	0.0002639	0.016229	1.50E-02	61.41923
0.6	0.000320	0.0003217	0.016624	5.44E-03	50.95000
0.7	0.000395	0.0003862	0.017026	2.24E-02	42.10380
0.8	0.000487	0.0004575	0.017437	6.05E-02	34.80493

MATLAB program. This plot shows that the shape of $F(x)$ is the same as that of $\hat{F}(x)$(i.e., the two approximations are identical) but differs from that of $F'(x)$. The plot suggests that the saddlepoint approximation for CDFs has the same accuracy as the 'exact' CDFs and is far superior to normal approximation. Table 1 shows the evaluation of the left tail probabilities for certain values of the exact $F(x)$ of the random sum in the second column, with the saddlepoint $\hat{F}(x)$ in the third column and the normal approximation in fourth column. However, based on the fifth column (the absolute relative errors), the accuracy of this method is very clear. For example, in the left tail probability, we obtained the following relative error values: 1.04E-01, 4.94E-02, 1.07E-02, 5.70E-02,1.50E-02..., and so on. All of these amounts and others suggest good approximations in the left tail. The maximum absolute relative error for the $F(x)$vs.$\hat{F}(x)$ approximation, based on our calculations for this example, appears in this tail and was 1.04E-01when $X = 0.1,\ F(x) = 0.000100$ and $\hat{F}(x) = 8.96E-05$. However, the approximation is still good with this amount of error (acceptable).

If we refer to table 2 to examine the relative error values near the center of the distribution, we obtain 3.76E-03, 3.09E-03, 2.69E-03,4.38E-03…, and so on. Based on these values and others, the accuracy is increased compared to that in the left tail probability.

The relative error values in the right tail probability, as shown in table 3, are3.10E-04,1.07E-05,4.91E-04,2.66E-04…, and so on. At this point, the accuracy is optimal.

Throughout the entire set of results (from x=0.1 to x=40.5 with step 0.1), with its corresponding figure 1carried out usingMATLAB program, the accuracy generally appears to be increasing. In general, for this application, the mean squared error of the saddlepoint approximation is MSE(1) = 1.28625E-06, that is, very close to zero, while the means squared error of the normal approximation is MSE(2) = 000476.

Table 2. Approximate center of the distribution of the saddlepoint approximation $\hat{F}(x)$, the exact $F(x)$ & the normal approximation $F'(x)$ for Poisson (9.565) Exponential (2.373) model.

x	$F(x)$	$\hat{F}(x)$	$F'(x)$	%RE1	%RE2
21.4	0.49764	0.49577	0.45025	3.76E-03	0.095229
21.5	0.50122	0.49967	0.45406	3.09E-03	0.09409
21.6	0.50492	0.50356	0.45788	2.69E-03	0.093163
21.7	0.50967	0.50744	0.46171	4.38E-03	0.094100
21.8	0.51366	0.51131	0.46554	4.58E-03	0.093681
21.9	0.51710	0.51518	0.46937	3.71E-03	0.092303
22.0	0.52150	0.51903	0.47320	4.74E-03	0.092617
22.1	0.52472	0.52287	0.47704	3.53E-03	0.090868

Table 3. Approximate right tail of the saddlepoint approximation $\hat{F}(x)$, the exact $F(x)$ & the normal approximation $F'(x)$ for random sum Poisson (9.565) Exponential (2.373) model.

x	$F(x)$	$\hat{F}(x)$	$F'(x)$	%RE1	%RE2
39.8	0.93567	0.93538	0.95030	3.10E-04	0.015636
39.9	0.93630	0.93629	0.95128	1.07E-05	0.015999
40.0	0.93764	0.93718	0.95225	4.91E-04	0.015582
40.1	0.93831	0.93806	0.95320	2.66E-04	0.015869
40.2	0.93923	0.93893	0.95413	3.19E-04	0.015864
40.3	0.93974	0.93980	0.95505	6.38E-05	0.016292
40.4	0.94101	0.94065	0.95596	3.83E-04	0.015887
40.5	0.94162	0.94149	0.95685	1.38E-04	0.016174

These results indicate that the saddlepoint approximation is almost exact. Thus, we conclude that the saddlepoint approximation method provides us with an accurate approximation for this difficult statistic, the accuracy of which appears to leave no room for doubt in either of the two tails or in the center of the distribution.

3. Real numerical comparisons of the Saddlepoint approximation for linear combination of Gamma distribution

Saddlepoint approximation plays an important role in helping us gain knowledge about unknown difficult distributional behavior, such as the linear combination of random variables. In this study, we discuss the linear combination of the Gamma distribution. This convolution model is given by

$$S_N = c_1X_1 + c_2X_2, \qquad (19)$$

where, X_1 and X_2 are both independent, following an Gamma distribution with parameters (θ,ρ) and (α,β), respectively. This paper investigates the saddlepoint approximations of the convolution, where $c_1 > 0$ and $c_2 > 0$ are real constants.

In the univariate case, a general saddlepoint approximation was given for the continuous CDFs. For the linear combinations of Gamma models, this method of approximation was applied where the root was found numerically. In this setting, the efficiency of this method was explored using the empirical CDFs found by simulation methods.

Figure 2 shows a comparative plot of the 'true' CDFs $F(x)$ with the saddlepoint $\hat{F}(x)$CDFs and the normal approximation CDFs for a linear combination of Gamma distribution. It is clear from this figure that the two approximations $F(x)$ and $\hat{F}(x)$ are very close, but differs from $F'(x)$. This result means that the saddlepoint approximation for CDFs has the same accuracy as the 'exact' CDFs and is far superior to the normal approximation. The first value of each cell of table 4 is 'exact'. The second and the third values are the saddlepoint approximation and normal approximation, respectively. The fourth and fifth columns show the absolute, relative errors between the saddlepoint approximation and the 'exact' CDFs and the relative errors between the normal approximation and the 'exact' CDFs, respectively.

The 'exact' CDFs were computed using the empirical distribution by simulating 10^6 independent values of $S_N = c_1X_1 + c_2X_2$, where $X_1 \sim Gamma(0.5,1)$, $X_2 \sim Gamma(1,2)$ and

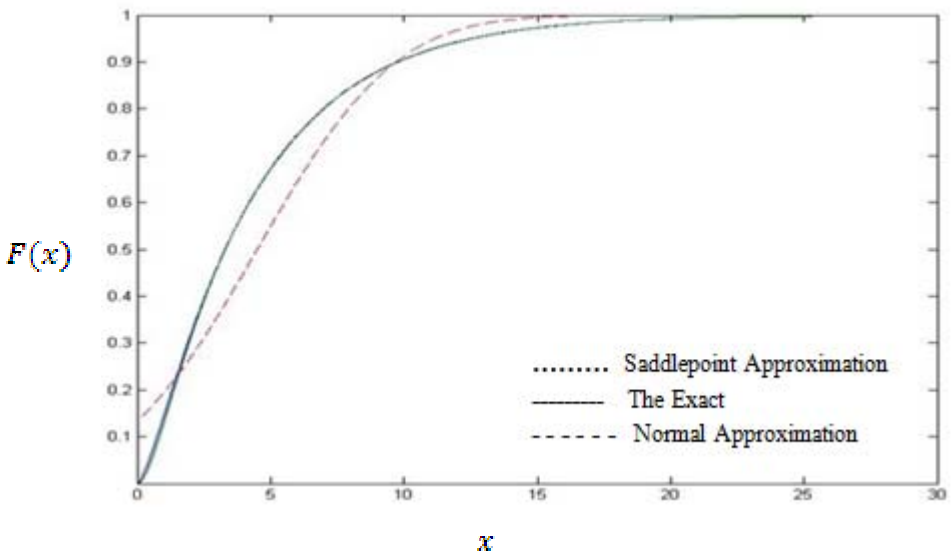

Fig. 2. Performance ofsaddlepoint approximation $\hat{F}(x)$ and the exact $F(x)$ with normal approximation $F'(x)$ for linear combination of Gamma (0.5,1,1,2).

Table 4. Comparison saddlepoint approximation $\hat{F}(x)$ and the exact $F(x)$ with normal approximation $F'(x)$ for linear combination of Gamma (0.5,1,1,2).

x	$F(x)$	$\hat{F}(x)$	$F'(x)$	%RE1	%RE2
3.5000	0.5242	0.5242	0.4028	0	0.231591
6.0000	0.7448	0.7433	0.6440	0.002014	0.135338
8.5000	0.8636	0.8621	0.8376	0.001737	0.030107
11.0000	0.9268	0.9260	0.9452	0.000863	0.019853
13.5000	0.9610	0.9603	0.9866	0.000728	0.026639
16.0000	0.9790	0.9787	0.9977	0.000306	0.019101
18.5000	0.9887	0.9886	0.9997	0.000101	0.011126
21.0000	0.9939	0.9939	1.0000	0	0.006137
23.5000	0.9968	0.9967	1.0000	0.000100	0.003210
26.0000	0.9983	0.9982	1.0000	0.000100	0.001703
28.5000	0.9991	0.9991	1.0000	0	0.231591

$c_1 = 1, c_2 = 2$ when $x = 0.01$.Generated by the MATLAB program.

Table 4 shows the relative errors for $F(x)$ vs. $\hat{F}(x)$ values of the distribution. The relative errors remain very small for the computations and the accuracy appears quite good, although the accuracy in the center is not quite as good as that in the left tail. Moreover, the numerical results indicate that the normal approximations are considerably less accurate than the saddlepoint approximations.

The values of the relative errors for $F(x)$ vs. $\hat{F}(x)$,for the right tail , the accuracy is good and very clear. However, the performance of the normal approximation in this tail appears to be much better than its performance in the center and in the left tail. Nevertheless, the saddlepoint approximation maintains its accuracy in the left, right and center of the distribution. In general, the numerical results indicate that the saddlepoint approximation is far more accurate than the normal approximation.

Table 5. Comparisonof saddlepoint approximation mid p-values and the exact with normal approximation for percentile modified linear rank tests.

Exact	Normal		Saddlepoint			
			First continuity correction		Second continuity correction	
	Mid-p-value	%RE	Mid-p-value	%RE	Mid-p-value	%RE
0.322	0.325	0.003106	0.323	0.009317	0.322	0
0.413	0.415	0	0.413	0.004843	0.413	0
0.377	0.378	0.002653	0.378	0.002653	0.377	0

Based on figure 2 with its corresponding numerical result using MATLAB program (from x = 3.5000 to x =28.5000 with step 2.5), this leads to

$$MSE(1) = \frac{1}{N}\sum_{i=1}^{N}(F(x_i) - \hat{F}(x_i))^2 = 0.000077696 \quad (20)$$

Additionally, the MSE (2) for $F(x)$ vs. $F^{'}(x)$ was calculated as

$$MSE(2) = \frac{1}{N}\sum_{i=1}^{N}(F(x_i) - F^{'}(x_i))^2 = 0.0019 \quad (21)$$

We note that the value of MSE(1) is far smaller than that of MSE(2) and that MSE(1) is itself very small and close to zero (i.e. the accuracy of the estimator with a smaller mean squared error is also higher). This result indicates that the saddlepoint approximation furnishes a good fit and is superior to the normal approximation.

4. The linear combinations of the rank-order statistics for percentile modified linear rank tests

P-value is associated with a test statistic. It is the probability if the test statistic really were distributed as it would be under the null hypotheses, of observing a test statistic (as extreme as, or more extreme than) the one actually observed.

The smaller p-value, the more strongly the test rejects the null hypothesis, that is, the hypothesis being tested. A p-value of 0.05 or less rejects the null hypothesis. However, this study uses saddlepoint methods to determine mid-p-values from the linear combinations of the rank-order statistics. The two methods suggest that normal approximation and permutation simulations can be used to determine mid-p-values from the null permutation distributions. The permutation simulations lead to intractable computations apart from the small sample size. The normal approximation demands that certain conditions be applied relative to the sample size; thus, without these conditions, the results will not attain the desired accuracy, particularly when the sample size is small.

The saddlepoint approximation provides a result using a highly accurate approximation without the need to place constraints or guidelines on the sample, and its accuracy is apparent even when the sample size is 1. Another advantage of these saddlepoint methods is that the required computational times are essentially negligible compared to the simulations. The real datasets used include small, intermediate and large sample sizes respectively,to show how accurate the saddlepoint method can be for all sample sizes.

For the third new estimators, table 5 shows the exact (true), normal and saddlepoint mid-p-values for linear combinations of the rank-order statistics for the two sample problems. In all examples, as a result, we determined how much the permutation simulations lead to complicated computations, apart from small values for the sample size. As indicated by the absolute relative errors, saddlepoint approximations can replace the permutation simulations and provide mid-p-values that are virtually exact for all practical purposes without the same required conditions or guidelines regarding the sample size as the normal approximation.And in most cases, the second correction is better than first corrections. Additionally, in both two continuity-corrected CDFs, the saddlepoint approximation is far more accurate than the normal approximation.All of the computations for this third new estimator were performed using FORTRAN software.

CONCLUSION

Estimating the CDFs for some linear combination of random variables is one of the problems we face in statistical inference that has many applications throughout life. The difficulty of estimating the CDFs for a given model should be detected. In this study, we used saddlepoint approximations as a better method to achieve an accurate approximation of the CDFs.Based on present study, three different versions of new saddlepoint approximations were developed. For the first approximation(the weighted random sums $S_{N(t)}$). We demonstrated the performance of the saddlepoint approximation in a wide range of applications.The

proposed new estimators using the saddlepoint approximationis highly accurate. The performance of the first new estimator for the random sumwas evaluated by the relative error between the exact value and the saddlepoint approximation and between the exact value and the normal approximation for each value. In addition,the mean squared error for the saddlepoint approximation was compared with the mean squared error for the normal approximation.For the second new estimators, saddlepoint approximation to a linear combination of Gamma models was considered. These models show close agreement between the exact, and saddlepoint and far superior accuracy to the normal approximation. Moreover, for the third new estimators, saddlepoint approximations can replace the permutation simulations and provide mid-p-values that are virtually exact for all practical purposes without the same required conditions or guidelines regarding the sample size as the normal approximation.In conclusion,we confirmed the accuracy of the saddlepoint approximation in these three different settings for the linear combination model.

ACKNOWLEDGEMENT

This study was supported financially by Taibah University, AlMadinah-M., Kingdom of Saudi Arabia.

REFERENCES

Ali, MM. and Obaidullah, M. 1982. Distribution of linear combination of exponential variates. Communications in Statistics-Theory and Methods. 11:1453-1463.

Daniels, HE. 1987. Tail probability approximations. International Statistical Review. 55:37-48.

Daniels, HE. 1954. Saddlepoint approximations in statistics. Annals of Mathematical Statistics. 25:631-650.

Gibbons, JD. and Chakraborti, S. 2003. Nonparametric statistical inference. (4th edi.). Marcel Dekker, New York, USA.

Johnson, NL., Kemp, AW. and Kotz, S. 2005. Univariate discrete distributions. (3rd edi.). John Wiley and Sons, Inc., USA.

Kasparaviciute, A. and Leonas S. 2013. Large deviations for weighted random sums. Non Llinear Analysis-Modeling and Control. 18:129-142.

Lugannani, R. and Rice, SO. 1980. Saddlepoint approximations for the distribution of the sum of independent random variables. Advances in Applied Probability. 12:475-490.

Skovgaard, IM. 1987. Saddlepoint expansions for conditional distributions. Journal of Applied Probability. 24:875-887.

Withers, CS. and Nadarajah, S. 2011. On the compound Poisson-gamma distribution. Kybernetika. 47:15-37.

Received: June 22, 2014; Accepted: July 7, 2014

SENRA Academic Publishers, British Columbia
Vol. 8, No. 3, pp. 3091-3103, October 2014
Online ISSN: 1920-3853; Print ISSN: 1715-9997

Canadian Journal of pure&applied sciences

CORROSION INHIBITION OF 2-AMINO-5 ETHYL-1, 3, 4-THIADIAZOLE ON MILD STEEL IN HYDROCHLORIC ACID

*Roland Tolulope Loto[1,2], Cleophas Akintoye Loto[1,2] and Patricia Abimbola Popoola[2]
[1]Department of Mechanical Engineering, Covenant University, Ota, Ogun State, Nigeria
[2]Department of Chemical, Metallurgical & Materials Engineering, Tshwane University of Technology Pretoria, South Africa

ABSTRACT

Corrosion inhibition of mild steel in 0.5M hydrochloric acid solutions by 2- amino- 5 ethyl- 1, 3, 4-thiadiazole(TTD) was studied using weight loss, open circuit potential measurement and potentiodynamic polarization technique. The compoundshowedmaximum inhibition efficiency of 93.7 and 97% at highest TTD concentration from weight-loss and potentiodynamic polarization test. Results from corrosion potential monitoring showed the inhibiting compound well within passivation values throughout the exposure period.Inhibition efficiency varied with inhibitor concentration and the mechanism of inhibition is attributed to chemical interaction and adsorption form thermodynamic calculations. Adsorption of the compound obeyed the Langmuir and Frumkin isotherm model. Scanning electron microscopy characterization showed the formation of protective precipitates on the steel surface while statistical derivations confirmed the overwhelming statistical significance of inhibitor concentration against exposure time on inhibition efficiency.

Keywords: Corrosion; thiadiazole; hydrochloric acid, steel, inhibition.

INTRODUCTION

Metallic corrosion has been a worldwide industrial problem that has the attention of scientist and engineers researching into and developing new corrosion control techniques (Liu *et al*., 2001; Collins *et al*., 1993; Ekpe *et al*., 1995). Corrosion inhibiting compounds are of immense importance and extensively employed in curtailing wastage of metallic alloys in applicationssuch as in acid pickling of steel, chemical cleaning and processing, ore production, chemical processing plants, automobile industries, oil well acidification etc (Ashassi-Sorkhabi *et al*., 2009; Singh *et al*., 1995). Chromate based compounds and inorganic inhibiting agents are commonly used for corrosion inhibition, however their application is being highly restricted due to their toxic nature and impact (Fontana, 1986; Abboud *et al*., 2009; Sinko, 2001; Manahan, 1994). Currently there has been unusual attention on the use of organic compounds due to their promising corrosion inhibition properties and environmentally friendly (Krim *et al*., 2008; Quraishi and Shukla, 2009; Devarayan, 2012). Application of nitrogen and sulphur containing heterocyclic organic compounds for the corrosion inhibition of mild steel in acidic solutions has been studied by a number of authors (Ita and Offiong, 1997; Abiola *et al*., 2004; Rastoyi *et al*., 2005; James *et al*., 2005; Ita and Offiong, 1997). Heterocyclic compounds act by adsorption onto the alloy surface through the heteroatom and triple or conjugated double bonds within their molecular structures (Thomas, 1980-1981). A number of heterocyclic compounds have been used for the corrosion inhibition of ferrous alloys in acid solutions (Bentiss*et al*., 2000; Cruz *et al*., 2004; Bouklah*et al*., 2005; Popova *et al*., 2004). In this investigation 2 Amino, 5 ethyl, 1, 3, 4-thiadiazole was observed for its corrosion inhibition properties and performance on mild steel in dilute hydrochloric acid.

*Corresponding author email: tolu.loto@gmail.com

MATERIALS AND METHODS

Material

The mild steel used for this research was obtained in the open market and analyzed at the Applied Microscopy and Triboelectrochemical Research Laboratory, Department of Chemical and Metallurgical Engineering, Tshwane University of Technology, South Africa. The mild steel has the nominal per cent composition: 0.301C, 0.169Si, 0.440Mn, 0.005P, 0.012S, 0.080Cu, 0.008Ni, 0.025Al, and the rest being Fe.

Inhibitor

2- Amino, 5- ethyl- 1, 3, 4-thiadiazole (TTD) a colorless, solid flakeobtained from SMM Instruments South Africa is the inhibitor used. The structural formula of TTD is shown in figure 1. The molecular formula is $C_4H_7N_3S$, while the molar mass is 129.18 g mol^{-1}.

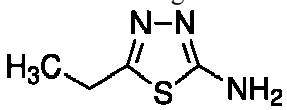

Fig. 1. Chemical structure of 2- Amino- 5 ethyl- 1, 3, 4-thiadiazole (TTD).

TTD was prepared in concentrations of 0.125%, 0.25%, 0.375%, 0.5%, 0.625% and 0.75%, respectively.

Test Media

0.5M hydrochloric acid with 3.5% recrystallised sodium chloride of Analar grade were used as the corrosion test media.

Preparation of Test Specimens

A cylindrical mild steel rod with a diameter of 14.5 mm was carefully machined and cut into a number of test specimens of average dimensions in length of 6 mm. A 3 mm hole was drilled at the centre for suspension. The steel specimens were then thoroughly rinsed with distilled water and cleansed with acetone for weight loss analysis. The linear polarization technique involved grinding the two surface ends of each specimen with silicon carbide abrasive papers of 80, 120, 220,800 and 1000 grits before being polished with 6.0μm to 1.0μm diamond paste, washed with distilled water, rinsed with acetone, dried and stored in a dessicator before the test.

Weight-loss Experiments

Weighted test species were fully and separately immersed in 200ml of the test media at specific concentrations of the TTD for 360 h at ambient temperature of 25^{o}C. Each of the test specimens was taken out every 72 h, washed with distilled water, rinsed with acetone, dried and re-weighed. Plots of weight-loss (mg), corrosion rate (mm/y) inhibitor concentration versus exposure time (h) (Figs. 2, 3 and 4) for the test media and those of percentage inhibition efficiency (%*IE*) (calculated) versus percentage TTD concentration (Fig. 5) were made from table 1.

The corrosion rate (R) calculation is from this equation 1:

$$R = \left[\frac{87.6W}{DAT}\right] \quad (1)$$

Where W is the weight loss in milligrams, D is the density in g/cm^3, A is the area in cm^2, and T is the time of exposure in hours. The %*IE* was calculated from the relationship in equation 2.

$$\%IE = \left[\frac{W1-W2}{W1}\right] = 100 \quad (2)$$

$W_1$and W_2 are the weight loss of mild steel coupon in free and inhibited acid chloride solutions respectively in the presence of predetermined concentrations of TTD. The %*IE* was calculated for all the inhibitors every 72 h during the course of the experiment, while the surface coverage is calculated from the relationship:

$$\theta = \left[1 - \frac{W2}{W1}\right] \quad (3)$$

Where θ is the substance amount of adsorbate adsorbed per gram (or kg) of the adsorbent.

Open Circuit Potential Measurement

A two-electrode electrochemical cell with a silver/silver chloride was used as reference electrode. The measurements of OCP were obtained with Autolab PGSTAT 30 ECO CHIMIE potentiostat. Resin mounted test electrodes/specimens with exposed surface of 165 mm^2 were fully and separately immersed in 200ml of the test media (acid chloride) at specific concentrations of TTD for a total of 288 h. The potential of each of the test electrodes was measured every 48 h. Plots of potential (mV) versus immersion time (hrs) (Fig. 6) for the test media were made from the tabulated values in table 2.

Linear Polarization Resistance

Linear polarization measurements were carried out using, a cylindrical coupon embedded in resin plastic mounts with exposed surface of 165 mm^2. The electrode was polished with different grades of silicon carbide paper, polished to 6μm, rinsed by distilled water and dried with acetone. The studies were performed at ambient temperature with Autolab PGSTAT 30 ECO CHIMIE potentiostat and electrode cell containing 200 ml of electrolyte, with and without the inhibitor. A graphite rod was used as the auxiliary electrode and silver chloride electrode (Ag/AgCl) was used as the reference electrode. The steady state open circuit potential (OCP) was noted. The potentiodynamic studies were then made from -1.5V *versus* OCP to +1.5 mV *versus* OCP at a scan rate of 0.00166V/s and the corrosion currents were registered. The corrosion current density (I_{corr}) and corrosion potential (E_{corr}) were determined from the Tafel plots of potential *versus* log I. The corrosion rate (R),the degree of surface coverage (θ) and the percentage inhibition efficiency (%*IE*) were calculated as follows

$$R = \frac{0.00327\ xicorrxeq.wt}{D} \quad (4)$$

Where I_{corr} is the current density in μA/cm^2, D is the density in g/cm^3; *eq.wt* is the specimen equivalent weight in grams. The percentage inhibition efficiency (%*IE*) was calculated from corrosion rate values using the equation.

$$\%IE = 1 - \left[\frac{R2}{R1}\right] = 100 \quad (5)$$

where$R1$and $R2$ are the corrosion rates in absence and presence of TTD, respectively.

Scanning Electron Microscopy Characterization

The surface morphology of the uninhibited and inhibited steel specimens were investigated after weight-loss

analysis in 0.5 M HCl solutions using Jeol scanning electron microscope for which SEM micrographs were recorded

Statistical Analysis

Two-factor single level statistical analysis using ANOVA test (F-test) was performed so as to investigate the significant effect of inhibitor concentration and exposure time, ascertaining their statistical significance on the inhibition efficiency values of TTD in the acid media.

RESULTS AND DISCUSSION

Weight-loss measurements

Weight-loss of mild steel at specific time intervals, in the absence and presence of TTD concentrations in 0.5M HCl acid at ambient temperature of 25^{o}C was studied. The values of weight-loss (*W*), corrosion rate (*R*) and the percentage inhibition efficiency (%*IE*) are presented in table 2. The corrosion rates decreased progressively in HCl with increase in TTD concentration. Figures 2, 3 and4shows the variation of weight-loss, corrosion rate and percentage inhibition efficiency versus exposure time at specific TTD concentrations while figure 5 shows the variation of %*IE* with TTD concentration. The curves obtained showa progressive increase in%*IE* values with the addition of TTD at all concentrations in HCl.

The inhibition efficiency in HCl declined from 0.125 - 0.5% TTD well below effective inhibiting values. This could be due to lateral repulsion between the molecules of TTD or formation of secondary precipitates resulting in desorption and penetration of the protective film by the corrosive species. At 0.625% TTD concentration there is a sharp increase in inhibition efficiency till 0.75% TTD concentration. Comparison of the %*IE* values of TTD in both acid solutions shows the inhibitor to be highly protective at specific concentrations.

Polarization studies

Potentiostatic potential was cursorily examined –1.5 V to +1.5 V vs. Ag/AgCl at a scan rate of 0.00166 mV s^{-1} for equilibrium state analysis. The effect of the addition of TTD on the anodic and cathodic polarization curves of

Table 1. Data obtained from weight loss measurements for MS in 0.5M HCl solution at specific concentrations of the TTD at 432 h.

Sample	Corrosion Rate (mm/y)	Inhibitor Concentration (%)	Inhibition Efficiency (%)	Weight Loss (mg)	Inhibitor Concentration (Molarity)	Surface Coverage (θ)
A	13.62	0	0	2.735	0	0
B	3.51	0.125	72.14	0.762	9.68E-06	0.721
C	4.97	0.25	62.74	1.019	1.94E-05	0.627
D	5.80	0.375	55.58	1.215	2.90E-05	0.556
E	7.65	0.5	39.23	1.662	3.87E-05	0.392
F	1.03	0.625	90.64	0.256	4.84E-05	0.906
G	0.66	0.75	93.6	0.175	5.81E-05	0.936

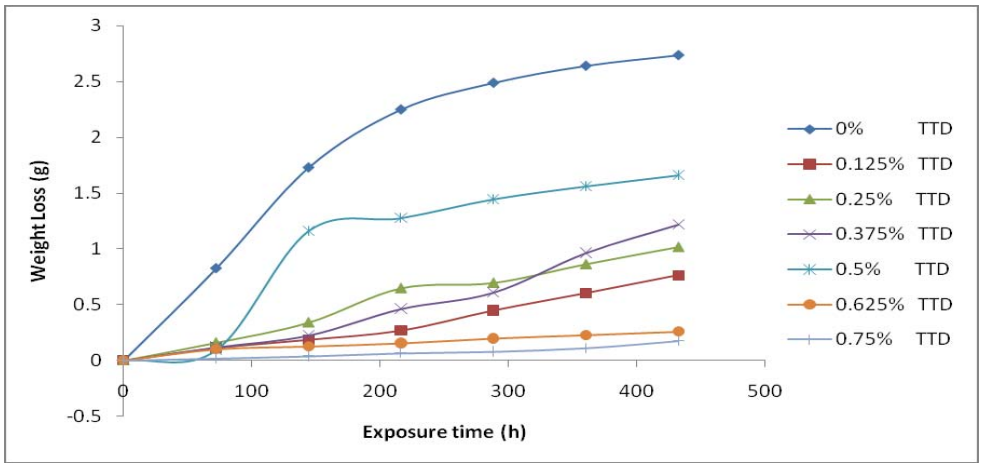

Fig. 2. Variation of weight-loss with exposure time for samples (A – G) in 0.5M HCl solution at specific TTD concentrations.

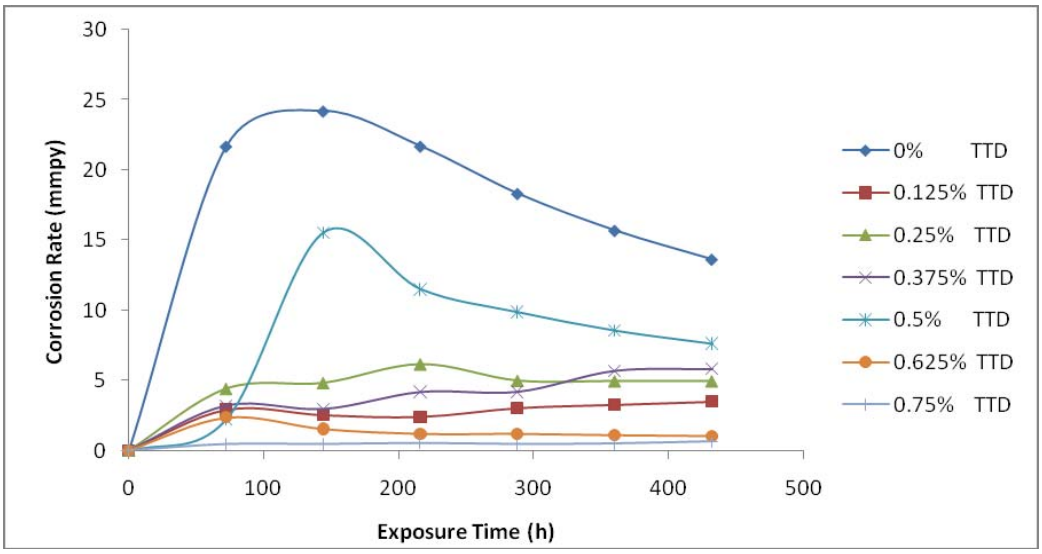

Fig. 3. Effect of percentage concentration of TTD on the corrosion rate of MS in 0.5M HCl.

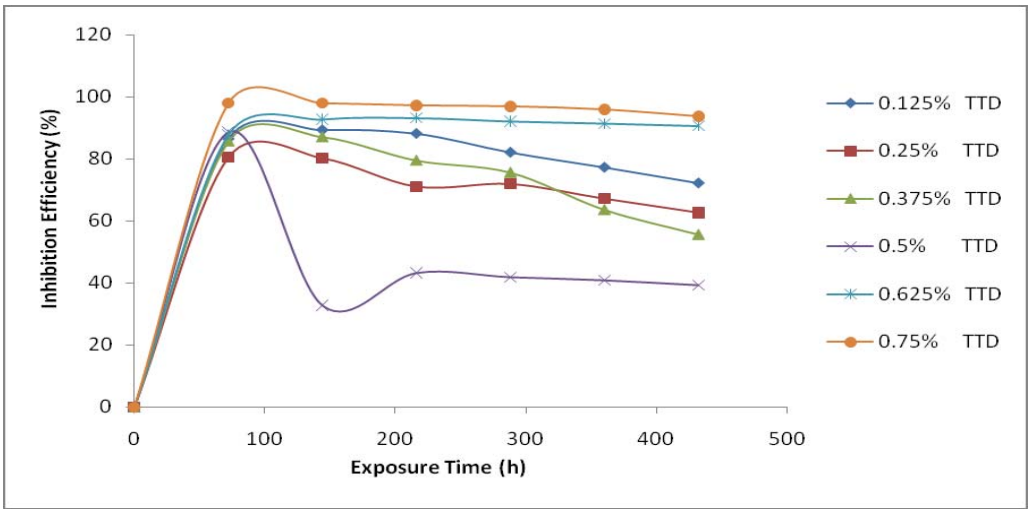

Fig. 4. Plot of inhibition efficiencies of sample (A-G) versus exposure time in 0.5M HCl solution/TTD during the exposure period.

mild steel in 0.5M HCl solutions is shown in figure 6. The performance of TTD on the corrosion inhibition of mild is independent of its concentration as observed in table 2. The corrosion rates in the acid solutions decreased in proportion despite the differential values in the electrochemical parameters while figure 7 depicts the electrochemical relationship between TTD concentration and inhibition efficiency of TTD. Changes in the redox Tafel constants occurred due to the electrolytic impact of TTD on the corrosion process. This altered the redox reactions responsible for corrosion as a result of the formation of a compact barrier film on the steel electrode surface.

The corrosion inhibition property of TTD on mild steel in the acid solution is of mixed inhibitiontype due to its electrochemical influence on the Tafel constants of the electrochemical reaction and differential values in the corrosion potential observed.The tendency for cathodic inhibition is much more dominant with the corrosion potential values shifting to less noble potentials over the TTD concentrations studied. The maximum displacement in HCl for the corrosion potential is 51mV in the cathodic direction, thus conventionally it is a mixed type inhibitor, but the mechanism of inhibition is dominantly cathodic (Eduok *et al*., 2010; Trowsdale *et al*., 1996). This causesthe selective precipitation of TTD cations on cathodic sites resulting in the suppression of hydrogen evolution and oxygen reduction reactions.

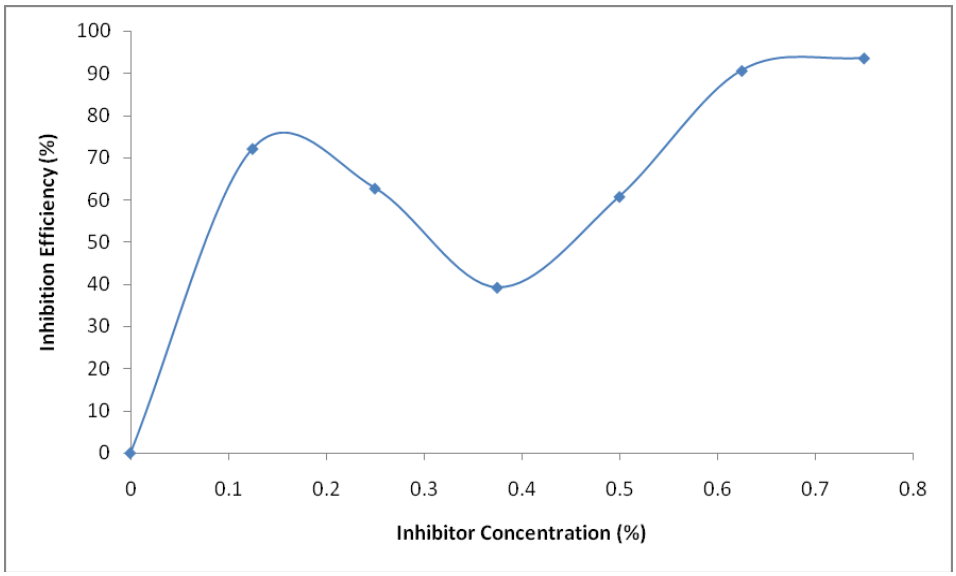

Fig. 5. Variation of Inhibition efficiency of versus inhibitor concentrations from weight loss analysis in 0.5 M HCl solution/TTD.

Table 2. Data obtained from polarization resistance measurements for MS in 0.5M HCl solution at specific concentrations of the TTD.

Sample	Inhibitor Concentration (%)	*ba* (V/dec)	*bc* (V/dec)	E_{corr}, Obs (V)	I_{corr} (A/cm²)	i_{corr} (A)	Corrosion rate (mm/yr)	*R*p (Ω)	Inhibition Efficiency (%)
A	0	0.249	0.070	-0.351	0.000401	0.000662	4.67	35.899	0
B	0.125	0.245	0.171	-0.384	7.47E-05	0.000123	0.87	355.41	81.37
C	0.25	0.279	0.161	-0.368	0.000111	0.000181	1.28	245.23	72.59
D	0.375	0.051	0.302	-0.396	0.000145	0.00024	1.69	79.040	63.81
E	0.5	0.201	0.087	-0.390	0.000236	0.000389	2.74	67.860	41.33
F	0.625	0.303	0.065	-0.318	2.93E-05	4.84E-05	0.34	480.77	92.72
G	0.75	0.082	0.042	-0.429	1.21E-05	1.99E-05	0.14	606.82	97.00

Open Circuit Potential Measurement

The corrosion potential values for TTD are shown in table 3, while figure 8 shows the corresponding relationship between corrosion potential values and exposure time. There is a potential displacement to less noble potentials from 0.125% TTD to 0.5% TTD even the potential values at 1.25% TTD - 2.5% TTD are well within passivity potentials, after which the potential values at 0.375% TTD – 0.5% TTD are within the zones of active corrosion. At 0.625% TTD – 0.75% TTD there is a sharp potential displacement to values within the zone of effective inhibition (total suppression of the corrosion process). This is further confirmed from the weight-loss method. The non linear potential values in HCl from 0.125% TTD to 0.75% TTD is most probably due to desorption of the inhibitor from the steel surface. The desorption is a product of the formation of secondary precipitates which accelerates the corrosion process and lateral repulsion between the cations of TTD compounds due to the specific nature of the inhibitor at the concentrations involved.Comparison of the potential values shows TTD influence to be more thermodynamically stable than in HCl due to the aggressive nature and adsorption of the chloride ions from the HCl solution.

Scanning Electron Microscopy Analysis

The SEM images of figure 9 (a & b) shows surfaces which has been electrochemically altered due to competitive adsorption of TTD molecules which results in the displacement of Cl^- ions initially adsorbed onto the specimen's surface. The resulting topography consist of solid and impervious precipitates of TTD molecules formed over the entire surface of MS due to charge transfer and chemical interaction with the valence orbital of iron constituting the bulk of MS constituent elements. This is responsible for the unusual topographic image because the cationic molecules of TTD form complexes on the surface which effective prevents diffusion of the corrosive anions. Results from weight loss and

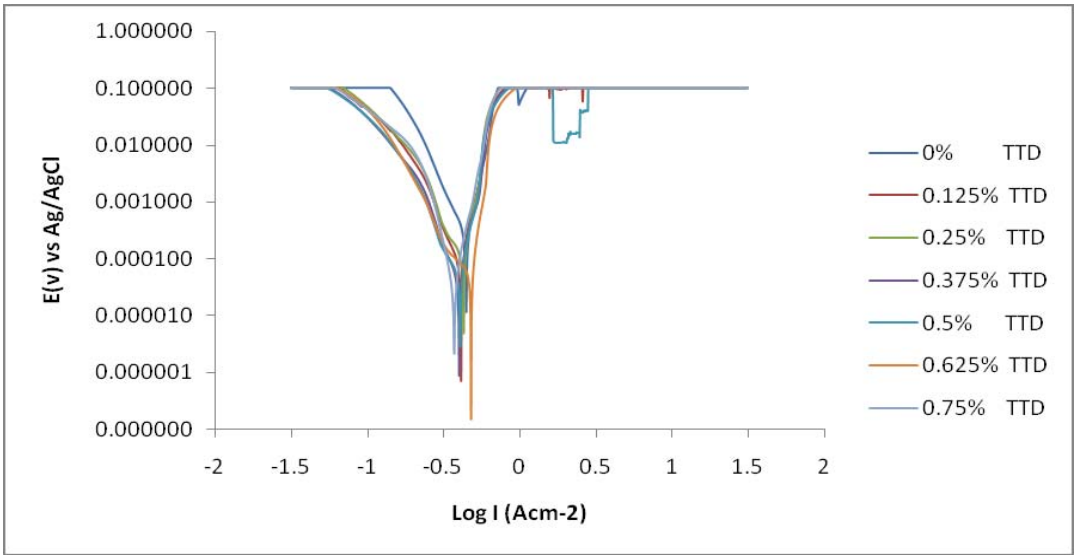

Fig. 6. Comparison plot of polarization scans for MS in 0.5M HCl solution at specific concentrations of TTD (0%-0.75% TTD).

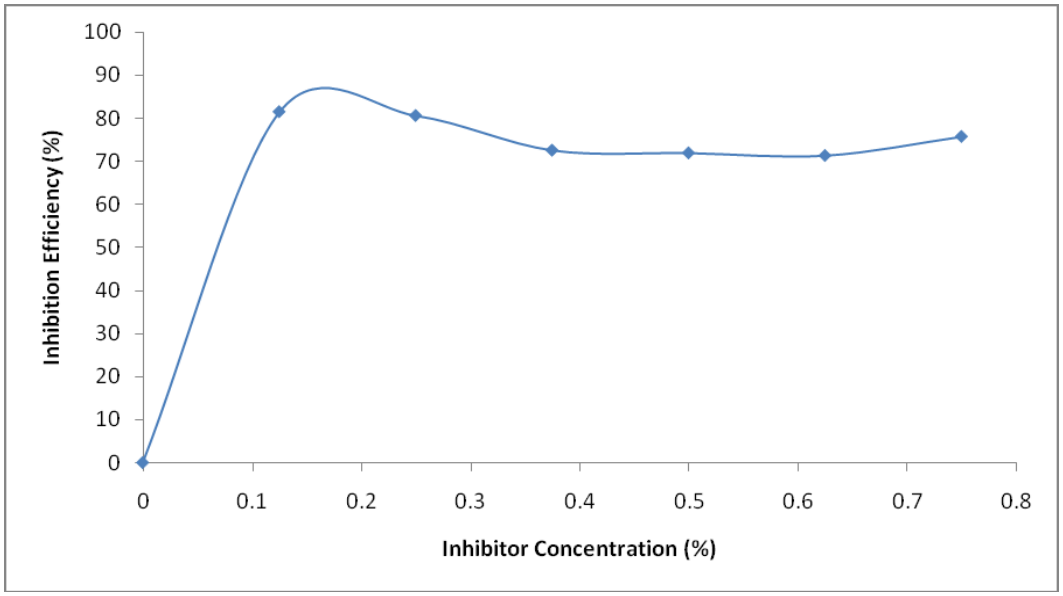

Fig. 7. The relationship between %*IE* and inhibitor concentration for polarization test in 0.5M HCl solution/TTD.

potentiodynamic polarization furthers corroborates the effectiveness of the protective film resulting from the significant electrochemical influence TTD has on the corrosion process. The contrast in the micrographs from both solutions is due to the molecular nature and specific inhibiting action of TTD the varying acid solutions.

Adsorption Isotherms and Thermodynamics of the Corrosion Process

The mechanism of corrosion inhibition can be explained on the basis of the adsorption behaviour of the adsorbate on the metal surface (Deyab and Abd El-Rehim, 2013). Adsorption isotherms are very important in determining the mechanism of organo - electrochemical reactions. The adsorptive behaviour of the organic compounds is an important part of this study, as it provides important clues to the nature of the metal-inhibitor interaction. Langmuir and Frumkin adsorption isotherms were applied to describe the adsorption mechanism for the inhibiting compounds in acid solutions, as they best fit the experimental results.

The isotherms are of the general form.

$$f(\theta, x) \exp(-2a\theta) = K \quad (6)$$

where f (θ, x) is the configurational factor which depends upon the physical model and assumption underlying the derivative of the isotherm, θ is the surface coverage, C is

Table 3. Data obtained from potential measurements for mild steel in 0.5M HCl in presence of specific concentrations of the TTD.

TTD Concentration (%) / Exposure Time (h)	0	0.125	0.25	0.375	0.5	0.625	0.75
0	-459	-346	-413	-438	-469	-314	-317
48	-451	-331	-397	-423	-450	-309	-312
96	-445	-324	-383	-415	-437	-304	-301
144	-431	-319	-374	-396	-413	-299	-293
192	-433	-313	-368	-388	-416	-295	-289
240	-438	-310	-359	-375	-411	-287	-281
288	-442	-302	-356	-367	-427	-282	-279

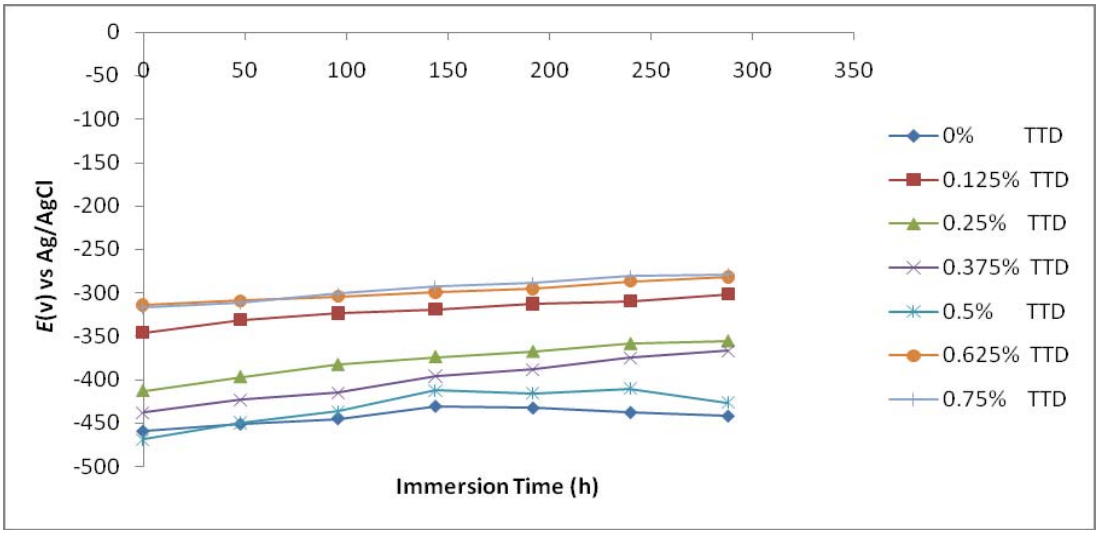

Fig. 8. Variation of potential with immersion time for TTD concentrations in 0.5M HCl.

the inhibitor concentration, x is the size ration, 'a' is the molecular interaction parameter and K is the equilibrium constant of adsorption process.

The conventional form of the Langmuir isotherm is,

$$\left[\frac{\theta}{1-\theta}\right] = K_{ads}C \quad (7)$$

and rearranging gives

$$K_{ads}C = \left[\frac{\theta}{1+K_{ads}\theta}\right] \quad (8)$$

whereθ is the degree of coverage on the metal surface, C is the inhibitor concentration in the electrolyte, and K_{ads} is the equilibrium constant of the adsorption process.

Langmuir isotherm proposes the following;

(i) The molecular interaction between the adsorbates on the metal surface is fixed.
(ii) The Gibbs free energy does not depend on the surface coverage values
(iii) There is no effect of lateral interaction among the adsorbates onthe value of Gibbs free energy (Ashish and Quraishi, 2011).

The plot of C/θ versus AMB concentration (C) (Fig. 10) fitted the Langmuir adsorption isotherm.

Frumkin isotherm assumes unit coverage at high inhibitor concentrations and that the electrode surface is inhomogeneous i.e. the lateral interaction effect is not negligible. In this way, only the active surface of the electrode, on which adsorption occurs, is taken into account. Frumkin adsorption isotherm can be expressed according to equation 9.

$$\text{Log } \{C \square(\frac{\theta}{1-\theta})\} = 2.303 \log K + 2\alpha\theta \quad (9)$$

Where K is the adsorption-desorption constant and α is the lateral interaction term describing the interaction in adsorbed layer.

Plots of θ/1- θ versus inhibitor concentration(C) as presented in figure 11 is linear with slight deviation which shows the applicability of Frumkin isotherm. The lateral interaction term (α) calculated from the slope of the Frumkin isotherm (Table 4) shows the intermolecular attraction between the TTD molecules on the surface of

MS decreases progressively with increase in TTD concentration; however its overall influence on the inhibition efficiency is negligible.

Table 4. Relationship between lateral interaction parameter and surface coverage (θ) in 0.5 M HCl MS.

Lateral Interaction Parameter (α)	Surface Coverage (θ)
0	0
2.156	0.721
2.478	0.627
2.798	0.556
3.964	0.392
1.716	0.906
1.661	0.936

Values of ΔG_{ads} around -20 kJ/mol are consistent with physisorption; those around -40 kJ/mol or higher involve charge sharing to form a coordinate type of bond chemisorption (Vračar and Drazic, 2002). The value of ΔG_{ads} in HCl for MS under the action of the organic compounds as shown in table 5 reveals the strong adsorption of TTD molecules onto the steel surface. The negative values of ΔG_{ads} showed that the adsorption of inhibitor molecules on the metal surface is spontaneous. The values of ΔG_{ads} calculated ranged between −38.00 and −40.94 kJ mol^{-1} for TTD (Table 5) in HCl. The values in HCl are consistent with chemical interaction and adsorption onto the MS surface.

The value of ΔG_{ads} obtained shows that the molecules chemisorb on the steel producing a bond resistant to penetration and competitive adsorption from the corrosive species. The intermolecular bonding is sufficiently strong to prevent displacement of adsorbed inhibitor molecules

(a)

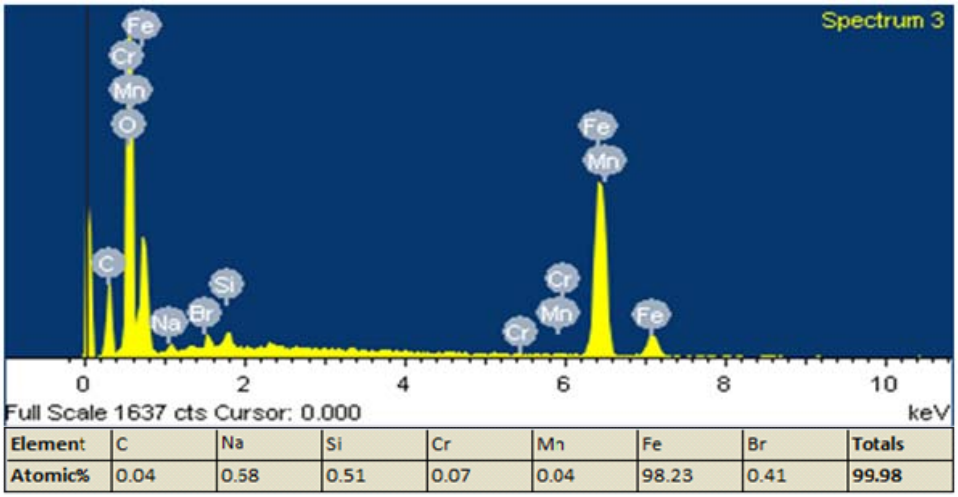

Element	C	Na	Si	Cr	Mn	Fe	Br	Totals
Atomic%	0.04	0.58	0.51	0.07	0.04	98.23	0.41	99.98

(b)

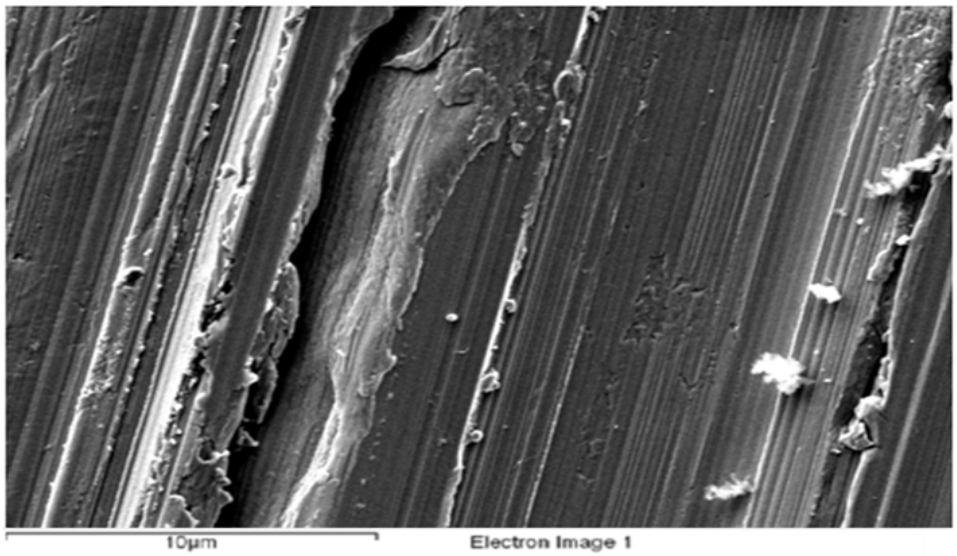

Fig. 9. SEM micrographs of: a) Energy dispersive spectrometer analysis of Mild, b) Mild steel before immersion in 0.5 M HCl.

(c)

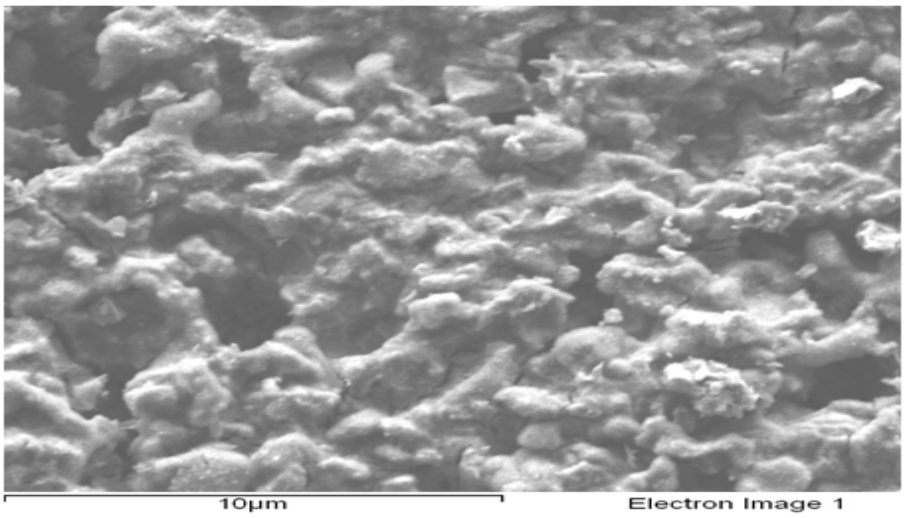

(d)

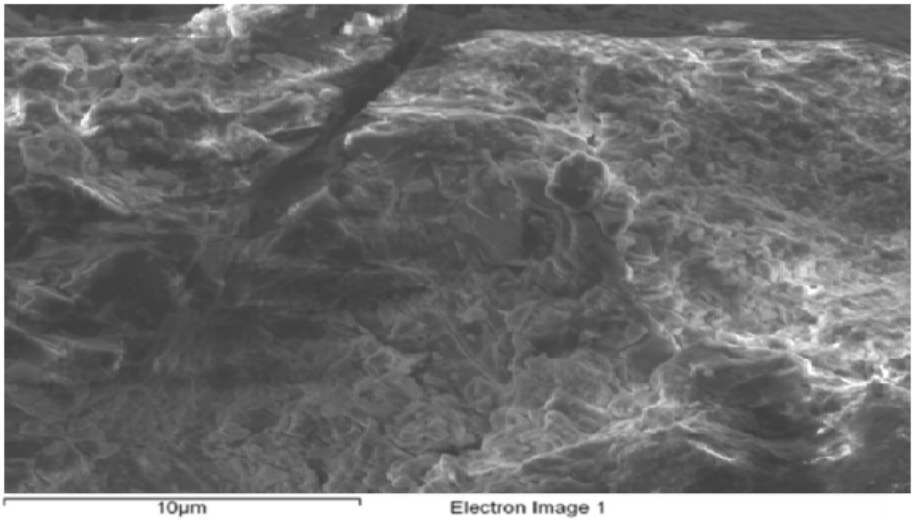

Fig. 9. SEM micrographs of: c) Mild steel after immersion in 0.5 M HCl, d) Mild steel after immersion in 0.5 M HCl with TTD addition.

along the surface. The precipitates formed are stable in the acid solution throughout the exposure period.

Statistical Analysis

Two-factor single level experimental ANOVA test (F-test) was used to analyse the separate and combined effects of the percentage concentrations of TTD and exposure time on the inhibition efficiency of TTD in the corrosion inhibition of mild steels in 0.5M HCl solutions and to investigate the statistical significance of the effects. The F-test was used to examine the amount of variation within each of the samples relative to the amount of variation between the samples.

The Sum of squares among columns (exposure time) was obtained with the following equations.

$$SS_c = \frac{\sum T_c^2}{nr} - \frac{T^2}{N} \qquad (10)$$

Sum of Squares among rows (inhibitor concentration)

$$SS_r = \frac{\sum T_r^2}{nc} - \frac{T^2}{N} \qquad (11)$$

Total Sum of Squares

$$SS_{Total} = \sum x^2 - \frac{T^2}{N} \qquad (12)$$

The results using the ANOVA test is tabulated (Table 4) as shown.

The ANOVA results (Table 6, Fig. 12) in the acid solution shows the overwhelming influence of inhibitor concentration on the inhibition efficiency with F-values of 98.46 (Table 6). This greater than significance factor at α=0.05 (level of significance or probability). The F-values of exposure time in both acids are less significant

Table 5. Data obtained for the values of Gibbs free energy, Surface coverage and equilibrium constant of adsorption at varying concentrations of TTD in 0.5 M HCl for MS.

Samples	Surface Coverage (θ)	Equilibrium Constant of Adsorption (K_{ads})	Free energy of Adsorption (ΔG_{ads}) (kJ/mol)
B	0.721	267483	-40.91
C	0.627	86804.3	-38.12
D	0.556	43138.9	-36.40
E	0.392	16682.4	-34.06
F	0.906	200074	-40.23
G	0.936	251783	-40.80

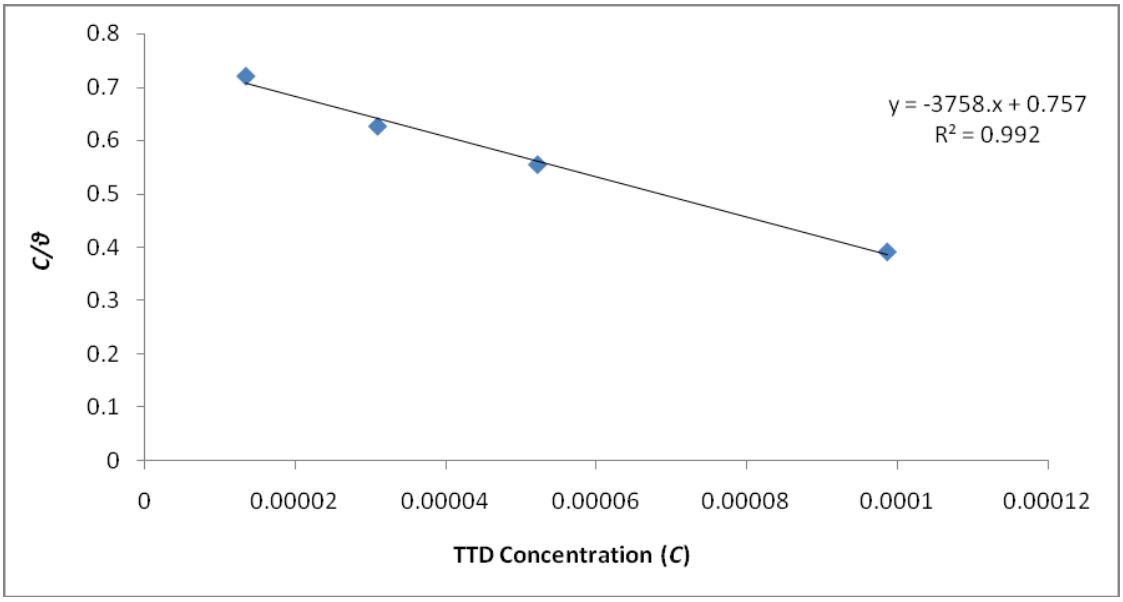

Fig. 10. Relationship between C/θ and TTD concentration (C) in 0.5 M HCl for MS.

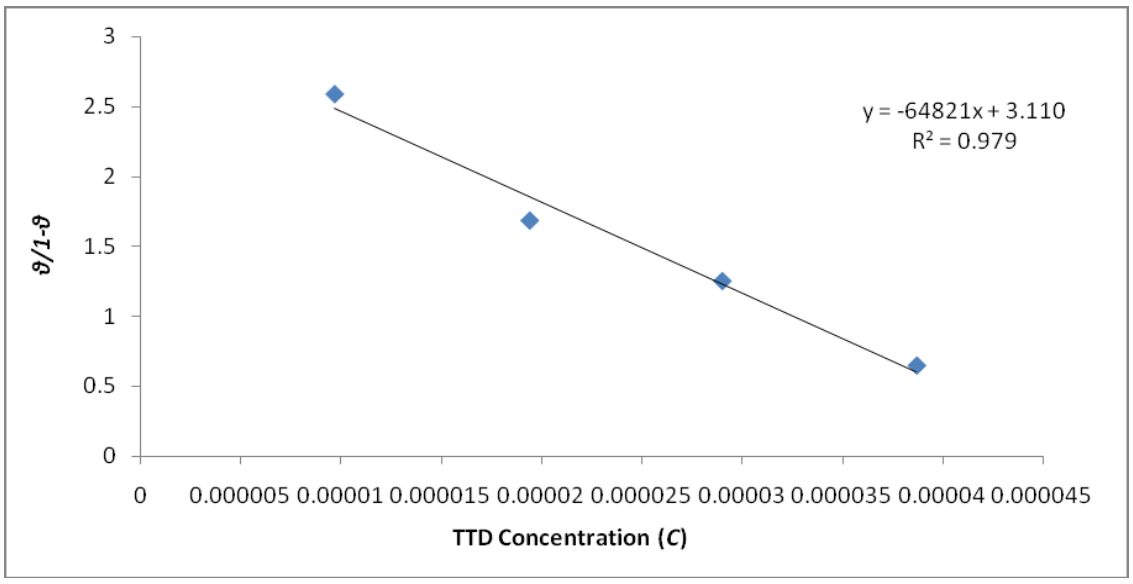

Fig. 11. Relationship between θ/1- θ and TTD concentration (C) in 0.5 M HCl for MS.

Table 6. Analysis of variance (ANOVA) for inhibition efficiency of TTD inhibitor in 0.5M HCl (at 95% confidence level).

TTD HCl					Min. MSR at 95% confidence	
Source of Variation	Sum of Squares	Degree of Freedom	Mean Square	Mean Square Ratio	Significance F	F(%)
Inhibitor concentration	7059.73	5	1411.95	139.41	2.71	85.7
Exposure Time	743.31	4	185.83	18.35	2.87	8.76
Residual	202.56	20	10.13			
Total	8005.60	29				

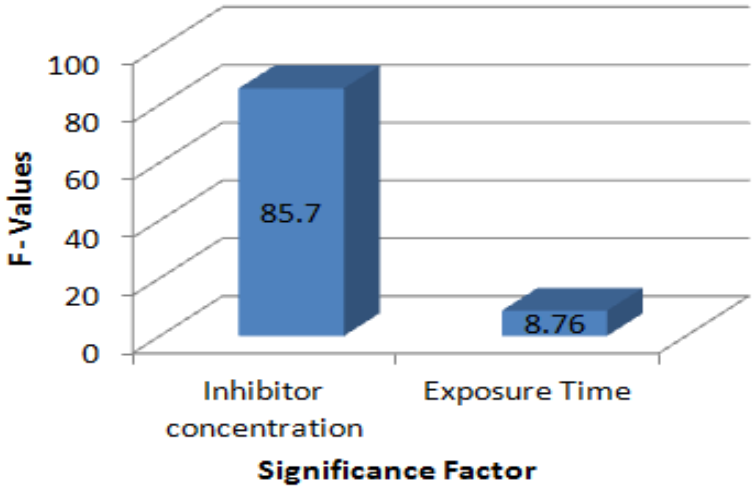

Fig. 12. Influence of inhibitor concentration and exposure time on inhibition efficiency of TTD in 0.5M HCl.

compared to inhibitor concentration but greater than the significant factor hence they are statistically relevant with F-values of 15.14. The statistical influence of the inhibitor concentration in HCl is 85.7% while the inf luence of the exposure time is 8.76%. The inhibitor concentration and exposure time are significant model terms influencing inhibition efficiency of TTD on the corrosion of the steel specimen with greater influence from the percentage concentration of TTD.

CONCLUSION

2-amino- 5 ethyl- 1, 3, 4 thiadiazole (TTD) performed effectively with excellent results in the acid media. Thecorrosion reduced with increase in TTD concentration. TTD showed mixed inhibiting tendencies at all concentration studied, though the tendency for cathodic inhibition is more pertinent with the corrosion potential values shifting to less noble values over the TTD concentrations studied. Results deduced from thermodynamic calculations showed the electrochemical interaction to be by chemisorption mechanism. SEM characterization shows surfaces which has been electrochemically altered due to adsorption of TTD molecules onto the specimen's surface resulting in topography which consists of solid and impervious precipitates of TTD compound. Statistical analysis through ANOVA revealed only the inhibitor concentration to be statistically relevant on the inhibition efficiency of TTD.

ACKNOWLEDGEMENT

The authors acknowledge the Department of Chemical, Metallurgical and Materials Engineering, Faculty of Engineering and the Built Environment, Tshwane University of Technology, Pretoria, South Africa for the provision of research facilities for this work.

REFERENCES

Abiola, OK., Oforka, NC. and Ebenso, EE. 2004. A potential corrosion inhibition for acid corrosion of mild steel. Electrochemistry. 2(9):409-413.

Abboud, Y., Abourriche, A., Saffaj, T., Berrada, M., Charrouf, M., Bennamara, A. and Hannache, H. 2009. A novel azo dye, 8-quinolinol-5-azoantipyrine as corrosion inhibitor for mild steel in acidic media. Desalination. 237:175-189.

Ashassi-Sorkhabi, H., Masoumi, B. and Ejbari, PE. 2009. Corrosion inhibition of mild steel in acidic media by Basic yellow 13 dye. Journal of Applied Electrochemistry. 39:1497-1501.

Ashish, KS. and Quraishi, MA. 2011. Investigation of the effect of disulfiram on corrosion of mild steel in hydrochloric acid solution. Corrosion Science. 53(4):1288-1297.

Bouklah, M., Ouassini, A., Hammouti, B. and El Idrissi, A. 2005. Corrosion inhibition of steel in 0.5 M H_2SO_4 by [(2-pyridin-4-ylethyl)thio]acetic acid. Applied Surface Science. 250: 50-56.

Bentiss, F., Traisnel, M., Gengembre, L. and Lagrenee, M. 2000. Inhibition of acidic corrosion of mild steel by 3,5-diphenyl-4H-1,2,4-triazole. Applied Surface Science. 161:194-202.

Cruz, J., Martez, R., Genesca, J. and Garcia-Ochoa, E. 2004. Experimental and theoretical study of1-(2-ethylamino)-2-methylimidazoline as an inhibitor of carbonsteel corrosion in acidmedia. Journal of Electroanalytical Chemistry. 566:111-121.

Collins, WD., Weyers, RE. and Al-Qadi, IL. 1993. Chemical Treatment of Corroding Steel Reinforcement after removal of chloride-contaminated concrete. Corrosion Nace. 49(1):74-88

Devarayan, K., Mayakrishnan, G. and Nagarajan, S. 2012. Green Inhibitors for Corrosion of Metals: A Review. Chemical Science Review and Letters.1(1):1-8.

Deyab, MA. and Abd El-Rehim, SS. 2013. Influence of Polyethylene Glycols on the corrosion Inhibition of carbon steel in butyric acid solution: Weight loss, EIS and theoretical studies. International Journal of Electrochemical Science. 8(12):12613-12627.

Eduok, UM., Umoren, SA. and Udoh, AP. 2010. Synergistic inhibition effects between leaves and stem extracts of *Sida acuta* and iodide ion for mild steel corrosion in 1 M H_2SO_4solutions. Arabian Journal of Chemistry. 5(3):325-337.

Ekpe, UJ., Ibok, UJ., Ita, BI., Offiong, OE. and Ebenso, EE. 1995. Inhibitory action of methyl and phenyl thiosemicarbazone derivatives on the corrosion of mild steel in hydrochloric acid. Materials Chemistry and Physics. 40:87-93.

Fontana, MG. 1986. Corrosion Engineering. (3rd edi.). McGraw-Hill, Singapore.

Ita, BI. and Offiong, OE. 1997. The inhibition of mild steel corrosion in hydrochloric acid by 2, 2'-pyridil and α-pyridoin. Materials Chemistry and Physics. 51:203-210.

Ita, BI. and Offiong, OE. 1997. Inhibition of steel corrosion in hydrochloric acid by pyridoxal, 4-methylthiosemicarbazide, pyridoxal-(4-methylthiosemicarbazone) and its Zn(II) complex. Materials Chemistry and Physics. 48:164-169.

James, AO., Oforka, NC. and Abiola, OK. 2005. Inhibition of the corrosion of aluminium in hydrochloric acid solutions by pyridoxal hydrochloride. Journal of Corrosion Science and Engineering. 7(21):1-10.

Krim, O., Bouachrine, M., Hammouti, B., Elidrissi, A. and Hamidi, M. 2008. 2.5-Difuryl-N-Methylpyrrole as Corrosion Inhibitor for Steel in 1 M HCl. Portuguese Electrochimical Acta. 26:283-289.

Liu, GQ., Zhu, ZY., Ke, W., Han, CI. and Zeng, CL. 2001. Corrosion Behavior of Stainless Steels and Nickel-Based Alloys in Acetic Acid Solutions Containing Bromide Ions. Corrosion Nace. 57(8):730-38.

Manahan, SE. 1994. Environmental Chemistry (6th edi.). Lewis, Boca Raton.

Popova, A., Christov, M., Raicheva, S. and Sokolova, E. 2004. Adsorption and inhibitive properties of benzimidazole derivatives in acid mild steel corrosion. Corrosion Science. 46:1333-1350.

Quraishi, MA. and Shukla, SK. 2009. Poly (aniline-formaldehyde): A new and effective corrosion inhibitor for mild steel in hydrochloric acid. Materials Chemistry and Physics. 113:685-689.

Rastogi, RB.,Singh, MM., Singh, K. and Yadav, KM. 2005. Organolic Dithiohydrazodicarbonamides as corrosion inhibitors for mild steel-dimethyl sulphoxide containing HCl. Portugaliae Electrochimica Acta. 22:315-332.

Singh, DDN., Singh, TB. and Gaur. B. 1995. The role of metal cations in improving the inhibitive performance of hexamine on the corrosion of steel in hydrochloric acid solution. Corrosion Science. 37:1005-1019.

Sinko, J. 2001. Challenges of chromate inhibitor pigments replacement in organic coatings. Progress in Organic Coating. 42:267-282.

Thomas, JGN. 1980-1981. Proceedings of the Fifth European Symposium on Corrosion Inhibitors, Ann. Univ. Ferrara. Italy. 453.

Trowsdale, AJ., Noble, B., Harris, SJ., Gibbins, ISR., Thompson, GE. and Wood, GC. 1996. The influence of silicon carbide reinforcement on the pitting behaviour of aluminium. Corrosion Science. 38(2):177-191.

Vračar, LM. and Dražić, DM. 2002. Adsorption and corrosion inhibitive properties of some organic molecules on iron electrode in sulfuric acid. Corrosion Science. 44:1669-1680.

Received: April 25, 2014; Accepted: June 23, 2014

SENRA Academic Publishers, British Columbia
Vol. 8, No. 3, pp. 3105-3114, October 2014
Online ISSN: 1920-3853; Print ISSN: 1715-9997

Canadian Journal of pure&applied sciences

RE-ACTIVATION OF A SMALL HYDROPOWER (SHP) PLANT: OYAN SHP STATION, NIGERIA

OR Adegboye[1], *KM Odunfa[1] and OS Ohunakin[2]
[1]Department of Mechanical Engineering, University of Ibadan, Nigeria
[2]Department of Mechanical Engineering, Covenant University, Nigeria

ABSTRACT

Electricity production in small hydropower (SHP) plants can be increased without the need for the construction of new SHP scheme, but by upgrading and optimizing different aspects of existing plant's operations. An assessment of the electromechanical equipment that suites the existing heads, discharge or flow rates and other electromechanical parameters at the Oyan SHP plant, using Retscreen Clean Energy Project Analysis Software and hydraulic turbine specific speed equation ($N_s = (N\sqrt{P_t})/H^{1.25}$) to evaluate plant performances was carried out in this work. Two cases involving upgrading of the electromechanical equipment to yield 10 and 12 MW of installed capacities respectively were considered, while at the same time maintaining the existing structures such as the weir, powerhouse and penstocks. The two cases were analysed and compared with a reference case (the existing installed capacity generation of 9 MW). Findings in terms of the financial and economic analysis for optimum installation and operation, favoured the 10 MW installation. Energy gain by installing the 10 MW is 33.37% relative to the reference case while the 12 MW is 5% compared with the reference. The simple payback for the 10 and 12 MW capacities is 11 and 13 months respectively. Hence, upgrade and optimization to 10 MW is found to be a more profitable option than the 12 MW capacity.

Keywords: Nigeria, re-activation, repowering, small hydropower plant, oyan dam.

INTRODUCTION

Background

The small and medium water flows represent an important power generation option that presents intrinsic advantages in eliminating the eventual social and environmental effects caused by large hydropower plants. Until 1973 during the worldwide energy crisis, the development of small hydropower schemes (micro, mini and small) was not considered economically viable because economies of scale was found to clearly favour the development of large hydro and thermal power plants (ECN, 2004).

Small hydropower (SHP) has been in existence in Nigeria since 1923, 45 years before the commissioning of the country's first large hydropower (Kainji). Today, SHP technology is still at its infancy in spite of the vast potential and the high energy need in the country; however, the situation is different in developed countries where SHP plants find broad adoption in electricity production and other applications (Ohunakin *et al*., 2011). Nigeria was divided into river basins in 1976 (through the establishment of River Basins Development Authorities), for purposes such as: irrigation, water supply, navigation, hydroelectric power generations, fisheries and recreational facilities; these river basins are accomplished through the construction of small, medium and large dams to impound surface waters thereby making most of the rivers and dams to be favoured with good heads and capacity for various SHP utilizations (Ohunakin *et al*., 2011). Summary of SHP potentials in the River Basins are shown in table 1.

Nowadays, new hydroelectric projects (in particular, large hydro plants) are facing great hindrances of initiation, due to existing environmental laws that resulted from the aggressive impacts of such projects on the environment (impacts such as (i) the commencement or acceleration of erosion process at the reservoir banks, (ii) a change in the water quality of the reservoir by organic decomposition which also favours the emission of greenhouse gases (GHGs), (iii) a reduction of the water oxygen concentration thus destroying most aquatic species and generating harmful compounds to human health (Maldonado *et al*., 2004). SHP on the other hand does not suffer any of these disadvantages associated with large hydro. However, the high initial cost of constructing new SHP plant may call for the need to re-power and upgrade existing SHP facilities, so as to increase the electrical power output, with negligible or no negative impacts. In ESHA (2005), the prospect of reinstating aged/obsolete SHP plants and upgrading existing/underutilized ones, is estimated at an annual electricity production of approximately 4,500 GWh. Provided plants to be re-powered are already installed for more than 30 years, most of the impending impacts would have been absorbed

*Corresponding author email: m.odunfa@mail.ui.edu.ng

by the boundary and nature would have re-adapted to the power plant environment; the emission of greenhouse gases will be practically null and there will be no need to compulsorily remove the riverside populations. A major task may be to find efficient alternatives (projects) to obtain profitable electrical energy supply in a manner that will meet any future demand, without necessarily having to distort nature through the expansion of power reservoirs (Maldonado *et al*., 2004). Acceptable projects under this guise, are those directed towards the increase of machine efficiency and reduction of water head losses (i.e. upgrading of the whole yield of transformation). The effect will lead to an increase of the plant capacity and production, under the same discharge conditions. These projects turn the hydro capacity increase to the advantage of the producer through the sale of more energy, and to the environment through growth of renewable energy production without negative impact (SHERPA, 2006). The aim of present work is to find the optimal power output that can be obtained, through the rehabilitation and upgrade of the existing SHP scheme of the Oyan dam, Ogun State, Nigeria.

Brief Description of an SHP

The SHP schemes are categorized into: (i) civil works and (ii) electromechanical equipment as shown in figure 1 (Singal *et al*., 2010). The civil works consist of intake, penstock (an intake structure or an enclosed pipe that delivers water to hydro turbines), power house building (a facility for the generation of electric power), and tail race channel (part of a hydropower facility that carries water away from a turbine) (Singal *et al*., 2010; Penstock, 2014; Tailrace, 2014). The electromechanical components are turbines with governing system, generator with excitation system, electrical and mechanical auxiliary, and transformer and switchyard equipment (Singal *et al*., 2010).

MATERIALS AND METHODS

Methodology

Oyan dam is earth filled on the Oyan river, 15 km North-West of Abeokuta on geographical coordinate 7°15′30″N and 3°15′20″E (Fig. 2). The dam and power plant parameters are shown in table 2. The Oyan hydropower plant was completed in 1982 and commissioned in 1983, but has not been put into operation till date. The power plant has a turbo-generator efficiency of 85%, alternator power factor of 80%, with three turbines of 3 MW each to yield 9 MW of total installed capacity and an annual firm energy production of 63.32 GWh. The possibility to re-activate the plant to increase its energy generation capacity was done using Retscreen International Clean/Renewable Energy Project Analysis Software.

SHP Turbine Selection

The hydraulic turbine plays an important role in an SHP station; the selection, type and specification of other equipment in the SHP station are dependent on the turbine (Singal *et al*., 2010). Furthermore in Singal *et al.* (2010), turbine selection is governed by head, discharge, capacity, speed, part load efficiency, number of units, and cavitation characteristics. Kaplan hydraulic turbine is selected for the power output of the scheme in this work, because it is directly related to low or medium head of the scheme; the relatively high specific speed of a Kaplan turbine also result in favourable economy of scale (i.e. smaller size of turbine and generator and hence reduction in installation and transportation cost) for SHP plants. The specific speed equation needed to improve the operating conditions of the turbine is expressed as:

$$N_s = (N\sqrt{P_t})/H^{1.25} \quad (1)$$

where N_s is the specific speed, N is the rotational speed of turbine (rev/min), P_t rated power output of the turbine (kW) and H is the rated net head (m). In addition, efficiency is maximum at the rated load as cavitation factor becomes higher, thus improving the plant's performance. Data related to the SHP generation is given in table 3.

ECONOMICS ANALYSIS

Generation Cost

Generation cost at different load factors for different type of turbines and generators is based on annual cost and annual energy generation. Annual cost for generation of electric energy includes operation and maintenance (O&M), insurance cost, depreciation of civil works and equipment, interest on the capital invested and replacement cost (Singal *et al*., 2008). Annual cost has been taken as 16% of the project cost. With the volatile cost of energy today, efficient use of energy in existing plants is as important as planning energy choices in new facilities. Energy performance and fuel selection for revamps and new plant designs will have a major impact on operating costs, capital costs and operating security (Jacob Consultancy, 2012).

Operating and maintenance cost (O & M)

According to Ohunakin and Akinnawonu (2012), manufacturers in recent years are attempting to lower costs arising from operation and maintenance (O&M) significantly, by developing new turbine designs that require fewer regular service visits and less turbine downtime. The O&M costs constitute a sizable share of the total annual costs of the turbine (Ohunakin and Akinnawonu, 2012). It consists of different cost components including land rent, insurance, regular maintenance, repair, spare parts and consumables, own

electricity consumption, administration etc. Information about actual values of O&M costs was not found and believed to vary depending on the particular location of the project. However, a value of 1.5% of the total project cost was adopted in this work in line with India's electricity sector (1998), since Nigeria and India have similarity of business and project terrain.

Depreciation
Equipment get depreciated over the life of the project. Based on the life of the project (hydropower plant) considered as 35 years, an annual rate of depreciation of 4% was adopted.

Interest
Interest rates between 10 to 12% are being charged by financial institutions for projects that exist within the small hydropower range. An interest rate of 11% has been taken for the analysis.

Benefit-Cost Ratio
The benefit-cost ratio (BCR) has been used to evaluate the economic viability of the project. The BCR is the ratio of the present value of future cash flows (benefits) to the present value of the original and subsequent cash out flows (Singal *et al*., 2008) it is often used to assess the value of a municipal project in relation to its cost (Sepulveda *et al*., 1984). Accordingly, benefits-cost ratio is worked out as follows:

$$\text{BCR} = \frac{\textbf{present value of benefits}}{\textbf{present value of expenditure}} \quad (2)$$

Present Value of Benefits
In order to get consistent values for both benefit and cost, the present value (PV) criterion has been adopted. Under the procedure, the present value at the time of first expenditure of the future stream of benefits was calculated by fixing the discount rate. The PV of the scheme has been evaluated by using the expression given in Equation 3 in Raghuvanshi (1995):

$$\mathbf{PV} = \sum_{i=1}^{n} \left[\mathbf{CF}_i / (1+d)^i \right] \quad (3)$$

where $\mathbf{PV}$ is the present value, $\mathbf{CF}$ is the cash flow, $\mathbf{n}$ is the last year of cash flow, $\mathbf{i}$ is the $\mathbf{ith}$ year starting with the initial investment and $\mathbf{d}$ is the discount rate. The life of the plant has been taken as 35 years and it was considered that after 25 years, major replacement of equipment and renovation of works may be required; power may not be generated during renovation of the units and other associated works. Hence, present value of benefits was computed for 25 years of the plant's operation (Singal *et al*., 2008).

Present Value of Expenditure
Duration of construction is taken as 2 years. In many situations, it is found that such plants were even installed in less than 2 years in recent past projects. The installation cost was divided as 77% in the first year and 23% in the second year (Forouzbakhsh, 2007). Present value of expenditure has been worked out by taking installation cost in 2 years followed by annual cost in the subsequent 25 years in the same way the present value of benefits was computed (Singal *et al*., 2008).

Discount Rate
Discount rate signifies the time value of money and is the cost of the capital investment. The source of capital is the equity and the loan (debt); equity and loan ratio has been taken in 30:70 proportion based on the guidelines for financing by leading financial institutions (Singal *et al.*, 2008). A discount rate of 15% is adopted in this work.

Inflation
The inflation, based on consumer price index for the years 1995 to 2007 varies from 3.3 to 8% in Nigeria. The average inflation during this period comes out to be around 5%, which has been taken as inflation on benefits from sale of electrical energy and the O&M cost.

Energy generation output
The amount of energy produced by a hydro power plant depends on: (i) the design capacity of the plant compared to the flow and head available in the stream and (ii) the variations in the load (Gupta, 2008). The annual energy output generated for a constant power (assuming some degree of load management) is expressed in Equation (3) as:

$$\mathbf{E\ (annual)\ =\ P\ (design)\ x\ 8760\ kWh} \quad (3)$$

where E (annual) is the annual energy output in kWh, P (design) is the firm power (kW) while the number of hours in a year is given as 8760.

Since it is not possible for load to be constant, the design capacity of the plant ($\mathbf{P\ (design)}$) would probably be greater than the maximum load in order to accomodate the possibility of future load increase. Furthermore, with occassional maintenance activities, shut down of the plant is also inevitable. Hence, the actual annual energy output will be less than that given in Equation (3). This calls for the inclusion of a plant or capacity factor ($\mathbf{PF}$) in the expression, thus giving rise to Equation (4) as expressed:

$$\mathbf{E\ (annual)\ =\ P\ (design)\ x\ PF\ x\ 8760\ kWh} \quad (4)$$

Model Simulation
Due to the time stepping of the Retscreen software (Fig. 3 shows the flowchart), the model developed is based on the following: (i) annual hydrological statistics (ii) annual production (which includes renewable energy delivered

and the excess renewable energy available) of the installed capacities to be considered and (iii) financial parameters like capital investment, annual cost, operating and maintenance (O&M) cost, production (generation) cost, energy savings income etc. Table 4 gives the basic data adopted for the simulation, considering the new capacities of 10 and 12MW.

RESULTS AND DISCUSSION

The output of production simulation is shown in Table 5. It can be observed from the result of the simulation shown in table 5, that the potential annual mean production at Oyan SHP plant ranges from 63.32 to 88.9 GWh for the installed capacities of 9 and 12 MW respectively. The results also showed an increase in power output for the 10 and 12 MW installed capacities. The increase in installed power from 9 to the 10 and 12 MW installed power is 16.67 and 15%, respectively. The 10 MW plant yielded 33.77% more energy production from the 9MW originally installed power than the 12MW. The plant capacity factor (0.92 of 8700 hours at full power) is quite high thus indicating that the installed capacity will be rather oriented towards the production of base load or energy.

Hydrological and load analysis

Oyan River possesses a steady stream flow whose annual inflow from the catchment area to the reservoir as modelled by the Retscreen Software, gave 56 m^3/s firm flow, occurring at 90 to 100% time of the river. This is shown in the flow duration curve in figure 4. The expected load duration for the 10 and 12MW installed capacities with an average load factor of 0.6 are as indicated in figures 5 and 6.

Economic estimates of re-powering the SHP plant with the consequent upgrade from the initial installed capacity of 9MW to 10MW (Case 1) and 12MW (Case 2) is depicted in table 6. The unit cost for the energy generated which is N10/kWh as given by the Retscreen simulation, is adopted in the computation of the energy generation cost at full load with a capacity factor of 0.92; this may be quite high to operate continuously for 8700 hours to be able to meet the highest production practices (i.e. the installed capacity is oriented towards the production of base load than peak energy). The percentage increase in generation cost from Case 1 to 2 was found to be 14%; this is fairly high and in favour of Case 1 relative to the respective energy output. Since the given average load factor is 60%, increase or decrease in demand of the grid or load centres will affect the load factor either upwardly or downwardly, leading to a decrease or increase in energy generation cost. Furthermore, a drop in plant factor as well as a fall in the firm flow below the rated, will certainly affect energy output. The energy savings income as simulated by Retscreen model resulted in N12/kWh, thus resulting into 5% energy savings from Case 1 to 2. This was found to be relatively small and also in favour of Case 1. The cummulative cash flow for 35 years of economic life were generated after subjecting the model to effective income tax, depreciation and discount rate and inflation.

The financial estimates, electromechanical equipment and O&M costs of the new projects (Cases 1 and 2) is shown in table 7. The depreciation rate, interest rate, insurance premiums and spare parts are found to be function of capital investment of the entire hydropower project. The cost implication of electromechanical equipment and the financial feasibility of the project as simulated by Retscreen are shown in tables 8 and 9, while table 10 depicts the results of the specific speed of the Reference case and Cases 1 and 2. The difference observed in the specific speeds is associated with variations in the power output. High specific speed can be obtained in Kaplan turbines because of their low heads and large output. Higher specific speed has been proved to give greater runner speed which gives smaller machine size, but characterized with greater cavitation factor. Furthermmore, smaller machine dimensions utilize space while greater rotational speed necessitates heavier mechanical designs due to the accompanying centrifugal force and the associated expensive construction materials.

CONCLUSION

In this research work, the following were concluded:

- An alternative to the development of a cost intensive new hydro plant, is to review old/existing hydropower sites via thorough evaluation of their various heads and discharges that can later be employed to upgrade and optimize their electromechanical equipment for more power output.
- This mode of repowering and reactivation was found to provide additional electrical energy in the average range of 10 to 30% and sometimes more of the total installed capacities, at less than one tenth the cost of a new project, with no negative social and environmental impacts as caused by new hydro power installations.
- The 10 MW (16.67% firm power gain of original installed capacity) installation is recommended for this research work because of its favourable economic, financial and technical feasibility.
- The 12MW (33.33% gain of original installed capacity) is also suitable but may be considered as an option which will become more financially and technically viable than 10MW in future, provided the hydrology of the Oyan river dam approach a firm flow of about 65 $\mathbf{m^3/s}$, especially with the ongoing trend of global warming effects.

Table 1. Summary of River Basins Small Scale Hydropower Potential.

River Basins	Discharge (m^3/s)	Available Head (m)	Total Theoretical Power (MW)
Sokoto-Rima	7.6 42.5 (27.0)	3.0 25.0 (14.5)	100.4
Hadeija-Jamaare	5.5 36.8 (23.4)	5.0 25.0 (14.5)	149.0
Chad	2.4 35 (14.6)	4.2 25.6 (12.6)	89.0
Niger	12.6 60 (55.0)	6.0 35.0 (30)	650.0
Upper Benue	8.4 106 (67.2)	5.6 120 (45)	985.0
Lower Benue	9.4 68 (47)	3.9 98 (38)	560.0
Cross River	12 86 (56)	5.2 76 (40)	350.0
Anambra-Imo	13 69 (45)	3.5 20 (12)	120.0
Owena	24 78 (56)	5.6 25 (14)	320.0
Ogun-Osun	24 56 (45)	4.5 28 (15)	187.0
Delta	N/A	N/A	N/A

Source: (ECN, 2004)

Table 2. Parameters related to the dam.

Catchment area	9000 km^2
Reservoir area	40 km^2
Embankment length	1100m
Maximum height	32.00m
Embankment top level	67.70 m
Normal water level	63.00m
Maximum water level	65.50m
Average annual flow volume	1770Mcm
Gross storage volume	270Mcm
Length of service spillway	75m
Number of gates of service spillway	4 x 15m x 7m
Crest of service spillway	56.00m
Capacity of service spillway	34.40m^3/s
Length of auxillary spillway	400m
Crest of auxillary spillway	63.25m
Capacity of auxillary spillway	19.90m^3/s
Number of outlets	3
Diameter of each outlet	1.8m
Centre line	43.3m
Capacity at low water level	15m^3/s
Penstock diameter	3.8m
Centre line	41.05m
Installed capacity	3 x 3MW

Table 3. Hydroelectric Power Generation Data (Reference Case).

Number of turbine/alternator	3
Turbine type	Vertically doubly regulated full Kaplan turbine
Turbo-generator efficiency	75%
Number of turbine/alternator	3
Turbine type	Vertically doubly regulated full Kaplan turbine
Turbine speed	375rpm
Turbine maximum head	25m
Alternator output power	3.750 kVA
Alternator output voltage	11kV
Alternator output current	196.8A
Alternator power factor	0.8
Alternator frequency	50Hertz
Annual firm energy generated	63.3GWh
Manufacturer	Garbe-Lahmeyer, Germany
Year of manufacture and completion of project	1982

Table 4. Basic data adopted for simulation.

Parameters	10 MW	12MW
Normal operating level (m)	63.00	63.00
Maximum operating level (m)	65.50	65.50
Minimum operating level (m)	55.00	55.00
Gross head (m)	25.00	25.00
Penstock elevation (m)	41.05	41.05
Firm flow (m^3/s)	56.00	56.00
Number of turbines	3.00	3.00
Rated turbine discharge (m^3/s)	18.00	18.00
Turbine efficiency (%)	90.40	90.40
Generator efficiency (%)	95.00	95.00
Power/Capacity factor (%)	92.00	92.00

Table 5. Results of Production Simulation.

Installed power	Change (%)	Firm power	Peak power	Firm annual production (GWh)	Change (%)	Peak annual production (GWh)	Change (%)
9 MW (Original)		9.00MW	9.00 MW	63.32		63.32	
10 MW (New)	+16.67	10.50MW	10.50MW	84.70	+33.77	84.70	+33.77
12 MW (New)	+15.00	11.00MW	12.00MW	88.90	+5.00	96.60	+14.1

Table 6. Economic Analysis of Cases 1 and 2.

Parameters	Values	Quantity	Case 1	Case 2	Change (%)
Unit cost for energy generation	N10/kWh		863,399,400	985,320,000	14.0
Annual energy savings/income	N12/kWh		1,015,760,700	1,066,800,000	5.0
Economic life			35 years	35 years	
Total cummulative cashflow		35 years	46,663,815,900 N/year	53,537,424,750 N/year	14.7
Effective income tax rate			35%	35%	
Depreciation rate			30%	30%	
Discount rate			15%	15%	
Inflation			5%	5%	

Table 7. Financial Analysis of Cases 1 and 2.

Parameters	Unit cost/charges	Quantity	Case 1 (10 MW)	Case 2 (12 MW)
Interest rate	11% / year			
Depreciation time	Year		35 years	35 years
Depreciation rate	4%/year			
Capital costs	N/year/new project		2,319,920,100	2,492,938,500
Turbines/generators, controls	N75000/kW		785,931,300	903,152,550
Equipment installation	10% of electromechanical		78,593,100	90,315,300
Transportation	10% of electromechanical		78,593,100	90,315,300
Feasibility study, Development and others			1,376,802,600	1,409,155,350
Total annual costs (O&M)			45,864,150	47,748,300
Insurance premiums	0.4% of capital costs (N)		9,279,750	9,971,700
Transmission line maintenance			5,625,000	5,625,000
Spare parts	0.5% of capital costs		11,599,650	12,464,700
O&M labour	N5,250,000/year	2	10,500,000	10,500,000
Travel and accomodation	N150,000/trip	6	900,000	900,000
General and administrative	10% of unit cost		3,790,500	3,946,200
Contingencies	10% of unit cost		4,169,400	4,340,700

Table 8. Cost implication of electromechanical equipment.

Parameters	Unit	Case 1	Case 2
Turbo-generator, control	N75,000/kW	N785,931,300	N903,152,550
Equipment installation	10% of turbo-generator, controls	N78,458,100	N90,315,300
Transportation	10% of turbo-generator, controls	N78,458,100	N90,315,300
Total		N942,847,500	N1,083,783,150

Table 9. Financial feasibilities.

Parameters	Unit	Case 1	Case 2
Pre-tax IRR and ROI	%	173.2%	187.5%
After tax IRR and ROI	%	159.6%	171.6%
Simple payback	month	11	11
NPV (N)	year	4,842,311,850	5,616,815,700

Exchange rate: $1=N150, subject to economic review

Table 10. Specific speed of the homologous turbine performance.

Parameters	Reference case	Case 1	Case 2
Specific speed (metric units)	759.0	806.5	862.2
Alternator output power (kVA)	9.80	11.40	13.00

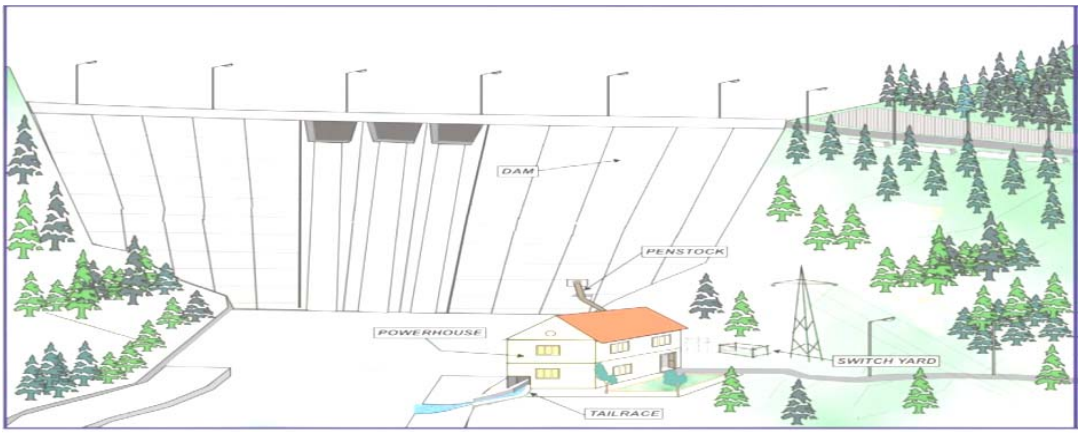

Fig. 1. Schematic of typical SHP scheme (Source: Singal *et al*., 2010**)**

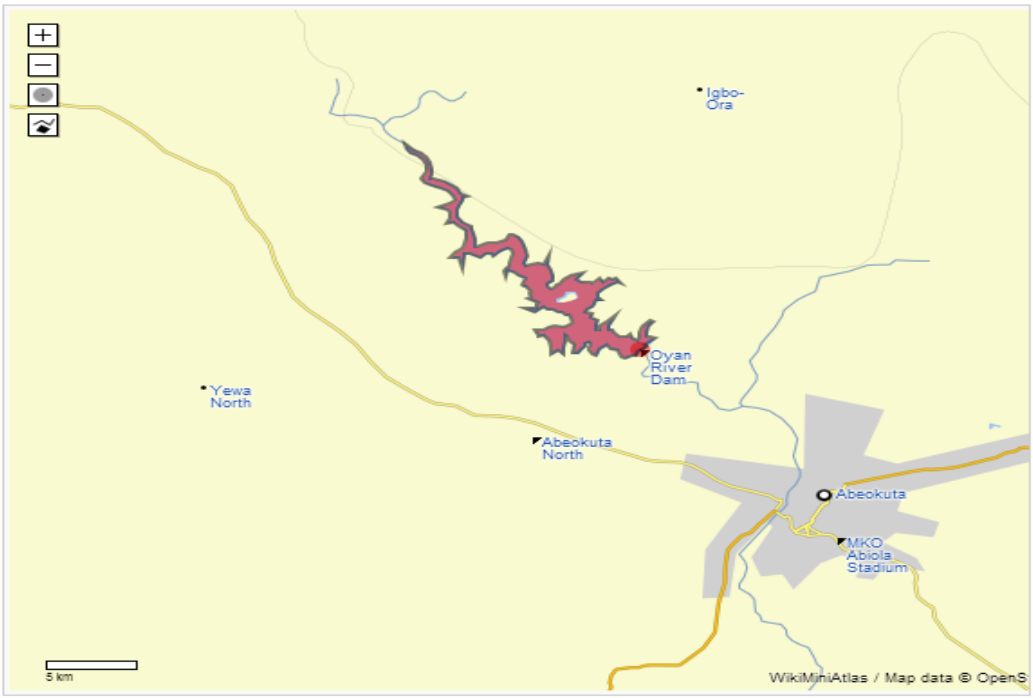

Fig. 2. Geographical view of the Oyan River Dam (Source: http://tools.wmflabs.org/geohack/geohack.php?pagename=Oyan_River_Dam&params=7_15_30_N_3_15_20_E_type:landmark)

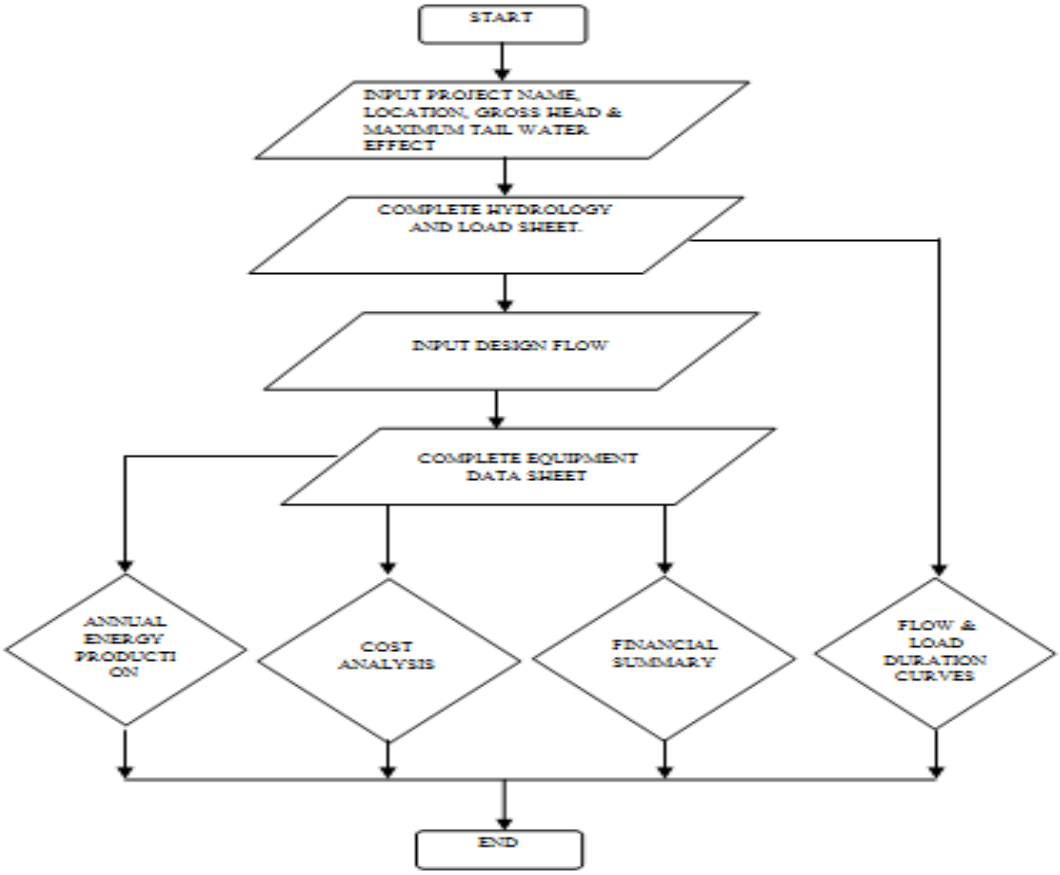

Fig. 3. Retscreen Analysis Flowchart.

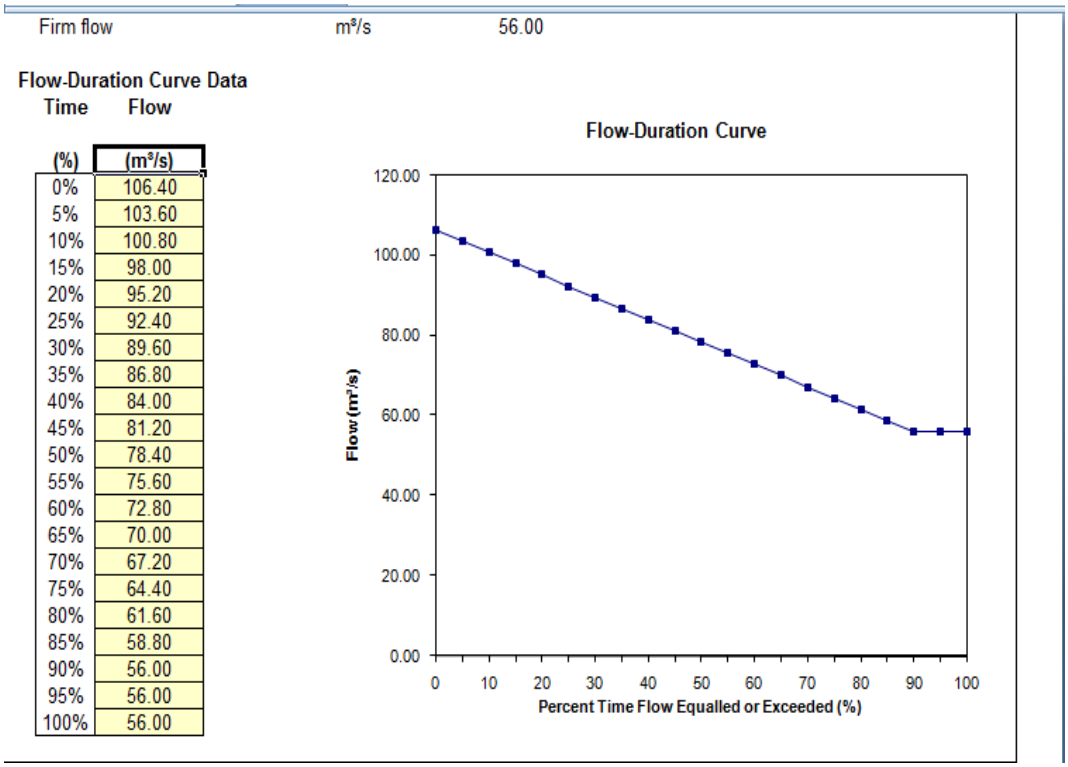

Firm flow m³/s 56.00

Flow-Duration Curve Data

Time (%)	Flow (m³/s)
0%	106.40
5%	103.60
10%	100.80
15%	98.00
20%	95.20
25%	92.40
30%	89.60
35%	86.80
40%	84.00
45%	81.20
50%	78.40
55%	75.60
60%	72.80
65%	70.00
70%	67.20
75%	64.40
80%	61.60
85%	58.80
90%	56.00
95%	56.00
100%	56.00

Fig 4. Hydrological Analysis for Oyan Dam.

Load-Duration Curve Data

Time (%)	Load (kW)
0%	10 547
5%	8 932
10%	8 476
15%	8 145
20%	7 850
25%	7 565
30%	7 280
35%	7 031
40%	6 792
45%	6 507
50%	6 221
55%	5 909
60%	5 632
65%	5 402
70%	5 209
75%	5 034
80%	4 786
85%	4 491
90%	4 095
95%	3 635
100%	3 083

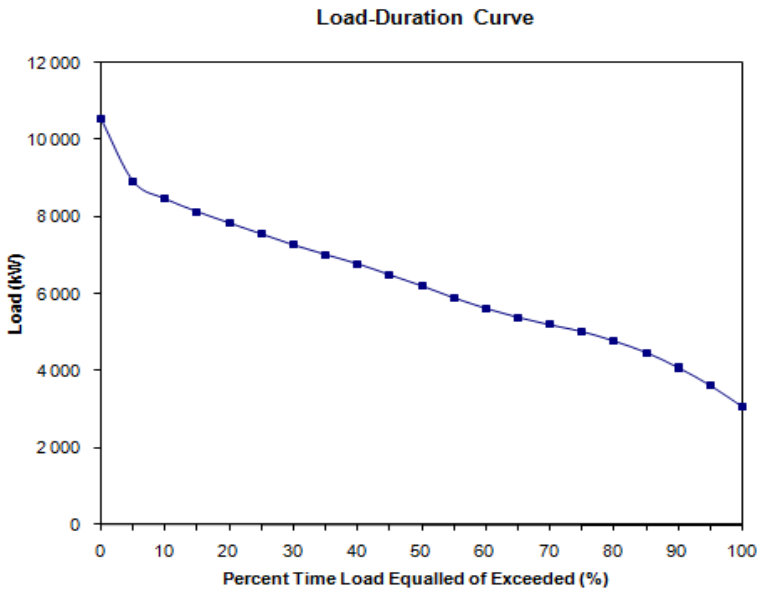

Fig. 5. Load Duration Curve for 10 MW with an Average Load Factor of 60%.

Load-Duration Curve Data

Time (%)	Load (kW)
0%	11 032
5%	9 343
10%	8 866
15%	8 519
20%	8 211
25%	7 913
30%	7 615
35%	7 355
40%	7 104
45%	6 806
50%	6 508
55%	6 180
60%	5 891
65%	5 651
70%	5 449
75%	5 266
80%	5 006
85%	4 698
90%	4 284
95%	3 802
100%	3 225

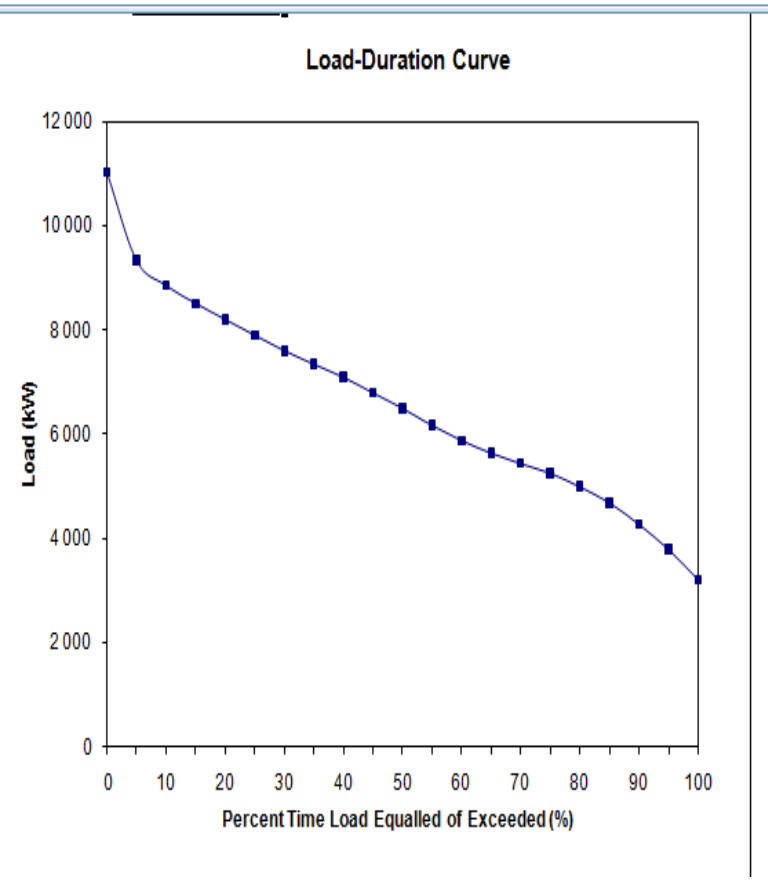

Fig. 6. Load Duration Curve for 12MW with an Average Load Factor of 60%.

ACKNOWLEDGMENT

The support provided by the Ogun-Osun River Basin Port Authority, Ogun State, Nigeria for the completion of the present work is gratefully acknowledged.

REFERENCES

Energy Commission of Nigeria (ECN). 2004. Guide book on Small Hydropower Development in Nigeria: Planning, Policy and Finance Issues. 55-94.

Forouzbakhsh, F., Hosseini, SMH. and Vakilian, M. 2007. An approach to the investment analysis of small and medium hydropower plants. Energy Policy. 35:1013-1024.

Gupta, BR. 2008. Generation of electrical energy: Energy Audit. (6^{th} edi.). India.

European Small Hydro Association (ESHA). 2005. Accessed online from www.esha.be, Available at: http://www.esha.be/fileadmin/esha_files/documents/publications/publications/BlueAGE.pdf

India's Electricity Sector. 1998. Widening Scope for Private Participation, Ministry of Power, Government of India, India. Accessed on 29 March 2013.

Jacobs Consultancy. 2012. Jacobs Consultancy Energy Optimization. Available online at: http://www.jacobsconsultancy.com/consultancy.asp?id=5532. Accessed on 29 March 2013.

Maldonado, OA., Panunzio, PA., Silva, DF. and Silveira, JL. 2004. Technique-economical viability of repowering of small hydroelectric power plant considering the social insert and environmental preservation. Departamento de Engenharia Elétrica, Universidade Estadual Paulista, Brasil. 333.

Ohunakin, OS., Ojolo, SJ. and Ajayi, OO. 2011. Small hydropower (SHP) development in Nigeria: An assessment. Renewable and Sustainable Energy Reviews. 15:2006-2013.

Ohunakin, OS. and Akinnawonu, OO. 2012. Assessment of wind energy potential and the economics of wind power generation in Jos, Plateau State, Nigeria. Energy for Sustainable Development. 16:78-83.

Penstock. Available online at: http://en.wikipedia.org/wiki/Penstock. Accessed on 29 April 2014.

Raghuvanshi, CS. 1995. Management and Organization of Irrigation System. Atlantic Publishers and Distributors. New Delhi, India.

Sepulveda, JA., Souder, WE. and Gottfried, BS. 1984. Schaum's Outline of Theory and Problems of Engineering Economics. Schaum's Outline Series Mcgraw-Hill.

Singal, SK., Saini, RP. and Raghuvanshi, CS. 2008. Cost Optimization Based on Electro-mechanical Equipment of Canal Based Low Head Small Hydropower Scheme. The Open Renewable Energy Journal. 26-35.

Singal, SK., Saini, RP. and Raghuvanshi, CS. 2010. Optimization of low-head, dam-toe, small hydropower projects. Journal of Renewable and Sustainable Energy. 043109:1-13.

Small Hydro Energy Efficient Promotion Campaign Action (SHERPA). 2006. Hydropower and Environment: Technical and Operational Procedures to better integrate Small Hydropower plants in the Environment. Available online at: http://www.esha.be/fileadmin/esha_files/documents/sherpa/annex_II_environmental_report.pdf. Accessed on 29 March 2013.

Tailrace. Available online at: http://en.wiktionary.org/wiki/tailrace. Accessed on 29 April 2014.

Received: May 30, 2014; Revised and accepted Aug 22, 2014

SENRA Academic Publishers, British Columbia
Vol. 8, No. 3, pp. 3115-3123, October 2014
Online ISSN: 1920-3853; Print ISSN: 1715-9997

Canadian Journal of pure&applied sciences

NEW INFORMATION THEORETIC MODELS, THEIR DETAILED PROPERTIES AND NEW INEQUALITIES

*Om Parkash[1] and Priyanka Kakkar[2]
[1]Department of Mathematics, Guru Nanak Dev University, Amritsar- 143005
[2]Department of Mathematics, Guru Nanak Dev University, Amritsar- 143005, India

ABSTRACT

New parametric models concerning measures of information including entropy, joint entropy, conditional entropy, directed divergence and inaccuracy have been introduced and their detailed properties have been studied. A new concept to be called alpha logarithm has been introduced and the chain rule for entropy, alpha mutual entropy and directed divergence has been studied. More desirable properties known as subadditivity and strong subadditivity of the entropy function have been studied and certain new inequalities useful in the literature of information theory has been derived.

Keywords: Entropy, directed divergence, inaccuracy, concavity, convexity.

INTRODUCTION

The notion of disorder or chaos, uncertainty or randomness, also known as entropy, was introduced by Clausius in the 19th century in thermodynamics- an integral part of Boltzmann's theory. Subsequently, the probabilistic nature of the concept emerged more clearly with Gibbs work on statistical mechanics. It was one of Shannon's (1948) great insights that entropy could be used as a measure of information content and one's freedom of choice when one selects a message to be communicated over a noisy or noiseless channel. Shannon also stressed the importance of the relative entropy, also known as directed divergence as a measure of redundancy which provides a comparison between two probabilistic systems and typically measures the actual entropy to the maximal possible entropy. This relative entropy played a key role in many of the later discoveries and applications in a various disciplines of mathematical sciences.

Shannon (1948) proposed the first most important and the simplest measure of additive entropy of a probability distribution $P = (p_1, p_2, ..., p_n)$, given by

$$H(P) = -\sum_{i=1}^{n} p_i \log p_i \ , \qquad (1.1)$$

with the convention that $0 \log 0 := 0$. Kullback and Leibler (1951) introduced the most important and desirable measure of divergence associated with the probability distributions $P = (p_1, p_2, ..., p_n)$ and $Q = (q_1, q_2, ..., q_n)$, given by

$$D(P:Q) = \sum_{i=1}^{n} p_i \log \frac{p_i}{q_i} \ . \qquad (1.2)$$

Another different concept in information theory is the measure of inaccuracy which was introduced by Kerridge (1961) and which connects the above mentioned two measures mathematically. This concept is basically associated with two probability distributions $P = (p_1, p_2, ..., p_n)$ and $Q = (q_1, q_2, ..., q_n)$ where Q is predicted and P is true probability distribution and this measure of inaccuracy is given by

$$I(P:Q) = \sum_{i=1}^{n} p_i \log q_i \ . \qquad (1.3)$$

The above mentioned measures have very nice mathematical properties and have tremendous applications in a variety of disciplines dealing with mathematical sciences. In spite of the fact that these measures are fundamental, we may face problems if we stick to these measures only because of their inadequacy towards applicability in every situation. An alternative is to use a generalized parametric measure of information where the parameter could hopefully be estimated from the data in the same way as ordinary statistical parameters are estimated from the data.

Many authors including Renyi (1961), Havrda Charvat (1967) and Tsallis (2009) introduced various generalized measures of information which are now increasingly used in many fields. Gupta and Bajaj (2013) studied the monotonic behaviour of the conditional Tsallis (2009) and Kapur (1967) entropies. Besenyei and Petz (2013) investigated a kind of partial subadditivity for Shannon and Tsallis entropy. Asgarani (2013) introduced a set of new three-parameter entropies which are expressed in terms of a generalized incomplete Gamma function and shown that for some special values of parameters, some known entropies are recovered. The uniqueness theorem for a two parameter extended relative entropy, that is, directed divergence is proved and its properties are studied by Furuichi (2010). Teixeira and Antunes (2012)

*Corresponding author email: omparkash777@yahoo.co.in

described three general definitions of conditional Renyi entropy and studied their properties and values as a function of parameter α. Bercher (2011) discussed the two families of two-parameter entropies and divergences, derived from the standard Renyi and Tsallis entropies and divergences. Furuichi and Mitroi (2012) introduced some parametric extended divergences combining J-divergence and Tsallis entropy defined by generalized logarithmic functions, which lead to new inequalities whereas several other inequalities on generalized entropies have been studied by Furuichi and Mitroi (2012).

The objective of the present study is to develop new information theoretic models and study their properties. The paper is organized as follows: In section 2, new measure of entropy to be called alpha entropy is introduced and its properties are studied. Section 3 deals with the new concept of alpha logarithm and provides the chain rule for alpha entropy and alpha mutual entropy by defining alpha joint entropy and alpha conditional entropy. Subadditivity and strong subadditivity property of entropy has been studied and various new inequalities has been derived. In section 4, new measure of directed divergence, its chain rule and new measure of inaccuracy is introduced.

2. New Measure of Entropy

In this section, we propose a new generalized measure of entropy for a probability distribution

$$P=\left\{\left(p_1, p_2, ..., p_n\right), p_i \geq 0, \sum_{i=1}^{n} p_i = 1\right\}$$

of the random variable $X=\left(x_1, x_2, ..., x_n\right)$ and studied its essential and desirable properties. This new entropy measure of order α to be called alpha entropy, is given by the following mathematical expression:

$$ {}_{\alpha}A\left(P\right)=\frac{\sum_{i=1}^{n} p_i \alpha^{\ln p_i}-1}{1-\alpha},\ \alpha>1, \qquad (2.1)$$

where ln(.) stands for the natural logarithm.

The expression (2.1) can also be written as

$$ {}_{\alpha}A\left(X\right)=\frac{\sum_{x} p\left(x\right) \alpha^{\ln p(x)}-1}{1-\alpha},\ \alpha>1.$$

The two notations $A_{\alpha}\left(X\right)$ and $A_{\alpha}\left(P\right)$ need not to be confused as they have the same meaning and will be used wherever required for simplicity.

Obviously, we have $\lim_{\alpha\to 1} {}_{\alpha}A\left(P\right)=-\sum_{i=1}^{n} p_i \ln p_i$.

Thus, $A_{\alpha}\left(P\right)$ is a generalization of well known Shannon (1948) entropy.

Next, to prove that ${}_{\alpha}A\left(P\right)$ is a valid measure of entropy, we study its essential and desirable properties as follows:

1. Obviously, ${}_{\alpha}A\left(P\right)\geq 0$.

2. ${}_{\alpha}A\left(P\right)$ is permutationally symmetric as it does not change if $p_1, p_2, p_3, ..., p_n$ are re-ordered among themselves.

3. ${}_{\alpha}A\left(P\right)$ is a continuous function of p_i for all p_i's.

4. **Concavity:** The Hessian matrix of second order partial derivatives of ${}_{\alpha}A\left(P\right)$ with respect to $p_1, p_2, \ldots, p_n$ is given by

$$\begin{bmatrix} \frac{\alpha^{\ln p_1}\left(1+\ln\alpha\right)\ln\alpha}{p_1\left(1-\alpha\right)} & 0 & \cdots & 0 \\ 0 & \frac{\alpha^{\ln p_2}\left(1+\ln\alpha\right)\ln\alpha}{p_2\left(1-\alpha\right)} & \cdots & 0 \\ \vdots & \vdots & \cdots & \vdots \\ 0 & 0 & \cdots & \frac{\alpha^{\ln p_n}\left(1+\ln\alpha\right)\ln\alpha}{p_n\left(1-\alpha\right)} \end{bmatrix},$$

which is negative definite.

Thus, ${}_{\alpha}A\left(P\right)$ is a concave function of p_i for all p_i's.

5. **Expansibility:** We have

${}_{\alpha}A\left(p_1, p_2, p_3, ..., p_n, 0\right)= {}_{\alpha}A\left(p_1, p_2, p_3, ..., p_n\right)$.

That is, the entropy does not change by the inclusion of an impossible event.

6. For degenerate distributions, ${}_{\alpha}A\left(P\right)=0$.

This indicates that for certain outcomes, the uncertainty should be zero.

7. Maximization of entropy: We use Lagrange's method to maximize the entropy measure (2.1) subject to the natural constraint $\sum_{i=1}^{n} p_i = 1$.

In this case, the corresponding Lagrangian is

$$L\equiv\frac{\sum_{i=1}^{n} p_i \alpha^{\ln p_i}-1}{1-\alpha}+\lambda\left(1-\sum_{i=1}^{n} p_i\right). \qquad (2.2)$$

Differentiating equation (2.2) with respect to p_i, $i=1,2,...,n$ and equating the derivatives to zero, we get

$p_i = e^{\log_{\alpha}\left(\frac{\lambda(1-\alpha)}{1+\ln\alpha}\right)},\ i=1,2,..,n$.

Using $\sum_{i=1}^{n} p_i = 1$, we get $e^{\log_{\alpha}\left(\frac{\lambda(1-\alpha)}{1+\ln\alpha}\right)}=\frac{1}{n}$,

that is, $p_i=\frac{1}{n},\ i=1,2,..,n$.

Now $\left(\frac{\partial^2 L}{\partial p_i^{\,2}}\right)_{p_i=\frac{1}{n}} = \frac{n\alpha^{-\ln n}(1+\ln\alpha)}{(1-\alpha)} < 0$ for every i.

Thus, we observe that the maximum value of ${}_\alpha A(P)$ arises for the uniform distribution and this result is most desirable.

8. The maximum value of the entropy is given by

${}_\alpha A\left(\frac{1}{n},\frac{1}{n},...,\frac{1}{n}\right) = \frac{\alpha^{-\ln n}-1}{1-\alpha}$.

Also, ${}_\alpha A'\left(\frac{1}{n},\frac{1}{n},...,\frac{1}{n}\right) = \frac{\alpha^{-\ln n}\ln\alpha}{n(\alpha-1)} > 0$,

which shows that ${}_\alpha A\left(\frac{1}{n},\frac{1}{n},...,\frac{1}{n}\right)$ is an increasing function of n, which is again a desirable result as the maximum value of an entropy should always increase.

9. Non-Additive property:

Let $P=(p_1,p_2,...,p_n)$ and $Q=(q_1,q_2,...,q_m)$ be two independent probability distributions of two random variables X and Y, so that

$P(X=x_i)=p_i$, $P(Y=y_j)=q_j$

$P(X=x_i,Y=y_j)=P(X=x_i)P(Y=y_j)=p_iq_j$.

For the joint distributions of X and Y, there are nm possible outcomes with probabilities p_iq_j; $i=1,2,...,n$ and $j=1,2,...,m$, so that the entropy of the joint probability distribution, denoted by $P*Q$, is given by

$$ {}_\alpha A(P*Q) = \frac{\sum_{i=1}^{n}\sum_{j=1}^{m} p_iq_j\alpha^{\ln p_iq_j}-1}{1-\alpha} = \frac{\sum_{i=1}^{n} p_i\alpha^{\ln p_i}\sum_{j=1}^{m} q_j\alpha^{\ln q_j}-1}{1-\alpha}. \quad (2.3)$$

Also, ${}_\alpha A(P)+{}_\alpha A(Q)+(1-\alpha)\,{}_\alpha A(P)\,{}_\alpha A(Q)$

$$ = \frac{\sum_{i=1}^{n} p_i\alpha^{\ln p_i}\sum_{j=1}^{m} q_j\alpha^{\ln q_j}-1}{1-\alpha}. \quad (2.4)$$

From (2.3) and (2.4), we have

${}_\alpha A(P*Q) = {}_\alpha A(P)+{}_\alpha A(Q)+(1-\alpha)\,{}_\alpha A(P)\,{}_\alpha A(Q)$.

So, measure of entropy ${}_\alpha A(P)$ is non-additive.

Thus, we claim that the new measure of entropy of order α introduced in (2.1) satisfies all the essential as well as desirable properties of being an entropy measure, it is a new generalized measure of entropy.

3 Alpha Logarithm-New Concepts

Let us introduce a new function to be called alpha logarithm given by

$$ \ln_\alpha x \equiv \frac{\alpha^{\ln x}-1}{\alpha-1},\ \alpha\neq 1, \quad (3.1)$$

for any non-negative real number x and α.

For $\alpha\to 1$, alpha logarithm tends to natural logarithm, that is, $\lim_{\alpha\to 1}\ln_\alpha x = \ln x$.

Its inverse is the alpha exponential function given by

$$ e_\alpha^x \equiv \left(1+(\alpha-1)x\right)^{\frac{1}{\ln\alpha}}. \quad (3.2)$$

For $\alpha\to 1$, alpha exponential tends to exponential function, that is, $\lim_{\alpha\to 1} e_\alpha^x = e^x$.

Now, let us state some results related to function (3.1) and (3.2)

1. $\ln_\alpha(xy) = \ln_\alpha x+\ln_\alpha y+(\alpha-1)\ln_\alpha x\,\ln_\alpha y$ (3.3)

2. $\ln_\alpha(xy) = \ln_\alpha x+\alpha^{\ln x}\ln_\alpha y$. (3.4)

3. $\ln_\alpha\left(\frac{1}{x}\right) = -\alpha^{-\ln x}\ln_\alpha x$. (3.5)

4. $e_\alpha^{x+y+(\alpha-1)xy} = e_\alpha^x e_\alpha^y$. (3.6)

Alpha entropy can be written as the alpha logarithm Shannon entropy in the following way:

$$ {}_\alpha A(P) = -\sum_{i=1}^{n} p_i\ln_\alpha p_i,\ \alpha>1. \quad (3.7)$$

Using result (3.5), (3.7) can further be written as

$$ {}_\alpha A(P) = \sum_{i=1}^{n} p_i\alpha^{\ln p_i}\ln_\alpha\frac{1}{p_i},\ \alpha>1. \quad (3.8)$$

Now, let us introduce the alpha joint entropy and alpha conditional entropy by means of following definitions:

Definition 3.1 For the conditional probability $p(x|y)=p(X=x|Y=y)$, we define alpha conditional entropy as

$$ {}_\alpha A(X|Y) = \sum_x\sum_y p(x,y)\alpha^{\ln p(x,y)}\ln_\alpha\frac{1}{p(x|y)},\ \alpha>1. \quad (3.9)$$

Definition 3.2 For the joint probability $p(x,y)=p(X=x,Y=y)$, we define alpha joint entropy as

$$ {}_\alpha A(X,Y) = \sum_x\sum_y p(x,y)\alpha^{\ln p(x,y)}\ln_\alpha\frac{1}{p(x,y)},\ \alpha>1 \quad (3.10)$$

or

$$ {}_\alpha A(X,Y) = \sum_x\sum_y\frac{p(x,y)\alpha^{\ln p(x,y)}-1}{1-\alpha},\ \alpha>1 \quad (3.11)$$

or

$$ {}_{\alpha}A(X,Y) = -\sum_x \sum_y p(x,y) \ln_{\alpha} p(x,y), \ \alpha > 1. \quad (3.12) $$

3.1 Chain rules for alpha entropy

Now, let us study the chain rule for alpha entropy given by means of following theorem:

Theorem 3.1 For the two random variables X and Y, we have

$$ {}_{\alpha}A(X,Y) = {}_{\alpha}A(X) + {}_{\alpha}A(Y|X), \ \alpha > 1. \quad (3.1.1) $$

Proof: Using $p(x,y) = p(y|x)\,p(x)$ and result (3.4), we have

$$ {}_{\alpha}A(X,Y) = \sum_x \sum_y p(x,y)\, \alpha^{\ln p(x,y)} \ln_{\alpha} \frac{1}{p(x,y)} $$

$$ = \sum_x \sum_y p(x,y)\, \alpha^{\ln p(x,y)} \ln_{\alpha} \frac{1}{p(y|x)} + \sum_x \sum_y p(x,y)\, \alpha^{\ln p(x)} \ln_{\alpha} \frac{1}{p(x)} $$

$$ = {}_{\alpha}A(Y|X) + {}_{\alpha}A(X). $$

Note: If X and Y are independent, that is, $p(y|x) = p(y)$ for all x and y, then from Theorem 3.1, we have the following pseudo-additivity:

$$ {}_{\alpha}A(X,Y) = {}_{\alpha}A(X) + {}_{\alpha}A(Y) + (1-\alpha)\, {}_{\alpha}A(X)\, {}_{\alpha}A(Y) $$

Theorem 3.2 The following chain rules hold:

$$ (1)\ {}_{\alpha}A(X,Y,Z) = {}_{\alpha}A(X,Y|Z) + {}_{\alpha}A(Z). \quad (3.1.2) $$

$$ (2)\ {}_{\alpha}A(X,Y|Z) = {}_{\alpha}A(X|Z) + {}_{\alpha}A(Y|X,Z) \quad (3.1.3) $$

Proof(1):

$$ {}_{\alpha}A(X,Y|Z) = \sum_x \sum_y \sum_z p(x,y,z)\, \alpha^{\ln p(x,y,z)} \ln_{\alpha} \frac{1}{p(x,y|z)} $$

$$ = \frac{1}{\alpha - 1} \sum_x \sum_y \sum_z p(x,y,z) \left(\alpha^{\ln \frac{p(x,y,z)}{p(x,y|z)}} - \alpha^{\ln p(x,y,z)} \right) $$

$$ = \frac{1}{\alpha - 1} \left(\sum_x \sum_y \sum_z p(x,y,z)\, \alpha^{\ln p(z)} - 1 \right) + \frac{1}{1-\alpha} \left(\sum_x \sum_y \sum_z p(x,y,z)\, \alpha^{\ln p(x,y,z)} - 1 \right) $$

$$ = -{}_{\alpha}A(Z) + {}_{\alpha}A(X,Y,Z) $$

that is, ${}_{\alpha}A(X,Y,Z) = {}_{\alpha}A(X,Y|Z) + {}_{\alpha}A(Z)$.

(2) On similar lines as proved in part (1), we have

$$ {}_{\alpha}A(Y|X,Z) = {}_{\alpha}A(X,Y,Z) - {}_{\alpha}A(X,Z). \quad (3.1.4) $$

Also, from (3.1.1), we have

$$ {}_{\alpha}A(X,Y) = {}_{\alpha}A(X) + {}_{\alpha}A(Y|X). \quad (3.1.5) $$

Therefore, equation (3.1.4) can further be written as

$$ {}_{\alpha}A(Y|X,Z) = {}_{\alpha}A(X,Y|Z) + {}_{\alpha}A(Z) - \left({}_{\alpha}A(Z) + {}_{\alpha}A(X|Z) \right) $$

that is, ${}_{\alpha}A(Y|X,Z) = {}_{\alpha}A(X,Y|Z) - {}_{\alpha}A(X|Z)$ which proves (3.1.3).

Remark 1. From (3.1.3), we have

$$ {}_{\alpha}A(X|Z) \le {}_{\alpha}A(X,Y|Z). $$

2. The part (2) of Theorem 3.2 can further be generalized in the following way:

$$ {}_{\alpha}A(X_1, X_2, ..., X_n|Y) = \sum_{i=1}^{n} {}_{\alpha}A(X_i|X_{i-1}, ..., X_1, Y). $$

Theorem 3.3 Let $X_1, X_2, ..., X_n$ be the random variables .Then we have the following chain rule:

$$ {}_{\alpha}A(X_1, X_2, ..., X_n) = \sum_{i=1}^{n} {}_{\alpha}A(X_i|X_{i-1}, ..., X_1) \quad (3.1.6) $$

Proof: We prove the theorem by induction on n. From Theorem 3.1, we have

$$ {}_{\alpha}A(X_1, X_2) = {}_{\alpha}A(X_1) + {}_{\alpha}A(X_2|X_1). $$

Let us assume that the result (3.1.6) is true for some n. From (3.1.1), we have

$$ {}_{\alpha}A(X_1, X_2, ..., X_{n+1}) = {}_{\alpha}A(X_1, X_2, ..., X_n) + {}_{\alpha}A(X_{n+1}|X_n, ..., X_1) $$

$$ = \sum_{i=1}^{n} {}_{\alpha}A(X_i|X_{i-1}, ..., X_1) + {}_{\alpha}A(X_{n+1}|X_n, ..., X_1), $$

which shows that (3.1.6) holds for $n+1$.

3.2 Subadditivities for alpha entropy

Theorem 3.4 Let X and Y be two random variables, then we have

$$ {}_{\alpha}A(X|Y) \le {}_{\alpha}A(X), \ \alpha > 1, \quad (3.2.1) $$

with equality if and only if $\alpha = 1$ and $p(x|y) = p(x)$ for all x and y.

Proof: Let $f(x) = \dfrac{x\alpha^{\ln x} - x}{1-\alpha}$, $\alpha > 1$.

This function is concave function of x. So, by concavity of $f(x)$, we have

$$ \sum_y p(y)\, f\left(p(x|y)\right) \le f\left(\sum_y p(y)\, p(x|y) \right) \quad (3.2.2) $$

Taking summation on x on both sides of (3.2.2), we get

$$ \sum_y p(y) \sum_x f\left(p(x|y)\right) \le \sum_x f\left(p(x)\right) $$

$$\Rightarrow \frac{\sum_y \sum_x p(x,y)\alpha^{\ln p(x|y)} - \sum_x \sum_y p(x,y)}{1-\alpha} \le \frac{\sum_x p(x)\alpha^{\ln p(x)} - 1}{1-\alpha},$$

that is,

$$\frac{\sum_y \sum_x p(x,y)\alpha^{\ln p(x|y)} - 1}{1-\alpha} \le \frac{\sum_x p(x)\alpha^{\ln p(x)} - 1}{1-\alpha} \quad (3.2.3)$$

Since $p(y)\alpha^{\ln p(y)} \le p(y)$ and $f(x) \ge 0$ for any $x > 0$, we have

$$p(y)\alpha^{\ln p(y)} \sum_x f\left(p(x|y)\right) \le p(y) \sum_x f\left(p(x|y)\right) \quad (3.2.4)$$

Taking summation on y on both sides of (3.2.4), we get

$$\sum_y p(y)\alpha^{\ln p(y)} \sum_x f\left(p(x|y)\right) \le \sum_y p(y) \sum_x f\left(p(x|y)\right)$$

$$\Rightarrow \sum_y \sum_x p(x,y)\alpha^{\ln p(x,y)} \ln_\alpha \frac{1}{p(x|y)} \le \frac{\sum_y \sum_x p(x,y)\alpha^{\ln p(x|y)} - 1}{1-\alpha} \quad (3.2.5)$$

From (3.2.3) and (3.2.5), we have

$$\sum_y \sum_x p(x,y)\alpha^{\ln p(x,y)} \ln_\alpha \frac{1}{p(x|y)} \le \frac{\sum_x p(x)\alpha^{\ln p(x)} - 1}{1-\alpha}$$

that is, ${}_\alpha A(X|Y) \le {}_\alpha A(X)$.

The equality holds when $\alpha = 1$ and $p(x|y) = p(x)$, that is, when X and Y are independent.

Theorem 3.5 Alpha entropy is sub-additive, that is,

$${}_\alpha A(X,Y) \le {}_\alpha A(X) + {}_\alpha A(Y). \quad (3.2.6)$$

Proof: The proof follows directly from Theorem 3.1 and Theorem 3.4.

Theorem 3.6 For the random variables $X_1, X_2, ..., X_n$, we have

$${}_\alpha A(X_1, X_2, ..., X_n) \le \sum_{i=1}^{n} {}_\alpha A(X_i), \quad (3.2.7)$$

with equality if and only if $\alpha = 1$ and the random variables are independent of each other.

Proof: The proof follows directly by making use of Theorem 3.3 and Theorem 3.4.

Theorem 3.7 For the random variables X, Y, Z with probabilities $p(X = x) = p(x)$, $p(Y = y) = p(y)$, $p(Z = z) = p(z)$ respectively and joint probability $p(x, y, z)$, strong subadditivity

$${}_\alpha A(X,Y,Z) + {}_\alpha A(Z) \le {}_\alpha A(X,Z) + {}_\alpha A(Y,Z) \quad (3.2.8)$$

holds with equality if and only if $\alpha = 1$ and the random variables X and Y are independent for a given random variable Z, that is, when $p(x|y,z) = p(x|z)$.

Proof: By making use of concavity of function $f(x)$ as defined in Theorem 3.4, we have

$$\sum_y p(y|z) f\left(p(x|y,z)\right) \le f\left(\sum_y p(y|z) p(x|y,z)\right)$$

$$\Rightarrow \sum_y p(y|z) f\left(p(x|y,z)\right) \le f\left(p(x|z)\right).$$

Multiply both sides of above inequality by $p(z)\alpha^{\ln p(z)}$ and taking the summation on z and x, we have

$$\sum_{z,x} p(z)\alpha^{\ln p(z)} \sum_y p(y|z) f\left(p(x|y,z)\right) \le \sum_{z,x} p(z)\alpha^{\ln p(z)} f\left(p(x|z)\right) \quad (3.2.9)$$

Now, $0 \le p(y|z) \le 1$

$$\Rightarrow p(y|z)\alpha^{\ln p(y|z)} \le p(y|z). \quad (3.2.10)$$

So, using the non-negativity of the function $f(x)$ and inequality (3.2.10), we have

$$p(y|z)\alpha^{\ln p(y|z)} \sum_x f\left(p(x|y,z)\right) \le p(y|z) \sum_x f\left(p(x|y,z)\right)$$

for any y, z.

Multiply both sides of above inequality by $p(z)\alpha^{\ln p(z)}$ and then taking the summation on y and z, we have

$$\sum_{y,z} p(z)\alpha^{\ln p(z)} p(y|z)\alpha^{\ln p(y|z)} \sum_x f\left(p(x|y,z)\right) \le \sum_{y,z} p(z)\alpha^{\ln p(z)} p(y|z) \sum_x f\left(p(x|y,z)\right)$$

$$\Rightarrow \sum_{y,z} p(y,z)\alpha^{\ln p(y,z)} \sum_x f\left(p(x|y,z)\right) \le \sum_{y,z} p(z)\alpha^{\ln p(z)} p(y|z) \sum_x f\left(p(x|y,z)\right) \quad (3.2.11)$$

From (3.2.9) and (3.2.11), we have

$$\sum_{y,z} p(y,z)\alpha^{\ln p(y,z)} \sum_x f\left(p(x|y,z)\right) \le \sum_{z,x} p(z)\alpha^{\ln p(z)} f\left(p(x|z)\right)$$

$$\Rightarrow \sum_{x,y,z} p(x,y,z)\alpha^{\ln p(x,y,z)} \ln_\alpha \frac{1}{p(x|y,z)} \le \sum_{x,z} p(x,z)\alpha^{\ln p(x,z)} \ln_\alpha \frac{1}{p(x|z)}$$

that is, ${}_\alpha A(X|Y,Z) \le {}_\alpha A(X|Z)$ (3.2.12)

$\Rightarrow {}_{\alpha}A(X,Y,Z) - {}_{\alpha}A(Y,Z) \le {}_{\alpha}A(X,Z) - {}_{\alpha}A(Z)$.
(Using Theorem 3.1)

The equality holds when $\alpha = 1$ and the random variables X and Y are independent for a given random variable Z, that is, when $p(x|y,z) = p(x|z)$.

Note: Inequality (3.2.6) can be recovered from inequality (3.2.8) by treating the random variable Z as a trivial one which proves that Theorem 3.7 is a generalization of Theorem 3.5.

The more generalized form of Theorem 3.7 is as follows:

Theorem 3.8 For the random variables $X_1, X_2, ..., X_n$, we have

$${}_{\alpha}A(X_{n+1}|X_1, X_2, ..., X_n) \le {}_{\alpha}A(X_{n+1}|X_2, ..., X_n). \quad (3.2.13)$$

Proof: The proof is on similar lines as in Theorem 3.7.

Theorem 3.9 For the random variables X, Y, Z, we have

$${}_{\alpha}A(X,Y|Z) \le {}_{\alpha}A(X|Z) + {}_{\alpha}A(Y|Z). \quad (3.2.14)$$

Proof: Adding $-2\,{}_{\alpha}A(Z)$ to both sides of inequality (3.2.8), we have

${}_{\alpha}A(X,Y,Z) - {}_{\alpha}A(Z) \le {}_{\alpha}A(X,Z) - {}_{\alpha}A(Z) + {}_{\alpha}A(Y,Z) - {}_{\alpha}A(Z)$

By making use of Theorem 3.1 in above inequality, we have result (3.2.14).

Above theorem can be generalized in the following way:

Theorem 3.10 For the random variables $X_1, X_2, ..., X_n, Z$, we have

$${}_{\alpha}A(X_1, X_2, ..., X_n|Z) \le {}_{\alpha}A(X_1|Z) + {}_{\alpha}A(X_2|Z) + ... + {}_{\alpha}A(X_n|Z) \quad (3.2.15)$$

Proof: The above result can be proved with the help of mathematical induction.

Theorem 3.11 For the random variables X, Y, Z, we have

$$2\,{}_{\alpha}A(X,Y,Z) \le {}_{\alpha}A(X,Y) + {}_{\alpha}A(Y,Z) + {}_{\alpha}A(Z,X). \quad (3.2.16)$$

Proof: From equation (3.2.12), we have

$${}_{\alpha}A(X|Y,Z) \le {}_{\alpha}A(X|Z). \quad (3.2.17)$$

From equation (3.2.1), we have

$${}_{\alpha}A(X|Z) \le {}_{\alpha}A(X). \quad (3.2.18)$$

So, (3.2.17) and (3.2.18) gives

$${}_{\alpha}A(X|Y,Z) \le {}_{\alpha}A(X). \quad (3.2.19)$$

Again from equation (3.2.12), we have

$${}_{\alpha}A(Z|X,Y) \le {}_{\alpha}A(Z|X). \quad (3.2.20)$$

Adding equation (3.2.19) and (3.2.20), we have

$${}_{\alpha}A(Z|X,Y) + {}_{\alpha}A(X|Y,Z) \le {}_{\alpha}A(Z|X) + {}_{\alpha}A(X) \quad (3.2.21)$$

Applying chain rule in (3.2.21), we have

${}_{\alpha}A(X,Y,Z) - {}_{\alpha}A(X,Y) + {}_{\alpha}A(X,Y,Z) - {}_{\alpha}A(Y,Z) \le {}_{\alpha}A(Z,X)$
which proves the theorem.

Theorem 3.12 For the random variables $X_1, X_2, ..., X_n$, we have

$${}_{\alpha}A(X_n|X_1) \le {}_{\alpha}A(X_2|X_1) + {}_{\alpha}A(X_3|X_2) + ... + {}_{\alpha}A(X_n|X_{n-1}) \quad (3.2.22)$$

Proof: From equation (3.1.6), we have

$${}_{\alpha}A(X_1, X_2, ..., X_n) = \sum_{i=1}^{n} {}_{\alpha}A(X_i|X_{i-1}, ..., X_1),$$

that is,

$${}_{\alpha}A(X_1, X_2, ..., X_n) = {}_{\alpha}A(X_1) + {}_{\alpha}A(X_2|X_1) + {}_{\alpha}A(X_3|X_2, X_1) + ... + {}_{\alpha}A(X_n|X_{n-1}, ..., X_1) \quad (3.2.23)$$

Using equation (3.2.12) in (3.2.23), we have

$${}_{\alpha}A(X_1, X_2, ..., X_n) \le {}_{\alpha}A(X_1) + {}_{\alpha}A(X_2|X_1) + {}_{\alpha}A(X_3|X_2) + ... + {}_{\alpha}A(X_n|X_{n-1}) \quad (3.2.24)$$

From the generalization of part (2) of Theorem 3.2, we have

$${}_{\alpha}A(X_n|X_1) \le_{\alpha} A(X_2, ..., X_n|X_1) = {}_{\alpha}A(X_1, ..., X_n) - {}_{\alpha}A(X_1)$$

(Using Theorem 3.1)

$$\le {}_{\alpha}A(X_2|X_1) + {}_{\alpha}A(X_3|X_2) + ... + {}_{\alpha}A(X_n|X_{n-1}),$$

which proves the theorem.

3.3 Alpha Mutual entropy

Alpha mutual entropy for the two random variables X and Y is defined as the difference between alpha entropy and alpha conditional entropy and is given by

$${}_{\alpha}I(X:Y) = {}_{\alpha}A(X) - {}_{\alpha}A(X|Y). \quad (3.3.1)$$

Also, alpha conditional mutual entropy for the three random variables X, Y, Z is given by

$${}_{\alpha}I(X:Y|Z) = {}_{\alpha}A(X|Z) - {}_{\alpha}A(X|Y,Z). \quad (3.3.2)$$

Theorem 3.13 (1) For the three random variables X, Y, Z, the following chain rule holds:

$${}_{\alpha}I(X:Y,Z) = {}_{\alpha}I(X:Z) + {}_{\alpha}I(X:Y|Z). \quad (3.3.3)$$

(2) For the random variables $X_1, X_2, ..., X_n$ and Y, the following chain rule holds:

$$ {}_{\alpha}I\left(X_1, X_2, ..., X_n : Z\right) = \sum_{i=1}^{n} {}_{\alpha}I\left(X_i : Y \middle| X_1, X_2, ..., X_{i-1}\right). \tag{3.3.4} $$

Proof: (1) We have

$$ \begin{aligned} {}_{\alpha}I\left(X : Y \middle| Z\right) &= {}_{\alpha}A\left(X \middle| Z\right) - {}_{\alpha}A\left(X \middle| Y, Z\right) \\ &= {}_{\alpha}A\left(X \middle| Z\right) - {}_{\alpha}A\left(X\right) + {}_{\alpha}A\left(X\right) - {}_{\alpha}A\left(X \middle| Y, Z\right) \\ &= -{}_{\alpha}I\left(X : Z\right) + {}_{\alpha}I\left(X : Y, Z\right), \end{aligned} $$

which proves the part (1).

(2) We have

$$ {}_{\alpha}I\left(X_1, X_2, ..., X_n : Z\right) = {}_{\alpha}A(X_1, X_2, ..., X_n) - {}_{\alpha}A(X_1, X_2, ..., X_n \middle| Y) $$

Using remark 2 and equation (3.18) in above equation, we have

$$ \begin{aligned} {}_{\alpha}I\left(X_1, X_2, ..., X_n : Z\right) &= \sum_{i=1}^{n} {}_{\alpha}A\left(X_i \middle| X_{i-1}, ..., X_1\right) \\ &\quad - \sum_{i=1}^{n} {}_{\alpha}A\left(X_i \middle| X_{i-1}, ..., X_1, Y\right) \\ &= \sum_{i=1}^{n} {}_{\alpha}I\left(X_i : Y \middle| X_1, X_2, ..., X_{i-1}\right), \end{aligned} $$

which proves part (2).

Note: Applications of inequalities

This is to be remarked that information theoretic inequalities play an important role in the theory of cryptography. To mention the fact, we consider Shannon's (1948) famous secret key cryptosystem model which consists of sender "S", a receiver "R", an eavesdropper "E", and an open channel from "S" to "R". The secret key Z is known to "S" and to "R" only whereas "S" encrypts the text X using Z according to the encryption rule which results in the cryptogram Y that is sent to "R" and can also be received by "E". "R" can recover X with his knowledge of Z. In the present model, a cipher is called perfect if and only if the text X and the cryptogram Y are independent random variables, that is, if and only if ${}_{\alpha}I\left(X, Y\right) = 0$ or equivalently, ${}_{\alpha}A\left(X\right) = {}_{\alpha}A\left(X \middle| Y\right)$ if we apply the parametric entropy introduced in section 2. "R" must be able to recover X uniquely from Y and Z, that is, ${}_{\alpha}A\left(X \middle| Y\, Z\right) = 0$.

Thus, applying this model, we have

$$ \begin{aligned} {}_{\alpha}A\left(X\right) &= {}_{\alpha}A\left(X \middle| Y\right) \\ &\le {}_{\alpha}A\left(XZ \middle| Y\right) \end{aligned} $$

(Using equation (3.1.3))

$$ \begin{aligned} &= {}_{\alpha}A\left(Z \middle| Y\right) + {}_{\alpha}A\left(X \middle| Y\, Z\right) \\ &= {}_{\alpha}A\left(Z \middle| Y\right) \\ &\le {}_{\alpha}A\left(Z\right) \end{aligned} $$

This inequality shows that the entropy of the secret key must be as large as the entropy of the text to be encrypted, and consequently provides a helpful tool for the removal of uncertainty to be removed.

4 New measures of Directed Divergence and Inaccuracy

4.1 Measure of directed divergence

We propose a new measure of divergence of probability distributions $P = (p_1, p_2, ..., p_n)$ from another probability distribution $Q = (q_1, q_2, ..., q_n)$ given by

$$ {}_{\alpha}D(P : Q) = \frac{\sum_{i=1}^{n} p_i \alpha^{\ln \frac{p_i}{q_i}} - 1}{\alpha - 1}, \ \alpha > 1. \tag{4.1.1} $$

This measure is to be called alpha directed divergence. The measure (4.1.1) can also be written in the following form:

$$ {}_{\alpha}D(P : Q) = \sum_{i=1}^{n} p_i \ln_{\alpha} \frac{p_i}{q_i}, \ \alpha > 1, \tag{4.1.2} $$

or

$$ {}_{\alpha}D(P : Q) = -\sum_{i=1}^{n} p_i \alpha^{\ln \frac{p_i}{q_i}} \ln_{\alpha} \frac{q_i}{p_i}, \ \alpha > 1. \tag{4.1.3} $$

Also, $\lim_{\alpha \to 1} {}_{\alpha}D(P : Q) = \sum_{i=1}^{n} p_i \ln \frac{p_i}{q_i}$,

which is Kullback-Leibler's (1951) measure of directed divergence.

Now, to prove the validity of this measure, we will resort to the definition of measure of directed divergence as given by Csiszer (1972) in the form of following theorem:

Theorem 4.1 If $\phi(.)$ is twice differentiable convex function such that $\phi(1) = 0$, then

$$ D\left(P : \mathrm{Q}\right) = \sum_{i=1}^{n} q_i \phi\left(\frac{p_i}{q_i}\right), \tag{4.1.4} $$

is a valid measure of directed divergence.

Now, let us take $\phi\left(x\right) = x \ln_{\alpha} x = \frac{x\left(\alpha^{\ln x} - 1\right)}{\alpha - 1}, \ \alpha > 1$.

Here $\phi(1) = 0$ and $\phi'\left(x\right) = \frac{1}{\alpha - 1}\left[\left(1 + \ln \alpha\right)\alpha^{\ln x} - 1\right]$,

$$ \phi''\left(x\right) = \frac{\alpha^{\ln x}\left(1 + \ln \alpha\right)\ln \alpha}{x\left(\alpha - 1\right)} > 0, $$

which shows that $\phi\left(x\right)$ is a convex function of x.

So, $\phi\left(x\right)$ satisfies all conditions of Theorem 4.1. Substituting it in equation (4.1.3), we get the measure of directed divergence (4.1.1). Hence, (4.1.1) is a valid measure of directed divergence.

Second Criteria to prove the validity of this measure is to

study its properties which are as follows:

1. ${}_\alpha D(P:Q) \geq 0$.

Proof: We will find the extremum of ${}_\alpha D(P:Q)$ subject to the constraint $\sum_{i=1}^{n} p_i = 1$. Let us consider the Lagrangian given by

$$L \equiv {}_\alpha D(P:Q) + \lambda\left(1 - \sum_{i=1}^{n} p_i\right).$$

Now, $\frac{\partial L}{\partial p_i} = \frac{\alpha^{\ln\frac{p_i}{q_i}}\left(1+\ln\alpha\right)}{\alpha - 1} - \lambda,\ i = 1,2,...,n$ and $\frac{\partial L}{\partial p_i} = 0$, gives

$$p_i = q_i e^{\log_\alpha \frac{\lambda(\alpha-1)}{1+\ln\alpha}}. \tag{4.1.5}$$

Now, using $\sum_{i=1}^{n} p_i = 1$ gives $e^{\log_\alpha \frac{\lambda(\alpha-1)}{1+\ln\alpha}} = 1$.

So, from equation (4.1.5), we get

$p_i = q_i,\ i = 1,2,...,n.$

Also, $\left(\frac{\partial^2 L}{\partial p_i^{\,2}}\right)_{p_i = q_i} = \frac{(1+\ln\alpha)\ln\alpha}{q_i(\alpha-1)} > 0,\ i = 1,2,...,n$.

and $\frac{\partial^2 L}{\partial p_i p_j} = 0,\ i \neq j.$

So, we see that the minimum value of ${}_\alpha D(P:Q)$ is obtained when $p_i = q_i,\ i = 1,2,...,n$ and $\left[{}_\alpha D(P:Q)\right]_{\min} = 0$. So, ${}_\alpha D(P:Q) \geq 0$.

2. ${}_\alpha D(P:Q) = 0$ when $P = Q$.

3. ${}_\alpha D(P:Q)$ is a convex function of P and Q.

Proof: The Hessian matrix of second order partial derivatives of ${}_\alpha D(P:Q)$ with respect to $p_1, p_2, \ldots, p_n$ is given by

$$\begin{bmatrix} \frac{\alpha^{\ln\frac{p_1}{q_1}}(1+\ln\alpha)\ln\alpha}{p_1(\alpha-1)} & 0 & \cdots & 0 \\ 0 & \frac{\alpha^{\ln\frac{p_2}{q_2}}(1+\ln\alpha)\ln\alpha}{p_2(\alpha-1)} & \cdots & 0 \\ \vdots & \vdots & \cdots & \vdots \\ 0 & 0 & \cdots & \frac{\alpha^{\ln\frac{p_n}{q_n}}(1+\ln\alpha)\ln\alpha}{p_n(\alpha-1)} \end{bmatrix}$$

which is positive definite. A similar result is also true with respect to $q_1, q_2, \ldots, q_n$. Thus, we conclude that ${}_\alpha D(P:Q)$ is a convex function of both $p_1, p_2, \ldots, p_n$ and $q_1, q_2, \ldots, q_n$.

Hence, ${}_\alpha D(P:Q)$ is a valid measure of directed divergence.

Next, we propose the measure of conditional directed divergence by taking in view the definition of alpha entropy and conditional alpha entropy.

Definition 4.1 For the two joint probability distributions $p(x,y)$ and $q(x,y)$ and the two conditional probability distributions $p(y|x)$ and $q(y|x)$, conditional directed divergence is given by the following mathematical expression:

$${}_\alpha D\left(p(y|x):q(y|x)\right) = -\sum_{i=1}^{n} p(x,y)\alpha^{\ln\frac{p(x,y)}{q(x,y)}} \ln_\alpha \frac{q(y|x)}{p(y|x)},\ \alpha > 1. \tag{4.1.6}$$

Theorem 4.2 The following chain rule holds for alpha directed divergence for general case, that is, when X and Y are not independent

$${}_\alpha D\left(p(x,y):q(x,y)\right) = {}_\alpha D\left(p(x):q(x)\right) + {}_\alpha D\left(p(y|x):q(y|x)\right) \tag{4.1.7}$$

Proof: The proof follows from the direct calculations:

$${}_\alpha D\left(p(x,y):q(x,y)\right) = \sum_x\sum_y p(x,y)\ln_\alpha \frac{p(x,y)}{q(x,y)}$$

$$= \sum_x\sum_y p(x,y)\left(\ln_\alpha \frac{p(x)}{q(x)} + \alpha^{\ln\frac{p(x)}{q(x)}} \ln_\alpha \frac{p(y|x)}{q(y|x)}\right)$$

(Using equation (3.4))

$$= \sum_x\sum_y p(x,y)\ln_\alpha \frac{p(x)}{q(x)} - \sum_x\sum_y p(x,y)\alpha^{\ln\frac{p(x)}{q(x)}}\alpha^{\ln\frac{p(y|x)}{q(y|x)}} \ln_\alpha \frac{q(y|x)}{p(y|x)}$$

(Using equation (3.5))

$$= \sum_x\sum_y p(x,y)\ln_\alpha \frac{p(x)}{q(x)} - \sum_x\sum_y p(x,y)\alpha^{\ln\frac{p(x,y)}{q(x,y)}} \ln_\alpha \frac{q(y|x)}{p(y|x)} \tag{4.1.8}$$

$$= {}_\alpha D\left(p(x):q(x)\right) + {}_\alpha D\left(p(y|x):q(y|x)\right).$$

Note: When X and Y are independent, that is, when $p(y|x) = p(y)$ and $q(y|x) = q(y)$, alpha directed divergence has a pseudoadditivity as shown below:

From (4.1.8)

$${}_\alpha D\left(p(x,y):q(x,y)\right) = \sum_x\sum_y p(x,y)\ln_\alpha \frac{p(x)}{q(x)} - \sum_x\sum_y p(x,y)\alpha^{\ln\frac{p(x,y)}{q(x,y)}} \ln_\alpha \frac{q(y|x)}{p(y|x)}$$

$$= {}_\alpha D\left(p(x):q(x)\right) + {}_\alpha D\left(p(y):q(y)\right)\sum_x p(x)\alpha^{\ln\frac{p(x)}{p(x)}}$$

$$= {}_\alpha D\left(p(x):q(x)\right) + {}_\alpha D\left(p(y):q(y)\right) + (\alpha-1)\,{}_\alpha D\left(p(x):q(x)\right){}_\alpha D\left(p(y):q(y)\right)$$

4.2 Measure of Inaccuracy

We propose the new parametric measure of inaccuracy given by the following mathematical expression:

$$ {}_{\alpha}I(P:Q) = \sum_{i=1}^{n} p_i \alpha^{\ln p_i} \ln_{\alpha} \frac{1}{q_i}, \ \alpha > 1 . \qquad (4.2.1) $$

Letting $\alpha \to 1$, measure (4.2.1) reduces to Kerridge's (1961) measure of inaccuracy given by

$$ I(P:Q) = -\sum_{i=1}^{n} p_i \ln q_i \ . $$

Measure (4.2.1) is a valid measure of inaccuracy as it satisfies the following properties:

1. $$ {}_{\alpha}I(P:Q) = \sum_{i=1}^{n} p_i \alpha^{\ln p_i} \ln_{\alpha} \frac{1}{q_i} \geq 0 . \qquad (4.2.2) $$

Since measure (4.2.1) is a sum of alpha entropy and alpha directed divergence given by (2.1) and (4.1.1) respectively, both of which are non-negative quantities, therefore (4.2.2) holds.

2. $ {}_{\alpha}I(P:P) = \sum_{i=1}^{n} p_i \alpha^{\ln p_i} \ln_{\alpha} \frac{1}{p_i}, \ \alpha > 1 $ is a valid measure of entropy as proved in Section 2.

3. $ {}_{\alpha}I(P:Q) \geq {}_{\alpha}I(P:P) $ and $ {}_{\alpha}I(P:Q) $ reduces to $ {}_{\alpha}I(P:Q) $ only when $Q = P$.

CONCLUDING REMARKS

The non-additive Tsallis entropy which is supposed to be a firm basis of the non-extensive statistical mechanics having applications in diverse disciplines of mathematical sciences motivated us to introduce the non-additive measure of entropy in the manuscript. It is expected that the proposed measure will perform equally well in all the application areas parallel to Tsallis entropy. Also, we have made the detailed study of the proposed entropy measure in the form of inequalities, theorems and developed corresponding measures of information applicable to a variety of mathematical disciplines.

ACKNOWLEDGEMENT

The authors are thankful to Council of Scientific and Industrial Research, New Delhi for providing the financial assistance for the preparation of the manuscript.

REFERENCES

Asgarani, S. 2013. A set of new three-parameter entropies in terms of a generalized incomplete Gamma function. Physica A. 392:1972-1976.

Bercher, JF. 2011. Escort entropies and divergences and related canonical distribution. Physics Letters A. 375:2969-2973.

Besenyei, A. and Petz, D. 2013. Partial subadditivity of entropies. Linear Algebra Appl. 439:3297-3305.

Csiszer, I. 1972. A class of measures of informativity of observation channels. Periodic Math. Hungarica. 2:191-213.

Furuichi, S. 2010. An axiomatic characterization of a two-parameter extended relative entropy. Journal of Mathematical Physics. 51:123302-123310.

Furuichi, S. and Mitroi, FC. 2012. Mathematical inequalities for some divergences. Physica A. 391:388-400.

Furuichi, S., Minculete, N. and Mitroi, FC. 2012. Some inequalities on generalized entropies. Journal of Inequalities and Applications. 2012:226-241.

Gupta, N. and Bajaj, RK. 2013. On partial monotonic behaviour of some entropy measures. Statistics and Probability Letters. 83:1330-1338.

Havrda, J. and Charvat, F. 1967. Quantification method of classification processes: concept of structural α-entropy. Kybernetika. 3:30-35.

Kapur, JN. 1967. Generalized entropy of order α and type β. The Maths. Seminar. 4:78-94.

Kerridge, DF. 1961. Inaccuracy and inference. J. R. Statist. Soc. B 23:184-194.

Kullback, S. and Leibler, RA. 1951. On information and sufficiency. Ann. Math. Statistics. 22:79-86.

Renyi, A. 1961. On measures of entropy and information. In: Proc. Fourth Berkeley Symp. Math. Statist. Prob. 1:547-561.

Shannon, CE. 1948. A mathematical theory of communication. Bell System Tech. J. 27:379-423.

Tsallis, C. 2009. Non-additive entropy: The concept and its use. Eur. Phys. J. A. 40:257-266.

Teixeira, A., Matos, A. and Antunes, L. 2012. Conditional Renyi entropies. IEEE Transactions on Information Theory. 58 (7):4273-4277.

Received: June 6, 2014; Revised and Accepted: July 14, 2014

SENRA Academic Publishers, British Columbia
Vol. 8, No. 3, pp. 3125-3129, October 2014
Online ISSN: 1920-3853; Print ISSN: 1715-9997

Canadian Journal of pure&applied sciences

EFFECTIVENESS OF DETECTIVE AND PREVENTATIVE INFORMATION SECURITY CONTROLS IN INFORMATION SYSTEMS ORGANIZATIONS

Muhammad Asif Khan
College of Computer Science and Engineering, Taibah University
Madina al Munawwara, Saudi Arabia

ABSTRACT

Information Systems (IS) organizations are experiencing a mounting pressure to contribute organizational success and to secure information asset, therefore, protection of information assets has become a paramount concern in IS organizations. IS organizations are more active in implementing technology and know the significance of IS audit and security controls in order to eliminate the risks for their IS asset and infrastructure. The aim of this paper is to analyze and demonstrate the effectiveness of network security controls in IS organizations that are implemented to ensure security and integrity of information assets. Also, the study evaluates the level of implementation of the detective and preventative security controls in organizations. In the present study we have collected data through survey from different organizations in Saudi Arabia. The purpose is to compare between the approaches for IS audit being used by these organizations and the industry standards of IS audit and controls set by organizations.

Keywords: Information systems organizations, security controls, audit and controls, information systems security controls.

INTRODUCTION

Organizations are becoming more dependent on information systems to provide fast, better and reliable services to their customers and to facilitate decision making and business strategy within the organizations. This trend is increased in the businesses with the advent of internet and electronic business and has grown IS security issue as a prime concern for organizations. Our business institutions are worldwide connected and rely on automated control systems (Warkentin and Willison, 2009). IS security is a process that protects information and maintains its integrity; however, it has not been a serious concern for the top management comparing to other IS issues (Brancheau *et al*., 1996). Most of the organizations do not provide IT security training to their employees and less than 50% of 459 CIOs and IT directors have said that they had IT security knowledge and training programs for their employees (Verton, 2002). For effective corporate governance a proper system of internal controls is essential and it is important to make sure the integrity of financial systems of organization remains intact without compromising and internal control is in place.

In organizations, there are external and internal security functions. External security functions consist of employees, administrative and physical while software and hardware are employed as internal security functions.

Corresponding author email: asifkhan2k@yahoo.com

It is reported that personnel in organizations cause key problem in information security (Puhakainen, 2006). Employees do not implement security controls seriously and poor compliance of security policies cause security breaches (Santon *et al*., 2005; Myyry *et al*., 2009). Deterrent measures attempt to deter people from using IS assets illegally. The deterrent measures can be policy statements or guidelines of using IS assets of an organization. Deterrent measures have been useful in keeping away people from unauthorized use of IS assets but a new theoretical model based on neutralization theory has been introduced (Siponen and Vance, 2010) that highlights neutralization as an important factor in order to implement and develop organizational security policies.

Preventive measures become effective when people do not pay attention to the deterrent measures and these measures are implemented by controls. Various security software are implemented in organizations to prevent unauthorized access to the IS assets. The security software provides different levels of access controls to IS assets (Weber, 1998). At basic level security software set in operating systems can enforce access to user account or any specific files. Security software in a middle level is set in database systems in order to access control of any particular records in a database. However, security software at an advanced level provides access control through high transaction means integrating audit and extensive security breach reports.

In organizations IS assets such as hardware, software, people and data are at risk of abuse by hackers through searching and exploiting vulnerabilities (Sun and Srivastava, 2006). Usually information is at risk during transmission over internet or information being stored in database of organization or information being stored in customers' computer. In financial institutions IS plays a strategic and significant role as compare to different business organizations. Therefore, financial institutions devote extra resources in IS in order to obtain more benefits than other organizations. Many companies face information security problems because senior management does not have a commitment and responsibility towards information security. Usually at management level absence of support from management is not considered in security rather information security is deemed a technical problem. Information security managers always find difficulties in implementing information security plans that take into account all security dimensions including human dimension, awareness dimension, policy dimension, measuring and monitoring dimension etc (Solms, 2001).

An effectiveness of information security depends on some organizational factors such as type of business, management interest and size of organization. To develop an effectiveness of information security, detective and preventive measures are taken into account. Organizations implement preventive security software that is assessed in terms of their sophistication.

There is no independent body that could conduct a systematic testing for the effectiveness of information security controls and usually the results of effectiveness testing carried out by vendors are never published. In a study Khan and Turki (2008) effectiveness of IS audit and control has been presented and an analysis of the effectiveness and efficiency of IS audit in reducing risks, vulnerabilities and security issues that are found within IS organizations is presented.

MATERIALS AND METHODS

In the present study we used a research survey instrument to collect data from various small to large organizations. We mailed out the survey instrument to 93 IS managers associated with small to large professional organizations. We followed up the survey by sending emails and phone calls whenever necessary. Out of 93 IS managers, 41 complete surveys were received and have been used for this study.

In the survey instrument we grouped questions in four categories in order to measure the IS security effectiveness in the organizations i.e. implementation of detective security controls, implementation of preventative security controls, management interest and open ended questions for respondents. We delivered the pilot questionnaires to few organizations in order to get the feedback. Based on the feedback we altered some questions, their wording and order before finalizing the survey instrument for the study.

To assess the implementation of detective security controls i.e. firewalls, intrusion detection system (IDS), encryption, check sums, logs/audit trails, capacity management, performance monitoring and anti-virus procedures, we formed questions to finding out any breach or abuse of IS security and the severity of actions taken by the organization: no abuse – no action - 0, little abuse – warning – 1, serious abuse – strict action – 2, destructive abuse – prosecution – 3. The detective efforts were measured using total man-hours expended on IS security purposes per week (Straub and Welke, 1998).

To evaluate the preventative security controls i.e. policies and procedures, honey pots, configuration management, incident handling, review of audit trails/logs, encryption and performance monitoring, we formulated questions to finding out the software for security used in the organization: software for security built in operating systems – 1, software for security built in databases – 2, software for security (special) – 3. The preventative efforts were measured using the level of sophistication of security software used in the organization.

We determined the size of an organization using the number of employees in the organization. We collected the nominal and ordinal data for this study. We used questions to find out involvement of top management in decisions with regard to security and security related activities. The questions have been helpful to know management's pro-active support for security functions within organizations. We asked these questions on Likert's scale i.e. from Strongly Agree - 5, Agree - 4, Neutral - 3, Disagree - 2 and Strongly Disagree - 1.

Perceptual responses from the respondents to six questions were used to measure the IS security effectiveness. The six questions were based on: preventative effect, detective effect, effect in hardware protection, effect in software protection, effect in data protection and effect in computer services protection. All questions were anchored on a Likert's scale i.e. from 'Maximum' (5), 'High' (4), 'Medium' (3), 'Low' (2) and 'Minimum' (1). Table I depicts the statistics of the organizations participated in the study:

Table 1. Statistics of participatory organizations.

Organization Type	Number of Organizations	% of Response Received
Banks, Financial Institutions	12	38.7
Manufacturing	3	9.6
Others	16	51.6

Since we have small size of sample nominal and ordinal data, we have used partial least square (PLS) method because this method does not require homogeneity and normality on data (Hair *et al.*, 1998).

RESULTS AND DISCUSSION

The questions in our survey instrument were based on different ensembles and the table 2 depicts the data

Based on our survey instrument it was determined that albeit many organizations recognize the importance of IS security effectiveness, but many of them had not properly placed IS security controls within the organizations. As we discussed above the effectiveness of network security controls was measured on Likert's scale, the table 3 depicts the IS effectiveness in organizations.

Reliability of the questions were tested by looking into the loadings of questions provided by PLS. Adequate reliability was proposed by Hair *et al*. (1998) as 0.5. On Cronbach's alpha, evidence of composite reliability could also be obtained. Nunnaly (1978) proposed the reliability of a construct should be at least 0.7. As an indication of adequate variance extracted 0.5 is a good indicator (Fornell, 1982). Table 4 depicts the results.

In this study we have used data collected from different types of organizations ranging from small to large conglomerates in Saudi Arabia where organizational culture, organizational maturity and employees behavior are generally varied. We suggest that this type of study should be carried out with different set of organizations and additional deterrent and preventive controls in order to generalize the results. This study has assessed various security controls and their effectiveness in different organizations. We have observed that small organizations do not have adequate security controls as compare to large organizations, and it is suggested to organizations to improve IS security effectiveness in future in order to prevent from a great damage.

As organizations are increasingly depending on IS and becoming more networked, further awareness of security controls is essential especially to the top management in order to have security measures in place.

A better IS security effectiveness is contributed by greater deterrent and preventive efforts. Many managers in organizations are either reluctant or unwilling to employ deterrent and preventive efforts to reduce risks in their organizations. The reason is they are unaware of the benefits of detective and deterrent measures and effects of preventive counter-measures. Since the penalty for IS abusers is not that high as compare to other crimes, organizations should take further steps to increase efforts for deterrent and preventive measures. The awareness of

Table 2. Ensembles and organizations data.

Ensemble	No. of Organizations	% of Organizations
Deterrent efforts (per day)		
Less than 1 hour	10	32.3
More than 1 but less than 3 hours	7	22.5
More than 3 but less than 9 hours	8	25.8
More than 9 hours	6	19.3
Deterrent Action		
No action	9	29.0
Warning	12	38.7
Suspension of services/ duties	8	25.8
Litigation/Prosecution	2	6.45
Preventive Action		
Security software	21	64.7
Operating systems	3	9.6
Database management systems	7	22.5

Table 3. Effectiveness of security controls in IS organizations.

Security Control	No. of Organizations	% of Organizations	Mean Significance of Security Control	Mean Security Control Effectiveness
Policies & Procedures	18	58.06	5	3
Firewalls	27	87.09	5	5
Intrusion Detection System	12	38.70	4	5
Honeypots	8	25.80	2	1
Encryption	22	70.97	4	4
Checksums	16	51.61	4	1
Audit Trails	13	41.93	5	2
Configuration Management	20	64.51	5	3
Incident Handling	24	77.41	4	3
Problem Escalation	17	54.83	4	4
Capacity Management	18	58.06	5	1
Performance Monitoring	25	80.64	5	1
Anti Virus Procedures	27	87.09	5	3

IS security effectiveness among top management is insufficient and it is suggested that some form of education may be useful in IS security context. Management should be emphasized different aspects of preventive efforts and the legitimate and illegitimate use of IS assets. It is important that IS auditors should have good experience in order to conduct audit on regular basis. Management should also be aware of security software to protect IS assets.

It is observed that small organizations do not invest in deterrent efforts as they believe and trust in employees while large organization invest more in deterrent efforts. It is advised to small organizations that they reassess their deterrent efforts to ensure there is assets are secure. Financial institutions tend to invest more for deterrent and preventive efforts due to large potential losses that may happen from IS security breach. The organizations which are related to other than financial business have lower IS security effectiveness as they are low deterrent efforts. These organizations must raise deterrent efforts to enhance IS security effectiveness as the businesses are increasingly adopting electronic networks in future.

REFERENCES

Brancheau, C., Janz, D. and Wetherbe, C.1996. Key Issues in Information Systems Management: 1994-95 SIM Delphi results MIS Quarterly. 20(2):225-242.

Fornell, C. 1982. A Second Generation of Multivariate Analysis. Methods, 1. New York, USA.

Hair, F., Anderson, E., Tatham, L. and Black, C. 1998. Multivariate Data Analysis with Readings. Englewood Cliffs, Prentice Hall, NJ, USA.

Khan, MA. and Turki, S. 2008. Evaluation of Software Development Controls in Information Systems Organizations. Canadian Journal of Pure and Applied Sciences. 2(2):463-468.

Myyry, L., Siponen M., Pahnila,S.,Vartiainen, T. and Vance, A. 2009. What levels of moral reasoning and values explain adherence to information security rules? An empirical study. European Journal of Information Systems. 18:126-139.

Nunnally, C. 1978. Psychometric theory. (2nd edi.). McGraw-Hill, New York, USA.

Puhakainen, P. 2006. A Design Theory for Information Security Awareness. University of Oulu, Oulu, Finland.

Siponen, M. and Vance, A. 2010. Neutralization: New Insights into the Problem of Employee Information Systems Security Policy Violations. MIS Quarterly. 34(3):487-502.

Solms, B. 2001. Corporate Governance and Information Security. Computers and Security. 20:215-218

Stanton, J., Stam, K., Mastrangelo, P. and Jolton, J. 2005. Analysis of End User Security Behaviors. Computers and Security. 24(2):124-133.

Straub, W. and Welke, J. 1998. Coping with Systems Risk: Security Planning Models for Management Decision Making. MIS Quarterly. 22(4):441-469.

Sun, l. and Srivastava, R. 2006. An Information Systems Security Risk Assessment Model under Dempster-Shafer Theory of Belief Functions. Journal of Management Information Systems. 22(4):109-142.

Verton, D. 2002. Disaster Recovery Plan Still Lags. Computer World. 36(14):10.

Warkentin, M. and Willison, R. 2009. Behavioral and policy issues in information systems security: the insider threat. European Journal of Information Systems. 18:101-105.

Weber, R. 1998. EDP auditing: Conceptual foundations and practice. McGraw Hills, NY, New York, USA.

Received: June 5, 2014; Accepted: Sept 6, 2014

SENRA Academic Publishers, British Columbia
Vol. 8, No. 3, pp. 3131-3137, October 2014
Online ISSN: 1920-3853; Print ISSN: 1715-9997

Canadian Journal of pure&applied sciences

LOGARITHMS OF IMAGINARY NUMBERS IN RECTANGULAR FORM: A NEW TECHNIQUE

Ashwani K Thukral
Department of Botanical and Environmental Sciences
Guru Nanak Dev University University, Amritsar -143005, India

ABSTRACT

Logarithms of imaginary numbers are defined by Euler's equation in polar form with real X-axis and imaginary Y-axis. In the present paper, a new concept of logarithms is developed from the basic principles to derive the logarithms of imaginary numbers in rectangular form with both X and Y axes being imaginary. Logarithms of imaginary numbers to a real base with an imaginary multiplicative coefficient are real numbers. This concept generalizes the multiplication and division of real and imaginary numbers using logarithms in rectangular form.

Keywords: Rectangular and polar form logarithms, Euler's equation, imaginary exponential function, logarithmic multiplication and division of imaginary numbers, computational sciences.

INTRODUCTION

The concept of logarithms was introduced by John Napier (1950-1617), a Scottish mathematician (Lexa, 2013). It took Napier about twenty years to complete his tables, which laid the foundation of a new computational technique to comprehend numerals of transcendental size (Clark and Montelle, 2011). Napier provided an arithmetic measure of a geometric ratio (Roegel, 2012). Several prominent scientists like Joost Burgi, Johannes Kepler, Gregoire de Saint-Vincent, Leonard Euler and others contributed to the development of logarithms (Lexa, 2013; Wikipedia, 2014a,b). The term "imaginary" for imaginary numbers was coined by Rene Descartes in 1637 (Wikipedia, 2014c). Gottfried Leibnitz and John Bernoulli-I were the first scientists who initiated discussion on the logarithms of real negative, and imaginary numbers in the year 1745 (Bal, 2014). Euler (1749) defined the exponential function and related it to the natural logarithm. He proved that Lebnitz was correct in claiming that the logarithms of negative numbers are imaginary (Cajori, 1913). Leibnitz and Newton gave the presently used terminology of the logarithms (Lefort, 2013). The logarithmic function has become indispensable to the understanding and development of science and technology, and computational techniques.

Neparian logarithms of real positive numbers (x) are defined as, $\log_b x = y$, such that $b^y = x$,

where y is a real number, and b is a real positive number base of the logarithm (generally 10, or 2 or e). In its integral form, the natural logarithmic function is defined as

$$\ln(x) = \int_1^x (1/t)dt, x > 0 \ .$$

Natural logarithm is the inverse function of natural exponential function. Logarithms were initially defined for all real positive numbers, until Euler described logarithms of complex and negative numbers, which expanded the field of logarithms.

Complex numbers can be represented using an Argand diagram, in which X-axis is a real axis and Y-axis is an imaginary axis (Fig. 1). A point in the Argand diagram represents a complex number, $x + iy$, where x and y are real numbers, and $i = \sqrt{-1}$.

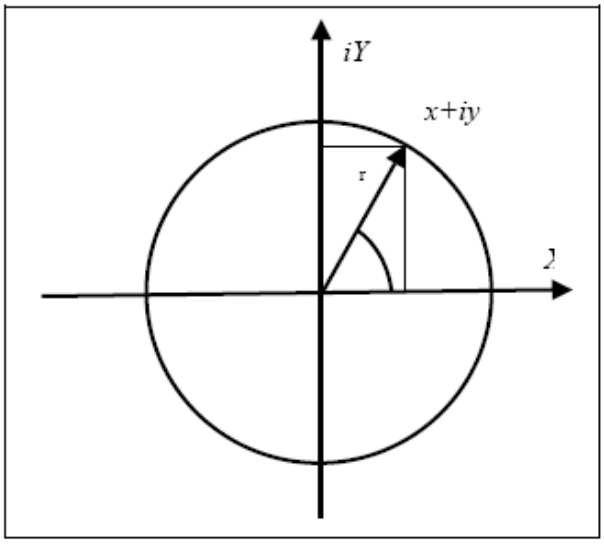

Fig. 1. Argand diagram for logarithms of complex numbers.

*Corresponding author email: akthukral.gndu@gmail.com

Euler (1749) gave a formula known as Euler's identity (Cajori, 1913):

$$e^{i\theta} = \cos x + i \sin x,$$

where, θ is the polar angle in radians between X-axis and the line joining the point (x, iy) with the origin. For $\theta = \pi$,

$$e^{i\pi} + 1 = 0$$

This defined the logarithm of (-1),

$$\log_e(-1) = i\pi .$$

Logarithms of complex numbers may be obtained by converting the rectangular coordinates of the complex number (x, iy) into polar coordinates as follows:

$$x + iy = re^{i\theta},$$

where, r is the magnitude of the radial line for the coordinates (x, iy), and θ is the polar angle in radians as given by,

$$r = \sqrt{x^2 + y^2},$$

$$\theta = \tan^{-1}\frac{y}{x}.$$

Thus started the field of logarithms of complex numbers. The logarithm of a complex number is obtained as follows:

$$r = y,$$

$$\log_e(x + iy) = \log_e r + i\theta .$$

The logarithms of imaginary numbers are obtained from the above equation with $x = 0$, and

$\theta = \pi/2$ radians (≈1.570796 radians),

$$\log_e(iy) = \log_e y + i(\pi/2).$$

This paper is intended to develop a general concept of logarithms applicable to both real and imaginary numbers on a rectangular coordinate system.

1. Logarithms of imaginary numbers

Recently, Thukral and Parkash (2014) generalized the logarithms of real positive numbers and real negative numbers in a rectangular coordinate system as follows:

$$\log_{c,b}(cx) = y, \text{ such that } c(b^y) = cx;\ x > 0, b > 1, \quad (1.1)$$

where c is +1 for logarithms of real positive numbers, and -1 for logarithms of real negative numbers. In this paper the author now extends this generalized concept to the logarithms of imaginary numbers. Putting the coefficient c equal to ($+i$) or ($-i$) in equation (1.1), logarithms of positive imaginary numbers and negative imaginary numbers on rectangular coordinate system may be defined:

Logarithms of positive imaginary numbers

$$\log_{+i,b}(+i)x = y, \quad (1.2)$$

such that $(+i)b^y = (+i)x$, $x > 0, b > 1$, and logarithms of negative imaginary numbers

$$\log_{-i,b}(-i)x = y, \quad (1.3)$$

such that $(-i)(b^y) = (-i)x$, $x > 0, b > 1$.

There thus follows the equivalence between the logarithms of positive and negative imaginary numbers (equations 1.2, 1.3):

$$\log_{+i,b}(+i)x = \log_{-i,b}(-i)x,\ x > 0, b > 1.$$

In a rectangular coordinate system with both X and Y axes are real, the area (integral) under the curve above X axis is real positive, and area above the curve under X axis is real negative (Fig. 2). However, since the reciprocals of imaginary numbers will also be imaginary numbers, that is, $1/ix = -ix$ and $1/(-ix) = ix$, the graph between ix and $1/ix$ can be better plotted on imaginary-imaginary (Im-Im) plot. Representing Im-Im axes as iX and iY, the nature of area (integral) under or above the curve gets reversed than in the Real-Real axes (X and Y) plot (Fig. 3).

A graph of the reciprocals of imaginary numbers on Im-Im plot shows the position of the hyperbolas (Fig. 4). Since, $(1/i) = -i$, the curve appears in the IV quadrant for positive imaginary numbers and in the II quadrant for negative imaginary numbers. The integral form of natural imaginary logarithms in rectangular plane will be

$$\log_{c,e}(cx) = \int_{c}^{cx} (1/t)dt, x > 0, c = +i, or, c = -i \quad (1.4)$$

By substitution, the integral for logarithm of positive imaginary numbers will be

$$\log_{+i,e}(+i)x = \int_{(+i)1}^{(+i)x} (1/(it))dit = \int_{(+i)1}^{(+i)x} (-i/t)dit$$

$$= -i^2 \int_{(+i)1}^{(+i)x} (1/t)dt, x > 0 \qquad (1.5)$$

$$\log_{+i,e}(+i)x = \int_{(+i)1}^{(+i)x} (1/t)dt\ ,\ x > 0\ .$$

It is seen that multiplication of lower and upper limits of the interval of integration (equations 1.4, 1.5) with a constant does not change the logarithm of a number,

$$\log_{c,e} cx = \int_{c}^{cx} (1/t)dt, x > 0\ ,$$

$$\log_{c,e} cx = \int_{1}^{cx} (1/t)dt - \int_{1}^{c} (1/t)dt = \log_e cx - \log_e c\ ,$$

$$\log_e c + \log_e x - \log_e c = \log_e x\ .$$

As for example, it may be verified from the computation of area under the curve with the help of a software, that

$$\ln(2) = \int_{1}^{2} (1/t)dt = \int_{2}^{4} (1/t)dt = \int_{0.5}^{1} (1/t)dt = \int_{-1}^{-2} (1/t)dt = 0.693$$

Therefore, the logarithms of imaginary numbers will be the same as for positive real numbers,

$$\log_{+i,e}(+i)x = \int_{1}^{x} (1/t)dt, x > 0\ . \qquad (1.6)$$

Similarly, the integral equation for logarithms of negative imaginary numbers will be

$$\log_{-i,e}(-i)x = -\int_{-x}^{-1} (1/t)dt\ ,\ x > 0\ . \qquad (1.7)$$

The logarithms of both positive and negative imaginary numbers will be real numbers (equations 1.6, 1.7).

A graph of logarithm of imaginary numbers in the rectangular coordinate system is given in figure 5. If the base of the function is Euler's constant *e*, then,

$i(e^y) = ix$, that is, $\log_{i,e}(ix) = y\ ,\ x > 0$, and

$-i(e^y) = -ix$, that is, $\log_{-i,e}(-ix) = y\ ,\ x > 0\ .$

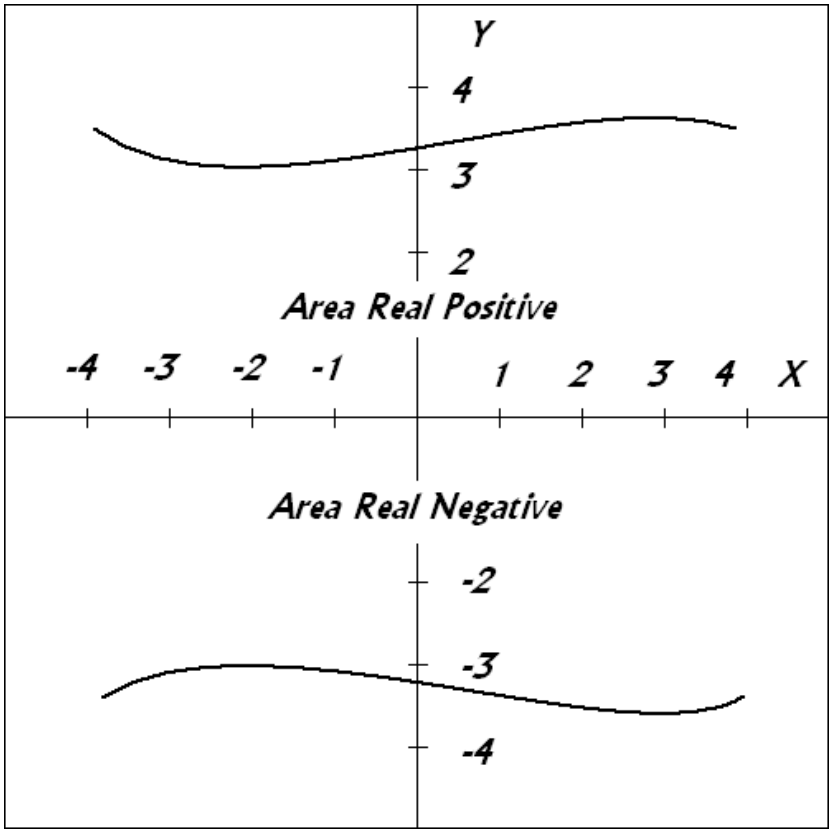

Fig. 2. Area graph for both axes being real (X, Y) (Re-Re plot).

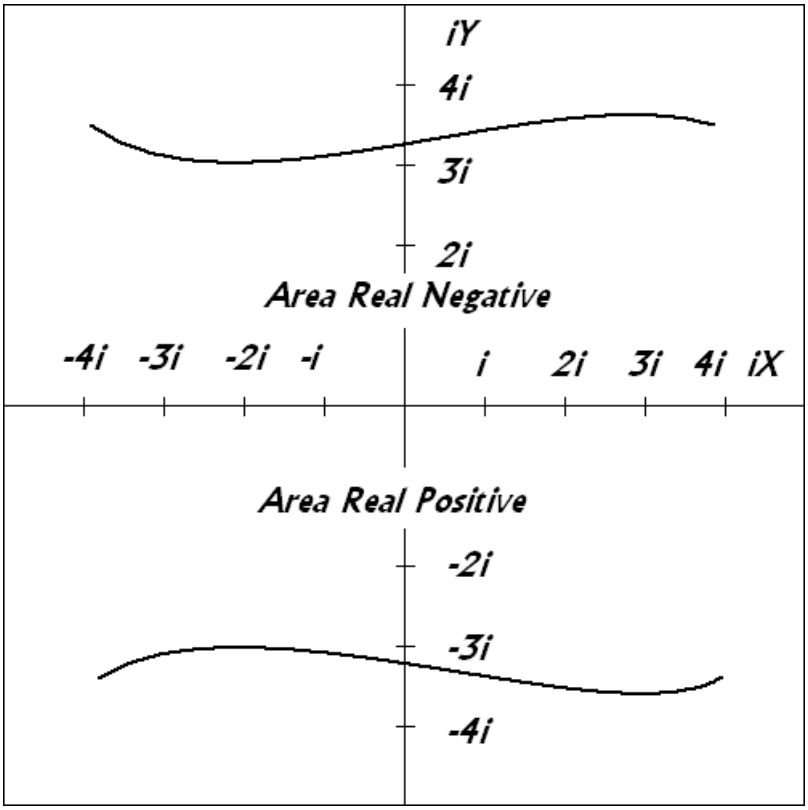

Fig. 3. Area graph for both axes being imaginary (iX, iY)(Im-Im plot).

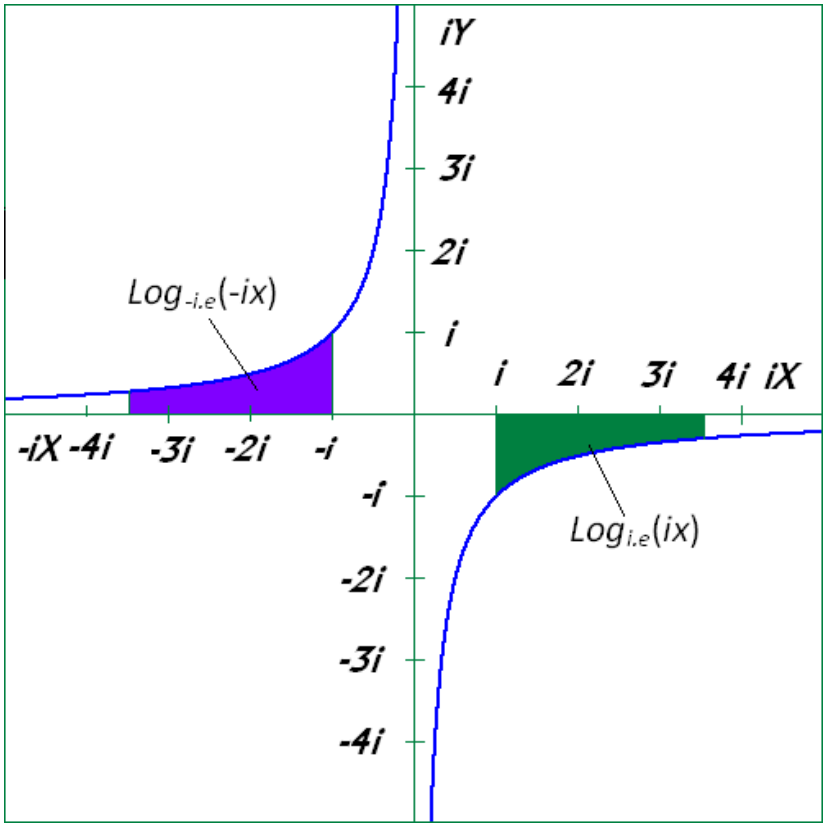

Fig. 4. Curves for hyperbolas transcribed by $y = 1/ix$ in rectangular plane with both X and Y axes being imaginary (Im-Im plot).

Table 1. Logarithms of some numbers in Euler's polar form and the proposed rectangular form.*

Imaginary number	Euler's polar form logarithm (Complex number)	Rectangular form logarithm with imaginary number base as per the present concept (Real number)
$(i)x$	$\log_e(i)x$	$\log_{i,e}(i)x$
0.5 *i*	-0.693+1.570 *i*	-0.693
i	0+1.570 *i*	0
1.5 *i*	0.405+1.570 *i*	0.405
2 *i*	0.693+1.570 *i*	0.693
$(-i)x$	$\log_e(i)x$	$\log_{-i,e}(-i)x$
-0.5 *i*	-0.693-1.570 *i*	-0.693
- *i*	0-1.570 *i*	0
-1.5 *i*	0.405-1.570 *i*	0.405
-2 *i*	0.693-1.570 *i*	0.693

*The software used in this paper are Function Calculator (Gang, 2014), Draw Function Graphs – Plotter – Recheronline, Complex Number Calculator (Pierce, 2014) and MS-Excel.

The logarithm of *i* will be, $\log_{i,b}(i) = 0$, since, $i(b^0) = i$, and the logarithm of $-i$ will be, $\log_{-i,b}(-i) = 0$, since, $-i(b^0) = -i$.

Log natural of imaginary number coefficient, *c*. For $c = +i$ or $c = -i$, $\log_{c,e} c = 0$. That is,

$\log_{+i,e}(+i) = 0$ and $\log_{-i,e}(-i) = 0$.

The inverse function of logarithm of natural positive imaginary logarithm will be $(+i)e^x$, $x > 0$. Similarly, the inverse function of logarithm of natural negative imaginary function will be $(-i)e^x$, $x > 0$, as given in figure 6.

A comparison of natural logarithms of imaginary numbers in polar and rectangular forms reveals that the real part of the two forms is equal (Table 1). The polar form logarithms have an imaginary part equal to $i(\pi/2)$ or $-i(\pi/2)$, for logarithms of $+ix$ or $-ix$ respectively.

2. Logarithmic operations on imaginary numbers

As per the present concept, logarithmic multiplication and division of imaginary and real numbers may be carried out.

Multiplication: For c_1 and c_2 same or different imaginary number coefficients $(c_1, c_2 = +i \text{ or } -i)$

$$\log_{c_1,b}(c_1x_1) + \log_{c_2,b}(c_2x_2) = \log_{c_1c_2,b}(c_1c_2x_1x_2),$$
$$x_1, x_2 > 0, b > 1. \quad (2.1)$$

For example if c_1=+*i*, c_2= -*i*, *b*=10, x_1=100, x_2=1000

$$\log_{+i,10}(+i)100 + \log_{-i,10}(-i)1000 = \log_{-(i^2),b} -(i^2)100000$$
$$= \log_{+1,b}(+1)100000$$

Real and imaginary numbers can be presented in terms of the powers of imaginary numbers, such as,

$(i^{-i} = -i)$, $(i^0 = +1)$, $(i^1 = +i)$, $(i^2 = -1)$, $(i^3 = -i)$, $(i^4 = +1)$.

Let $(c_1, c_2 = i^m, i^n)$. Following general equation for the multiplication of real numbers and imaginary numbers is thus derived

$$\log_{i^m,b}(i^m x_1) + \log_{i^n,b}(i^n x_2) = \log_{i^{m+n},b}(i^{m+n} x_1 x_2),$$
$$x_1, x_2 > 0, b > 1. \quad (2.2)$$

Division: If c_1, c_2 are the same or different imaginary number coefficients, $(c_1, c_2 = +i \text{ or } -i)$

$$\log_{c_1,b}(c_1x_1) - \log_{c_2,b}(c_2x_2) = \log_{(c_1/c_2),b}(c_1x_1)/(c_2x_2),$$
$$x_1, x_2 > 0, b > 1$$
$$\log_{i^m,b}(i^m)x_1 - \log_{i^n,b}(i^n)x_2 = \log_{i^{m-n},b}(i^{m-n})x_1/x_2 \quad (2.3)$$

Power: Log of power function, $c(x^n)$, $c = +i$ or $c = -i$ will be,

$$\log_{c,b} c(x^n) = n(\log_{c,b} cx),\ x > 0, b > 1$$

For $c = +i$

$$\log_{+i,b}[(+i)(x^n)] = n[\log_{+i,b}(+i)(x)],\ x > 0, b > 1$$

For $c = -i$

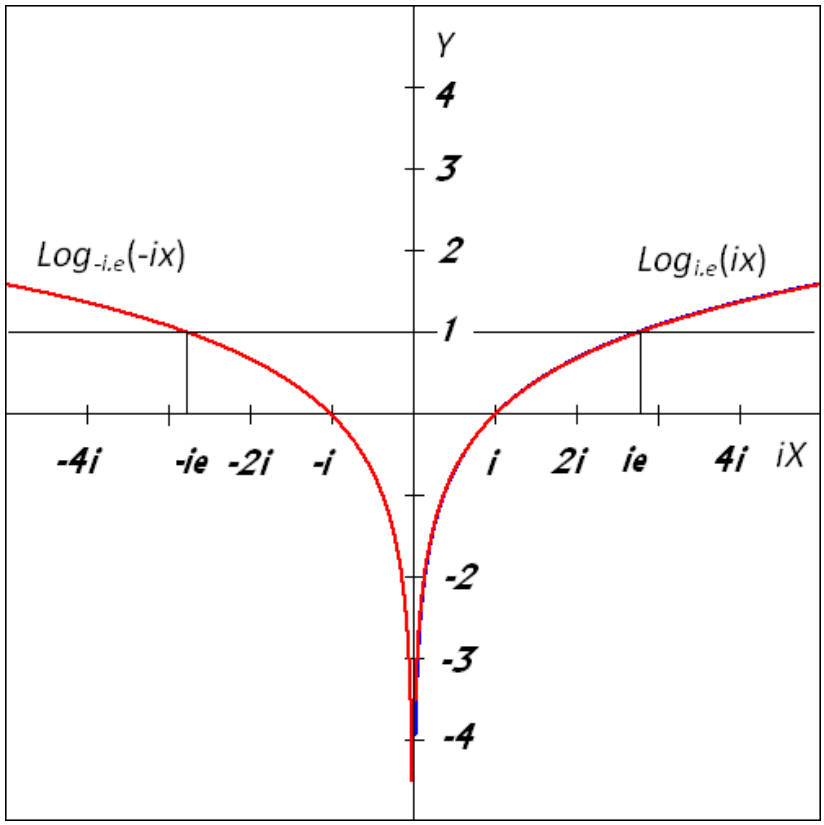

Fig. 5. Logarithmic curve for positive (right) and negative (left) imaginary numbers.

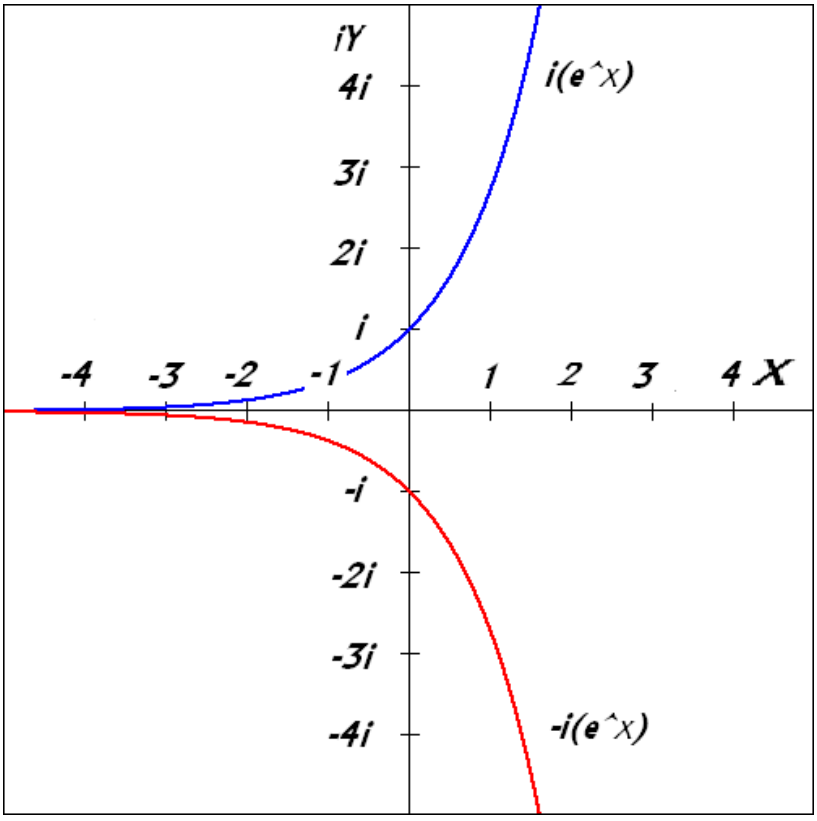

Fig. 6. Graph for positive (upper curve) and negative (lower curve) imaginary exponential functions.

$$\log_{-i,b}[(-i)(x^n)] = n[\log_{-i,b}(-i)x)], x > 0, b > 1$$

Given below is an example involving the multiplication and division of real and imaginary numbers with the help of $\log_{c,e} cx$, where $b = e$; $c = +1, -1, +i$, or $-i$; and $x>0$. The symbol * represents multiplication.

$$y = \frac{25 * (-10) * (+15i) * (-30i)}{50 * 20i},$$

$$\log_{c,e}(y) = \log_{1,e}(1*25) + \log_{-1,e}(-1*10) + \log_{i,e}(i*15)$$
$$+ \log_{-i,e}(-i*30) - \log_{1,e}(1*50) - \log_{i,e}(i*20)$$

= 3.21887+2.30258+2.70805+3.4012-3.91202-2.99573
= 4.72295.

$$c = [1*(-1)*i*(-i)]/[1*i] = i.$$
$$y = i*\exp(4.72295) = 112.5i.$$

Therefore, the logarithms of imaginary numbers and real numbers in the rectangular form may provide an effective tool for calculations.

CONCLUSION

Logarithms of imaginary numbers were defined by Euler on a polar coordinate system with imaginary Y axis and real X axis. In the present paper, logarithms of imaginary numbers have been defined on a rectangular coordinate system consisting of both X and Y axes as imaginary axes. Hyperbolas formed in the IV and II quadrants may be used to define logarithms of positive and negative imaginary numbers respectively. Logarithms of imaginary numbers with (+*i*) or (-*i*) coefficient to the base are real numbers. This concept of logarithms will provide a useful technique to multiply and divide real and imaginary numbers using logarithms on a rectangular coordinate system, similar to the logarithms of real positive numbers.

ACKNOWLEDGEMENTS

Thanks are due to the University Grants Commission, and Department of Science and Technology, Government of India, New Delhi, for financial assistance.

REFERENCES

Bal, D. 2014. Leibniz, Bernoulli and the logarithms of negative numbers. (http://www.math.ryerson.ca/~dbal/files/LeibBernLogs.pdf)

Cajori, F. 1913. History of the expontial and logarithmic concepts: The creation of a theory of logarithms of complex numbers by Euler. The American Mathematical Monthly (Published by the Mathematical Association of America). 20:75-84. (http://www.jstor.org/stable/2973441).

Clark, KM. and Montelle, C. 2011. Logarithms: The early history of a familiar function- John Napier introduces logarithms. Loci. pp. 1-6. (Published by the Mathematical Association of America). DOI:10.4169/loci003495. (http://www.maa.org/publications/periodicals/convergence/logarithms-the-early-history-of-a-familiar-function-john-napier-introduces-logarithms).

Euler, L. 1749. On the logarithms of negative and imaginary numbers. Actor. Acad. Berolinensis tomo VA. p. 139 Number 807 in the Enestrom index. Translation copy right © with 2005 Todd Doucet. (http://eulerarchive.maa.org/docs/translations/E807en.pdf)

Gang, XIAO. 2014. Function calculator. (http://wims.unice.fr/wims/en_tool~analysis~function.en.html).

Lefort, X. 2013. History of the logarithms. An example of the development of a concept in mathematics. pp. 1-9. (www.gobiernodecanarias.org).

Lexa, MA. 2013. Remembering John Napier and his logarithms. pp. 1-13. (www.see.ed.ac.uk/~mlexa/supportingdoc/mlexa_napier_revised.pdf).

Pierce, Rod. 2014. Complex Number Calculator. Math is Fun. (http://www.mathsisfun.com/numbers/complex-number-calculator.html).

Recheronline. 2010. http://rechneronline.de/function-graphs/

Roegel, D. 2012. Napier's ideal construction of logarithms. LOCOMAT project, the LORIA Collection of Mathematical Tables. (http://locomat.loria.fr/napier1619construction.pdf).

Thukral, AK. and Parkash, O. 2014. A new approach for the logarithms of real negative numbers. Canadian Journal of Pure and Applied Sciences. 8(2):2955-2961.

Wikipedia. 2014[a]. Logarithm. pp. 1-20. (http://en.wikipedia.org/wiki/Logarithm).

Wikipedia. 2014[b]. Contributions of Leonhard Euler to mathematics.1-6. (http://en.wikipedia.org/wiki/Contributions_of_Leonhard_Euler_to_mathematics).

Wikipedia. 2014[c]. Complex number. pp. 1-25. En.wikipedia.org/wiki/Complex_number.

Received: June 4, 2014; Accepted: July 3, 2014

SENRA Academic Publishers, British Columbia
Vol. 8, No. 3, pp. 3139-3145, October 2014
Online ISSN: 1920-3853; Print ISSN: 1715-9997

Canadian Journal of pure&applied sciences

AN EXAMINATION OF ZERO-ORDER MODES OF PLATE PEM-SH DISPERSIVE ACOUSTIC WAVES: MAGNETICALLY OPEN AND ELECTRICALLY CLOSED PLATE SIDES

A A Zakharenko
International Institute of Zakharenko Waves (IIZWs)
Address: 660037, Krasnoyarsk-37, 17701, Krasnoyarsk, Russia

ABSTRACT

This report copes with the examination of dispersive shear-horizontal (SH) wave propagation in the piezoelectromagnetic (PEM) thin film. The studied plate must represent an anisotropic solid with bulk properties. Its symmetry must be hexagonal pertaining to 6 *mm* point group of crystal symmetries. The changes in the velocities of the inspected dispersive waves versus the dimensionless plate thickness *kd* are graphically examined for some values of the coefficient of the magnetoelectromechanical coupling (CMEMC). The obtained results have clarified that the inspected waves are slightly dispersive when the CMEMC < 0.2. The dispersion must be significant for larger values. It was found that the zero-order mode of one inspected dispersive wave can commence only at some $kd > 0$. The same mode of the second inspected dispersive wave can begin at $kd = 0$. For a very large value of *kd*, the wave velocities approach the speed of the nondispersive surface Bleustein-Gulyaev-Melkumyan wave. Also, these academic results can be useful for design of dispersive wave technical devices: chemi-bio-sensors, labs on tiny chips, filters, dispersive delay lines, etc., and their further prospective miniaturization.

PACS: 74.25.Ld, 81.70.Cv, 68.60.Bs, 51.40.+p, 75.80.+q, 62.65.+k, 75.20.En, 68.35.Gy

Keywords: Magneto-electro-elastic thin film, magnetoelectric effect, dispersive acoustic anti-plane waves, zero-order modes.

INTRODUCTION

These theoretical examinations are based on and develop the achievements recently obtained in book (Zakharenko, 2012a). This is constructive because allow one to get more complete picture of the behavior of some dispersive waves recognized as the shear-horizontally (SH) polarized processes flowing inside thin solid films, also known as piezoelectromagnetic (PEM) plates. This study uses only the homogeneous case: the lower and upper faces of the PEM plate can be mechanically, electrically, and magnetically conditioned in the same manner. Thus, the mechanical condition at the plate faces is called the mechanically free surface. Besides, the magnetic and electrical ones are the magnetically open and electrically closed surfaces, respectively. The comprehension of assorted boundary conditions is perfectly stated in 1992 by Al'shits *et al*.

The PEM composites, also known as the magneto-electro-elastics are multi-promising for modern employments in a set of technological arenas. These smart solids can concurrently enjoy several effects such as magnetoelectric (ME), piezomagnetic (PM), piezoelectric (PE). Accordingly, these effects and smart solid compounds are reviewed in the academic literature cited in Kimura (2012), Park and Priya (2012), Pullar (2012), Bichurin *et al*. (2012), Zakharenko (2013a), Chen *et al*. (2012), Bichurin *et al*. (2011), Srinivasan (2010), Özgür *et al*. (2009), Zhai *et al*. (2008), Nan *et al*. (2008), Eerenstein *et al*. (2006), Fiebig (2005), Spaldin and Fiebig (2005), Kimura (2007), Kimura *et al*. (2003), Wang *et al*. (2009), Ramesh (2009), Delaney *et al*. (2009), Gopinath *et al*. (2012), Fert (2008), Chappert and Kim (2008), Bibes and Barthélémy (2008), Priya *et al*. (2007), Grossinger *et al*. (2008); Ahn *et al*. (2009); Fang *et al*. (2008) and Prellier (2005).

Today there are the trends toward device microminiaturization and multifunctionality. Therefore, various multiferroic solids that can combine two or more ferroic attributes have been widely applied to sensing, actuating, and storage devices (Nan *et al*., 2008; Eerenstein *et al*., 2006). PEM composites, as one typical nature of multiferroic matter, have attracted intensive attention in the last decades because they can possess a large ME constant (Fiebig, 2005; Spaldin and Fiebig, 2005). For that reason, various theoretical and experimental investigations have been carried out on the mechanical behavior of such multiphase compounds in the form of different representative structures. The understanding of wave propagation behavior in the composites (Fiebig, 2005) is very important in designs of acoustic wave devices and related applications.

Corresponding author email: aazaaz@inbox.ru

It is evident that the PEM solid can be used together or instead of PE or PM solid. It is also apparent that the PEMs are excellent candidates for smart matter technical devices (Özgür *et al*., 2009; Fiebig, 2005) because they possesses electrical, magnetic, and mechanical subsystems and it is possible to control the electrical subsystem by the magnetic one through the mechanical one. The ME solids can be divided into two groups: monocrystals and composites. The relatively large ME effect was revealed in several PEM monocrystals such as Cr_2O_3 (Fiebig, 2005), $LiCoPO_4$ (Rivera, 1994), $TbPO_4$ (Rado *et al*., 1984). However, ME compounds can exhibit a significantly larger ME effect. They possess both the magnetic and electric phases. The famous candidates for the PM phase are Terfenol-D and Metglas and PZT is fitting as the PE phase.

ME multiferroics can couple electric and magnetic dipoles (Kimura, 2012) and so, have a big potential for expected ME devices. Modern discoveries have revealed that ferroelectricity can be induced by complex internal arrangements of magnetic moments in magnetically induced ferroelectrics. Such ferroelectrics can demonstrate giant ME effects: the changes in ferroelectric polarization as soon as an external magnetic field acts. However, none of them can have combined big electric and magnetic polarizations at ~ 20^oC, but the $Sr_3Co_2Fe_{24}O_{41}$ Z-type hexaferrite (Kitagawa *et al*., 2010). A comprehensive review of M, W, X, Y, Z, and U-type hexaferrites can be found in (Pullar, 2012).

A set of wave phenomena in solids can be studied in the frameworks of the multidisciplinary modern ultrasonics (Ensminger and Bond, 2012). Ultrasonics includes the basic science of the energy-matter interaction, the associated technologies for generation and detection, and an increasingly diverse range of applications, which are now encountered in almost every field of engineering, many of the sciences and in medicine. It is also well-known that different SH-SAWs can be produced by the electromagnetic acoustic transducers (EMATs) (Ribichini *et al*., 2010). The noncontact methods such as the EMAT can offer a series of advantages in comparison with the traditional piezoelectric transducers (Thompson, 1990; Hirao and Ogi, 2003).

However, the PEs are widely used, probably, due to the fact that their properties are well-known compared with the PEM solids. For instance, Fu *et al*. (2010) have represented recent developments on the application of ZnO films (6 *mm* PEs) for microfluidics and biosensors based on acoustic waves. Tan *et al*. (2010) have presented a numerical-experimental study of capillary wave motion excited by high frequency SAWs. The plate wave technical devices (Rocha-Gaso *et al*., 2009) can be also used because the interdigital transducers can be formed on the lower side of the plate and the upper side can be in a contact with a fluid. It is thought that employment of suitable PEM thin films can also give a significant rise to various investigations of the complex biosystems. Thus, it is necessary to be familiar with the SAW and plate wave characteristics of the smart substances that can be also apt for wireless tools. Wireless sensing tools (Rocha-Gaso *et al*., 2009) can have the following applications: engine metrology, safety, tracing and tracking, internal and external monitoring, etc. In addition, passive sensors can really have a big potential: it is expected that they can successively replace existing sensors and actually create new sensing applications.

According to recent review (Giannitsis, 2011), chip-like laboratories are a group of miniaturized analytical devices that integrate fluidics, electronics, sensorics, and they are capable of analyzing biochemical liquid samples: solutions of metabolites, proteins, macromolecules, nucleic acids, viruses. In addition to their measuring capabilities, these complex laboratories-devices can facilitate fluidic transportation, mixing, sorting, separation of liquids. It is also possible to mention that the SAWs can result in exhibition of the acoustowetting phenomenon (Rezk *et al*., 2012a) when the SAW propagation causes the formation of a liquid layer from a fluid drop situated on the solid surface. Recent work (Rezk *et al*., 2012b) has studied paper-based microfluidics and stated that it can offer an alternative to typical polymers. Review work (Fair, 2007) discusses the suitability of electrowetting-on-dielectric microfluidics for applications in true chip-like labs. It is well-known that microfluidic devices can offer unique advantages in sample handling, reagent mixing, separation, and detection. Flow-injection analysis method, techniques of microconstruction, and microfluidics are reviewed in (Weigl *et al*., 2003) and interesting work (Yoon and Kim, 2012) reviews pathogen chip-like lab sensors for food safety.

This examination acquaints the reader with some recent accomplishments in the field of the acoustic wave propagation in the PEM thin films. The wave propagation can possess some peculiarities that must be recorded for the research community to make use of the PEM matter in a list of smart practical devices: actuators, filters, sensors, MEMs, laboratories on chips, etc.

THEORETICAL PART AND RESULTS

The theory of the shear-horizontally (SH) polarized wave processes in the 6 *mm* PEM plates is given in (Zakharenko, 2012a). This theory naturally starts with the consideration of the suitable thermodynamic variables and functions, writes the corresponding constitutive relations, and thermodynamically defines the PEM material constants. Next, the mechanical equilibrium equations must be written together with the Maxwell equations for

electrostatics and magnetostatics in the quasi-static approximation. The coupled equations of motion in the differential forms can be then constituted. With the solutions in the plane wave form for them, the tensor form of the equations of motion can be represented.

It is now necessary to discuss the suitable propagation direction in order to cope with propagation of pure waves (Lardat *et al*., 1971; Dieulesaint and Royer, 1980) with the anti-plane polarization (perpendicular to the sagittal plane.) The propagations of pure SH-waves are possible only in the high symmetry directions (Lardat *et al*., 1971; Dieulesaint and Royer, 1980). For the hexagonal (6 *mm*) solids (Nye, 1989, Newnham, 2005, Lovett, 1999, Auld, 1990) the wave process direction must be parallel to the free surface and perpendicular to both the surface normal and the six fold symmetry axis. The mentioned normal must be also perpendicular to the mentioned axis. All such apt propagation directions are true for PEs, PMs, and PEMs when they relate to the broaden family of the 6 *mm* solids. In these directions, the PEM SH-wave process must also attach the magnetic (ψ) and electrical (φ) potentials.

Using the coupled equations of motion written in the tensor form and the suitable high symmetry propagation direction in the PEM plate, it is possible to find the eigenvalues and the corresponding eigenvectors (Zakharenko, 2013b; Zakharenko, 2013c; Zakharenko, 2014) for the problem of the SH-wave propagation. Also, it is worth noting that in such direction, the following independent nonzero material constants exist: the stiffness constant C, PM coefficient h, PE constant e, dielectric permittivity coefficient ε, magnetic permeability coefficient μ, and electromagnetic constant α, where $C = C_{44} = C_{66}$, $e = e_{16} = e_{34}$, $h = h_{16} = h_{34}$, $\varepsilon = \varepsilon_{11} = \varepsilon_{33}$, $\mu = \mu_{11} = \mu_{33}$, and $\alpha = \alpha_{11} = \alpha_{33}$ (Zakharenko, 2010; Zakharenko, 2012a; Zakharenko, 2012b). The found eigenvalues and eigenvectors are employed to figure the complete mechanical displacement, complete magnetic and electrical potentials dependent on the weight factors that can be calculated treating the boundary conditions. The mechanical, electrical, and magnetic boundary conditions for the lower and upper PEM plate sides are as follows: the mechanically free, electrically closed ($\varphi = 0$), and magnetically open ($\psi = 0$) faces. The boundary conditions in the case when the treated medium concurrently owns the PM, PE, and ME effects are perfectly recorded by Al'shits *et al*. (1992). With the book by Zakharenko (2012a), the following dispersion relation for the determination of the phase velocity V_{new1} of the first new plate SH-wave can be written:

$$\sqrt{1-\left(V_{new1}/V_{tem}\right)^2}\tanh(kd)-\frac{K_{em}^2}{1+K_{em}^2}\tanh\left(kd\sqrt{1-\left(V_{new1}/V_{tem}\right)^2}\right)=0 \tag{1}$$

where kd is the normalized plate thickness: k and d are the wavenumber in the direction of wave process propagation and the plate half-thickness, respectively.

The dispersion relation written above pertains to the case when the velocity V_{new1} is smaller than the SH bulk acoustic wave (BAW) speed V_{tem} tied with the magnetic and electrical potentials. This is the case of the lowest or zero-order mode. The V_{tem} is defined by

$$V_{tem}=\sqrt{C/\rho}\left(1+K_{em}^2\right)^{1/2} \tag{2}$$

where ρ is the mass density.

In expressions (1) and (2), K_{em}^2 stands for the coefficient of the magnetoelectromechanical coupling (CMEMC) that equals to

$$K_{em}^2=\frac{\mu e^2+\varepsilon h^2-2\alpha e h}{C\left(\varepsilon\mu-\alpha^2\right)} \tag{3}$$

For this set of the boundary conditions mentioned above, it is necessary to state that there is the second dispersion relation (Zakharenko, 2012a). For the case when the propagation velocity is smaller than the speed V_{tem}, the second dispersion relation can be extra determined. The velocity V_{new2} for the second-type lowest mode ($V_{new2} < V_{tem}$) of the second new plate SH-wave can be calculated with the following formula:

$$\tanh\left(kd\sqrt{1-\left(V_{new2}/V_{tem}\right)^2}\right)\sqrt{1-\left(V_{new2}/V_{tem}\right)^2}-\frac{K_{em}^2}{1+K_{em}^2}\tanh(kd)=0 \tag{4}$$

One can find in (1) and (4) that for a very big value of kd, the velocities V_{new1} and V_{new2} for both the new plate SH-waves will approach the SH-SAW velocity corresponding to the surface Bleustein-Gulyaev-Melkumyan (BGM) wave (Melkumyan, 2007; Zakharenko, 2011). The speed of the nondispersive BGM-wave can be evaluated with the following explicit formula:

$$V_{BGM}=V_{tem}\left[1-\left(\frac{K_{em}^2}{1+K_{em}^2}\right)^2\right]^{1/2} \tag{5}$$

The main purpose of this report is to examine the behaviors of the velocities V_{new1} and V_{new2} versus the dimensionless parameter kd. These dependencies of $V_{new1}(kd)$ and $V_{new2}(kd)$ are defined by dispersion relations (1) and (4) that can be investigated only numerically. Also, it is convenient to carry out the numerical study for different values of K_{em}^2 which couples all the PEM

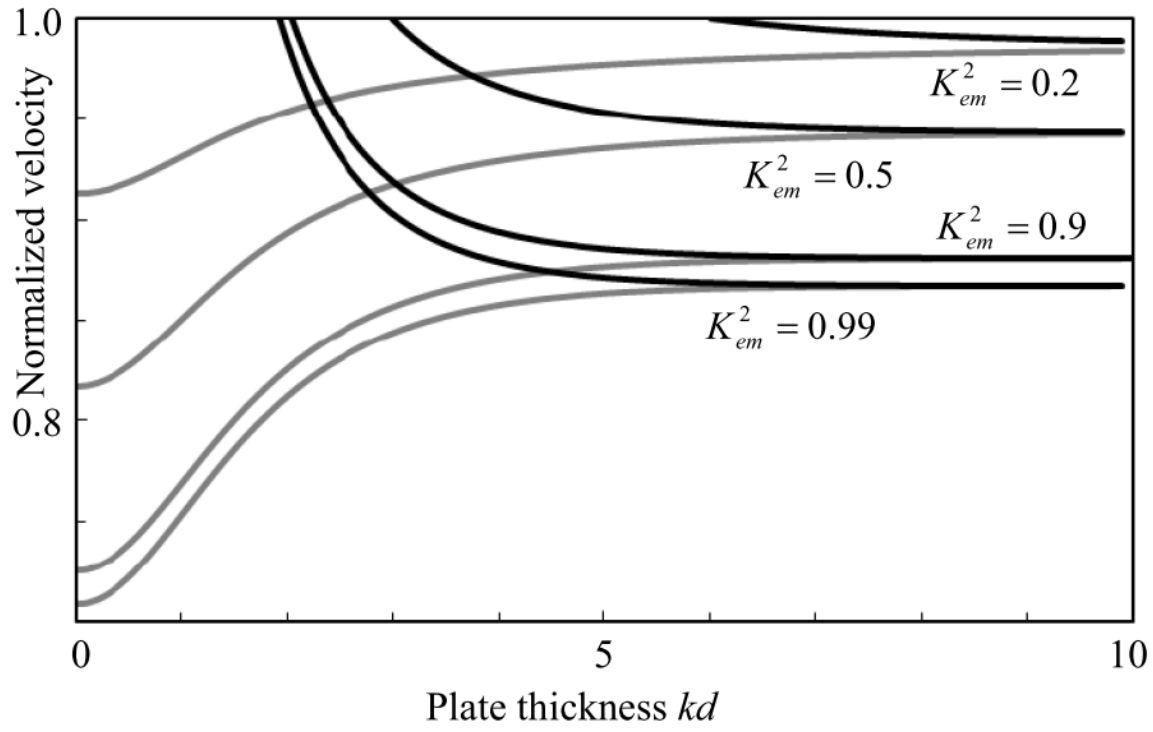

Fig. 1. The zero-order modes for K_{em}^2 several values: the normalzed velocities V_{new1}/V_{tem} and V_{new2}/V_{tem} are shown by the black and grey lines, respectively.

constants, see formula (3). In the book by Zakharenko (2012a), the dependencies of $V_{new1}(kd)$ and $V_{new2}(kd)$ for the lowest modes were performed only for K_{em}^2 = 0.3. The study of book (Zakharenko, 2012a) is incomplete because the following questions remain: what is the *kd* threshold minimum for the first lowest mode corresponding to the V_{new1} and what is the minimum value of the V_{new2} of the second lowest mode for $kd \rightarrow 0$. It is also essential to say that $K_{em}^2 < 1$.

Figure 1 shows the dependence of the normalized velocities V_{new1}/V_{tem} and V_{new2}/V_{tem} of the new dispersive SH-waves propagating in the 6 *mm* PEM plate. The figure graphically shows the zero-order mode dispersion relations for K_{em}^2 = 0.2, 0.5, 0.9, 0.99. The velocities V_{new1}/V_{tem} and V_{new2}/V_{tem} are shown by the black and grey lines, respectively. First of all, it is necessary to state that at very big values of *kd*, the values of both the velocities approach the value of the surface BGM-wave. It is also clearly seen in the figure that for a relatively small value of K_{em}^2 = 0.2, the values of the velocities are situated quite close to the value of the V_{tem} (2). This is so due to the fact that for a small K_{em}^2, the value of V_{BGM} (5) is situated slightly below the value of V_{tem}. For K_{em}^2 = 0.2, the velocity V_{new1} starts at *kd* ~ 6.0 and the relation V_{BGM}/V_{tem} is ~ 0.986. For large values of K_{em}^2 = 0.9 and 0.99, this mode shown by the black lines starts at *kd* ~ 2.04 and ~ 1.92, respectively. Therefore, it is possible to state that this report has determined the minimum threshold value of *kd* ~ 1.9. This is a quite large value.

It is also possible to further analyze the behavior of the second zero-order mode shown by the grey lines. For K_{em}^2 = 0.2, the V_{new2} starts with the minimum value of V_{new2}/V_{tem} ~ 0.913 at *kd* = 0 and can reach V_{BGM}/V_{tem} at a big *kd*. This means that the second lowest mode with such small value of K_{em}^2 = 0.2 cannot exist below the minimum value of V_{new2}/V_{tem} ~ 0.913. Therefore, the V_{tem} value must be certainly large to deal with significant velocity dispersion. For K_{em}^2 = 0.9 and 0.99, the second lowest mode starts at *kd* = 0 with the following minimum values: V_{new2}/V_{tem} ~ 0.726 and V_{new2}/V_{tem} ~ 0.709. This means that the velocity V_{new2} cannot have values smaller than ~ $0.7V_{tem}$. This is very important finding and differs this type of the dispersive SH-wave with the anti-plane polarization from the dispersive Lamb type waves with the in-plane polarization because the Lamb wave asymmetric mode starts with zero speed at *kd* = 0.

Based on the results revealed in this work, it is also possible to discuss some 6 *mm* PEM composites. The material characteristics of the $BaTiO_3$-$CoFe_2O_4$ composites can be borrowed from (Aboudi, 2001; Annigeri *et al*., 2006). These compounds can be classified as the composites with (0-3) connectivity when the 3D matrix consisting of the $BaTiO_3$ PE phase or the $CoFe_2O_4$ PM phase has the PM or PE 0D inclusions, respectively. For the $BaTiO_3$-$CoFe_2O_4$ composites with 20% and 80% volume part of $BaTiO_3$, the V_{BGM} values (~2794.045 m/s and ~2956.340 m/s) are very close to the corresponding V_{tem} values (~2794.094 m/s and ~2956.343 m/s) and K_{em}^2 << 0.2. Therefore, the plate SH-waves characterized by the velocities V_{new1} and V_{new2} will be weakly dispersive and the velocity V_{new1} for the first lowest mode can start at $kd >> 6.0$. On the other hand, it is also possible to discuss the other composite plate such as PZT-5H–Terfenol-D with the (2-2) connectivity when the 2D planes of the PZT-5H PE phase and the Terfenol-D PM phase follow each other to form a sandwich structure. It has K_{em}^2 ~ 0.788, V_{tem} ~ 1746.253 m/s, and V_{BGM} ~ 1644.243 m/s (Wang and Mai, 2007; Liu and Chue, 2006; Zakharenko, 2012c). This value of K_{em}^2 is close to 0.9 shown in the figure. Therefore, it is possible to say that using figure 1, it is possible to compare different composites. It is also possible to state that to study the PEM plates instead of the corresponding bulk solids is more preferable because at $kd \rightarrow 0$ the V_{new2} values can be significantly smaller than the V_{BGM} value. This fact can be convenient for experimentalists to study these waves. Also, it is obvious that the PEM plates can be used to further miniaturize the technical devices based on such smart matter. Indeed, they are good candidate to constitute new technical devices. The most famous tools on the dispersive SH-waves are delay lines, bio-chemi-sensors, and the devices with a higher level of integration: chip-like complex laboratories, etc. These waves can be readily generated and detected in the noncontact manner with the electromagnetic acoustic transducers (Ribichini *et al*., 2010; Thompson, 1990; Hirao and Ogi, 2003).

Finale note

For any peculiarities' documentation, this analysis of the dispersive wave propagation (anti-plane polarized zero-order modes) in the solid magneto-electro-elastic plates was carried out for several K_{em}^2 values. It was solidly recorded that the propagation velocity cannot be equal to zero even for $kd = 0$ and when $K_{em}^2 \sim 1$. With $K_{em}^2 \sim 1$, the corresponding inspected wave velocity approaches some original velocity ~ $0.7V_{tem}$ at $kd = 0$. Concerning the second inspected wave process, the velocity never starts at $kd = 0$ for the reason that this zero-order mode is connected with the other branch existing above the V_{tem}. For a large K_{em}^2, both the inspected wave velocities approach the BGM wave rapidity. Also, these discussions can be useful in the constitution of list of dispersive wave technical tools. The delay lines can be the right application. Besides, the anti-plane polarized waves are exhaustively exploited to constitute sensors, filters, smart matter technical devices, complex laboratories on a single chip, etc., and can supplementary develop the device miniaturization.

REFERENCES

Aboudi, J. 2001. Micromechanical analysis of fully coupled electro-magneto-thermo-elastic multiphase composites. Smart Materials and Structures. 10(5):867-877.

Ahn, CW., Maurya, D., Park, CS., Nahm, S. and Priya, S. 2009. A generalized rule for large piezoelectric response in perovskite oxide ceramics and its application for design of lead-free compositions. Journal of Applied Physics. 105(11):114108, pp6.

Al'shits, VI., Darinskii, AN. and Lothe, J. 1992. On the existence of surface waves in half-infinite anisotropic elastic media with piezoelectric and piezomagnetic properties. Wave Motion. 16(3):265-283.

Annigeri, AR., Ganesan, N. and Swarnamani, S. 2006. Free vibrations of simply supported layered and multiphase magneto-electro-elastic cylindrical shells. Smart Materials and Structures. 15(2):459-467.

Auld, BA. 1990. Acoustic Fields and Waves in Solids. Krieger Publishing Company (vol. I and II, 2nd edi.). pp878.

Bibes, M. and Barthélémy, A. 2008. Multiferroics: Towards a magnetoelectric memory. Nature Materials. 7(6):425-426.

Bichurin, M., Petrov, V., Zakharov, A., Kovalenko, D., Yang, SCH., Maurya, D., Bedekar, V. and Priya, SH. 2011. Magnetoelectric interactions in lead-based and lead-free composites. Materials. 2011(4):651-702.

Bichurin, MI., Petrov, VM. and Petrov, RV. 2012. Direct and inverse magnetoelectric effect in layered composites in electromechanical resonance range: A review. Journal of Magnetism and Magnetic Materials. 324(21):3548-3550.

Chappert, C. and Kim, JV. 2008. Metal spintronics: Electronics free of charge. Nature Physics. 4(11):837-838.

Chen, T., Li, S. and Sun, H. 2012. Metamaterials application in sensing. MDPI Sensors. 12(3):2742-2765.

Delaney, KT., Mostovoy, M. and Spaldin, NA. 2009. Superexchange-driven magnetoelectricity in magnetic vertices. Physical Review Letters. 102(15):157203.

Dieulesaint, E. and Royer, D. 1980. Elastic waves in solids: Applications to signal processing. J. Wiley, New York, USA. (Translated by Bastin, A. and Motz, M., Chichester). pp511.

Eerenstein, W., Mathur, ND. and Scott, JF. 2006. Multiferroic and magnetoelectric materials. Nature. 442(7104):759-765.

Ensminger, D. and Bond, LJ. 2012. Ultrasonics: Fundamentals, Technologies, and Applications. (3rd edi.). A series of textbooks and reference books on mechanical engineering. Ed. Faulkner, LL. CRC Press: Taylor & Francis Group, Boca Raton – London – New York. pp728.

Fair, RB. 2007. Digital microfluidics: is a true lab-on-a-chip possible? Microfluid and Nanofluid. 3(3):245-281.

Fang, D., Wan, YP., Feng, X. and Soh, AK. 2008. Deformation and fracture of functional ferromagnetic. ASME Applied Mechanics Review. 61(2):020803. pp23.

Fert, A. 2008. Origin, development, and future of spintronics (Nobel lectures). Reviews of Modern Physics. 80(4):1517-1530.

Fiebig, M. 2005. Revival of the magnetoelectric effect. Journal of Physics D: Applied Physics. 38(8):R123-R152.

Fu, YQ., Luo, JK., Du, XY., Flewitt, AJ., Li, Y., Markx, GH., Walton, AJ. and Milne, WI. 2010. Recent developments on ZnO films for acoustic wave based biosensing and microfluidic applications: A review. Sensors and Actuators B: Chemical. 143(2):606-619.

Giannitsis, AT. 2011. Microfabrication of biomedical lab-on-chip devices. A review. Estonian Journal of Engineering. 17(2):109-139.

Gopinath, SCB., Awazu, K. and Fujimaki, M. 2012. Waveguide-mode sensors as aptasensors. MDPI Sensors. 12(2):2136-2151.

Grossinger, R., Duong, GV. and Sato-Turtelli, R. 2008. The physics of magnetoelectric composites. Journal of Magnetism and Magnetic Materials. 320(14):1972-1977.

Hirao, M. and Ogi, H. 2003. EMATs for science and industry: Non-contacting ultrasonic measurements. Boston, MA, Kluwer Academic.

Kimura, T., Goto, T., Shintani, H., Ishizaka, K., Arima, T. and Tokura, Y. 2003. Magnetic control of ferroelectric polarization. Nature. 426(6962):55-58.

Kimura, T. 2007. Spiral magnets as magnetoelectrics. Annual Review of Materials Research. 37(1):387-413.

Kimura, T. 2012. Magnetoelectric hexaferrites. Annual Review of Condensed Matter Physics. 3(1):93-110.

Kitagawa, Y., Hiraoka, Y., Honda, T., Ishikura, T., Nakamura, H. and Kimura, T. 2010. Low-field magnetoelectric effect at room temperature. Nature Materials. 9(10):797-802.

Lardat, C., Maerfeld, C. and Tournois, P. 1971. Theory and performance of acoustical dispersive surface wave delay lines. Proceedings of the IEEE. 59(3):355-364.

Liu, TJCh. and Chue, ChH. 2006. On the singularities in a bimaterial magneto-electro-elastic composite wedge under antiplane deformation. Composite Structures. 72(2):254-265.

Lovett, DR. 1999. Tensor properties of crystals. (2nd edi.). Taylor and Francis. pp480.

Melkumyan, A. 2007. Twelve shear surface waves guided by clamped/free boundaries in magneto-electro-elastic materials. International Journal of Solids and Structures. 44(10):3594-3599.

Nan, CW., Bichurin, MI., Dong, SX., Viehland, D. and Srinivasan, G. 2008. Multiferroic magnetoelectric composites: Historical perspective, status, and future directions. Journal of Applied Physics. 103(3):031101.

Newnham, RE. 2005. Properties of Materials: Anisotropy, Symmetry, Structure. (Kindle edi.). Oxford University Press Inc., Oxford-New York. pp391.

Nye, JF. 1989. Physical Properties of Crystals. Their Representation by Tensors and Matrices. Oxford, Clarendon Press. pp385.

Özgür, Ü., Alivov, Ya. and Morkoç, H. 2009. Microwave ferrites, part 2: Passive components and electrical tuning. Journal of Materials Science. Materials in Electronics. 20(10):911-952.

Park, ChS. and Priya, Sh. 2012. Broadband/Wideband Magnetoelectric Response. Advances in Condensed Matter Physics. Hindawi Publishing Corporation. 2012:323165. pp12.

Prellier, W., Singh, MP. and Murugavel, P. 2005. The single-phase multiferroic oxides – from bulk to thin film. Journal of Physics: Condensed Matter. 17(30):R803-R832.

Priya, S., Islam, RA., Dong, SX. and Viehland, D. 2007. Recent advancements in magnetoelectric particulate and laminate composites. Journal of Electroceramics. 19(1):147-164.

Pullar, RC. 2012. Hexagonal ferrites: A review of the synthesis, properties and applications of hexaferrite ceramics. Progress in Materials Science. 57(7):1191-1334.

Rado, GT., Ferrari, JM. and Maisch, WG. 1984. Magnetoelectric susceptibility and magnetic symmetry of magnetoelectrically annealed $TbPO_4$. Physical Review B. 29(7):4041-4048.

Ramesh, R. 2009. Materials science: Emerging routes to multiferroics. Nature. 461(7268):1218-1219.

Rezk, AR., Manor, O., Friend, JR. and Yeo, LY. 2012[a]. Unique fingering instabilities and soliton-like wave propagation in thin acoustowetting films. Nature Communications. 3:1167. pp7.

Rezk, AR., Qi, A., Friend, JR., Li, WH. and Yeo, LY. 2012[b]. Uniform mixing in paper-based microfluidic systems using surface acoustic waves. Lab on a Chip. 12(4):773-779.

Ribichini, R., Cegla, F., Nagy, PB. and Cawley, P. 2010. Quantitative modeling of the transduction of electromagnetic acoustic transducers operating on ferromagnetic media. IEEE Transactions on Ultrasonics, Ferroelectrics, and Frequency Control. 57(12):2808-2817.

Rivera, JP. 1994. The linear magnetoelectric effect in $LiCoPO_4$ revisited. Ferroelectrics. 161(1):147-164.

Rocha-Gaso, MI., March-Iborra, C., Montoya-Baides, Á. and Arnau-Vives, A. 2009. Surface generated acoustic wave biosensors for the detection of pathogens: A review. MDPI Sensors. 9(7):5740-5769.

Spaldin, NA. and Fiebig, M. 2005. The renaissance of magnetoelectric multiferroics. Science. 309(5733):391-392.

Srinivasan, G. 2010. Magnetoelectric composites. Annual Review of Materials Research. 40(1):153-178.

Tan, MK., Friend, JR., Matar, OK. and Yeo, LY. 2010. Capillary wave motion excited by high frequency surface acoustic waves. Physics of Fluids. 22(11):112112.

Thompson, RB. 1990. Physical principles of measurements with EMAT transducers. In: Physical Acoustics. Eds. Mason WP. and Thurston, RN. Academic Press, New York, USA. 19:157-200.

Wang, BL. and Mai, YW. 2007. Applicability of the crack-face electromagnetic boundary conditions for fracture of magnetoelectroelastic materials. International Journal of Solids and Structures. 44(2):387-398.

Wang, KF., Liu, JM. and Ren, ZF. 2009. Multiferroicity: The coupling between magnetic and polarization orders. Advances in Physics. 58(4):321-448.

Weigl, BH., Bardell, RL. and Cabrera, CR. 2003. Lab-on-a-chip for drug development. Advanced Drug Delivery Reviews. 55(3):349-377.

Yoon, JY. and Kim, BS. 2012. Lab-on-a-chip pathogen sensors for food safety. MDPI Sensors. 12(8):10713-10741.

Zakharenko, AA. 2010. Propagation of seven new SH-SAWs in piezoelectromagnetics of class 6 *mm*. LAP LAMBERT Academic Publishing GmbH & Co. KG, Saarbruecken-Krasnoyarsk. pp84.

Zakharenko, AA. 2011. Analytical investigation of surface wave characteristics of piezoelectromagnetics of class 6 *mm*. ISRN Applied Mathematics (India). 2011:408529. pp8.

Zakharenko, AA. 2012[a]. Thirty two new SH-waves propagating in PEM plates of class 6 *mm*. LAP LAMBERT Academic Publishing GmbH & Co. KG, Saarbruecken-Krasnoyarsk. pp162.

Zakharenko, AA. 2012[b]. Twenty two new interfacial SH-daves in Dissimilar PEMs. LAP LAMBERT Academic Publishing GmbH & Co. KG, Saarbruecken – Krasnoyarsk. pp148.

Zakharenko, AA. 2012[c]. On wave characteristics of piezoelectromagnetics. Pramana – Journal of Physics. 79(2):275-285.

Zakharenko, AA. 2013[a]. Piezoelectromagnetic SH-SAWs: A review. Canadian Journal of Pure & Applied Sciences. 7(1):2227-2240.

Zakharenko, AA. 2013[b]. Peculiarities study of acoustic waves' propagation in piezoelectromagnetic (composite) materials. Canadian Journal of Pure and Applied Sciences. 7(2):2459-2461.

Zakharenko, AA. 2013[c]. New nondispersive SH-SAWs guided by the surface of piezoelectromagnetics. Canadian Journal of Pure and Applied Sciences. 7(3):2557-2570.

Zakharenko, AA. 2014. Some problems of finding of eigenvalues and eigenvectors for SH-wave propagation in transversely isotropic piezoelectromagnetics. Canadian Journal of Pure and Applied Sciences. 8(1):2783-2787.

Zhai, J., Xing, ZP., Dong, Sh-X., Li, JF. and Viehland, D. 2008. Magnetoelectric laminate composites: An overview. Journal of the American Ceramic Society. 91(2):351-358.

Received: Jan 20, 2014; Revised: Sept 1, 2014: Accepted: Sept 6, 2014

SENRA Academic Publishers, British Columbia
Vol. 8, No. 3, pp. 3147-3153, October 2014
Online ISSN: 1920-3853; Print ISSN: 1715-9997

Canadian Journal of pure&applied sciences

A COMPARATIVE STUDY OF HEURISTIC AND METAHEURISTIC FOR THREE IDENTICAL PARALLEL MACHINES

*Omar Selt[1] and Rachid Zitouni[2]
[1]Department of Mathematics, University of M'sila, Algeria
[2]Laboratory of Fundamental and Numerical Mathematics, University of Setif 1, Algeria

ABSTRACT

In this paper, we propose a comparative study between metaheuristic and a new heuristic for solving scheduling problems of *n* tasks on *m* identical parallel machines with unavailability periods. This problem is NP-complete in the strong sense of the expression and finding an optimal solution appears unlikely. In this frame, we suggested a new heuristic in which availability periods of each machine are filled with the highest weighted tasks. To improve the performance of this heuristic, we used three diversification strategies (T_1, T_2 and T_3) with the aim of exploring unvisited regions of the solution space and two well-known neighborhoods (neighborhood by swapping and neighborhood by insertion). The computational experiment was carried out on three identical parallel machines with different availability periods. It must be noted that tasks movement can be within one machine or between different machines. Note that all data in this problem are integer and deterministic. The weighted sum of the end dates of tasks constitutes the optimization performance criterion in the problem treated in this paper.

Keywords: Scheduling, parallel identical machines, unavailability periods, metaheuristic, tabu search.

INTRODUCTION

A scheduling problem consists in organizing tasks realization time with consideration of time constraints (time limits, tasks series character) and constraints related to using and availability of required resources. The scheduling constitutes a solution to the considered problem, describes the tasks execution and resources location during time and aims to satisfy one or many objectives.

A scheduling problem under machines availability constraints has been studied by many authors. For example $P_m // N-\boldsymbol{C} // C_{\max}$ has been studied by Lee (1996, 1997, 1999), Schmidt (2000) and Yun-Chia *et al*. (2013). The tabu search is a metaheuristic originally developed by Glover (1986), Glover and Hanafi (2002) and independently by Hancen (1986).

This method combines a local search procedure with a certain number of rules and mechanism which allows surmounting the obstacle of local optima without cycling. Toward furthermore, it proved hight efficiently in resolution of the problems NP-complet and approximate more the optimal solution.

The scheduling problem of a single machine with minimization of the weighted sum of the end dates of tasks. without unavailability constraint is optimally resolved by using the WSPT (weighted shortest processing time) rules. The case of several machines is studied by many authors like Belouadeh *et al*. (1992), Sadfi (2002) and Haouari and Ladhari (2003).

In 1984, Schmidt has studied the scheduling problem of parallel identical machines with different unavailability intervals and different tasks deadlines. He used the method of Branch and Bound based on two procedures: the first is the generation by decomposition and cut approach and the second is the hybridization of procedures of generation by cut. He also built an admissible preemptive scheduling of a complexity $O(n/m \ln n)$ where n is the number of tasks and m is the number of machines. Lee (1999) have studied the simultaneous scheduling of production works and maintenance activities in parallel identical machines to minimize the weighted sum of the end dates of tasks. They have studied two cases: The first, with sufficient number of resources, concerns the case where several machines can be checked up simultaneously (overlap of unavailability periods). The second case, with insufficient number of resources, concerns the case where only one machine can be checked up (overlap of unavailability periods not allowed). They could demonstrate that even if all tasks have the same weight, the problem is NP-hard. They proposed the method of Branch and Bound based on the approach of columns generation to solve the two cases. They have published an experimental study on average size instances.

Zribi *et al*. (2005) have studied the problem

*Corresponding author email: selt.omar@yahoo.fr

$1//N-\boldsymbol{C}//\sum_{j=1}^{n} w_j C_j$ and have compared two exact methods: one is the Branch and Bound, the other is the integer programming.They have concluded that Branch and Bound method have better performance and it allowed resolving instances of more than 1000 tasks.

Another study Adamu and Adewunmi (2012) have studied the problem $P_m//\sum_{j=1}^{n} w_j\left(U_j+V_j\right)$, they proposed some metaheuristics for scheduling on parallel identical machines to minimize weighted number of early and tardy jobs.

In 2013, they carried out a comparative study of different (a genetic algorithm, particle swarm optimization and simulated annealing with their hybrids) metaheuristics for identical machines. In this paper, the results of Adamu and Adewunmi (2012) research works are exploited to develop a different new metaheuristic to solve the scheduling problem under different constraints.

PROBLEM STATEMENT

This problem consists in scheduling n tasks for m parallel identical machines $\{M_1, M_2, ..., M_m\}$ where $n >> m \geq 2$, with unavailability periods.

We assume that the tasks $\{j_1, j_2, ..., j_n\}$ are all available at $t=0$ and their operation times are independent from the choice of machines performing these tasks. In the generic case of the problem, each one of the m machines can show some unavailability periods during scheduling horizon and each task must be executed onetime.

This problem noted by $P_m//N-\boldsymbol{C}//\sum_{j=1}^{n} w_j C_j$ consists in assigning n tasks to m machines over availability intervals in a manner to enforce the weighted sum of the end dates of tasks. referred to as $\sum_{j=1}^{n} w_j C_j$ to be minimal.

It must be noted that there is $(n!)^m$ possibility to assign n tasks to m machines (Sakarovitch, 1984).

NEIGHBORHOOD STRUCTURE

Neighborhood determination constitutes the most important stage in metaheurstic methods elaboration. In the following part, we use two Neighborhoods, (neighborhood by swapping) and (neighborhood by insertion).

It must be noted that tasks movement can be within one machine or between different machines.

NEIGHBORHOOD BY SWAPPING

Definition. *Consider a sequence σ composed of n tasks. A neighborhood σ' is obtained by permuting two tasks. j and j' of respectively k and k' positions σ with $k' = k+1, k+2, ..., n$.*

The set :

$N_1(\sigma) = \{\sigma, \sigma \text{ is obtained by permutation of two tasks}\}$

is called neighborhood of σ This set is consequently obtained by permutation of all tasks of σ two by two.

Proposition. *Consider a sequence σ, the set's cardinal of $N_1(\sigma)$ is $\frac{n(n-1)}{2}$.*

Proof . The permutation of all tasks. two by two consists in permuting each task of the sequence with all remained tasks. without identical ones. The number of possible permutations in a sequence σ composed of n tasks. is : $(n-1)+(n-2)+..+2+1=\frac{n(n-1)}{2}$.

NEIGHBORHOOD BY INSERTION

Definition. *Consider a sequence σ composed of n tasks.*

A neighborhood σ' is obtained by inserting one task j of a position k in a new position k' in the sequence σ. The set

$N_2(\sigma) = \{\sigma', \sigma' \text{ is obtained by inserting a task of position } k \text{ in } k'\}$

is a neighborhood of σ. This set is consequently obtained by realizing all possible insertions of all tasks of σ.

Proposition. *Consider a sequence σ, the set's cardinal of $N_2(\sigma)$ is $(n-1)^2$.*

Proof . Inserting a task j of position k in an other position k' in the sequence σ allows getting $n-1$ possible insertions. Hence, for n tasks, there is $n(n-1)$ insertions to be done. To avoid getting identical sequences, adjacent tasks insertions are counted once. Consequently $n-1$ insertions will be deleted. Finally, the number of obtained insertions is: $n(n-1)-(n-1)=(n-1)^2$.

TABU LIST STRUCTURE

The tabu method is based on the principle that consists in maintaining in memory the last visited solutions and in forbidding the return to them for a certain number of iterations. The aim is to provide sufficient time to the algorithm so it can leave the local optimum. In other words, the tabu method conserves in each stage a list L of solutions (Tabu's) which it is forbidden to pass-by temporarily. The necessary space for saving a set of solutions tabus in the memory is indispensable.

The list, that we propose, contains the found solutions sequences. After many tests, a dynamic size list, which varies according to the search amelioration state, is conceived. The initial size of this list is considered to be $\frac{3\sqrt{n}}{2}$ where n is the tasks number. After that, during the search, when 5 successive iterations pass without amelioration of solution, the list is reduced to a number inferior or equal to $\sqrt{n}$. On the other hand, when 5 successive iterations pass and the solution is ameliorated, the list is increased to a number superior or equal to $2\sqrt{n}$. The Tabu list is consequently dynamic and its size varies within the interval $[\sqrt{n}, 2\sqrt{n}]$. The decrease or the increase of list size must always be done at the end of the list.

HEURISTIC FOR THE PROBLEM (P).

An initial solution is always necessary. For this reason, we suggest in this part the following heuristic: assigne the (best) task h where $\left(\frac{p_h}{w_h} = \min_{j \in J}\left\{\frac{p_j}{wj}\right\}\right)$ to the best machine (the most available[1]) based on two principles justified by the two following propositions :

Proposition 3. In an optimal scheduling, it is necessary to schedule the tasks. in each availability period of the machine according to the order SWPT.

Proof . It results directly by adjacent task exchange like used by Smith (1956) for the corresponding periods.

Proposition 4. It is not useful to let the machine (idle) if a task can be assigned to this machine.

Notations:

We denote by :

$J = \{1, 2, ..., n\}$: The set of tasks.

p_h : Execution time of the task h.

$p_h^{(i)}$: Execution time of the task h assigned to the machine $i \in I$.

$I = \{1, 2, ..., m\}$: The set of machines

I_{NA} : The set of non-assigned machines.

α : Number of availability zones.

$Z = \{1, 2, ..., \alpha\}$: Availability zones.

$S_z^{(i)}$ ($z \in Z$) : The beginning of the unavailability time of the machine $i \in I$.

T_F : Final time.

$T_z^{(i)}$ $(z \in Z)$: The end of the unavailability time of the machine $i \in I$.

$\sigma_z^{(i)}(z \in Z)$: The set of partial sequences assigned to the machine $i \in I$.

$\sigma_z = \sigma_z^{(1)} \cup \sigma_z^{(2)} \cup ... \cup \sigma_z^{(m)}$.

$$J_z^{(i)}(z \in Z) = \left\{ \begin{matrix} j \,/\, j \text{ task assigned to the machine } i \\ \text{with } T_z^{(i)} \le C_j^{(i)} \le S_z^{(i)} \end{matrix} \right\}.$$

$C_z^{(i)}$ $(z \in Z)$: Execution time of the task $j \in J_z^{(i)}$.

We assume that for each task $h \in J$, there is at least one machine $i \in I$ such that $P_h \le S_z^{(i)} - T_z^{(i)}$.

FORMULATIONS MATHEMATICS

Consider $I = \{1, 2, ..., m\}$, $J = \{1, 2, ..., n\}$,
$\sigma = (\sigma(1), \sigma(2), ..., \sigma(n))$ a sequence of n tasks. and **P** the set of all possible sequences permutations.
This problem is formulated as an integer linear programming model:

$$f = \min_{\sigma \in \mathbf{P}} \sum_{j=1}^{n} w_{\sigma(j)} C_{\sigma(j)}$$

$$(P) \quad \sum_{j \in \sigma_{(j)}^{(i)}} p_{\sigma(j)}^{(i)} \le S_z^{(i)} \quad , \tag{1}$$

$$S_z^{(i)} \in \mathrm{N};\ z = 1, 2, ..., \alpha;\ \sigma(j) = \sigma_{(j)}^{(1)} \cup \sigma_{(j)}^{(2)} \cup ... \cup \sigma_{(j)}^{(i)}$$

$$C_{\sigma(j)}^{(i)} = \sum_{j \in \sigma_{(j)}^{(i)}} p_{\sigma(j)}^{(i)} + T_z^{(i)} \quad , T_z^{(i)} \in \mathrm{N}; \tag{2}$$

$$i = 1, 2, ..., m;\ j = 1, 2, ..., n \tag{3}$$

$$\sum_{\substack{j=1,2,..,n \\ z=1,2,..,\alpha}} X_{j_z} = 1 \text{ and } X_{j_z} \in \{0, 1\}$$

ALGORITHM

Initialization

$J = \{1, 2, ..., n\}$, $I = \{1, 2, ..., m\}$; $Z = \{1, 2, ..., \alpha\}$; $I_{NA} = I$;

$S_\alpha^{(i)} = T_F$ (given), $\sigma = \phi$, $f_\sigma = 0$, $z = 1, C_z^{(i)} = 0$ and $T_1^{(i)} = 0$.

Sort task $h \in J$ in increasing order according to the criterion p_h / w_h in a list L_1

Sort task $h \in J$ in increasing order according to the criterion p_h in a list L_2

While

$(L_1 \neq \phi \text{ and } z \le \alpha)$ **do**

Begin

[1] A machine is supposed to be the most available if it has an availability period the most close to t=0 and it is able to realize the required task.

Set $p_{h_1} = p_h / w_h$ from the top list of L_1.
$p_{h_2} = p_h$ from the top list of L_2.

Determine the machine $k \in I_{NA}$ and the task $h \in J$ such that
$S_z^{(k)} - C_z^{(k)} = \max_{i \in I_{NA}} \{S_z^{(i)} - C_z^{(i)}\} >= \min(p_{h_1}, p_{h_2})$
If $\{k\} = \phi$ **then**

Determine the machine $k \in I$ and the task $h \in J$ such that
$S_z^{(k)} - C_z^{(k)} = \max_{i \in I} \{S_z^{(i)} - C_z^{(i)}\} >= \min(p_{h_1}, p_{h_2})$

Endif
If $\{k\} \neq \phi$ **then**
Begin
Assigned the task h to the machine k
Delete the task h from the two lists L_1 and L_2
Compute $C_z^{(k)} = \sum_{j \in J_z^{(k)}} p_j + T_z^{(k)}$;
Determine $\sigma_z^{(k)} = \sigma_z^{(k)} \cup \{h\}$ and $f_\sigma = f_\sigma + w_h C_z^{(k)}$;
Set $I_{NA} = I_{NA} \setminus \{k\}$
End
Else
Begin
Set $z = z + 1$; $I_{NA} = I$;
End
Endif
End

COMPUTATIONAL ANALYSIS

Data generation

The heuristic were tested on problems generated with 500 tasks similar to that used in previous studies (Adamu and Abass, 2010; Ho and Chang, 1995; M'Hallah and Bulfin, 2005) for each task j an integer processing time p_j was randomly generated in the interval $(1,99)$ with a weight randomly w_j chosen in interval $(1,10)$.

The search time to define a neighborhood and to determine minimal cost is chosen equal to $90s$.

The number of machines fixed (3 machines) with (3 availability zones for each machine).

Diversification strategies

The final time to execute this problem is chosen as $T_F = 1200s$. It is divided according to diversification strategy to three times T_1, T_2 and T_3. After many experiments, these periods are chosen as follows:

$T_1 = 700s$ Initial starting time: uses long term memory to store the frequency of the moves executed throught of the search.

$T_2 = 300s$ First restarting time makes use of influential moves.

$T_3 = 200s$ Second restarting time also makes use of influential moves.

The table 1 below presents:

1- The initial mean values of objective function corresponding to initial sequence.
2- The initial mean values of objective function obtained by using on one hand, the neighborhood by swapping and on the other hand, the neighborhood by insertion.
3- The average times corresponding to the two neighborhoods.
4- The percentage of cost improvement.
5- The best costs.

RESULTS

The results listed in table 1 shows clearly that the tabu method based on neighborhood by insertion presents best costs compared with tabu method based on neighborhood by swapping. This is due to the fact that the first neighborhood ensures a faster tasks movement besides that the search space is richer with optimals partials sequences in each availability periods. This can also be explained by the nature of used neighborhoods, besides the left shifting of other tasks in the swapping neighborhood. The results show that execution time obtained by the first neighborhood is acceptable.

On the other hand, the heuristic amelioration rate between the two neighborhoods is remarkable (Figs. 1 and 2). It is also noted that the cost amelioration rate of the proposed tabu search heuristic is situated between 0.4% and 14%.

RECAPITULATED TABLE

In table 1 below one use the following abbreviations:
AC: Average costs
AT: Average time
PIIC: Percentage of improvement of the initial costs

Table 1. Percentage of heuristic cost amelioration based on metaheuristic.

n	Initial cost by heuristic (AC of 5 instances)	Tabu search by Swapping			Tabu search by Insertion			Best Cost
		AC	AT (second)	PIIC	AC	AT (second)	PIIC	
50	46290	41142	131	11%	41012	81	12%	41012
	54046	50550	179	6%	50444	139	7%	50444
	44648	43134	146	3%	43030	107	4%	43030
100	198110	179808	197	9%	179640	252	10%	179640
	176650	169064	314	4%	168868	480	5%	168868
	202408	186198	256	8%	195082	418	4%	186198
200	735058	633146	431	14%	733038	403	0.5%	633146
	692042	688068	327	1%	688962	498	1%	688068
	700578	699438	535	0.4%	699360	434	3.8%	699360
400	2773407	2771998	255	0.5%	2671898	583	4%	2671898
	2807046	2693834	325	6%	2793712	298	5%	2693834
	2756238	2638554	470	4%	2628452	428	5%	2628450
500	4289054	4273518	249	1%	4273400	378	1%	4273400
	4422156	4386046	360	1%	4384956	354	1%	4384956
	4649564	4497934	486	4%	4497822	707	4%	4497822

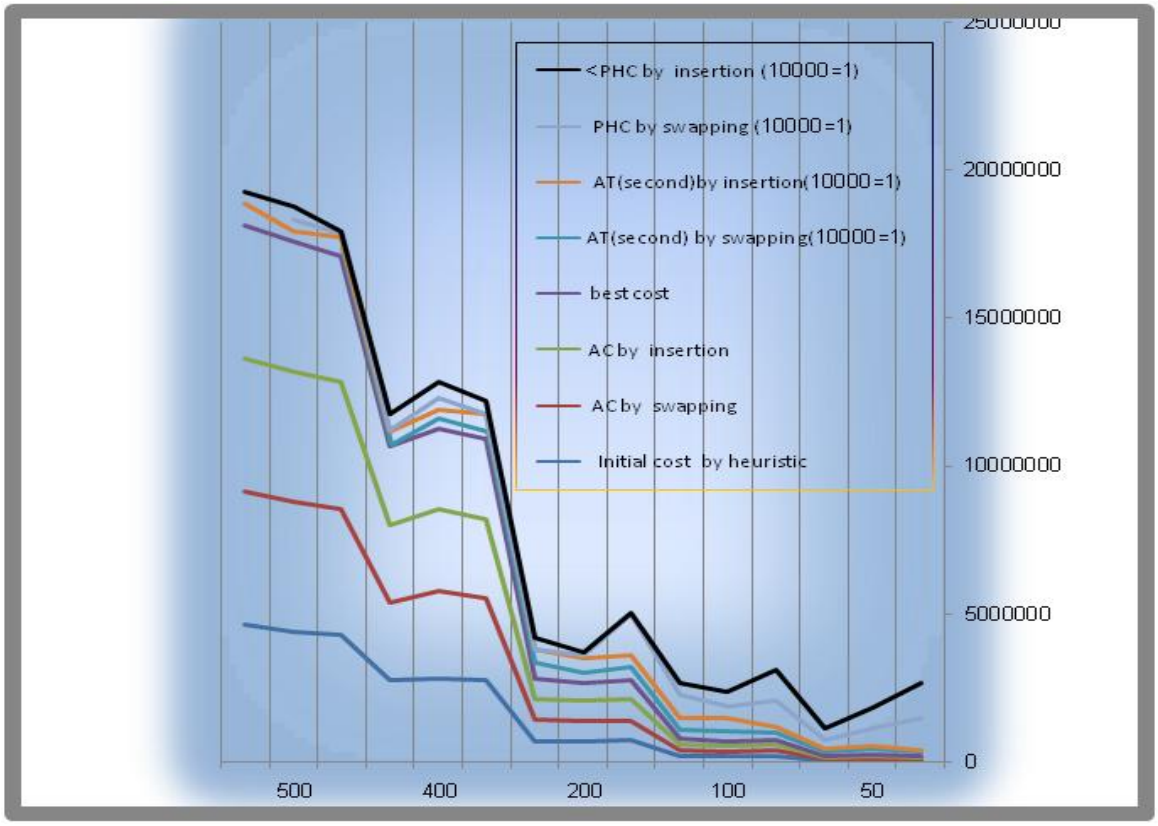

Fig 1. Comparison of heuristic and metaheuristic for n=500.

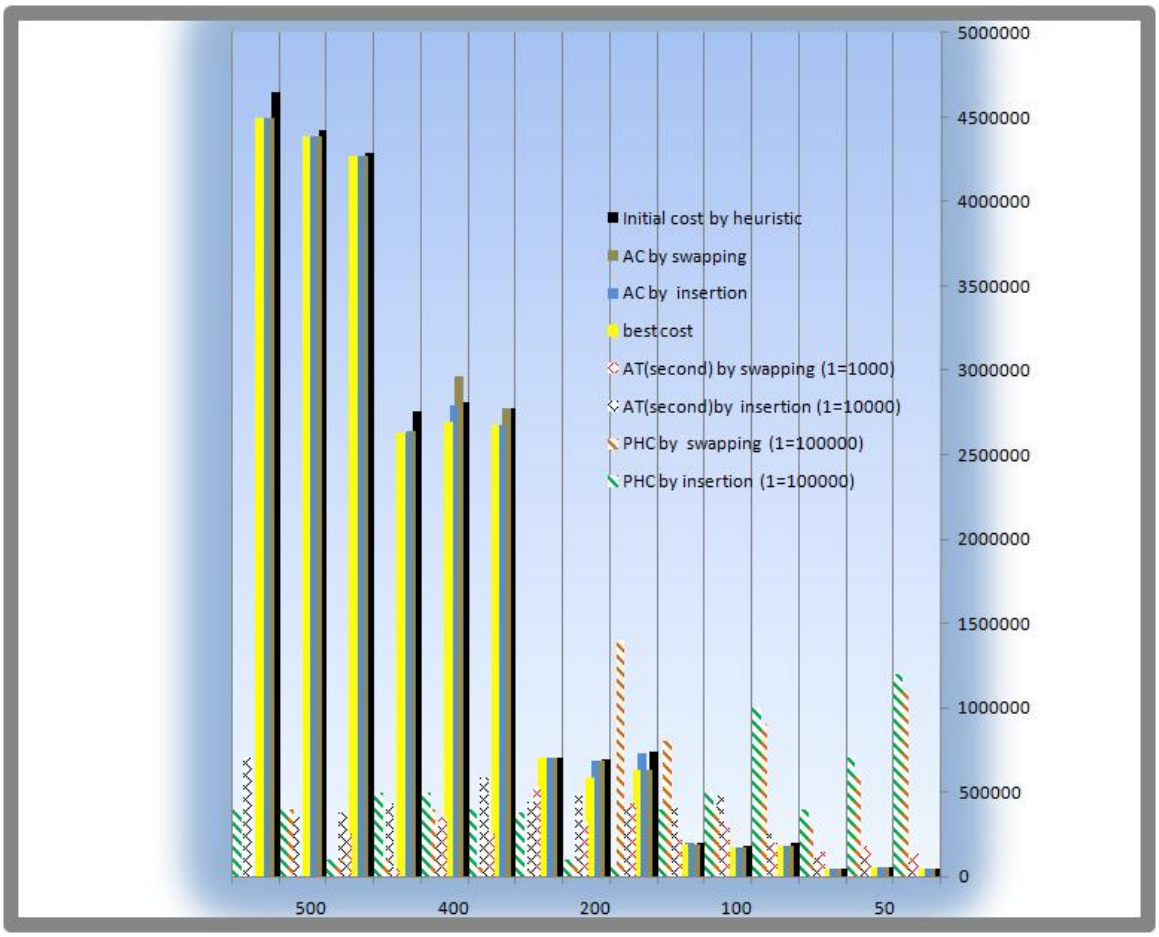

Fig 2. Comparison of heuristic and metaheuristic for n=500.

CONCLUSION

In this paper, a metaheuristic polynomial approach (Tabu search) as solution for tasks scheduling problem with parallel identical machines and availability periods is presented. The developed approach uses a diversification technique based on search restarting from the point of the solution that was chosen among the earlier best unmaintained found solutions, by considering that the tabu list is dynamic and its size varies according to amelioration state of the solution. According to the curried out tests, it can be concluded that the proposed approach ensure better results (heuristic amelioration cost up to14%). It must be noted that the neighborhood by insertion presents the best costs with an acceptable execution time.

ACKNOWLEDGEMENT

My special thanks to Professor Hocine Belouadah, Mohamed Said Hamani and Tarak Benslimane for their advises to achieved this work.

REFERENCES

Adamu, MO. and Abass, O. 2010. Paralell machine sheduling to maximize the weighted number of just-in-time jobs. J. App. Sci. Technol. 15(1&2):12-34.

Adamu, MO. and Adewunmi, A. 2013. Comparative study of metaheuristics for identical parallel machines. J. Eng.Technol. Res. 5(7):207-216.

Adamu, MO. and Adewunmi, A. 2012. Metaheuristics for scheduling on parallel machine to minimize weighted number of early and tardy jobs. Int. J. Phys. Sci. 7(10): 1641-1652.

Belouadah, H., Posner, ME. and Potts, CN. 1992. Scheduling with relates dates on a single machine to minimize total weighted completion time. Discrete Appl. Math. 36:213-231.

Glover, F. and Hanafi, S. 2002. Tabu Search and Finite Convergence, Special Issue on Foundations of heuristics in Combinatorial Optimization. Discrete Appl. Math. 119:3-36.

Glover, F. 1986. Futurepathsfo rinteger programming and

links to artificial intelligence, Comput. Open Res. 13: 533-549.

Hansen, P. 1986. The steepest ascent mildest descent heuristic for combinatorial programming. In: Proceedings of the Congress on Numerical Methods.

Haouari, M. and Ladhari, T. 2003. Branch and bound-based local search method for the flow shop problème. J. Oper. Res. Soc. 54:1076-1084.

Ho, JC. and Chang, YL. 1995. Minimizing the number of tardy jobs for m paralell machines. Eur. J. Oper. Res. 84: 334-355.

Lee, CY. 1996. Machine scheduling with an availability constraints. J. Global Optim. 9:395-416.

Lee, CY. 1997. Minimising the makespan in two machines flow shop scheduling problem with availability constraints. Oper. Res. Lett. 20:129-139.

Lee, CY. 1999. Two machines flow shop scheduling problem with availability constraints. European J. Oper. Res. 114:420-429.

M'Hallah, R. and Bulfin, RL. 2005. Minimizing the weighted number of tardy jobs of paralell processors. Eur. J. Oper. Res.160 :471-484.

Sadfi, C. 2002. Problèmes d'ordonnancement avec minimisation des encours Thèse PhD. Institut National Polytechnique de Grenoble, France.

Schmidt, G. 2000. Scheduling with limited machine availability. European J. Oper. Res. 121:1-15.

Smith, WE. 1956. Various optimizes for single-stage production. Naval Res. Logist. 3:59-66.

Yun-Chia, L., Yu-Ming, H. and Chia-Yun, T. 2013 Metaheuristics for drilling operation scheduling in Taiwan PCB industries. Int. J. Prod. Econ. 141(1):189-198.

Zribi, N., Kacem, I., El-Kamel, A. and Borne. P. 2005. Minimisation de la somme des retards dans un jobshop flexible. Revue e-STA (SEE). 2(2):2.

Received: April 11, 2014; Revised and Accepted: Sept 11, 2014

SENRA Academic Publishers, British Columbia
Vol. 8, No. 3, pp. 3155-3161, October 2014
Online ISSN: 1920-3853; Print ISSN: 1715-9997

Canadian Journal of pure&applied sciences

SOIL MODULUS AND UNDRAINED COHESION OF CLAYEY SOILS FROM STRESS-STRAIN MODELS

*SB Akpila and IW Omunguye
Department of Civil Engineering, Rivers State University of Science and Technology
PM B 5080, Port Harcourt, Nigeria

ABSTRACT

A study based on the stress-strain behaviour of soils in four areas within Port Harcourt has been carried out. In this study, deformation trends on stress and strain, derivative of stress and strain, and ratio of deviator stress to undrained cohesion to strain were established. Higher stability and lower deformation of soils response to loading were in descending order of Rukpoku, Ada George, Borikiri and Abuloma areas. At low strains, soil modulus E, generally reduced with increase in strain converging towards 3.5% strain and subsequently, exhibited slight increase in value on Rukpoku and Ada George Road soils. Predicted soil moduli for the areas are generally within the range of E, identified as soft to medium clay soils, except for Rukpoku soils that are within the range of hard clay. Predicted values of the ratio of deviator stress to undrained cohesion and strain, at strain level of 1% are generally lower than reported field values frequently used for intact blue London clay, but are within the value used for routine work in London clay. Shallow foundation settlement input parameter of soil modulus can easily be obtained from the predictive models or values, for preliminary analysis and design.

Keywords: Deviator stress, undrained cohesion, deformation, foundation settlement.

INTRODUCTION

Soils are generally subjected to various loads, which in this context can be those from load bearing walls, columns, vehicular wheel loads, and machine foundations, etc, causing stresses in the soil mass. The soils correspondingly experience varying levels of strain. This relationship can be exemplified in the laboratory for soils subjected to, for instance, triaxial compression, or direct shear on fully saturated soils. Hence, it becomes imperative to understand the shape of stress-strain curves of these soils in general. Problems involving the application of stresses to soils may be divided into those in which (a) deformation of the foundation soil control design and (b) failure of the foundation soil controls design. In deformation-controlled design, the deformation of a mass of soil must be computed and this ensures that the shape of the stress-strain curve must be taken into account. But for failure-controlled design, the precise shape of the stress-strain curve need not be known if shear stress reaches a maximum and subsequently remains constant even at very large strain (Poulos, 1971). Literatures in stability analysis reports stress-strain curves of soils reaching a maximum shear stress which then undergoes constant deformation under continuous strain. But in the laboratory, compressive triaxial test are generally not continued to attain continuous deformation under shear stress. Four major factors are considered to significantly control the shape of stress-strain curves of soils; soil type, initial structure, initial state and method of loading. The sections of stress-strain curve are affected to varying degree by these factors; before the steady state, the stress-strain curve is affected by all the factors whereas in the steady state, the shear stress is not influenced by initial structure, the stress path followed during loading or the initial state. However, the strain required to attain the steady state may be dependent on method of loading, initial state, initial structure and soil type (Poulos, 1971). Soils exhibit nonlinear stress-strain curve, and different soil moduli can be deduced from the slope of the curve. Depending on where the slope is determined, the secant modulus, tangent modulus, unloading modulus or reload modulus can be obtained. Consequently, appropriate selection of these moduli in engineering applications is important. For instance, the secant modulus is appropriate in predicting spread footing movement due to first load application; the tangent modulus is used in cases of evaluating incremental movement due to incremental load from one more storey in a high–rise building. Also, the unloading modulus is useful in calculating heave at bottom of excavation or rebound on pavement on removal of truck tyre load, while reload modulus is used in calculating bottom excavation movement on replacement of excavated soil or equivalent overburden (Briaud, 2010). The classical elasticity modelassumes soil behaviour under loading to be elastic and under axi-symmetric loading, the following equations are expressed (Bolton, 1979):

*Corresponding author email: sakpilab@gmail.com

$$\epsilon_1 = \frac{1}{E}(\sigma_1 - \mu\sigma_2 - \mu\sigma_3) \quad (1)$$

$$\epsilon_2 = \frac{1}{E}(-\mu\sigma_1 + \sigma_1 - \mu\sigma_3) \quad (2)$$

$$\epsilon_3 = \frac{1}{E}(-\mu\sigma_1 - \mu\sigma_2 + \sigma_3) \quad (3)$$

Where σ_1, σ_2 and σ_3 are three dimensional stresses, ϵ_1, ϵ_2, and ϵ_3 are three-dimensional strains, μ is poison ratio and E is modulus of soil.

Under uniaxial loading ($\sigma_2 = \sigma_3 = 0, and \ \epsilon_2 = \epsilon_3 = 0$) Equation (1) becomes;

$$E = \frac{\sigma_1}{\epsilon_1} \quad (4)$$

If the stress-strain curve is represented by $f(x)$, then incorporating Equation (4), the slope of the stress-strain curve can be expressed as;

$$\frac{d}{dx} f(x) = \frac{\sigma_1}{\epsilon_1} = E \quad (5)$$

Given that the deviator stress is $\sigma_1 - \sigma_3$ then the slope of

$(\sigma_1 - \sigma_3)/c_u$ versus axial strain, ϵ can be represented as

follows;

$$\frac{d}{d\epsilon}\{(\sigma_1 - \sigma_3)/c_u\} = \alpha \quad (6)$$

Where $\alpha = \frac{E}{c_u}$ and c_u = undrained cohesion.

Immediate settlement of shallow foundations placed on cohesive soils can be evaluated with value of undrained modulus, E_u, of the supporting soil as input parameter. However, determination of E_u is faced with several challenges and in Barnes (2000) and Jamiolkowski *et al.* (1979) proposed ratio of undrained modulus to undrained cohesion (E_u/c_u) depending on overconsolidation ratio and plasticity index. Butler (1974) proposed E_u/c_u ratio of 400 that is frequently used for intact blue overconsolidated London clay, while E_u/c_u ratio of 140 is proposed by Padfield and Sharrock (1983) for routine work in London clay. A procedure for obtaining undrained modulus directly from triaxial test results by determining the strain corresponding to 65% of the maximum deviator stress and dividing this value into its corresponding stress is outlined by Skempton (1951) and Smith (1982). In many literatures, E_u for various soils is presented in a wide range of values with little emphasis as to whether they are secant modulus, tangent modulus, unload modulus or reload modulus (Bowles, 1997). However, the initial tangent modulus is quite often used to represent the stress-strain modulus of a soil. This application is due to the elastic response of soils generally observed only near the origin and which is almost the same for different test plots. The adoption of re-load modulus has been emphasised as a better choice and it is generally higher than the initial tangent modulus of the first cycle due to the effect of strain hardening (Raj, 2008). Recent studies on the development of predictive models on evaluation of settlement parameters of void ratios e, coefficient of volumetric compressibility m_v, and compression modulus E_c, on clayey soils have been reported (Akpila, 2013a,b). It was observed that values of e, and m_v, generally showed a decreasing trend with increase in pressure, while E_c increased with pressure.

Based on the difficulty in evaluating the relevant soil modulus needed in the analysis and design of foundation, an attempt is made in this paper to develop a predictive model for the studied areas.

MATERIALS AND METHODS

Acquisition and Analysis of Data

A total of 81 unconsolidated undrained triaxial test results were analysed from each of the four areas studied in Port Harcourt: Abuloma, Ada George Road, Rukpoku and Borikiri**.** The deviator stresses, induced strains, cross-sectional area, major(σ_1)and minor (σ_3)principal stresses were evaluated. For instance, the deviator stress ($\sigma_1 - \sigma_3$), is evaluated noting that the average cross-sectional area (A) of the specimen does not remain constant throughout the test. When the original cross-sectional area of the specimen is A_o and the original volume is V_o then, for a decrease in volume of the specimen during the test, the average cross-sectional area (A) is expressed as;

$$A = A_o \frac{1 - \varepsilon_v}{1 - \varepsilon_a} \quad (7)$$

If the volume of specimen increases during the test, then Equation (1) becomes;

$$A = A_o \frac{1 + \varepsilon_v}{1 - \varepsilon_a} \quad (8)$$

Where ε_v is the volumetric strain ($\Delta v/v_o$), and ε_a is the axial strain ($\Delta l/l_o$). Deviator stresses were evaluated by dividing the load with corresponding cross-sectional area of the sample.

RESULTS AND DISCUSSION

Deviatorstress - strain curve

The various nonlinear stress-strain curves and soil modulus-strain curves of clayey soils from four studied areas are shown in figures 1- 4. The variation of applied deviator stress to strain induced on the soils is observed to have increased in the order of soils obtained from Abuloma, Borokiri, Ada George Road and Rukpoku. This is indicative of the tendency of soils within Rukpoku to exhibit higher stability and lower deformation as against the response of loading to stability and deformation on soils within the three other areas. Soils within Ada George Road showed middle bound response to loading, while soils within Borokiri have higher stability compared to those within Abuloma. Their predictive trends are given

by Equations (9-12). For cell pressure of 300 kN/m^2, the stress-strain curves are represented by Equations (13-16). The failure curve is typical of the non-linear behaviour of soils under deformation and the stress magnitudes sustained by the soils are highest on Rukpoku soils and lowest on Abuloma soils. Soils within Ada George Road had middle bound values, while those of Borikiri were higher than those from Abuloma.

Soil Modulus

The slope of stress-strain curves of Equations (9-12) are presented in Equations (17-20) while the variation of soil modulus E, with strain for cell pressure of 100 kN/m^2 is presented in figure 3. Soil modulus E, generally had a decreasing trend, with maximum values obtained at zero strain; Rukpoku soils had highest values, while Abuloma soil had lowest E. For strains exceeding 3%, soil modulus of Rukpoku soils showed a characteristic increase in value.

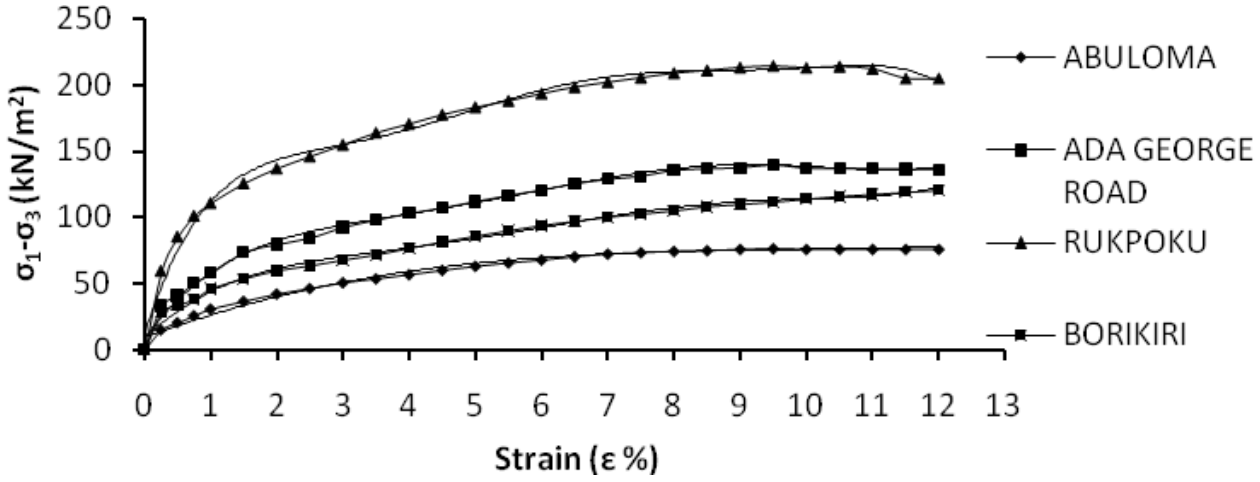

Fig. 1. Deviator stress and strain (σ_3 =100kN/m^2).

$\sigma_1 - \sigma_3$ = - 0.004ε^6 + 0.169ε^5 - 2.634ε^4 + 20.09ε^3 - 78.35ε^2 + 159.8ε + 13.44; R² = 0.991 Rukpoku (9)

$\sigma_1 - \sigma_3$ = 0.065ε^3 - 1.909ε^2 + 19.08ε + 9.137; R² = 0.986 Abuloma (10)

$\sigma_1 - \sigma_3$ = 0.007ε^5 - 0.234ε^4 + 2.846ε^3 - 15.88ε^2 + 47.99ε + 9.233; R² = 0.992 Borokiri (11)

$\sigma_1 - \sigma_3$ = 0.009ε^5 - 0.325ε^4 + 3.9816ε^3 - 22.54ε^2 + 68.11ε + 9.005; R²= 0.994 Ada George (12)

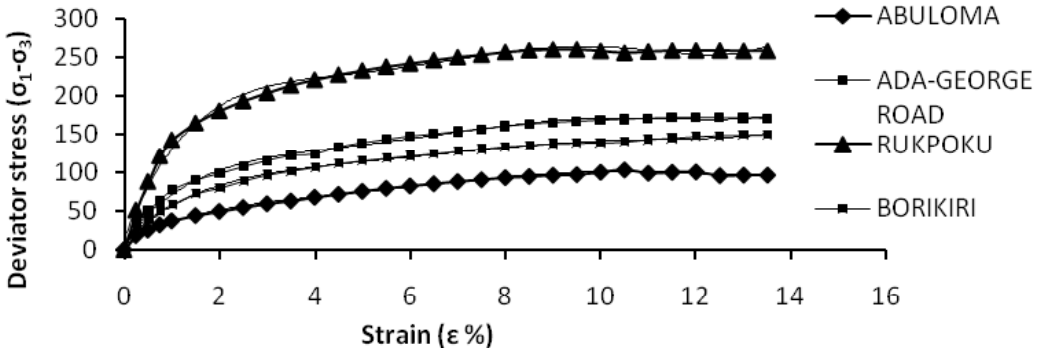

Fig. 2. Deviator Stress and Strain (σ_3 = 300 kN/m^2).

$\sigma_1 - \sigma_3$ = 0.013ε^5 - 0.496ε^4 + 7.037ε^3 - 46.85ε^2 + 155.1ε + 15.44; R² = 0.992 Rukpoku (13)

$\sigma_1 - \sigma_3$ = 0.006ε^5 - 0.237ε^4 + 3.374ε^3 - 22.48ε^2 + 78.76ε + 12.34; R² = 0.993 Ada George (14)

$\sigma_1 - \sigma_3$ = 0.003ε^5 - 0.149ε^4 + 2.207ε^3 - 15.70ε^2 + 60.56ε + 9.673; R² = 0.995 Borokiri (15)

$\sigma_1 - \sigma_3$ = 0.003ε^5 - 0.115ε^4 + 1.597ε^3 - 10.26ε^2 + 37.58ε + 6.408; R² = 0.994 Abuloma (16)

$E = -0.024\varepsilon^5 + 0.845\varepsilon^4 - 10.536\varepsilon^3 + 60.27\varepsilon^2 - 156.7\varepsilon + 159.8$; $R^2 = 0.991$ Rukpoku (17)

$E = 0.195\varepsilon^2 - 3.818\varepsilon + 19.08$; $R^2 = 0.986$ Abuloma (18)

$E = 0.035\varepsilon^4 - 0.936\varepsilon^3 + 8.538\varepsilon^2 - 31.76\varepsilon + 47.99$; $R^2 = 0.992$ Borokiri (19)

$E = 0.045\varepsilon^4 - 1.3\varepsilon^3 + 11.944\varepsilon^2 - 45.08\varepsilon + 68.11$; $R^2 = 0.992$ Ada George (20)

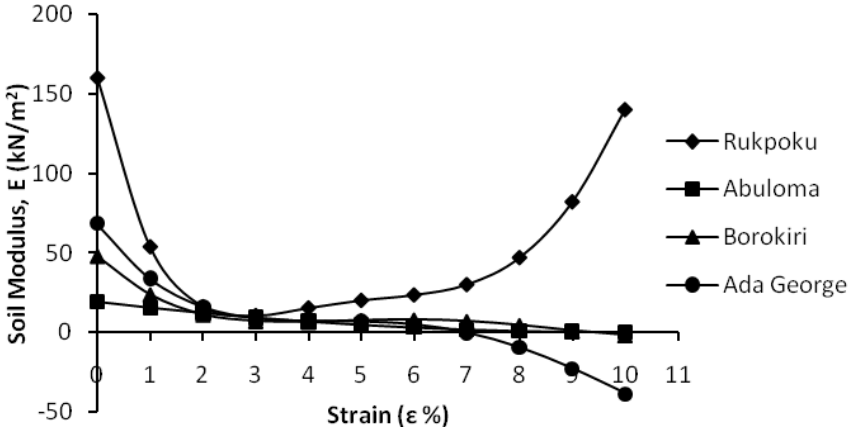

Fig. 3. Soil Modulus and Strain ($\sigma_3 = 100$ kN/m^2).

$E = 0.065\varepsilon^4 - 1.96\varepsilon^3 + 21.11\varepsilon^2 - 93.7\varepsilon^2 + 155.1$; $R^2 = 0.992$ Rukpoku (21)

$E = 0.030\varepsilon^4 - 0.948\varepsilon^3 + 10.12\varepsilon^2 - 44.96\varepsilon + 78.76$; $R^2 = 0.993$ Ada George (22)

$E = 0.015\varepsilon^4 - 0.596\varepsilon^3 + 6.621\varepsilon^2 - 31.4\varepsilon + 60.56$; $R^2 = 0.995$ Borokiri (23)

$E = 0.015\varepsilon^4 - 0.46\varepsilon^3 + 4.791\varepsilon^2 - 20.52\varepsilon + 37.5$; $R^2 = 0.994$ Abuloma (24)

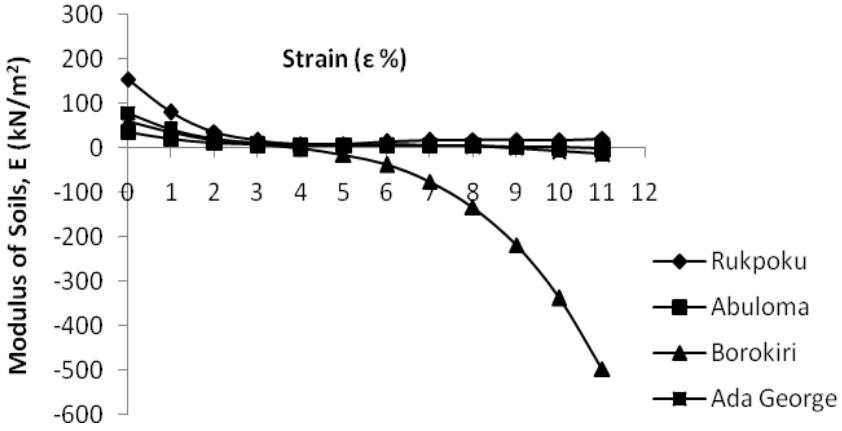

Fig. 4. Variation of Modulus with Strain ($\sigma_3 = 300$ kN/m^2).

The rate of change of stress with strain, expressed by the soil modulus, for cell pressure of 300kN/m^2 is presented in Equations (21-24) and depicted in figure 4. At low strains, soil modulus generally reduced with increase in strain converging towards 3.5% strain. Thereafter, E exhibited slight increase in value on Rukpoku and Ada George Road soils.

Stress to Undrained cohesion, $(\sigma_1 - \sigma_3)/c_u$, and Strain

Soils response in terms of the ratio of deviator stress to undrained cohesion, $(\sigma_1 - \sigma_3)/c_u$and strain for cell pressure of 100 and 300 kN/m^2 are presented in figures 5 and 6, respectively. The response trend is generally non-linear with highest values found on soils within Borikiri, and lowest values on Abuloma soils. Middle bound value is

$(\sigma_1 - \sigma_3)/c_u = - 0.011\varepsilon^4 + 0.135\varepsilon^3 - 0.755\varepsilon^2 + 2.284\varepsilon + 0.435$; $R^2 = 0.992$ Borokiri (25)

$(\sigma_1 - \sigma_3)/c_u = - 0.009\varepsilon^4 + 0.115\varepsilon^3 - 0.660\varepsilon^2 + 1.905\varepsilon + 0.338$; $R^2 = 0.984$ Rukpoku (26)

$(\sigma_1 - \sigma_3)/c_u = - 0.005\varepsilon^4 + 0.068\varepsilon^3 - 0.391\varepsilon^2 + 1.189\varepsilon + 0.155$; $R^2 = 0.994$ Ada George Rd (27)

$(\sigma_1 - \sigma_3)/c_u = - 0.004\varepsilon^4 + 0.052\varepsilon^3 - 0.305\varepsilon^2 + 1.010\varepsilon + 0.117$; $R^2 = 0.996$ Abuloma (28)

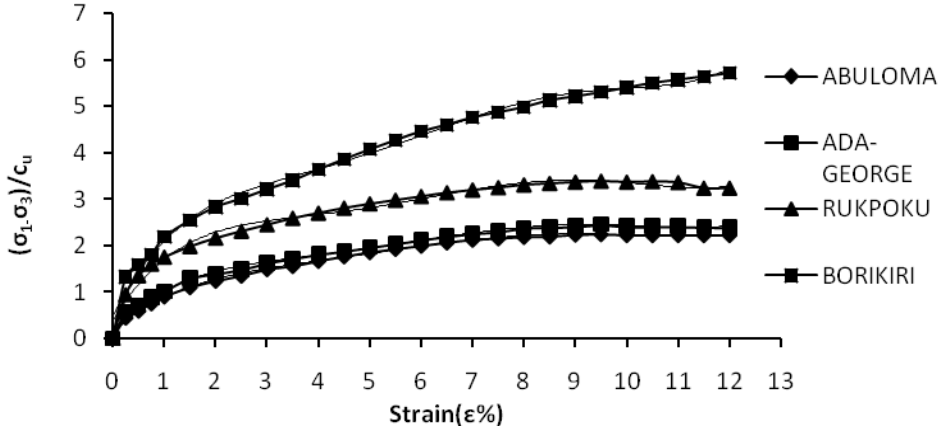

Fig. 5. Deviator stress to undrained cohesion and strain (σ_3 =100 kN/m^2).

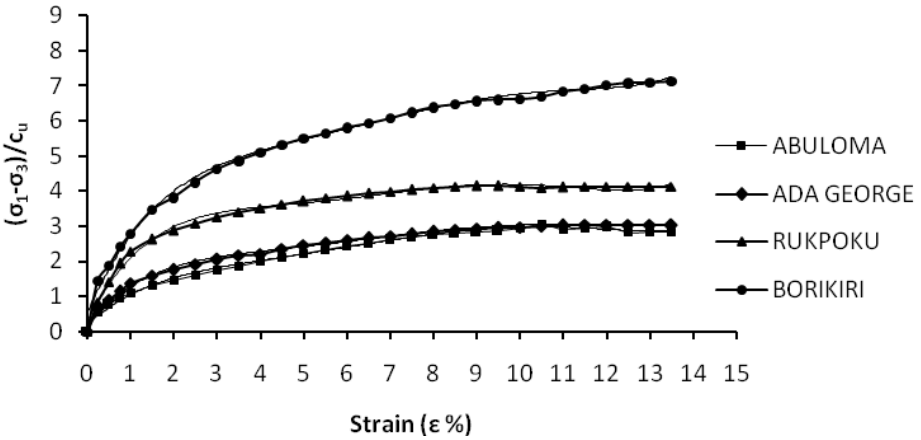

Fig. 6. Deviator Stress to Undrained cohesion and Strain (σ_3 = 300kN/m^2).

$(\sigma_1 - \sigma_3)/c_u = - 0.007x^4 + 0.105x^3 - 0.747x^2 + 2.884x + 0.460$; $R^2 = 0.995$ Borokiri (29)

$(\sigma_1 - \sigma_3)/c_u = - 0.007x^4 + 0.111x^3 - 0.743x^2 + 2.463x + 0.245$; $R^2 = 0.992$ Rukpoku (30)

$(\sigma_1 - \sigma_3)/c_u = - 0.004x^4 + 0.059x^3 - 0.394x^2 + 1.381x + 0.216$; $R^2 = 0.993$ Ada George Rd (31)

$(\sigma_1 - \sigma_3)/c_u = - 0.003x^4 + 0.047x^3 - 0.301x^2 + 1.105x + 0.188$; $z^2 = 0.994$ Abuloma (32)

associated with Rukpoku soils but soils around Ada George Road had values that are slightly higher than those within Abuloma. Their respective trend lines are given by Equations (25-28).

MODEL VERIFICATION

Soil Modulus

Evaluation of tangent modulus of the soils at 1% strain level for cell pressures of 100 kN/m^2 and 300 kN/m^2 based on deviator stress-strain models of Equations (9-12) and (13-16) respectively are shown in table1. The predicted soil modulus are generally in the range of E, identified as soft to medium clay soils, except for Rukpoku soils that are in the range of hard clay. From the derivatives of the deviator stress-strain models of Equations (17-20) and (21-24), the soil modulus at 1% strain level are also presented in table 2. The predicted soil moduli for the areas suggested Abuloma soils as soft

Table 1. Model verification of soil modulus (Stress-strain models).

Location	Predicted Tangent Modulus E (MPa)	E from field values (MPa)	
		Clay soil	Range
Rukpoku	99-115	Very soft	2-15
Ada George Rd	45-59	Soft	15-25
Borikiri	35-47	Medium	25-50
Abuloma	17-29	Hard	50-100

Table 2. Model verification of soil modulus ($\frac{d}{d\varepsilon}(\sigma_1 - \sigma_3)$).

Location	Predicted Tangent Modulus E (MPa)	E from field values (MPa)	
		Clay soil	Range
Rukpoku	54-81	Very soft	2-15
Ada George Rd	23-43	Soft	15-25
Borikiri	16-43	Medium	25-50
Abuloma	15-21	Hard	50-100

clays, those within Borikiri and Ada George Road as soft to medium clays, but Rukpoku having E of hard clays.

Stress to Undrained cohesion, $(\sigma_1 - \sigma_3)/c_u$and Strain

The predicted values of E/c_u based on the ratio of deviator stress to undrained cohesion**,** $(\sigma_1 - \sigma_3)/c_u$, and strain for cell pressure of 100 and 300 kN/m^2 at strain level of 1% is presented in Tables 3. Predicted E/c_u values are generally lower than reported field values frequently used for intact blue London clay, but are within the value used for routine work in London clay.

CONCLUSION

The stress-strain curve of the soils showed nonlinear deformation behaviour and the predicted soil modulus for the areas are generally in the range of E identified as soft to medium clay soils, except for Rukpoku soils that are within the range of hard clays.

Based on the derivatives of the deviator stress-strain models, Abuloma soils have E described as soft clays, those within Borikiri and Ada George Road have E associated with soft to medium clays, but Rukpoku area has E described as hard clays. The predicted values of E/c_u based on the ratio of deviator stress to undrained cohesion**,** $(\sigma_1 - \sigma_3)/c_u$and strain at strain level of 1% generally gave values lower than reported field values frequently used for intact blue London clay, but are within the values used for routine work in London clay.

Ultimately, foundation settlement input parameter of soil modulus in the studied areas can easily be obtained from generated predictive models or values, for purposes of preliminary analysis and design of shallow foundations placed on cohesive soils.

REFERENCES

Akpila, SB. 2013[a]. Predictive Approach on Evaluation of Settlement Parameters on Clayey Soils in Parts of Port Harcourt. Scientific Journal of Pure and Applied Sciences. 2(2):66-71.

Akpila, SB. 2013[b]. Predictive Models on Settlement Parameters of Clayey Soils: A Case Study in Port Harcourt City of Nigeria. Canadian Journal of Pure and Applied Sciences. 7(3):2649-2653.

Barnes, GE. 2000. Soil Mechanics, Principles and Practice. (2nd edi.). MacMillan Press Ltd, London. pp267.

Bolton, M. 1979. Guide to Soil Mechanics. The MacMillan Press Ltd, London. pp120.

Bowles, JE. 1997. Foundation Analysis and Design. (5th edi.). MacGraw- Hill International Editions. pp125.

Briaud, JL. 2010. Introduction to Soil Moduli. Static2.docstoccdn.com/docs/42184625/1

Butler, FG. 1974. Review Paper: Heavily Over-consolidated Clays. In: Proceedings of the Conference on Settlement of Structures. Pentech Press, Cambridge. 531-578.

Jamiolkowski, M., Lancellotta, R., Pasqualini, E., Marchetti, S. and Nava, R. 1979. Design Parameters for Soft Clays. General Report. Proc. 7th European Conf. on Soil Mechanics and Foundation Engineering. 5:27-57.

Padfield, CJ. and Sharrock, MJ. 1983. Settlement of Structures on Clay Soils. Construction Industry Research and Information Association. Special Pub. pp27.

Poulos, CJ. 1971. Stress-Strain Curves of Soils, Geotechnical Engineers, Inc. Winchester, Massachusetts. 01890.

Raj, PP. 2008. Soil Mechanics and Foundation Engineering. Dorling Kindersley Pvt Ltd., India. pp171.

Skempton, AW. 1951. The Bearing Capacity of Clays. Building Research Congress.

Smith, GN. 1982. Elements of Soil Mechanics for Civil and Mining Engineers. (5th edi.). Billing and Sons Ltd, UK. 348-349.

Received: June 27, 2014; Revised and Accepted: Aug 1, 2014

SENRA Academic Publishers, British Columbia
Vol. 8, No. 3, pp. 3163-3165, October 2014
Online ISSN: 1920-3853; Print ISSN: 1715-9997

Canadian Journal of pure&applied sciences

Short Communication

ON FUZZY COMPLEX DERIVATIVES II

Pishtiwan O. Sabir
Department of Mathematics, Faculty of Science and Science Education
University of Sulaimani, Sulaimani, Kurdistan Region, Iraq

ABSTRACT

In this paper, an important theorem of fuzzy derivative for fuzzy complex functions which map a regular complex numbers into bounded closed complex complement normalized fuzzy numbers is proved. This is a modification and generalization of the fuzzy derivative in Sabir *et al.* (2012).

Keywords: Fuzzy complex numbers, Fuzzy Functions, Fuzzy derivatives.

INTRODUCTION

Fuzzy complex analysis was first introduced by Buckley and Qu (1991, 1992) that extends definitions and results of Dubois and Prade (1982) to the complex case. Buckley (1989) suggested the notion of convergence, differentiation and continuity of complex fuzzy function (Guangquan, 1991; Chun and Ma, 1998; Dianjun, 2000; Qiu *et al.*, 2009; Ousmane and Congxin, 2003; Shengquan, 2006; Cai, 2009). As a generalization of Buckley's work, several scholars continued research in fuzzy analysis like Wu and Qiu (1999), Zengtai and Shengquan (2006), Qiu and Shu (2008), Sun and Guo (2010), Ma and Chen (2012) and Sabir (2012).

PRILIMINARIES

Zadeh (1965) firstly introduced the concept of fuzzy subset which is a function $\mu(\tilde{A},x)\colon X \to [0,1]$ and a generalization of the classical set operations.

Definition 1. Let $\tilde{A}$ be a fuzzy subset and $\alpha \in [0,1]$, then
(1) The α–level of $\tilde{A}$, denoted by ${}^{\alpha+}\tilde{A}$, is the crisp set $\{x \in X\colon \mu(\tilde{A},x) \geq \alpha\}$.
(2) The weak α–level ${}^{\alpha-}\tilde{A}$ of a fuzzy subset $\tilde{A}$ is the non-fuzzy set of all elements of X that grade of memberships are greater than α.
(3) The height of a fuzzy subset $\tilde{A}$ is the number obtained by $\alpha_{\tilde{A}}^{max} = sup_{x\in X}\,\mu(\tilde{A},x)$.

Definition 2. For any collection, $\{\tilde{A}_i\colon i \in I\}$, of fuzzy subsets of X, where I is a nonempty index set.
(1) The union of fuzzy subsets $\tilde{A}_i$ is defined by $\mu(\cup_i \tilde{A}_i, x) = sup_x\,\mu(\tilde{A}_i,x)$.
(2) The intersection of fuzzy subsets $\tilde{A}_i$ is defined by $\mu(\cap_i \tilde{A}_i, x) = inf_x\,\mu(\tilde{A}_i,x)$.
(3) The complement of $\tilde{A}_i$ is defined by $\mu(\neg\tilde{A}_i,x) = 1-\mu(\tilde{A}_i,x)$, for all x belongs to X.

Definition 3. A fuzzy number $\tilde{a}$ defined on the set of real numbers $\mathcal{R}$ is a function $\mu(\tilde{a},x)\colon \mathcal{R} \to [0,1]$, which satisfies:
(1) $\tilde{a}$ is upper semicontinuous.
(2) $\mu(\tilde{a},x) = 0$ outside some interval $[c,d]$.
(3) There are real numbers a,b such that $c \leq a \leq b \leq d$, $\mu(\tilde{a},x)$ is increasing on [c, a], $\mu(\tilde{a},x)$ is decreasing on $[b,d]$, and $\mu(\tilde{a},x) = 1$, $a \leq x \leq b$.

Definition 4. A fuzzy complex number $\hat{Z}$ is a mapping $\mu(\hat{Z},z)\colon \mathbb{C} \to [0,1]$ if and only if:
(1) $\mu(\hat{Z},z)$ is continuous.
(2) ${}^{\alpha-}\hat{Z}$ is open, bounded, and connected.
(3) ${}^{1+}\hat{Z}$ is non-empty, compact, and arcwise connected.

RESULTS

Definitions, results and notations on fuzzy complex analysis which are used in this section can be found in Sabir *et al.* (2012).

Theorem 1. Let $\tilde{Z},\widetilde{W}$ be BCCCNFNs and $\tilde{f}$ be a fuzzy meromorphic function. If $\tilde{f}(z) = \widetilde{W}$ and $\tilde{f}'(z) = \widetilde{W}$ have the same zeros, $\tilde{f}(z) = \tilde{Z}$ and $\tilde{f}'(z) = \tilde{Z}$ have the same zeros with the same order, and $\bar{N}(r,{}^{z,\gamma+}\tilde{f}) = o(T(r,{}^{z,\gamma+}\tilde{f}))$ then ${}^{z,\gamma+}\dot{\tilde{f}} = {}^{z,\gamma+}\tilde{f}$.

Proof: By hypothesis, we have
$2T(r,{}^{z,\gamma+}\tilde{f}) \leq \bar{N}(r,{}^{z,\gamma+}\tilde{f}) + \bar{N}\left(r,\frac{1}{{}^{z,\gamma+}\tilde{f}-{}^{\gamma+}\tilde{Z}}\right)$

*Corresponding author email: pishtiwan.sabir@gmail.com

$$+\bar{N}\left(r,\frac{1}{z,\gamma+\tilde{f}-\gamma+\tilde{W}}\right)+\bar{N}\left(r,\frac{1}{z,\gamma+\tilde{f}}\right)+o\big(T(r,{}^{z,\gamma+}\tilde{f})\big)$$

$$=\bar{N}\left(r,\frac{1}{z,\gamma+\tilde{f}}\right)+\bar{N}\left(r,\frac{1}{z,\gamma+\dot{\tilde{f}}-\gamma+\tilde{Z}}\right)+\bar{N}\left(r,\frac{1}{z,\gamma+\dot{\tilde{f}}-\gamma+\tilde{W}}\right)+o\big(T(r,{}^{z,\gamma+}\tilde{f})\big)$$

$$=\bar{N}\left(r,\frac{1}{z,\gamma+\tilde{f}}\right)+N\left(r,\frac{{}^{z,\gamma+}\dot{\tilde{f}}}{z,\gamma+\tilde{f}}\right)+o\big(T(r,{}^{z,\gamma+}\tilde{f})\big)$$

$$=\bar{N}\left(r,\frac{1}{z,\gamma+\tilde{f}}\right)+\bar{N}\big(r,{}^{z,\gamma+}\tilde{f}\big)+\bar{N}\left(r,\frac{1}{z,\gamma+\tilde{f}}\right)+o\big(T(r,{}^{z,\gamma+}\tilde{f})\big)$$

$$=2\bar{N}\left(r,\frac{1}{z,\gamma+\tilde{f}}\right)+o\big(T(r,{}^{z,\gamma+}\tilde{f})\big)$$

$$\leq 2T\big(r,{}^{z,\gamma+}\tilde{f}\big)+o\big(T(r,{}^{z,\gamma+}\tilde{f})\big).$$

It follows that,

$$\bar{N}\left(r,\frac{1}{z,\gamma+\tilde{f}}\right)=\bar{N}\left(r,\frac{1}{z,\gamma+\dot{\tilde{f}}-\gamma+\tilde{Z}}\right)+\bar{N}\left(r,\frac{1}{z,\gamma+\dot{\tilde{f}}-\gamma+\tilde{W}}\right)+o\big(T(r,{}^{z,\gamma+}\tilde{f})\big),\text{ and}$$

$$m\left(r,\frac{1}{z,\gamma+\tilde{f}-\gamma+\tilde{W}}\right)\leq m\left(r,\frac{\left(z,\gamma+\dot{\tilde{f}}-\gamma+\tilde{Z}\right)-\left(z,\gamma+\tilde{f}-\gamma+\tilde{Z}\right)}{z,\gamma+\dot{\tilde{f}}\left(z,\gamma+\dot{\tilde{f}}-\gamma+\tilde{Z}\right)-z,\gamma+\ddot{\tilde{f}}\left(z,\gamma+\tilde{f}-\gamma+\tilde{Z}\right)}\right)+m\left(r,\frac{{}^{z,\gamma+}\dot{\tilde{f}}}{\left(z,\gamma+\tilde{f}-\gamma+\tilde{Z}\right)\left(z,\gamma+\tilde{f}-\gamma+\tilde{W}\right)}\right)+m\left(r,\frac{{}^{z,\gamma+}\ddot{\tilde{f}}}{z,\gamma+\dot{\tilde{f}}\left(z,\gamma+\dot{\tilde{f}}-\gamma+\tilde{Z}\right)}\right)+m\left(r,\frac{{}^{z,\gamma+}\dot{\tilde{f}}}{\left(z,\gamma+\tilde{f}-\gamma+\tilde{W}\right)}\right)$$

$$\leq T\left(r,\frac{{}^{z,\gamma+}\dot{\tilde{f}}}{z,\gamma+\tilde{f}-\gamma+\tilde{Z}}-\frac{{}^{z,\gamma+}\ddot{\tilde{f}}}{z,\gamma+\dot{\tilde{f}}-\gamma+\tilde{Z}}\right)+o\left(T\big(r,{}^{z,\gamma+}\tilde{f}\big)\right)+o\big(T(r,{}^{z,\gamma+}\tilde{f})\big)+o\left(T\big(r,{}^{z,\gamma+}\dot{\tilde{f}}\big)\right)$$

$$=N\left(r,\frac{{}^{z,\gamma+}\dot{\tilde{f}}}{z,\gamma+\tilde{f}-\gamma+\tilde{Z}}-\frac{{}^{z,\gamma+}\ddot{\tilde{f}}}{z,\gamma+\dot{\tilde{f}}-\gamma+\tilde{Z}}\right)+m\left(r,\frac{{}^{z,\gamma+}\dot{\tilde{f}}}{z,\gamma+\tilde{f}-\gamma+\tilde{Z}}-\frac{{}^{z,\gamma+}\ddot{\tilde{f}}}{z,\gamma+\dot{\tilde{f}}-\gamma+\tilde{Z}}\right)+o\big(T(r,{}^{z,\gamma+}\tilde{f})\big)$$

$$\leq \bar{N}\big(r,{}^{z,\gamma+}\tilde{f}\big)+m\left(r,\frac{{}^{z,\gamma+}\dot{\tilde{f}}}{z,\gamma+\tilde{f}-\gamma+\tilde{Z}}\right)+m\left(r,\frac{{}^{z,\gamma+}\ddot{\tilde{f}}}{z,\gamma+\dot{\tilde{f}}-\gamma+\tilde{Z}}\right)+o\big(T(r,{}^{z,\gamma+}\tilde{f})\big)$$

$$=o\left(T\big(r,{}^{z,\gamma+}\tilde{f}\big)\right)+o\left(T\big(r,{}^{z,\gamma+}\tilde{f}\big)\right)+o\left(T\left(r,{}^{z,\gamma+}\dot{\tilde{f}}\right)\right)+o\big(T(r,{}^{z,\gamma+}\tilde{f})\big).$$

Hence,

$$N\left(r,\frac{1}{z,\gamma+\dot{\tilde{f}}-\gamma+\tilde{Z}}\right)+N\left(r,\frac{1}{z,\gamma+\tilde{f}-\gamma+\tilde{W}}\right)+o\left(T\big(r,{}^{z,\gamma+}\tilde{f}\big)\right)$$

$$=N\left(r,\frac{1}{z,\gamma+\dot{\tilde{f}}-\gamma+\tilde{Z}}\right)+N\left(r,\frac{1}{z,\gamma+\tilde{f}-\gamma+\tilde{W}}\right)+o\left(T\big(r,{}^{z,\gamma+}\tilde{f}\big)\right)$$

$$=N\left(r,\frac{1}{z,\gamma+\tilde{f}-\gamma+\tilde{W}}\right)+o\left(T\big(r,{}^{z,\gamma+}\tilde{f}\big)\right),\text{ and}$$

$$m\left(r,\frac{1}{z,\gamma+\dot{\tilde{f}}-\gamma+\tilde{W}}\right)+N\left(r,\frac{1}{z,\gamma+\dot{\tilde{f}}-\gamma+\tilde{W}}\right)\leq T\big(r,{}^{z,\gamma+}\tilde{f}\big)+o\left(T\big(r,{}^{z,\gamma+}\tilde{f}\big)\right)=\bar{N}\left(r,\frac{1}{z,\gamma+\tilde{f}-\gamma+\tilde{W}}\right)+o\left(T\big(r,{}^{z,\gamma+}\tilde{f}\big)\right)$$

$$\leq N\left(r,\frac{1}{z,\gamma+\dot{\tilde{f}}-\gamma+\tilde{W}}\right)+o\left(T\big(r,{}^{z,\gamma+}\tilde{f}\big)\right).$$

Therefore,

$$T\left(r,\frac{1}{z,\gamma+\tilde{f}-\gamma+\tilde{Z}}\right)+T\left(r,\frac{1}{z,\gamma+\dot{\tilde{f}}-\gamma+\tilde{Z}}\right)+T\left(r,\frac{1}{z,\gamma+\tilde{f}-\gamma+\tilde{W}}\right)+T\left(r,\frac{1}{z,\gamma+\dot{\tilde{f}}-\gamma+\tilde{W}}\right)$$

$$=m\left(r,\frac{1}{z,\gamma+\tilde{f}-\gamma+\tilde{Z}}\right)+m\left(r,\frac{1}{z,\gamma+\dot{\tilde{f}}-\gamma+\tilde{Z}}\right)+m\left(r,\frac{1}{z,\gamma+\tilde{f}-\gamma+\tilde{W}}\right)+m\left(r,\frac{1}{z,\gamma+\dot{\tilde{f}}-\gamma+\tilde{W}}\right)+N\left(r,\frac{1}{z,\gamma+\tilde{f}-\gamma+\tilde{Z}}\right)+N\left(r,\frac{1}{z,\gamma+\dot{\tilde{f}}-\gamma+\tilde{Z}}\right)+N\left(r,\frac{1}{z,\gamma+\tilde{f}-\gamma+\tilde{W}}\right)+N\left(r,\frac{1}{z,\gamma+\dot{\tilde{f}}-\gamma+\tilde{W}}\right)+o\left(T\big(r,{}^{z,\gamma+}\tilde{f}\big)\right)$$

$$\leq m\left(r,\frac{1}{z,\gamma+\ddot{\tilde{f}}}\right)-m\left(r,\frac{1}{z,\gamma+\dot{\tilde{f}}}\right)+N\left(r,\frac{1}{z,\gamma+\dot{\tilde{f}}-\gamma+\tilde{W}}\right)+m\left(r,\frac{1}{z,\gamma+\dot{\tilde{f}}}\right)+T\big(r,{}^{z,\gamma+}\tilde{f}\big)+o\left(T\big(r,{}^{z,\gamma+}\tilde{f}\big)\right)$$

$$\leq T\left(r, {}^{z,\gamma+}\dot{\tilde{f}}\right) + T\left(r, \frac{1}{z,\gamma+\dot{\tilde{f}}-\gamma+\widetilde{W}}\right) + T\left(r, {}^{z,\gamma+}\tilde{f}\right)$$

$$+o\left(T\left(r, {}^{z,\gamma+}\tilde{f}\right)\right) \text{ a Contradiction.}$$

ACKNOWLEDGMENT

This study was financial supported by Science Faculty of Higher Education Commission under the University of Sulaimani Scientific Research Program is highly acknowledged. The author is highly thankful to Scientific Committee of Mathematics Department, Scientific Committee of Faculty of Sciences and Science Education for facilitating the project.

REFERENCES

Buckley, JJ. and Qu, Y. 1991. Fuzzy complex analysis I: Differentiation. Fuzzy Sets and Systems 41. Elsevier. 269-284.

Buckley, JJ. and Qu, Y. 1992. Fuzzy complex analysis II: Integration. Fuzzy Sets and Systems. 49. Elsevier. 71-179.

Buckley, JJ. 1989. Fuzzy complex numbers. Fuzzy Sets and Systems. 33. Elsevier. 333-345.

Cai, QP. 2009. The continuity of complex fuzzy function. Adv. in Int. and Soft Computing. 2:695-704.

Chun, C. and Ma, S. 1998. The differentiation of complex fuzzy functions. Proc. of the 9th NCFMFS, Baoding, Hebei U. Press. 162-166.

Dianjun, Y. 2000. On the complex fuzzy derivative. BUSEFAL. 81:90-92.

Dubois, D. and Prade, H. 1982. Towards fuzzy differential calculus, Part 3: Differentiation. Fuzzy Sets and systems 8. Elsevier. 225-233.

Guangquan, Z. 1991. Fuzzy continuous function and its properties. Fuzzy Sets and Systems 43. Elsevier. 159-171.

Ma, S. and Chen, F. 2012. Fuzzy complex valued integral and its convergence. Adv. in Int. and Soft Computing. 147:265-273.

Ousmane, M. and Congxin, W. 2003. Semi continuity of complex fuzzy functions. Tsinghua Science and Technology. 8:65-70.

Qiu, D. and Shu, L. 2008. Notes on: On the restudy of fuzzy complex analysis: Part I and Part II. Fuzzy Sets and Systems 159. Elsevier. 2185-2189.

Qiu, D., Shu, L. and Mo, ZW. 2009. Notes on fuzzy complex analysis. Fuzzy Sets and Systems 160. Elsevier. 1578-1589.

Sabir, PO. 2012. On fuzzy complex analysis. PhD. Thesis. University of Sulaimani, , Kurdistan Region, Iraq.

Sabir, PO., Adil, KJ., Munir, AA. 2012. On fuzzy complex derivatives. IOSR Journal of Mathematics. 2(5): 47-52.

Shengquan, M. 2006. The series of complex fuzzy valued and its convergence. Journal of Fuzzy Mathematics. 5: 200-211.

Sun, J. and Guo, S. 2010. The solution algorithm of complex fuzzy valued function integral by fuzzy element. ACFIE. 78:55-63.

Wu, C. and Qiu, J. 1999. Some remarks for fuzzy complex analysis. Fuzzy Sets and Systems 106. Elsevier. 231-238.

Zadeh, LA. 1965. Fuzzy sets. Inform. & Control. 8:338-353.

Zengtai, G. and Shengquan, M. 2006. The research advances in fuzzy complex analysis. Math. in Prac. and Theory. 36:200-211.

Received: July 1, 2014; Revised: Sept 7, 2014; Accepted: Sept 12, 2014